SR P T01
Form 1
WAIVER

THE UNIVERSITY OF NEW SOUTH WALES

DECLARATION RELATING TO DISPOSITION OF PROJECT REPORT/THESIS

This is to certify that I being a candidate for the degree of am fully aware of the policy of the University relating to the retention and use of higher degree project reports and theses, namely that the University retains the copies submitted for examination and is free to allow them to be consulted or borrowed. Subject to the provisions of the Copyright Act, 1968, the University may issue a project report or thesis in whole or in part, in photostat or microfilm or other copying medium.

In the light of these provisions I grant the University Librarian permission to publish, or to authorize the publication of my project report/thesis, in whole or in part.

I also authorize the publication by University Microfilms of a 350 word abstract in *Dissertation Abstracts International* (applicable to doctorates only).

I hereby declare that this submission is my own work and that, to the best of my knowledge and belief, it contains no material previously published or written by another person nor material which to a substantial extent has been accepted for the award of any other degree or diploma of a university or other institute of higher learning, except where due acknowledgement is made in the text.

PARAMETER IDENTIFICATION OF VIBRATING STRUCTURES

by

YONGLIN PI

A thesis submitted in fulfilment of
the requiement for the degree of
Doctor of Philosophy

The University of New South Wales
AUSTRALIA
June, 1990

TABLE OF CONTENTS

TABLE OF FIGURES

ACKNOWLEDGEMENTS

The author wishes to express his sincere gratitude to his supervisor, Dr. N. C. Mickleborough for invaluable and consistent guidance, encouragement and enthusiasm throughout the course of this research. He is particularly indebted to Dr. N. C. Mickleborough for his support, advice and generosity with time on the preparation of this thesis. The author is grateful to Professor H. M. Irvine, Head of the Department of Structural Engineering, for his assistance and direction in the present study.

The thanks are extended to the staff members and research fellows of the Department of Structural Engineering for their kindness, valuable suggestions and encouragement in many instances.

The author is grateful to the staff of the Laboratory of Structural Engineering at the University of New South Wales for their assistance in the laboratory testing.

The author also wishes to record his sincere thanks to the School of Civil Engineering of The University of New South Wales for the financial support granted to him in the form of a University Scholarship and a Civil Engineering Scholarship to enable him to carry out this research work.

The author's special gratitudes are due to his wife Xuelan, his sons Yibin and Yixin, who encouraged, supported and assisted in immeasurable ways throughout the course of this research, without which this ambition may not have been fulfilled.

Finally, the author wishes to dedicate this humble contribution to his mother Zhang Sulan, who passed away during this period of the author's course of research. A mother who gave so generously of her kindness and brought the love into his whole life in so many ways.

ABSTRACT

The aim of this research is to develop methods for modal and structural identification of linear vibrating structures in the time domain.

Two methods for the modal identification of a vibrating structure are developed on the basis of the ARMAX model (auto-regressive and moving average model with the control excitation) of a linear damped dynamic structural system.

The first method, called direct method in this thesis, uses the time domain response data in the case of free vibration test, or the time domain excitation and response data in the case of forced vibration test, to identify the coefficient matrices of the ARMAX model. The modal parameters, such as mode shapes, natural frequencies and damping ratios, are then computed from the identified coefficient matrices.

The second method, called indirect method in this thesis, is also developed from the ARMAX model of a vibrating structure. This method identifies the mode shapes separately from the identification of natural frequencies and damping ratios. The natural frequencies and damping ratios are identified using a univariate ARMAX model of the vibrating structure. Once the transfer function of the univariate ARMAX model is estimated from test data, the zeros of the transfer function are used to determine the natural frequencies and damping ratios of the vibrating structure. The impulse response function matrices of the vibrating structure are identified from a multiple variate ARMAX model. These impulse function matrices are used with the identified frequencies and damping ratios to compute the mode shapes.

Some practical methods are also developed for hammer impact vibration tests, single shaker vibration tests and multiple shaker vibration tests based on Z-transformation. In contrast with the conventional frequency domain methods, which usually require the performance of Fourier or Laplace transformation, these methods use the time domain test data directly to identify the modal parameters of the vibrating structure without really performing Z-transformation.

These methods can be applied in the free vibration modal tests or the forced vibration modal tests. They can be used with either the deterministic excitation signal or the random excitation signal. Since the time domain data is directly used, the instrumentation is much simpler compared with the frequency domain methods. The closely spaced frequencies can be identified by the present methods in this thesis. The direct method is a general modal identification method in the time domain and can be reduced to most specific time domain modal identification methods under specific sets of conditions.

As an applications of the modal identification, a method is developed to identify the structural parameters of a vibrating structure with non-proportional damping using the complex modal parameters. The method is the generalization and improvement of the Automated Model Improvement (AMI) method. The method can identify the structural parameters directly using normal or complex modal parameters while most present methods for structural parameter identification use the normal modal parameters. Since the modal parameters obtained from a modal test for the vibrating structure with nonproportional damping is complex, the method is therefore suitable to the use of the modal testing data.

The procedure followed in this thesis mainly is the theoretical development and

verification of the developed methods using computer simulation tests. The laboratory test investigation was also carried out.

In order to further verify the developed methods and investigate their application in the laboratory environment, laboratory tests of a steel cantilevered beam and a steel high rise building model were conducted. Practical procedures are suggested for the application of the developed methods in the laboratory testing. Some important aspects for modal identification testing and analysis of test data, such as, excitation signals, the measurement of excitations and responses, instrumentation of modal testing, the determination of the degrees of freedom contained in the test data, the decision of the sampling rate, the identification of observation noise are discussed and some useful techniques are suggested for dealing with these important aspects.

Chapter 1

INTRODUCTION

"The time has come", the Walrus said "To talk of many things: of shoes - and ships - and sealing wax - of cabbages and Kings - of why the sea is boiling hot - and whether pigs have wings"

- L. Carroll

§ 1.1 BACKGROUND OF THE RESEARCH

Some projects studying different facets of the offshore structures have been continuing over the last five years in the School of Civil Engineering at The University of New South Wales. These projects are

1. System identification for offshore structures;
2. Mechanics of the response of tubular members to collisions;
3. Nonlinear analysis of offshore platforms;
4. Lifting and laying of offshore pipelines
5. Mechanics of spanning in submarine pipelines.

Brief descriptions of these works can be found in a paper by Irvine (1986) in which a portrait of the general aspects concerning the resources available and the coordination of research work in the area of offshore engineering in Australia is also given.

The continuous efforts made in these past years in offshore engineering research by a group of researchers in the School of Civil Engineering at The University of New South Wales have in general achieved most of the prescribed goals. The research findings are expected to be eventually applied in practical, user-oriented systems or codes of practice in the future.

Research into the numerous problems inherent in offshore engineering is important to the oil and gas industry, especially in Australia. It is estimated the about 80% of the total oil and gas reserves in Australia are deposited under the sea bed on the continental shelf or margin. A well-established network for coordinated research work, conducted by both academic institutions and industry, would therefore form a sound basis for providing technical support for future explorations of oil and gas deposits, and for the efficient maintenance of existing structures in Australia.

The continental margins, located on the slopes between the continental shelf breaks and the edges of the continental rises, usually lie between 200m and 3500m in water depth, and may include sediments of shallow water origin subsequently depressed into deeper water as a result of marginal subsidence. To design a structure, for instance a jacket platform, in a water depth of this order to withstand the continuous environmentally hazardous conditions is quite a formidable task. To quote an example, one of the tallest deep-water platforms to date is the Cognac Platform standing 385m tall in the Gulf of Mexico in a water depth of 312m. Designers of these types of platforms have to consider a large number of factors in order to cater for the potentially hazardous situations jeopardizing both the lives of workers on the platform and the structure itself.

Nevertheless, accidents, due to both human errors and acts of nature, do occur in many instances. One of the worst accidents was that of the semi-submersible platform "Alexander L. Kielland" in the North sea. In the early evening of March 27, 1980, one of the five legs of Kielland broke off with "an almighty crack", as one worker recalled. The platform began to quiver and rig tilted steeply. The wind caught the tilting deck, pushing the rig over much faster than expected. The accident resulted in a death toll of 123 out of a total of 212 persons working on the platform. The cause of the accident was believed to be due to a three inch crack in a weld, covered with paint. The crack was reported to be present well before the rig was even launched. The flaw was aggravated by the characteristic growth due to fatigue loading during platform operation until the metal finally broke apart.

This accident clearly demonstrated the high risk of accident characteristics inherent in offshore operations. Amongst the other causes, the change of structural behavior in offshore structures may be significant due to the change of structural parameters,

which is caused by member damage, marine growth or other reasons. It is important that the vibration levels encountered in service or operation be anticipated and brought under control so that some measures could be taken to prevent the disasters. Therefore, it is necessary to determine the change of the structural parameters from time to time in order to provide a thorough and precise knowledge of the dynamic characteristics for the anticipation of dynamic behavior and the vibration control. Determination of the structural parameters, i.e. the system identification, will meet these needs.

The system identification can be carried out using either direct measurements of excitation and response, or more often using modal data from tests. Hence, identification of the modal parameters of a vibrating structure is important.

The primary motivation of the present research is to develop useful methods which can be applied to modal and structural identification problems associated with offshore structures. The methods can be used directly with time domain data without transformation of this data to the frequency domain. Whilst actual offshore structures possess some nonlinear behavior, the present work has been limited to the assumption of linearity. The present work has concentrated on the analytical tools in linear structures with general damping. In this thesis, therefore, the presentation is in a way general enough to meet this purpose. Throughout the thesis, full derivations are usually given and all applications illustrated by simple examples, though not necessarily of offshore structures.

§ 1.2 INTRODUCTION TO SYSTEM IDENTIFICATION

There are two types of problems in structural dynamics: direct problem and inverse problem as shown in Fig. 1.1.

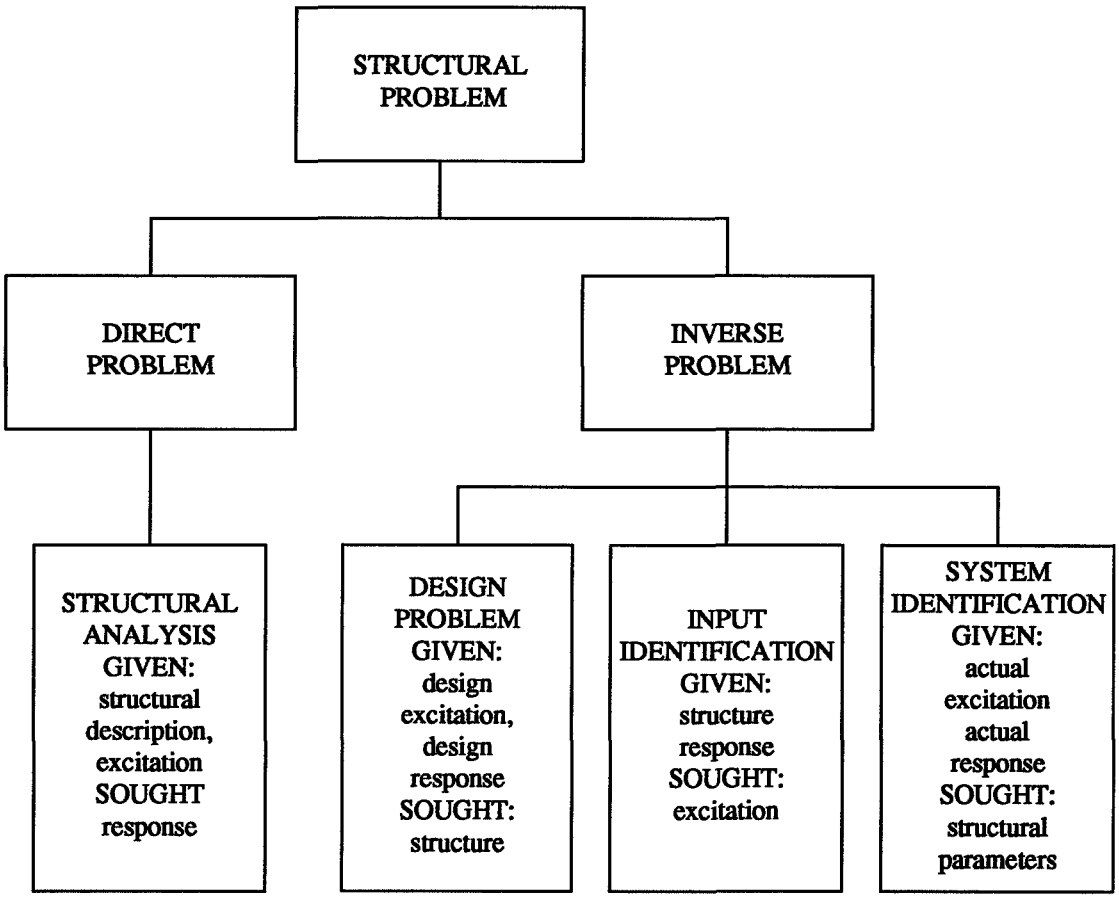

Fig. 1.1 Classification of Problems in Structural Dynamics

The structural analysis is the direct problem. With the dynamic analysis, the dynamic behavior of novel and complicated structures has to be investigated by structural analysis based on a structure envisaged often only by engineering drawings. Starting from a physical model, and neglecting all physical effects which may not appear relevant to the problem under consideration, a mathematical model has to be built up using some mathematical expression. In almost every case it has to

be simplified compared to the physical model. The parameter values of the model have to be determined within limitations. With this mathematical model, and taking into account the loadings, the dynamic structural response can be predicted. Structural analysis results therefore in a parametric computational model. Its accuracy depends on the influence of the introduced simplifications and assumptions. If the structure to be investigated is novel and experiences of comparable structures are not available, the errors of the predicted results are largely unknown. The results may be useful for investigations but some doubts must exist in proving the qualification of the structure. Structural engineers are familiar with this Direct Problem, since it is generally adopted practice to calculate and compare these responses with acceptable response levels to satisfy safety and comfort requirements. This method of analysis is relatively advanced and sophisticated at present. However, the usefulness of such analytical solutions is limited by the degree of realistic representation of the mathematical models to adequately represent the physical structure.

The inverse problem includes the design problem, the excitation identification problem, and the system identification problem. The first two inverse problems will not discussed in this dissertation although they are very important components of design and analysis. The third problem - system identification - involves the determination of the mathematical model and structural parameters, or determination of structural parameters on the basis of assumed mathematical description. The system identification of a vibrating structure requires using the measured data from structural response to known or unknown disturbances in a vibration test.

An example of the identification of vibrating structures may be illustrated by a building as shown in Fig. 1.2.

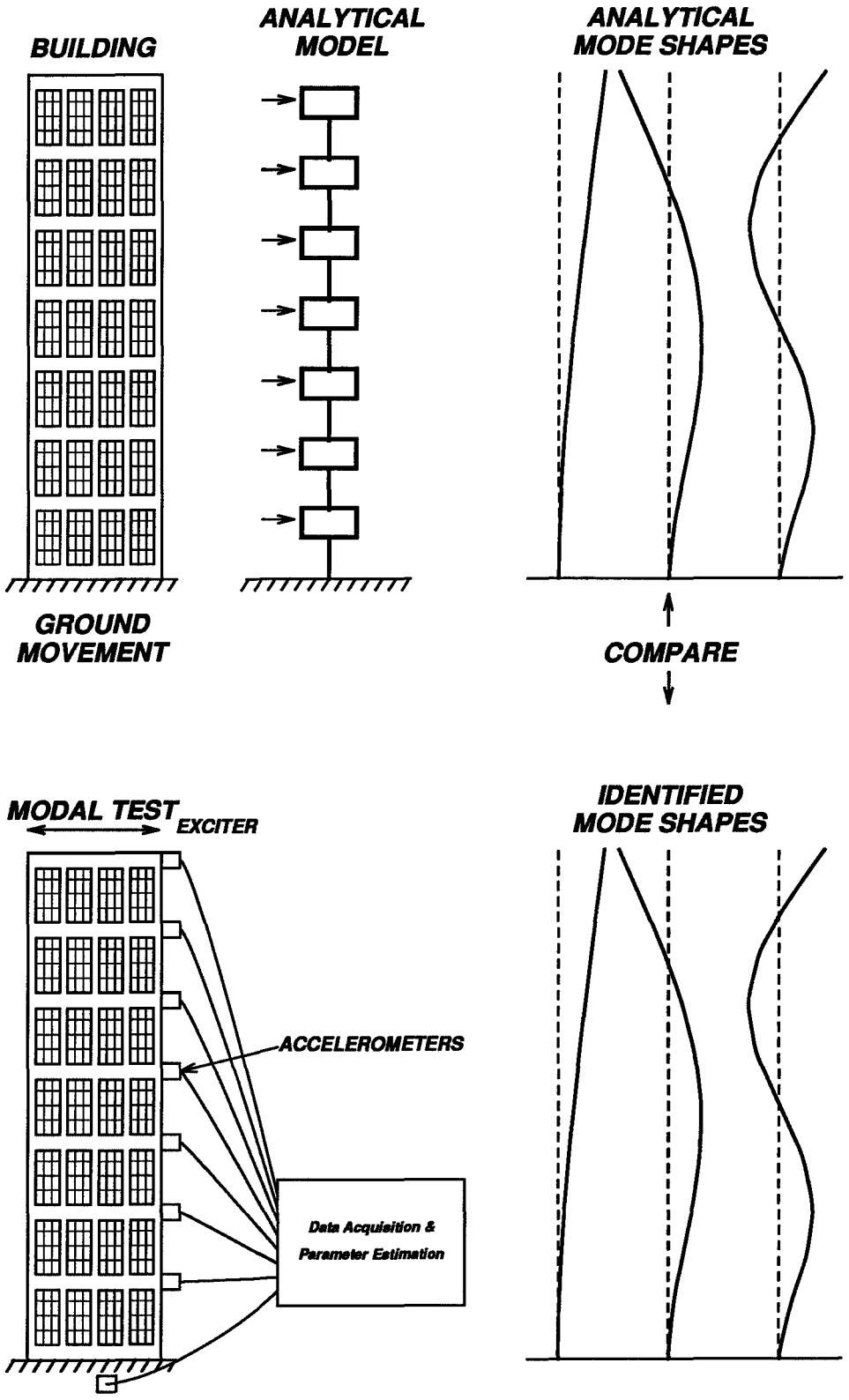

Fig. 1.2 Foundational problem in system identification

The building could undergo imposed vibration. The imposed excitation and the response to the excitation are measured. At the same time a theoretical model could be proposed and its response to the imposed vibration is predicted using the theoretical model. The measured and predicted responses are then compared. If the theoretical model can adequately describe the structure, the predicted response would coincide with the measured response. When these comparisons do not agree with each other within given tolerance, the parameters or equations of the analytical model does not describe the structure adequately and needs to be changed in order to improve the comparison. The equations and parameters thus identified could be taken as a better description of the system.

These inverse problems have always been of interest to structural engineers. However, in the past, because of limitations of instrumentation costs, measuring capabilities and computer capabilities, it has not been possible to satisfactorily solve this kind of inverse problem. In the recent years, with the simultaneous decrease in instrumentation costs and the increase of response-measuring capabilities and the development of computer hardware and software it has become possible to acquire and process the necessary test data to obtain necessary information of a vibrating system and the identification of parameters of a vibrating system becomes feasible.

Methods for identification of a vibrating structure may be classified into two groups. The first group of the methods use the excitation and response data to directly identify the structural parameters. The second group of methods use the modal parameter obtained from the modal test to indirectly identify the structural parameters. The second group of methods are more often used. Therefore, to accurately determine modal parameters is essential for the identification of structural parameters. In addition to that the results obtained from modal identification may be

applied in identification of the mathematical model of a vibrating structure, the identified modal model itself can be applied in many circumstances. For example,

- A theoretical model such as finite element model can be validated by comparison of the identified modal parameters with the theoretical modal values. The validated theoretical model can then be used for predicting the response of the structure to some complex excitation. For example, prediction of the modal spectral response to the ground shaking caused by earthquake requires modal parameters of a structure. If the theoretical model is validated by modal test, it can be further used in the modal spectral and other analysis as necessary. In engineering practice, if major modes of vibration of a structure can be validated by modal tests, the validity of the theoretical model representing the structure can be assured and the model can be further used in other stages of analysis. For this application, accurate estimates of natural frequencies of the major modes are necessary, but accurate mode shape data are not essential although the correlation of the mode shapes from modal test with those from theoretical model is still required. Usually, it is impossible to predict the damping of each mode at the theoretical modeling stage and hence there is nothing with which to compare identified modal damping from the tests. However, this measured damping can be incorporated into the theoretical model to predict specific response levels. For example, in predicting the response of a structure to the earthquake ground shaking using modal spectral method, different response spectra will be used according to the damping of the structure.

- In addition to the use of identified structural model in vibration control, the modal model identified from testing can be incorporated with the modal control of structural vibration. One of requirements for good control performance is to have an accurate modal description of the structure. In particular, the active

modal control utilizes the response of the structure in feedback in order to modify the eigenvalues and eigenvectors of the structure and this requires quick and accurate modal identification.

- In many instances, complete structures are frequently very complex. Methods have thus been developed to permit this kind of structures to be broken down into their components, or substructures, with much of the analysis being carried out on the components. The whole structure will then be assembled in terms of the individual components. One main advantage of the method is that it can combine substructures or components from different resources, both from theoretical or experimental studies. In particular, when some substructures are very difficult to be mathematically modeled, the modal test can provide the necessary information for these components.

- Modifications to a structure may be carried out because of design alterations for operational reasons and in this case it will generally be necessary to ensure the modification would not create any inappropriate changes in dynamic behavior of the structure. In some other cases, it is desirable to change some natural frequencies or to add some damping to avoid a resonance without introducing new unwanted effects. Sometimes the modification procedures involve relatively minor changes to the original one, in order to fine tune a structure's dynamics, and this situation can relax the data requirements somewhat. However, there are a large number of possible modifications which may meet the requirement of the small change. Hence it is necessary to determine which of the modifications would be the most effective for the desired change. A sensitivity analysis based on the identified modal model of the original structure can be used in this aspect.

- The model produced by a modal test can be applied to response prediction and force determination. For the response prediction, a set of measurements is performed under relatively simple excitation conditions and this measured data is analyzed appropriately to derive a model for the structure. The prediction of the structure's response to more complicated excitation, based on the model obtained from the modal test, can then be made. In case of determination of excitation force, the measured responses are used together with a mathematical description of the structure in order to deduce the excitation forces. This process can be very sensitive to the accuracy of the model used for the structure and so it is often necessary for the model itself to be derived from modal test before it can be used in determination of the excitation forces.

The normal procedure for the modal identification consists of three steps: (a) to measure response and/or excitation data, (b) to analyze the measured data and then (c) to derive a modal model of the structure. Accordingly, in the modal identification problem there are three main aspects. First, the fundamental theory of a vibrating structure is essential for the the development of the various identification methods and experimental techniques. Second, the accurate experimental techniques are very important to provide necessary and precise test data for the modal identification. Third, the methods for identification of modal parameters, i.e., methods for processing the test data, play a significant role to obtain the modal parameters.

This research is designed to mainly deal with the third aspect. Some methods for modal identification, which can be used with time domain data, are developed. The relationships between excitations, initial conditions and responses in the time domain will be derived. On the basis of these relationships, some methods for the modal identification are developed. The proposed methods consist of two groups: the first

group of methods will be developed using the ARMAX model of a vibrating structure which describes the relationship between excitations and responses in the time domain. The second group of methods will be developed using a *Z*-transformation which is the transformation of a discrete time signal as a power series in z^{-1} coefficients of which are the amplitudes of the discrete-time signals. The application of proposed methods in laboratory experiments for modal identification will also be investigated. Further, a method for identification of structural parameters of vibrating structures using modal data is developed, which can also be considered as an application of modal identification.

§ 1.3 OBJECTIVES AND SCOPE

The main objectives of this thesis are detailed in the following. They are listed approximately in order in which they are dealt with in this thesis.

1. to study various models representing the dynamics of a vibrating structure in the frequency domain and the time domain.

2. to investigate relationships between the various models and to establish the bases for the development of the proposed methods for modal identification.

3. to develop the ARMAX model of a vibrating structure and to investigate the relationship between the coefficient matrices of the ARMAX model and modal parameters of the vibrating structure.

4. to develop methods for modal identification on the basis of the ARMAX model of a vibrating structure.

5. to study techniques for detection of the excessive modes caused by observation noise.

6. to investigate methods for the determination of the degrees of freedom of a vibrating structure in a test.

7. to develop methods for the modal identification using *Z*-transformation.

8. to present a technique for extraction of mode shapes from *Z*-transfer function of a vibrating structure.

9. to explore the application of the proposed methods to laboratory testing and to discuss the practice of modal experiments.

10. to investigate methods for identification of structural parameters using modal test data.

Although not all the structures or systems encountered in practice will be linear, this thesis is based on the assumption of linearity of structures and this has two main implications:

1. that doubling the magnitude of the excitation force would simply result in a doubling of the response,

2. that if two or more excitation patterns are applied simultaneously then the response thus produced will be equal to the sum of the responses caused by each excitation individually.

§ 1.4 LAYOUT OF THESIS

Since the review of the research topics involves the fundamental theory of vibrating

structures, Chapter 2 will discuss the general theory of vibrating structures and this will provide an overall view on the various models of a vibrating structure and the relationships between these models. The structural model in configuration space and in the state space will be introduced. The modal model of vibrating structures in several cases will be derived. The relationship of structural model and modal model in the state space will be discussed and this will play an important role in the identification of structural parameters using modal test data. In this chapter, the relationship of the modal model and response model of the vibrating structures will also be derived. The relationship will provide the basis for the development of methods for the modal identification using the excitation and response data in the time domain.

Chapter 3 will review modal identification methods and more attentions will be paid to the time domain methods. A variety of methods for modal identification will be discussed, and the basic principles and implementations will be described. The advantages and disadvantages of these methods will also be discussed.

Chapter 4 will be devoted to the development of two methods for modal identification using an ARMAX model. The ARMAX model describes the relationship between excitations and responses of vibrating structures in terms of the discrete time series. The proposed methods will identify the coefficient matrices of the ARMAX model, and the modal parameters of vibrating structures will be determined through the relationship between the coefficient matrices and the modal parameters.

In chapter 5, the discrete response and excitation signals in the time domain will be studied from another point of view. Use will be made of Z-transformation in discrete

time domain to replace the Laplace-transformation in continuous time domain. Methods for modal identification will be developed on the basis of *Z*-transformation.

One necessary and important ingredient of modal identification is the modal testing. In real modal testing, the basic measurement system, excitation methods used in a test and various aspects related to the modal testing are necessary for the success of modal identification. In chapter 6, the application and experimental procedures will be discussed with relation to structures tested in the laboratory.

An important application of modal identification is to verify and correct or adjust the analytical model. The procedure of the correction and adjustment of the analytical model is called structural identification. Chapter 7 will tackle the structural identification problem. A method using modal test data will be developed for the identification of structural system with non-proportional damping.

General conclusions and recommendations for future developments are given in Chapter 8.

Complete computer program listings will not be given in the thesis. An extensive list of bibliography is included at the end of this thesis.

§ 1.5 LIST OF PUBLICATIONS

Some of the work described in this thesis has already been published or presented at conferences. These papers are:

[1] PI, Y.L. and MICKLEBOROUGH, N.C. "Modal Identification of a Vibrating Structure In the Time Domain", *Computers & Structures*, Vol. 32, No. 5

August, 1989.

[2] PI, Y.L. and MICKLEBOROUGH, N.C., "Modal Identification of Vibrating Structures Using ARMA Model", *Journal of Engineering Mechanics, American Society of Civil Engineers*, Vol. 115, No. 10, October, 1989.

[3] MICKLEBOROUGH, N.C. and PI, Y.L., "Modal Parameter Identification Using Z-Transforms", *International Journal for Numerical Methods in Engineering* Vol. 28, No. 10, 1989.

[4] MICKLEBOROUGH, N.C. and PI, Y.L., " System Modal Identification Using Free Vibration Data", *Structural Engineering/Earthquake Engineering*, Vol. 6, No. 2, 1989.

[5] PI, Y.L. and MICKLEBOROUGH, N.C., " Identification of Parameters for Offshore Structures Using Modal Test Data", *Proc. Eighth Australasian Conference on Coastal and Ocean Engineering*, Institute of Engineers(Australia), Launceston, 1987.

[6] PI, Y.L. and MICKLEBOROUGH, N.C., "Modal Identification from Auto-regressive Model Using Free Vibration Data", *Proc. Eleventh Australasian Conference on the Mechanics of Structures and Materials*, Auckland, New Zealand, 1988.

[7] PI, Y.L. and MICKLEBOROUGH, N.C., "Determination of Modal Parameters using ARMA Model of Vibrating Structures", *UNICIV Report, No. R-250*, The University of New South Wales, 1988.

[8] PI, Y.L. and MICKLEBOROUGH, N. C., "Time Domain Modal Identification of a Linear Vibrating Structure", *UNICIV Report, No. R-249,*

The University of New South Wales, 1988.

[9] PI, Y.L. and MICKLEBOROUGH, N.C., "Identification of Parameters of Vibrating Structure with Non-proportional Damping", *Proc. First Structural Engineering Conference*, Institute of Engineers(Australia), Melbourne, 1987.

[10] MICKLEBOROUGH, N.C. and PI, Y.L., "Estimate of Modal Parameters for a Dynamic System Using Z-Transform", *UNICIV Report, No. R-253*, The University of New South Wales, July 1988.

Chapter 2

LINEAR DAMPED VIBRATING STRUCTURES

The purpose of the present course is the deepening and development of difficulties underlying contemporary theory.

- A. A. Blasov

§ 2.1 GENERAL CONSIDERATION

Theoretical fundamentals of a vibrating structure are very important in the structure system identification. Before tackling the system identification problem, it is appropriate in this chapter to briefly study the theoretical fundamentals which will provide an overall view on the various models of a vibrating structure and the relationships between these models. Foss (1958) derived the basic modal model for

vibrating structures using a first-order state variable representation of the structural parameter model for classical normal modes analysis. His derivation is well known and extensively used, for example, by Meirovitch (1967) and Ewins (1984). Development using state variable formulations different from Foss's were given by Beliveau (1977, 1979) and Brandon (1984). Richardson (1974) used Laplace Transformations of the structural model and analyzed the resulting second-order algebraic matrix equation to derive the modal model. Vigneron (1986) developed the natural modes and modal model for an elastic structure with linear viscous damping, via a formulation that is comparable to that of the classical normal modes formulation of the undamped case. In this chapter, attempts will be made to present the fundamentals of vibrating structures in a manner which are suitable for study of modal identification in this thesis.

Generally, the vibration of a vibrating structure is described in terms of *structural parameters*, i.e., its *mass, stiffness and damping* properties. This description is mathematically in the form of partial differential equations for continuous vibrating structures, or in the form of ordinary differential equations for discrete or discretized vibrating structure systems. This description is called the *structural model* of the vibrating structure.

Once the structural model is established, a modal analysis is usually performed to yield another description of the vibrating structure's behavior in terms of *modal parameters* of the structure, i.e., a set of *natural frequencies* with corresponding vibration *mode shapes* and *modal damping factors*. This description is referred to as a *modal model* of the vibrating structure. This model describes the various behavior of the structure under natural vibration, i.e., without external forcing or excitation, and hence the modal analysis is also known as free vibration analysis.

One of the main aims of the structural analysis is to predict the responses of the structure to the possible external excitations. The response analysis will be able to predict exact theoretical responses of how the structure will vibrate under given excitation conditions and especially, the amplitudes of vibration. Without doubt, this will be determined not only by the structure's inherent properties but also by the nature and magnitude of the imposed excitation. The response description is called the *response model* of the vibrating structure, which usually consists of two parts: the response caused by the initial conditions, i.e., general solution, and the response caused by the external excitation, i.e., particular solution. The *response model* may be classified into two groups: frequency domain response in terms of response spectra and time domain response in terms of *displacements, velocities or accelerations*. Using the latter group of data to identify the modal and structural parameters of a vibrating structure is the main concern of this thesis.

The analysis procedure described above can be summarized in Fig. 2.2-1.

Fig. 2.2-1 Analysis procedure

As mentioned in the introduction, the analysis is classified as the direct problem in structural dynamics, while the structural system identification procedure is one of inverse problems in structiral dymanics. The system identification procedure can be illustrated in Fig. 2.2-2. As shown, the identification route is in the reverse direction of the analysis route.

Fig. 2.2-2 Identification procedure

Since damping is very important for the damped linear vibrating structure, some aspects of the damping are to be discussed next. There are many mathematical models representing damping. The most important type of damping in vibration study is *linear viscous damping*. According to this model the damping takes the form of a force proportional in magnitude to the velocity and acting in the direction opposite to the direction of the velocity. *Coulomb damping* also gives rise to a force opposing the motion, but, in contrast with viscous damping, it has a constant magnitude. This damping is also referred to as *dry friction*. Another widely used model is *structural damping*. It is associated with internal energy dissipation due to the hysteresis effect in cyclic stress, for which reason it is also called *hysteresis damping*. Without loss of generality, the chapter will describe the theoretical fundamentals with consideration of linear viscous damping.

It is well known that the coupled equations of motion describing an undamped multi-degree-of-freedom structure can be uncoupled by means of modal analysis, which uses a linear transformation to express the equations of motion in terms of different set of coordinates, the principal coordinates. The linear transformation is represented in matrix form by the *normal modal matrix*, obtained from the eigenvalue problem associated with the undamped structure. In some special cases the normal modal matrix can also be used successfully to uncouple the equations of motion of a linear viscously damped structure. Unfortunately, this is not always possible. The general case of viscous damping can however be treated by transforming a set of n ordinary differential equations of second order into a set of $2n$

ordinary differential equations of first order, i.e., state variable representations. The eigenvalues and eigenvectors associated with the latter set of equations are, for the case with which this thesis is primarily concerned, complex quantities.

§ 2-2 is devoted to the formulation of the equations of motion of the vibrating structure in the configuration space and in the state space by invoking the Lagrangian equation. The modal model of the structure for several cases will then be discussed in § 2-3. The relationship between the modal parameters and structural parameters will be briefly investigated. § 2-4 will deal with the response model in the various cases. Finally, § 2-5 summurizes the various models discussd in this chapter.

§ 2.2 STRUCTURAL MODEL

This section will discuss the *structural model* of a linear viscously damped vibrating structure. The motion of a vibrating structure can be described by a set of variables. The minimum number of independent variables required to fully describe the motion of a discrete or discretized structure is referred to as the number of degrees of freedom of the structure. These variables are called coordinates. Usually, these coordinates represent physical quantities, but at times they represent more abstract quantities, such as coefficients of a series. Hence they are known as generalized coordinates.

The motion of an n-degree-of-freedom structure can be fully described by n generalized coordinates $y_i(t)$ $(i = 1, 2, \cdots, n)$. The system kinetic energy has the form

$$T = \frac{1}{2}\sum_{i=1}^{n}\sum_{j=1}^{n} m_{ij}\dot{y}_i\dot{y}_j \tag{2.2-1}$$

where the coefficients m_{ij} are symmetric inertia or mass coefficients and $\dot{y}_i$ are generalized velocities. The kinetic energy, in Eqn. (2.2-1), is a positive definite quadratic expression. Similarly, the potential energy can be written in the form

$$T = \frac{1}{2}\sum_{i=1}^{n}\sum_{j=1}^{n} k_{ij} y_i y_j \tag{2.2-2}$$

where the coefficients k_{ij} are symmetric stiffness coefficients. The potential energy is a positive definite expression when the system is positive definite.

The system Lagrangian will then be

$$L = T - V \tag{2.2-3}$$

Another important class of forces is that consisting of viscous damping forces. The damping forces depend on the generalized velocities $\dot{y}_i$ and are assumed to be obtained from the quadratic function

$$Q = \frac{1}{2}\sum_{i=1}^{n}\sum_{j=1}^{n} c_{ij} \dot{y}_i \dot{y}_j \tag{2.2-4}$$

which is called the dissipation function initially named by Lord Rayleigh. The coefficients c_{ij}, called damping coefficients, are generally constant and they are symmetric, $c_{ij} = c_{ji}$. The remaining forces, not falling into any of the above categories are denoted by f_i and assumed to be derivable from the virtual work expression

$$\overline{\delta w} = \sum_{i=1}^{n} f_i \delta y_i \tag{2.2-5}$$

where δy_i are the generalized virtual displacements. The generalized forces f_i generally depend on time but not on displacements or velocities.

With all these definitions in mind, the equations of motion of the vibrating structure take the form of Lagrange's equations

$$\frac{d}{dt}\left[\frac{\partial L}{\partial \dot{y}_i}\right] - \frac{\partial L}{\partial y_i} + \frac{\partial Q}{\partial \dot{y}_i} = f_i \tag{2.2-6}$$

The solution of Eqn. (2.2-6) consists of functions of the n generalized coordinates $y_i(t)$ $(i = 1, 2, \cdots, n)$.

These n generalized coordinates do not describe the state of a vibrating structure uniquely, and to define the state uniquely it is necessary to specify also the generalized velocities $\dot{y}_i(t)$. If the generalized velocities are used as a set of auxiliary variables, then the motion can be described in a $2n$-dimensional Euclidean space defined by y_i and $\dot{y}_i$ and known as the *state space.*

In order to obtain the solution of Eqn. (2.2-6) in the configuration space, Eqns. (2.2-1) through (2.2-4) are substituted into Eqn. (2.2-6) leading to a set of n coupled ordinary differential equations describing the motion of a linear viscously damped structure. These equations can be written in the matrix form

$$\mathbf{M}_0\ddot{\mathbf{y}}(t) + \mathbf{C}_0\dot{\mathbf{y}}(t) + \mathbf{K}_0\mathbf{y}(t) = \mathbf{f}(t) \tag{2.2-7}$$

where $\ddot{\mathbf{y}}(t)$, $\dot{\mathbf{y}}(t)$ and $\mathbf{y}(t)$ are the acceleration, velocity and displacement of the vibrating structure; $\mathbf{f}(t)$ is the external loading or excitation. Mass matrix $\mathbf{M}_0$, damping matrix $\mathbf{C}_0$ and stiffness matrix $\mathbf{K}_0$ are of order $n \times n$ and symmetric positive for a positive system.

The solution of Eqn. (2.2-6) in the state space can be obtained by introducing the state vector

$$\mathbf{x}^T(t) = \{\mathbf{y}^T(t)\ \dot{\mathbf{y}}^T(t)\} \tag{2.2-8}$$

as

$$\mathbf{M}^*\dot{\mathbf{x}}(t) + \mathbf{K}^*\mathbf{x}(t) = \mathbf{D}\mathbf{f}(t) \tag{2.2-9}$$

where $\mathbf{M}^*$ and $\mathbf{K}^*$ are $2n \times 2n$ symmetric matrices with

$$\mathbf{M}^* = \begin{bmatrix} -\mathbf{K}_0 & \mathbf{0} \\ \mathbf{0} & \mathbf{M}_0 \end{bmatrix} \tag{2.2-10}$$

and

$$\mathbf{K}^* = \begin{bmatrix} \mathbf{0} & \mathbf{K}_0 \\ \mathbf{K}_0 & \mathbf{C}_0 \end{bmatrix} \tag{2.2-11}$$

and $\mathbf{D}$ is a $2n \times n$ matrix with

$$\mathbf{D} = \begin{bmatrix} \mathbf{0} \\ \mathbf{I} \end{bmatrix} \tag{2.2-12}$$

Eqns. (2.2-9) can also be expressed in another form

$$\dot{\mathbf{x}}(t) = \mathbf{A}\mathbf{x}(t) + \mathbf{B}\mathbf{f}(t) \tag{2.2-13}$$

where

$$\mathbf{A} = -\mathbf{M}^{*-1}\mathbf{K}^* = \begin{bmatrix} \mathbf{0} & \mathbf{I} \\ -\mathbf{M}_0^{-1}\mathbf{K}_0 & -\mathbf{M}_0^{-1}\mathbf{C}_0 \end{bmatrix} \tag{2.2-14}$$

and

$$\mathbf{B} = \mathbf{M}^{*-1}\mathbf{D} = \begin{bmatrix} \mathbf{0} \\ \mathbf{M}_0^{-1} \end{bmatrix} \tag{2.2-15}$$

Eqn. (2.2-7) represents the structural model of a linear vibrating structure system in the configuration space, while Eqn. (2.2-9) or (2.2-13) represents the structural model in the state space.

§ 2.3 MODAL MODEL

Using linear system theory, a general closed-form solution of Eqn. (2.2-7) can be shown to exist. However, an attempt to produce the actual numerical solution is likely to meet with serious computational difficulties, particularly for a high-order system. A convenient method of deriving the solution is by modal analysis, which requires the solution of the eigenvalue problem for the system. The solution will form the modal model of the vibrating structure. In the following, the modal model for various cases will be derived and their properties will be discussed.

§ 2.3.1 Undamped Vibrating Structures

For undamped vibrating structures, Eqn. (2.2-7) reduces to

$$\mathbf{M}_0\ddot{\mathbf{y}}(t) + \mathbf{K}_0\mathbf{y}(t) = \mathbf{0} \tag{2.3-1}$$

where $\mathbf{M}_0$ and $\mathbf{K}_0$ are real symmetric matrices of rank n. Further, $\mathbf{M}_0$ is positive definite. The solution of Eqn. (2.3-1) has the exponential form

$$\mathbf{y}(t) = e^{-\omega t}\boldsymbol{\phi} \tag{2.3-2}$$

where ω is a constant scalar and $\boldsymbol{\phi}$ is a constant n-vector. Substituting Eqn. (2.3-2) into Eqn. (2.3-1) and dividing through by $e^{-\omega t}$ yield

$$\mathbf{K}_0\boldsymbol{\phi} = \lambda\mathbf{M}_0\boldsymbol{\phi} \tag{2.3-3}$$

with $\lambda = -\omega^2$. The problem of determining the constants λ for which Eqn. (2.3-3) possesses nontrivial solutions $\boldsymbol{\phi}$ is known as the *eigenvalue problem.* It is known from linear algebraic theory that the necessary and sufficient condition for a set of homogeneous algebraic equations to possess a nontrivial solution is that the determinant of the coefficients be zero. Hence,

$$\det(\mathbf{K}_0 - \lambda\mathbf{M}_0) = 0 \tag{2.3-4}$$

this equation is known as the *characteristic equation*, or the *frequency equation* of Eqn. (2.3-3). Because $\mathbf{K}_0$ and $\mathbf{M}_0$ are square matrices of rank n, the characteristic determinant represents a polynomial of degree n in λ. In general, the solution has n

distinct roots λ_i $(i = 1, 2, \cdots, n)$ called *characteristic values or eigenvalues*. To each of these eigenvalues there corresponds a vector $\boldsymbol{\phi}_i$ satisfying the equation

$$\mathbf{K}_0\boldsymbol{\phi}_i = \lambda_i\mathbf{M}_0\boldsymbol{\phi}_i \quad (i = 1, 2, \cdots, n) \tag{2.3-5}$$

where $\boldsymbol{\phi}_i$ is known as the characteristic vector or eigenvector corresponding to λ_i.

Since $\mathbf{K}_0$ and $\mathbf{M}_0$ are symmetric and positive definite, it can be shown that the roots of the characteristic equation are real and positive. The roots are denoted $\lambda_i = -\omega_1^2, -\omega_2^2, \cdots, -\omega_n^2$. The positive square roots of these values are the *natural frequencies* ω_i of the structure. The frequencies are arranged in order of increasing magnitude such as $\omega_1 \leq \omega_2 \leq \omega_2 \leq \cdots \leq \omega_n$. In general all ω_i are distinct, although it is quite possible that two natural frequencies possess the same value. The eigenvectors $\boldsymbol{\phi}_i$ represent the mode shapes of the undamped vibrating structure. Mode shapes $\boldsymbol{\phi}_i$ and natural frequencies ω_i form the modal model of a undamped vibrating structure.

The eigenvalue problem in Eqn. (2.3-3) is in terms of two real symmetric matrices. The eigenvalue problem can also be transformed into *standard form* of an eigenvalue problem in terms of a single real symmetric matrix. In fact, because $\mathbf{M}_0$ is a positive definite real symmetric matrix, it can be decomposed into

$$\mathbf{M}_0 = \mathbf{Q}^T\mathbf{Q} \tag{2.3-6}$$

where $\mathbf{Q}$ is a real nonsingular matrix. Introducing Eqn. (2.3-6) into Eqn. (2.3-3)

$$\mathbf{K}_0\boldsymbol{\phi} = \lambda\mathbf{Q}^T\mathbf{Q}\boldsymbol{\phi} \tag{2.3-7}$$

Considering the linear transformation

$$\boldsymbol{\phi} = \mathbf{Q}^{-1}\boldsymbol{\kappa} \tag{2.3-8}$$

where $\mathbf{Q}^{-1}$ exists because $\mathbf{Q}$ is nonsingular. Substituting Eqn. (2.3-8) into Eqn. (2.3-7) yields the eigenvalue problem in standard form

$$\mathbf{A}_0\boldsymbol{\kappa} = \lambda\boldsymbol{\kappa} \tag{2.3-9}$$

with

$$\mathbf{A}_0 = (\mathbf{Q}^T)^{-1}\mathbf{K}_0\mathbf{Q}^{-1} \tag{2.3-10}$$

being a real symmetric matrix, which is positive definite if $\mathbf{K}_0$ is positive definite. Hence, the eigenvalue problems in Eqns. (2.3-3) and (2.3-9) can be regarded as being equivalent. Whereas both eigenvalue problems yield the same eigenvalues λ_i, the eigenvectors are not the same but related by Eqn. (2.3-8).

The eigenvectors of the eigenvalue problem in Eqn. (2.3-9) have the following important property: The two eigenvectors corresponding to distinct eigenvalues are orthogonal. This statement can be shown by considering two eigenvectors $\boldsymbol{\kappa}_i$ and $\boldsymbol{\kappa}_j$ corresponding to the distinct eigenvalues λ_i and λ_j, so that

$$\mathbf{A}_0\boldsymbol{\kappa}_i = \lambda_i\boldsymbol{\kappa}_i \tag{2.3-11}$$

$$\mathbf{A}_0\boldsymbol{\kappa}_j = \lambda_j\boldsymbol{\kappa}_j. \tag{2.3-12}$$

Premultiply Eqn. (2.3-11) by $\boldsymbol{\kappa}_j^T$, postmultiply the transpose of Eqn. (2.3-12) by $\boldsymbol{\kappa}_i$, subtract one result from the other, recall $\mathbf{A}_0^T = \mathbf{A}_0$ and write

$$0 = (\lambda_i - \lambda_j)\boldsymbol{\kappa}_j^T \boldsymbol{\kappa}_i. \tag{2.3-13}$$

But the eigenvalues are distinct, $\lambda_i \neq \lambda_j$, so that Eqn (2.3-13) is satisfied if and only if

$$\boldsymbol{\kappa}_j^T \boldsymbol{\kappa}_i = 0, \quad \lambda_i \neq \lambda_j. \tag{2.3-14}$$

Considering Eqn. (2.3-8), the following orthogonal property of the eigenvectors $\boldsymbol{\phi}_i$ about $\mathbf{M}_0$ for the eigenvalue problem in Eqn. (2.3-3), is obtained

$$\boldsymbol{\phi}_j^T \mathbf{M}_0 \boldsymbol{\phi}_i = 0. \tag{2.3-15}$$

The matrix $\mathbf{M}_0$ plays the role of a weighting matrix. Premultiply both sides of Eqn. (2.3-3) by $\boldsymbol{\phi}_j^T$, postmultiply its both sides by $\boldsymbol{\phi}_i$

$$\boldsymbol{\phi}_j^T \mathbf{K}_0 \boldsymbol{\phi}_i = \lambda_i \boldsymbol{\phi}_j^T \mathbf{M}_0 \boldsymbol{\phi}_i. \tag{2.3-16}$$

Hence, for instance, the orthogonality condition can also be written

$$\boldsymbol{\phi}_j^T \mathbf{K}_0 \boldsymbol{\phi}_i = 0. \tag{2.3-17}$$

When $i = j$ the products in Eqns. (2.3-15) and (2.3-16) are not zero, but yield mass and stiffness coefficients

$$m_{ii} = \boldsymbol{\phi}_i^T \mathbf{M}_0 \boldsymbol{\phi}_i \tag{2.3-18}$$

$$k_{ii} = \boldsymbol{\phi}_i^T \mathbf{K}_0 \boldsymbol{\phi}_i. \tag{2.3-19}$$

As mentioned above, the eigenvectors are not uniquely determined but can be normalized uniquely. Hence, the eigenvectors can be normalized such as

$$\boldsymbol{\phi}_i^T \mathbf{M}_0 \boldsymbol{\phi}_i = 1 \tag{2.3-20}$$

$$\boldsymbol{\phi}_i^T \mathbf{K}_0 \boldsymbol{\phi}_i = \lambda_i. \tag{2.3-21}$$

The following orthogonality properties will then hold

$$\boldsymbol{\Phi}^T \mathbf{M}_0 \boldsymbol{\Phi} = \mathbf{I} \tag{2.3-22}$$

$$\boldsymbol{\Phi}^T \mathbf{K}_0 \boldsymbol{\Phi} = \boldsymbol{\Lambda} \tag{2.3-23}$$

where $\boldsymbol{\Lambda}$ is a diagonal matrix with λ_i being its diagonal elements, and $\boldsymbol{\Phi}$ is the eigenvector matrix with the $\boldsymbol{\phi}_i$ being its i-th column. The orthogonality relationships (2.3-22) and (2.3-23) will play an important role in the structure system identification.

§ 2.3.2 Damped Vibrating Structures

A viscously damped structure can be described by recalling the Eqn. (2.2-7)

$$\mathbf{M}_0 \ddot{\mathbf{y}}(t) + \mathbf{C}_0 \dot{\mathbf{y}}(t) + \mathbf{K}_0 \mathbf{y}(t) = \mathbf{f}(t). \tag{2.3-24}$$

Consider the free vibration case, $\mathbf{f}(t) = \mathbf{0}$, by assuming a solution of the homogeneous

set of equations in the form

$$\mathbf{y}(t)=\boldsymbol{\phi} e^{\lambda t} \tag{2.3-25}$$

so that a set of n homogeneous algebraic equations representing the eigenvalue problem is obtained

$$[\,\lambda^2\mathbf{M}_0 + \lambda\mathbf{C}_0 + \mathbf{K}_0\,]\boldsymbol{\phi} = [\mathbf{p}(\lambda)]\boldsymbol{\phi} = \mathbf{0} \tag{2.3-26}$$

where $[\mathbf{p}(\lambda)]$ is a square matrix as a function of λ. Eqn. (2.3-26) has a nontrivial solution only if the determinant of the coefficients is zero,

$$|\,[\,\mathbf{p}(\lambda)\,]\,| = 0. \tag{2.3-27}$$

This is the characteristic equation or determinant equation of order $2n$ in λ of matrix $[\,\mathbf{p}(\lambda)\,]$. The roots of the characteristic equation can be real, purely imaginary, or complex. If the roots are real they must be negative, which corresponds to an overdamped structure for which an aperiodic decaying motion is obtained. If the roots are complex they must appear in pairs of complex conjugates with a negative real part such as

$$\lambda = -\eta\omega \pm i\omega\sqrt{1-\eta^2} \tag{2.3-28}$$

and the corresponding modal columns $\boldsymbol{\phi}$ must also be complex conjugates. A pair of complex conjugate modes multiplied by the corresponding time-dependent exponential functions can be combined to obtain a damped oscillatory motion. This is the case in which the structure is underdamped. For an undamped structure, purely

imaginary roots will be obtained in pairs of complex conjugates. But the eigenvector $\boldsymbol{\phi}$ in Eqn. (2.3-25) are not orthogonal about any one of matrices $\mathbf{M}_0$, $\mathbf{C}_0$ and $\mathbf{K}_0$. However, the orthogonality property for the state representation of a damped structure can be derived similarly to the undamped case. Recall the state representation Eqn. (2.2-9)

$$\mathbf{M}^*\dot{\mathbf{x}}(t) + \mathbf{K}^*\mathbf{x}(t) = \mathbf{D}\mathbf{f}(t). \tag{2.3-29}$$

Consider the corresponding homogeneous equation to Eqn. (2.3-29)

$$\mathbf{M}^*\dot{\mathbf{x}}(t) + \mathbf{K}^*\mathbf{x}(t) = \mathbf{0}. \tag{2.3-30a}$$

Assume the solution of the form $\mathbf{x}(t) = e^{\lambda t}\boldsymbol{\psi}$, the eigenvalue problem is then obtained as

$$\lambda\mathbf{M}^*\boldsymbol{\psi} + \mathbf{K}^*\boldsymbol{\psi} = \mathbf{0} \tag{2.3-30}$$

where $\mathbf{M}^*$ and $\mathbf{K}^*$ are symmetric matrices as shown in Eqns. (2.2-10) and (2.2-11), and so $\mathbf{M}^{*T} = \mathbf{M}^*$ and $\mathbf{K}^{*T} = \mathbf{K}^*$.

Because matrices $\mathbf{M}^*$ and $\mathbf{K}^*$ are not positive definite, the problem cannot be reduced to one in terms of a single real symmetric matrix. However, since the original eigenvalue problem is in terms of symmetric matrices $\mathbf{M}^*$ and $\mathbf{K}^*$, it possesses certain properties which are not shared by an eigenvalue problem in terms of general non-symmetric matrices. In particular, the eigenvectors $\boldsymbol{\psi}_i$ corresponding to the eigenvalues λ_i are orthogonal with respect to both matrices $\mathbf{M}^*$ and $\mathbf{K}^*$. To prove this two solutions with distinct eigenvalues are written in the form

$$\lambda_i \mathbf{M}^* \boldsymbol{\psi}_i + \mathbf{K}^* \boldsymbol{\psi}_i = \mathbf{0} \tag{2.3-31}$$

$$\lambda_j \mathbf{M}^* \boldsymbol{\psi}_j + \mathbf{K}^* \boldsymbol{\psi}_j = \mathbf{0}. \tag{2.3-32}$$

Premultiplying Eqn. (2.3-31) by $\boldsymbol{\psi}_j^T$ and Eqn. (2.3-32) by $\boldsymbol{\psi}_i^T$ yields

$$\lambda_i \boldsymbol{\psi}_j^T \mathbf{M}^* \boldsymbol{\psi}_i + \boldsymbol{\psi}_j^T \mathbf{K}^* \boldsymbol{\psi}_i = \mathbf{0} \tag{2.3-33}$$

and

$$\lambda_j \boldsymbol{\psi}_i^T \mathbf{M}^* \boldsymbol{\psi}_j + \boldsymbol{\psi}_i^T \mathbf{K}^* \boldsymbol{\psi}_j = \mathbf{0}. \tag{2.3-34}$$

Subtracting the transpose of Eqn. (2.3-34) from Eqn. (2.3-33) the following is obtained

$$(\lambda_i - \lambda_j) \boldsymbol{\psi}_j^T \mathbf{M}^* \boldsymbol{\psi}_i = 0. \tag{2.3-35}$$

Since eigenvalues are distinct, $\lambda_i \neq \lambda_j$, from Eqn. (2.3-35) the orthogonal relationships are obtained

$$\boldsymbol{\psi}_j^T \mathbf{M}^* \boldsymbol{\psi}_i = 0, \qquad \lambda_i \neq \lambda_j, \qquad i, j = 1, 2, \cdots, 2n \tag{2.3-36}$$

and it follows from Eqn. (2.3-33) that

$$\boldsymbol{\psi}_j^T \mathbf{K}^* \boldsymbol{\psi}_i = 0, \qquad \lambda_i \neq \lambda_j, \qquad i, j, = 1, 2, \cdots, 2n. \tag{2.3-37}$$

The eigenvectors $\boldsymbol{\psi}_i$ can be normalized by setting

$$\boldsymbol{\psi}_i^T \mathbf{M}^* \boldsymbol{\psi}_i = 1, \qquad i = 1, 2, \cdots, 2n \tag{2.3-38}$$

so that, if $\boldsymbol{\Psi} = [\boldsymbol{\psi}_1 \ \boldsymbol{\psi}_2 \ \cdots \ \boldsymbol{\psi}_{2n}]$ represents the square matrix of the normalized eigenvectors, then Eqns. (2.3-36) and (2.3-37) can be combined into

$$\boldsymbol{\Psi}^T \mathbf{M}^* \boldsymbol{\Psi} = \mathbf{I} \tag{2.3-39}$$

from which it follows automatically that

$$\boldsymbol{\Psi}^T \mathbf{K}^* \boldsymbol{\Psi} = \boldsymbol{\Lambda} \tag{2.3-40}$$

where the $\boldsymbol{\Lambda}$ is the diagonal matrix of the eigenvalues. Because the eigenvalues are distinct, the eigenvectors $\boldsymbol{\psi}_i$ are independent. Eqns. (2.3-39) and (2.3-40) will play a very important role in the system identification of a vibrating structure with general damping. Further, Eqn. (2.3-30) can be reduced to the form

$$\mathbf{A}\boldsymbol{\psi} = \lambda \boldsymbol{\psi} \tag{2.3-41}$$

where, assuming $\mathbf{M}^*$ is nonsingular,

$$\mathbf{A} = -\mathbf{M}^{*-1}\mathbf{K}^* = \begin{bmatrix} \mathbf{0} & \mathbf{I} \\ -\mathbf{M}_0^{-1}\mathbf{K}_0 & -\mathbf{M}_0^{-1}\mathbf{C}_0 \end{bmatrix}. \tag{2.3-42}$$

Hence, the eigenvalue problem (2.3-30) and (2.3-41) have the same eigenvectors $\boldsymbol{\psi}_i$ and the same eigenvalues λ_i. By assuming $\boldsymbol{\psi} = \begin{Bmatrix} \boldsymbol{\psi}^{(1)} \\ \boldsymbol{\psi}^{(2)} \end{Bmatrix}$ and substituting this expression and Eqns. (2.2-10) and (2.2-11) into Eqn. (2.3-30), the lower part of

expansion of Eqn. (2.3-30) yields

$$\lambda \mathbf{M}_0 \boldsymbol{\psi}^{(2)} + \mathbf{C}_0 \boldsymbol{\psi}^{(2)} + \mathbf{K}_0 \boldsymbol{\psi}^{(1)} = \mathbf{0}. \tag{2.3-43}$$

It can be seen, by comparison Eqn. (2.3-43) with Eqn. (2.3-26), $\boldsymbol{\psi}^{(1)} = \boldsymbol{\phi}$ and $\boldsymbol{\psi}^{(2)} = \lambda \boldsymbol{\phi}$, so that the eigenvectors $\boldsymbol{\psi}_i$ can relate to the eigenvectors $\boldsymbol{\phi}_i$ by the following equation

$$\boldsymbol{\psi}_i = \begin{Bmatrix} \boldsymbol{\psi}_i^{(1)} \\ \boldsymbol{\psi}_i^{(2)} \end{Bmatrix} = \begin{Bmatrix} \boldsymbol{\phi}_i \\ \lambda_i \boldsymbol{\phi}_i \end{Bmatrix}. \tag{2.3-44}$$

Once eigenvectors $\boldsymbol{\psi}_i$ are obtained, eigenvectors $\boldsymbol{\phi}_i$, i.e. mode shapes of the vibrating structure, can be extracted from this relationship. Eigenvalues λ_i are expressed in terms of natural frequencies ω_i and damping ratios η_i as Eqn. (2.3-28).

As previously mentioned in the case of undamped structures, the amplitude of the eigenvector is arbitrary, and the modes are determined within a multiplicative constant. For a damped structure not only the amplitude but also the phase angle is arbitrary. From Eqn. (2.3-44), the ratios of the magnitudes of corresponding complex elements of both the upper and lower part of an eigenvector are the same and the difference in phase angles of the corresponding complex elements are equal to each other. This can be illustrated in Fig. 2.3-1.

For the *i*-th eigenvector the following relations must hold

$$\frac{|\boldsymbol{\psi}_{ri}|}{|\boldsymbol{\psi}_{ji}|} = \frac{|\boldsymbol{\psi}_{(r+n)i}|}{|\boldsymbol{\psi}_{(j+n)i}|} = const \tag{2.3-45}$$

and

$$\theta_r - \theta_j = \theta_{r+n} - \theta_{j+n} = const \tag{2.3-46}$$

where $|\psi_{ri}|$ is the magnitude and θ_r is the phase angle of the rth element of the ith eigenvector ψ_i.

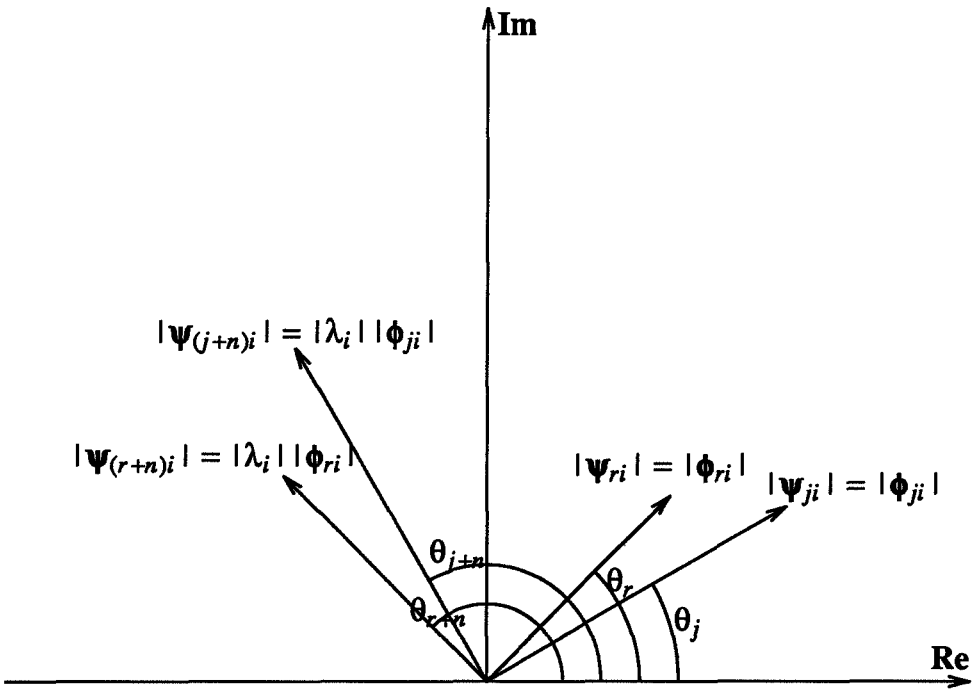

Fig. 2.3-1 Magnitude and Phase of the Elements of Eigenvector

The complex mode can be normalized and this means removing the arbitrariness both from the magnitudes and phase angles of the complex elements of the eigenvector ψ_i.

§ 2.4 RESPONSE MODEL

For the structural and modal identification, it is important to explicitly express the responses in terms of modal parameters and excitations. This expression is called *response model* of the linear structure. The response model may be described in the time domain or frequency domain. Three types of time domain response model: impulse response, free response and forced response are discussed in this section. Frequency domain response of undamped and damped structure is also introduced.

§ 2.4.1 Impulse Response Model

Impulse response is a very basic concept in the vibrating structure analysis. It describes the relationship between the excitation and response and is very explicit and attractive computationally.

For convenience, scalar excitation and scalar response is to be discussed first and the results will be extended to the case of multiple excitation and multiple response. Before proceeding with the derivation of the impulse response, it is necessary to introduce the unit impulse, or *Dirac's delta function.* The mathematical definition of the unit impulse is

$$\delta(t-\tau)=0, \text{ for } t\neq\tau \text{ and } \int_{-\infty}^{\infty}\delta(t-\tau)dt=1 \tag{2.4-1}$$

and the unit impulse has units $time^{-1}$.

The unit impulse is depicted in Fig. 2.4-1 in the form of a thin rectangle of infinitesimal width ε and height $1/\varepsilon$. In the limit, as ε approaches zero, the width

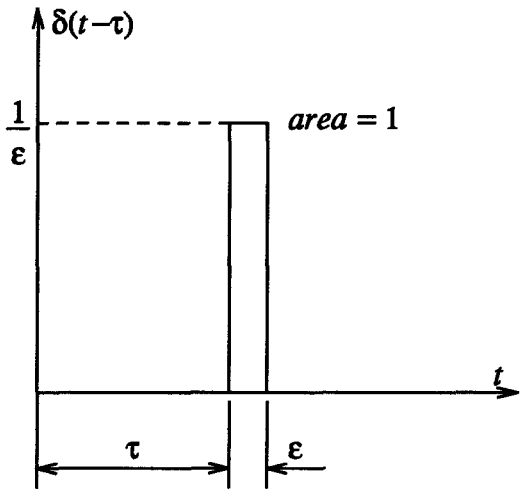

Fig. 2.4-1 Unit Impulse

tends to zero while height tends to infinity in a way that the area under the curve remains constant and equal to unity. Actually, the shape of the delta function is immaterial as the width is very thin and the area is equal to unity. In fact, the delta function should really resemble a 'spike'. Note that the unit impulse defined by Eqn. (2.4-1) is applied at $t = \tau$. A unit impulse applied at $t = 0$ is denoted by $\delta(t)$.

The *impulse response*, denoted by $h(t)$, is defined as the response of a structure to a unit impulse applied at t=0.

$$y(t) = \int_0^t h(t-\tau)\delta(\tau)d\tau = h(t). \tag{2.4-2}$$

The impulse response embodies all the structure characteristics including modal characteristics, so that it provides a way for the modal identification. The impulse response is not merely a convenient method of describing the structure characteristics but is also a useful method for evaluation of the response, as it permits the synthesis of the response to any arbitrary excitation. The relationship between the impulse response function, excitation and response can be depicted by

the diagram shown in Fig. 2.4-2.

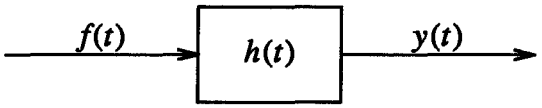

Fig. 2.4-2 Impulse Response Model Diagram

Assume that a linear structure is subjected to the arbitrary excitation $f(t)$ and consider a thin rectangular area of width $\Delta\tau$ and height $f(\tau)$, as shown in Fig. 2.4-3.

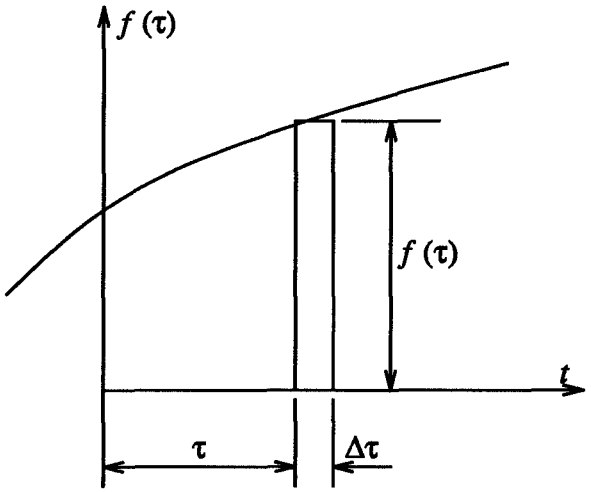

Fig. 2.4-3 Impulse Response

This particular increment of area can be regarded as an impulse of magnitude $f(\tau)$ applied at $t = \tau$, so that the contribution to the structure response attributable to this excitation is simply

$$\Delta y(t,\tau) = f(\tau)h(t-\tau)\Delta\tau \tag{2.4-3}$$

where $h(t-\tau)$ is the impulse response function delayed by $t = \tau$. The response can therefore be approximated by a collection of corresponding impulse response, or

$$y(t) \approx \sum_{\tau} f(\tau)h(t-\tau)\Delta\tau. \tag{2.4-4}$$

The response can be rendered exact by letting $\Delta\tau \to 0$ and replacing the summation by integration, so as to obtain

$$y(t) = \int_{-\infty}^{t} f(\tau)h(t-\tau)d\tau \tag{2.4-5}$$

which is known as the convolution integral. It should be pointed out that Eqn. (2.4-5) represents only the response to the excitation $f(t)$. The response to any possible initial excitation must be evaluated separately and added to it. The convolution integral is symmetric in $f(t)$ and $h(t)$. Indeed, it is not difficult to show that the integral can also be written in the form

$$y(t) = \int_{-\infty}^{t} f(t-\tau)h(\tau)d\tau. \tag{2.4-6}$$

If a structure has n excitation stations and n response stations, and the initial condition is zero, the impulse response model in Eqn. (2.4-6) can extended to

$$\mathbf{y}(t) = \int_{-\infty}^{t} \mathbf{H}(t-\tau)\mathbf{f}(\tau)d\tau \tag{2.4-7}$$

where

$$\mathbf{H}(t-\tau) = \begin{bmatrix} h_{11}(t-\tau) & h_{12}(t-\tau) & \cdots & h_{1n}(t-\tau) \\ h_{21}(t-\tau) & h_{22}(t-\tau) & \cdots & h_{2n}(t-\tau) \\ \vdots & \vdots & & \vdots \\ h_{n1}(t-\tau) & h_{n2}(t-\tau) & \cdots & h_{nn}(t-\tau) \end{bmatrix} \tag{2.4-8}$$

and $h_{ij}(t-\tau)$ is the response at time t at the ith response station due to impulse function applied at time τ at the jth excitation station, the excitation at other stations being identically zero. Equivalently, $h_{ij}(t-\tau)$ is the impulse response between the jth excitation station and ith response station. Hence **H** is called the impulse response matrix of the vibrating structure.

§ 2.4.2 Time Domain Free Response Model

A structure in a static equilibrium state would not vibrate until some external excitation is imposed on it. But if a structure is not in an equilibrium state, it may vibrate. The non-equilibrium state is called the initial condition, which could be initial displacements, velocities or accelerations, or any of their combinations. The response model to the initial condition is known as *free response model.* The free response model of undamped vibrating strctures can be obtained by recalling Eqn. (2.3-2) and (2.3-3). In the case of an undamped structure, Eqn. (2.3-2) is used to derive the free responses. Each eigenvalue λ_i corresponds two exponents, $\omega_i = \pm\sqrt{-\lambda_i}$ and so Eqn. (2.3-2) admits solutions of the form

$$\mathbf{y}_i(t) = (a_i e^{\sqrt{-\lambda_i}t} + b_i e^{-\sqrt{-\lambda_i}t})\boldsymbol{\phi}_i, \quad i = 1, 2, \cdots, n \tag{2.4-9}$$

which are often referred to as eigen solutions, where a_i and b_i are constant. Because the structure under consideration is linear, the general solution of Eqn. (2.3-3) is a linear combination of the eigen solutions, or

$$\mathbf{y}(t) = \sum_{i=1}^{n} (a_i e^{\sqrt{-\lambda_i}t} + b_i e^{-\sqrt{-\lambda_i}t})\boldsymbol{\phi}_i \tag{2.4-10}$$

where the constants a_i and b_i depend on the initial conditions $\mathbf{y}(0)$ and $\dot{\mathbf{y}}(0)$. This solution must be real. For nonzero eigenvalues, therefore, $\omega_i \neq 0$, a_i and b_i must be complex conjugates and the solutions reduce to

$$\mathbf{y}(t) = \sum_{i=1}^{n} (a_i e^{i\omega_i t} + \bar{a}_i e^{-i\omega_i t})\boldsymbol{\phi}_i \tag{2.4-11}$$

where $\bar{a}_i$ is the complex conjugate of a_i.

In the case of a damped structure, Eqn. (2.3-3) is used to obtain the free responses. As mentioned in § 2.3, a constituent solution of free vibration is

$$\mathbf{x}_i(t) = e^{\lambda_i t}\boldsymbol{\psi}_i, \quad i = 1, 2, \cdots, 2n. \tag{2.4-12}$$

Because of linearity of the structure, the solution of Eqn. (2.3-3) is

$$\mathbf{x}(t) = \sum_{i=1}^{2n} e^{\lambda_i t}\boldsymbol{\psi}_i \tag{2.4-13}$$

The free vibration response expressions (2.4-12) and (2.4-13) imply the relationships between the free response time history, and eigenvalues λ_i and eigenvectors $\boldsymbol{\phi}_i$ or $\boldsymbol{\psi}_i$.

§ 2.4.3 Time Domain Forced Response Model

In order to obtain the time domain forced response, Eqn. (2.2-13) is used. The solution of Eqn. (2.2-13) with **A** and **B** as constant matrices can be obtained in analogy to the method used in the scalar case by first obtaining the homogeneous solution, then the particular solution, and finally adding both together. The

homogeneous component of Eqn. (2.2-13) is

$$\dot{\mathbf{x}}(t) = \mathbf{A}\mathbf{x}(t), \quad \mathbf{x}(0) = \mathbf{x}(t=0) \tag{2.4-14}$$

and a suggested solution of

$$\mathbf{x}(t) = \exp[\mathbf{A}t]\mathbf{x}(0) \tag{2.4-15}$$

where $\exp[\mathbf{A}t]$ is the exponential function of the matrix $\mathbf{A}t$ defined by the Taylor series

$$\exp(\mathbf{A}t) = \sum_{i=0}^{\infty} \frac{(\mathbf{A}t)^i}{i!}. \tag{2.4-16}$$

Defining the derivative of a function,

$$\frac{d}{dt}\exp[\mathbf{A}t] = \lim_{h\to 0} \frac{1}{h}(\exp[\mathbf{A}(t+h)] - \exp[\mathbf{A}t])$$

$$= \lim_{h\to 0} \frac{\exp[\mathbf{A}t]}{h}(\exp[\mathbf{A}h] - \mathbf{I}). \tag{2.4-17}$$

Applying the series expansion for $\exp[\mathbf{A}h]$ yields

$$\frac{d}{dt}\exp[\mathbf{A}t] = \exp[\mathbf{A}t]\mathbf{A} = \mathbf{A}\exp[\mathbf{A}t] \tag{2.4-18}$$

Thus if the right-hand side of Eqn. (2.4-15) is differentiated,

$$\frac{d}{dt}(\exp[\mathbf{A}t]\mathbf{x}(0)) = \mathbf{A}\exp[\mathbf{A}t]\mathbf{x}(0) = \mathbf{A}\mathbf{x}(t). \tag{2.4-19}$$

and Eqn. (2.4-15) is seen to be the homogeneous solution of Eqn. (2.2-13). For notational simplicity, it is written

$$\mathbf{T}(t,\ t_0) = \exp[\mathbf{A}(t-t_0)], \tag{2.4-20}$$

where $\mathbf{T}(t,\ t_0)$ is called the *state transition matrix*. When $t_0 = 0$,

$$\mathbf{T}(t) = \exp[\mathbf{A}t] \tag{2.4-21}$$

and the homogeneous solution in Eqn. (2.4-15) is as

$$\mathbf{x}(t) = \mathbf{T}(t)\mathbf{x}(0). \tag{2.4-22}$$

From the equations derived above, it is relatively easy to show the following properties of the state transition matrix:

$$\mathbf{T}^{-1}(t) = \mathbf{T}(-t), \tag{2.4-23}$$

$$\mathbf{T}(0) = \mathbf{I} \tag{2.4-24}$$

and

$$\mathbf{T}(t_1)\mathbf{T}(t_2) = \mathbf{T}(t_1 + t_2). \tag{2.4-25}$$

The complete solution can therefore be derived as follows. It can be seen that

$$\dot{\mathbf{T}}(t) = \mathbf{A}\mathbf{T}(t) \tag{2.4-26}$$

Postmultiplying both sides of this equation by $\mathbf{T}^{-1}(t)$ yields

$$\dot{\mathbf{T}}(t)\mathbf{T}^{-1}(t) = \mathbf{A}. \tag{2.4-27}$$

Thus

$$\mathbf{A} = \dot{\mathbf{T}}(t)\mathbf{T}^{-1}(t) = \dot{\mathbf{T}}(t)\mathbf{T}(-t). \tag{2.4-28}$$

But noting $\mathbf{T}^{-1}(t)\mathbf{T}(t) = \mathbf{I}$ and differentiating both sides of the equation with respect to t,

$$\mathbf{A} = -\mathbf{T}(t)\dot{\mathbf{T}}(-t). \tag{2.4-29}$$

Substituting Eqn. (2.4-29) into Eqn. (2.2-13) yields

$$\dot{\mathbf{x}}(t) = \mathbf{A}\mathbf{x}(t) + \mathbf{B}\mathbf{f}(t) = -\mathbf{T}(t)\dot{\mathbf{T}}(-t)\mathbf{x}(t) + \mathbf{B}\mathbf{f}(t) \tag{2.4-30}$$

Premultiplying by $\mathbf{T}(-t)$ and noting that $\mathbf{T}(-t)\mathbf{T}(t) = \mathbf{T}(0) = \mathbf{I}$ yields

$$\mathbf{T}(-t)\dot{\mathbf{x}}(t) + \dot{\mathbf{T}}(-t)\mathbf{x}(t) = \mathbf{T}(-t)\mathbf{B}\mathbf{f}(t) \tag{2.4-31}$$

The left-hand side of Eqn. (2.4-31) is a perfect differential. Therefore,

$$\frac{d}{dt}(\mathbf{T}(-t)\mathbf{x}(t)) = \mathbf{T}(-t)\mathbf{B}\mathbf{f}(t) \tag{2.4-32}$$

and integrating gives

$$\mathbf{T}(-t)\mathbf{x}(t) = \int_0^t \mathbf{T}(-\tau)\mathbf{B}\mathbf{f}(\tau)d\tau + \mathbf{T}(0)\mathbf{x}(0) \tag{2.4-33}$$

This can now be premultiplied by $\mathbf{T}(t)$ to yield, with $\mathbf{T}(0) = \mathbf{I}$,

$$\mathbf{x}(t) = \mathbf{T}(t)\mathbf{x}(0) + \int_0^t \mathbf{T}(t-\tau)\mathbf{B}\mathbf{f}(\tau)d\tau \tag{2.4-34}$$

Eqn. (2.4-34) represents the solution of Eqn. (2.2-13), which consists of two parts: the response due to initial condition of the structure $\mathbf{T}(t)\mathbf{x}(0)$ and the response due to external excitation $\int_0^t \mathbf{T}(t-\tau)\mathbf{B}\mathbf{f}(\tau)d\tau$. This permits the calculation of the state $\mathbf{x}(t)$ and hence the response $\mathbf{y}(t)$ at any time t, given the initial condition $\mathbf{x}(0)$, the excitation function $\mathbf{f}(t)$ and , of course, the matrices **A** and **B**.

§ 2.4.4 Discrete Time Response Model

The measurements in the modal test are digital signals which are not continuous in the time domain and since most identification algorithms are conveniently implemented on digital computers, it is appropriate to define discrete time structure models and investigate the response models in the discrete time domain.

The basic difference to be used here between the continuous time and discrete time formulations is simply stated. In the continuous time domain all variables such as

$\mathbf{x}(t)$ and $\mathbf{f}(t)$ are continuous in the sense of being specified for all values of the variable t; in the discrete time domain $\mathbf{x}(t)$ and $\mathbf{f}(t)$ are assumed to be known or specified only at certain discrete values of t.

The discrete time signals are frequently generated through the process of sampling the functions $f(t)$ and $y(t)$ of continuous time. A model for the process of sampling the function of continuous time, for example, $f(t)$, is shown in Fig. 2.4-4.

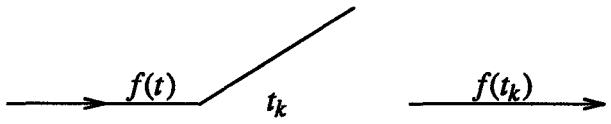

Fig. 2.4-4 Sampling Process

The sampler switch is thought of as closing instantaneously at time instants $t = t_k$ and being open otherwise. At the output terminal of the sampler, the number $f(t_0)$, $f(t_1)$, ··· will appear at the time instants t_0 , t_1, ···. In this manner the function of the continuous time has been converted into a sequence of numbers. Fig. 2.4-5 illustrates a typical function $f(t)$ and sequence of numbers generated when $f(t)$ is sampled.

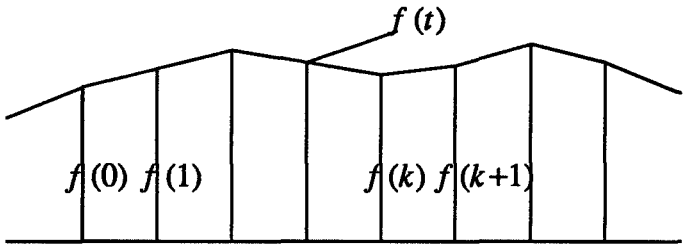

Fig. 2.4-5 Example of Sampling

The sampling process most frequently used in applications, particularly in this thesis,

is one in which the sampling switch closes every T seconds. This is called equally spaced sampling and will be illustrated as shown in Fig. 2.4-6.

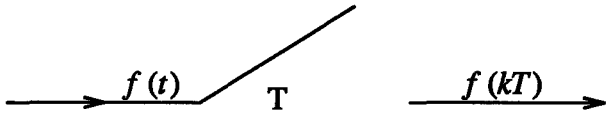

Fig. 2.4-6 Model of process of equally spaced samping

In this case the signal picking up interval Δt is fixed,

$$t_{k+1} - t_k = \Delta t = T, \tag{2.4-35}$$

where T is called the sampling period and is constant for any k, thus

$$t_k = kT, \tag{2.4-36}$$

since t_0 is taken to be zero.

Consider next the solution of the continuous time response model as given by Eqn. (2.4-34),

$$\mathbf{x}(t) = \mathbf{T}(t)\mathbf{x}(0) + \int_0^t \mathbf{T}(t-\tau)\mathbf{B}\mathbf{f}(\tau)d\tau \tag{2.4-37}$$

If $t=T$ and if $\mathbf{f}(t)$ is assumed to be held constant and equal to $\mathbf{f}(0)$ over the time period $t=0$ to $t=T$, then it follows that

$$\mathbf{x}(T) = \mathbf{T}(T)\mathbf{x}(0) + [\int_0^T \mathbf{T}(T-\tau)\mathbf{B}d\tau]\mathbf{f}(0) \tag{2.4-38}$$

Assuming

$$\Delta(T) = [\int_0^T \mathbf{T}(T-\tau)d\tau]\mathbf{B} \tag{2.4-39}$$

with **B** being constant, then

$$\mathbf{x}(T) = \mathbf{T}(T)\mathbf{x}(0) + \Delta(T)\mathbf{f}(0). \tag{2.4-40}$$

Eqn. (2.4-40) thus yields the value of the state variable $\mathbf{x}(T)$ at time $t=T$. If the entire procedure is repeated from $t=T$ to $t=2T$ using a constant value of $\mathbf{f}(T)$ and the time over which the integration is performed is the same length as the the previous step, then

$$\mathbf{x}(2T) = \mathbf{T}(T)\mathbf{x}(T) + \Delta(T)\mathbf{f}(T) \tag{2.4-41}$$

Continuing the entire process

$$\mathbf{x}((k+1)T) = \mathbf{T}(T)\mathbf{x}(kT) + \Delta(T)\mathbf{f}(kT) \qquad (k = 0, 1, 2, \cdots) \tag{2.4-42}$$

In simpler terms

$$\mathbf{x}(k+1) = \mathbf{T}(T)\mathbf{x}(k) + \Delta(T)\mathbf{f}(k) \qquad (k = 0, 1, 2, \cdots) \tag{2.4-43}$$

This equation may be used recursively to generate $\mathbf{x}(1)$, $\mathbf{x}(2)$, $\cdots$. Using the simple nomenclature that $\mathbf{T}(T) = \mathbf{T}$= constant matrix and that $\Delta(T) = \Delta$ = constant matrix, then

$$\mathbf{x}(k+1) = \mathbf{T}\mathbf{x}(k) + \Delta\mathbf{f}(k)$$

$$\mathbf{x}(k+2) = \mathbf{T}\mathbf{x}(k+1) + \Delta\mathbf{f}(k+1)$$

$$= \mathbf{T}^2\mathbf{x}(k) + \mathbf{T}\Delta\mathbf{f}(k) + \Delta\mathbf{f}(k+1)$$

$$\mathbf{x}(k+3) = \mathbf{T}^3\mathbf{x}(k) + \mathbf{T}^2\Delta\mathbf{f}(k) + \mathbf{T}\Delta\mathbf{f}(k+1) + \Delta\mathbf{f}(k+2)$$

and

$$\mathbf{x}(k+i) = \mathbf{T}^i\mathbf{x}(k) + \sum_{l=0}^{i-1}\mathbf{T}^{i-1-l}\Delta\mathbf{f}(k+i). \qquad (2.4\text{-}44a)$$

This equation shows how the state variable $\mathbf{x}(k+i)$ after i sampling periods, is predicted on the basis of the state $\mathbf{x}(k)$ and sequence of inputs $\mathbf{f}(k)$, $\mathbf{f}(k+1)$, ··, $\mathbf{f}(k+i-1)$. From the above, the free response model of the strcuture can also be represented by

$$\mathbf{x}(k+1) = \mathbf{T}\mathbf{x}(k) \qquad or \qquad \mathbf{x}(k) = \mathbf{T}^k\mathbf{x}(0) \qquad (2.4\text{-}44b)$$

§ 2.4.5 Frequency Response Model

For the convenience of reviewing the modal identification methods in the frequency domain, *frequency response model* is briefly discussed in this section. The frequency response function of a vibrating structure is related to its modal parameters the and this constitutes the basis for identification of modal parameters from the frequency response data. The case where the vibrating structure is excited sinusoidally by a set of forces having the same frequency ω, but with various

amplitudes and phases is considered here to derive the frequency response model.

Undamped Structures

For an undamped structure, the equation of motion in Eqn. (2.2-7) becomes

$$\mathbf{M}_0\ddot{\mathbf{y}}(t) + \mathbf{K}_0\mathbf{y}(t) = \mathbf{f}(t). \tag{2.4-45}$$

Taking Fourier transformation of both sides of Eqn. (2.4-45) yields

$$(\mathbf{K}_0 - \omega^2\mathbf{M}_0)\mathbf{y}(\omega) = \mathbf{f}(\omega) \tag{2.4-46}$$

where $\mathbf{y}(\omega)$ and $\mathbf{f}(\omega)$ are Fourier transformations of $\mathbf{y}(t)$ and $\mathbf{f}(t)$, respectively, and

$$\mathbf{y}(\omega) = \int_{-\infty}^{+\infty} \mathbf{y}(t)e^{-i\omega t}dt$$

$$\mathbf{f}(\omega) = \int_{-\infty}^{+\infty} \mathbf{f}(t)e^{-i\omega t}dt.$$

Rearranging to solve for the unknown responses

$$\mathbf{y}(\omega) = (\mathbf{K}_0 - \omega^2\mathbf{M}_0)^{-1}\mathbf{f}(\omega) \tag{2.4-47}$$

and which may be written as

$$\mathbf{y}(\omega) = \mathbf{H}(\omega)\mathbf{f}(\omega) \tag{2.4-48}$$

where $\mathbf{H}(\omega)$ is the $n \times n$ frequency response function matrix for the structure. This expression can be written as

$$\mathbf{H}(\omega) = \begin{bmatrix} h_{11}(\omega) & h_{12}(\omega) & \cdots & h_{1n}(\omega) \\ h_{21}(\omega) & h_{22}(\omega) & \cdots & h_{2n}(\omega) \\ \vdots & \vdots & & \vdots \\ h_{n1}(\omega) & h_{n2}(\omega) & \cdots & h_{nn}(\omega) \end{bmatrix} \tag{2.4-49}$$

and $h_{ij}(\omega)$ is the response at frequency ω at the ith station due to an excitation applied at the jth station, the excitation at other stations being identically zero. Eqn. (2.4-48) is called the *frequency response model.* The frequency response model can be depicted by a diagram shown in Fig. 2.4-7.

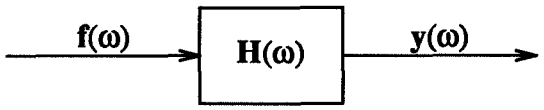

Fig. 2.4-7 Frequency Response Model Diagram

The general element in the frequency response function matrix, $\mathbf{H}(\omega)$, is defined as follows:

$$h_{jk}(\omega) = \frac{y_j(\omega)}{f_k(\omega)}, \quad when \quad f_m(\omega) = 0 \quad \text{and} \quad m = 1, \cdots, n \neq k. \tag{2.4-50}$$

It is clearly possible to determine values of the elements of $\mathbf{H}(\omega)$ at any frequency of interest simply by substituting the appropriate values of ω into Eqn. (2.4-48). However, it does not reveal the relationship between the frequency response function and modal parameters. For this and other reasons an alternative means of deriving

the frequency response function parameters is used which makes use of the modal properties for the structure.

Returning to Eqn. (2.4-47)

$$\mathbf{K}_0 - \omega^2\mathbf{M}_0 = \mathbf{H}(\omega)^{-1}. \tag{2.4-51}$$

Premultipling both sides by $\mathbf{\Phi}^T$ and postmultipling both sides by $\mathbf{\Phi}$ to obtain

$$\mathbf{\Phi}^T(\mathbf{K}_0 - \omega^2\mathbf{M}_0)\mathbf{\Phi} = \mathbf{\Phi}^T\mathbf{H}(\omega)^{-1}\mathbf{\Phi} \tag{2.4-52}$$

or

$$diag[\omega_r^2 - \omega^2] = \mathbf{\Phi}^T\mathbf{H}(\omega)^{-1}\mathbf{\Phi} \tag{2.4-53}$$

which gives

$$\mathbf{H}(\omega) = \mathbf{\Phi}diag[\omega_r^2 - \omega^2]^{-1}\mathbf{\Phi}^T. \tag{2.4-54}$$

It is clear from this equation that the frequency response function matrix $\mathbf{H}(\omega)$ is symmetric and this will be recognized as the principle of reciprocity which applies to many structural characteristics. Its implications in this situation are that

$$h_{jk}(\omega) = \frac{y_j(\omega)}{f_k(\omega)} = h_{kj}(\omega) = \frac{y_k(\omega)}{f_j(\omega)}. \tag{2.4-55}$$

Eqn. (2.4-54) can be used to calculate any individual frequency response function parameter $h_{jk}(\omega)$ by the following formula

$$h_{jk}(\omega) = \sum_{r=1}^{n} \frac{{}_r\phi_j \, {}_r\phi_k}{\omega_r^2 - \omega^2} = \sum_{r=1}^{n} \frac{{}_rA_{jk}}{\omega_r^2 - \omega^2}. \tag{2.4-56}$$

${}_rA_{jk}$ is referred to as a *modal constant* of the structure.

Damped Structures

In the case of damped structure, taking Laplace transform of Eqn. (2.4-34) and considering $\mathbf{T}(t) = \exp[\mathbf{A}t]$

$$\hat{\mathbf{x}}(s) = [s\mathbf{I} - \mathbf{A}]^{-1}\mathbf{x}(0) + [s\mathbf{I} - \mathbf{A}]^{-1}\mathbf{B}\hat{\mathbf{f}}(s) \tag{2.4-57}$$

where the circumflex $\hat{}$ denotes the Laplace transform of a variable and

$$\hat{\mathbf{x}}(s) = \int_0^{+\infty} \mathbf{x}(t)e^{-st}dt \tag{2.4-58}$$

and

$$\hat{\mathbf{f}}(s) = \int_0^{+\infty} \mathbf{f}(t)e^{-st}dt. \tag{2.4-59}$$

Substituting Eqns. (2.2-14) and (2.2-15) into Eqn. (2.4-57) and assuming $\mathbf{x}(0) = \mathbf{0}$

$$\hat{\mathbf{x}}(s) = [s\mathbf{M}^* - \mathbf{K}^*]^{-1}\mathbf{D}\hat{\mathbf{f}}(s). \tag{2.4-60}$$

That is

$$\hat{\mathbf{x}}(s) = \boldsymbol{\Psi}[\boldsymbol{\Psi}^T(s\mathbf{M}^* - \mathbf{K}^*)\boldsymbol{\Psi}]^{-1}\boldsymbol{\Psi}^T\mathbf{D}\hat{\mathbf{f}}(s). \tag{2.4-61}$$

Considering the orthogonal properties in Eqns. (2.3-39) and (2.3-40) yields

$$\hat{\mathbf{x}}(s) = \boldsymbol{\Psi}[s\mathbf{I} - \boldsymbol{\Lambda}]^{-1}\boldsymbol{\Psi}^T\mathbf{D}\hat{\mathbf{f}}(s). \tag{2.4-62}$$

Since $\hat{\mathbf{x}}(s) = \begin{Bmatrix} \hat{\mathbf{y}}(s) \\ \dot{\hat{\mathbf{y}}}(s) \end{Bmatrix}$, assuming $\mathbf{x}(0) = \mathbf{0}$,

$$\hat{\mathbf{y}}(s) = \mathbf{C}[s\mathbf{I} - \mathbf{A}]^{-1}\mathbf{B}\hat{\mathbf{f}}(s) \tag{2.4-63}$$

or

$$\hat{\mathbf{y}}(s) = \mathbf{C}\boldsymbol{\Psi}[s\mathbf{I} - \boldsymbol{\Lambda}]^{-1}\boldsymbol{\Psi}^T\mathbf{D}\hat{\mathbf{f}}(s) \tag{2.4-64}$$

where

$$\mathbf{C} = [\mathbf{I} \quad \mathbf{0}] \tag{2.4-65}$$

and

$$\mathbf{D} = \begin{bmatrix} \mathbf{0} \\ \mathbf{I} \end{bmatrix}. \tag{2.4-66}$$

Hence the transfer function matrix is

$$\mathbf{H}(s) = \mathbf{C}[s\mathbf{I} - \mathbf{A}]^{-1}\mathbf{B} \tag{2.4-67}$$

or

$$\mathbf{H}(s) = \mathbf{C}\boldsymbol{\Psi}[s\mathbf{I} - \boldsymbol{\Lambda}]^{-1}\boldsymbol{\Psi}^T\mathbf{D} \tag{2.4-68}$$

and

$$\mathbf{y}(s) = \mathbf{H}(s)\mathbf{f}(s). \tag{2.4-69}$$

Taking $s = i\omega$, the frequency response function matrix is

$$\mathbf{H}(\omega) = \mathbf{C}\boldsymbol{\Psi}[i\omega\mathbf{I} - \boldsymbol{\Lambda}]^{-1}\boldsymbol{\Psi}^T\mathbf{D}. \tag{2.4-70}$$

The element of the transfer function matrix h_{jk} may then be written as

$$h_{jk}(\omega) = \sum_{r=1}^{2n} \frac{{}_r\psi_j \, {}_r\psi_{k+n}}{i\omega - \lambda_r} = \sum_{r=1}^{2n} \frac{{}_rA_{jk}}{i\omega - \lambda_r}. \tag{2.4-71}$$

Eqns. (2.4-56) and (2.4-71) describe the relationships between the modal parameters of a vibrating structure and its frequency response functions.

Fig. 2.4-8 shows a typical frequency response function. Since the frequency response function is complex, the figure indicates its magnitutes.

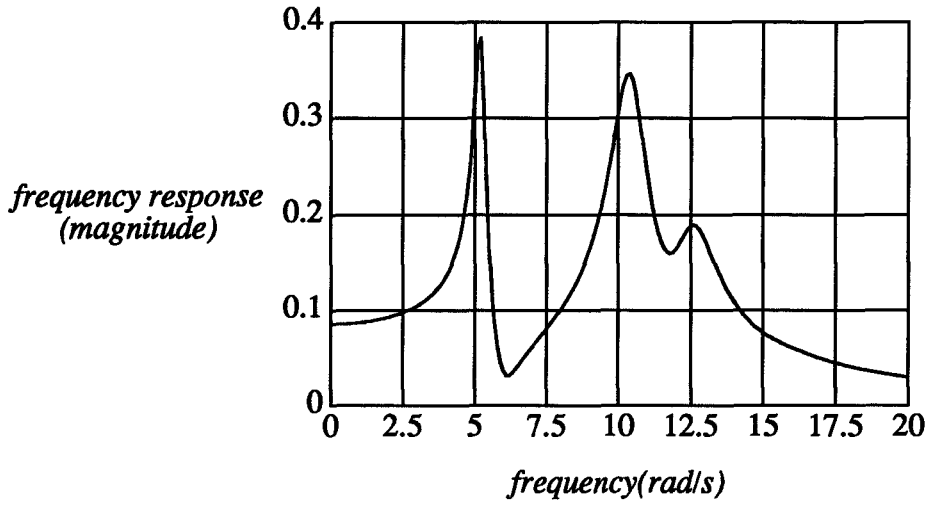

Fig. 2.4-8 Frequency Response Function (Magnitude)

Corresponding real and imaginary parts of the frequency response function are depicted in Figs. 2.4-9 and 2.4-10.

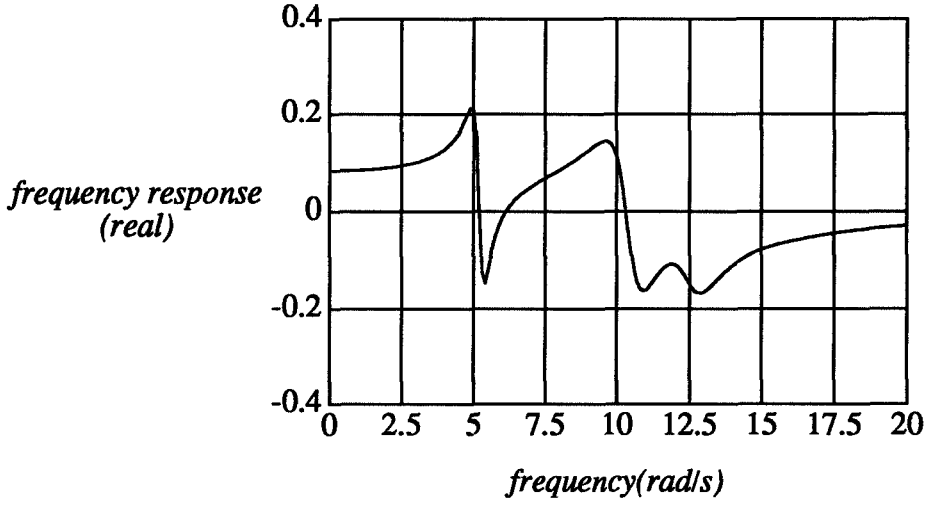

Fig. 2.4-9 Real Part of Frequency Response Function

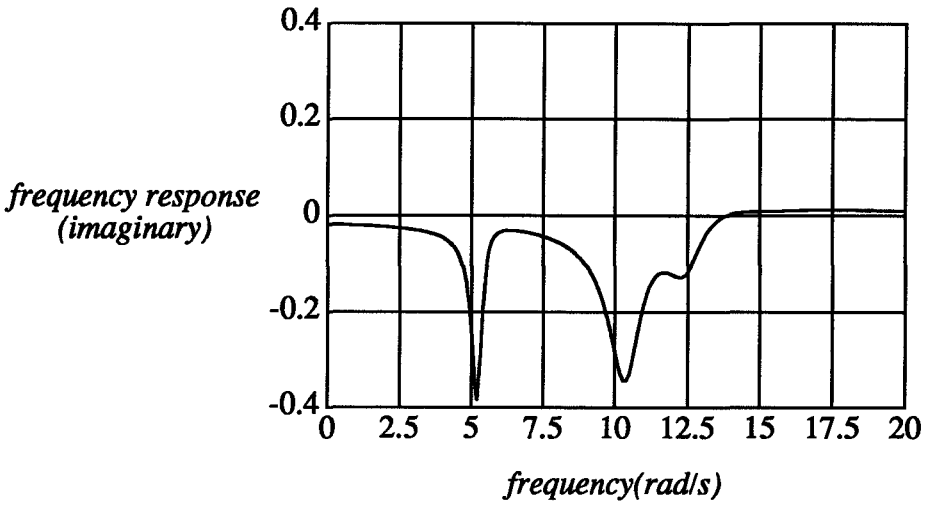

Fig. 2.4-10 Imaginary Part of Frequency Response Function

The phase of the frequency response function is also shown in Fig. 2.4-11.

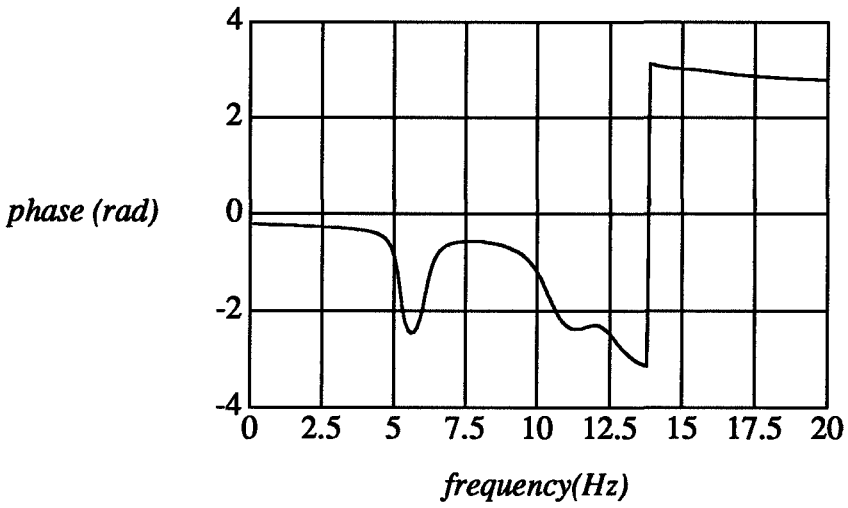

Fig. 2.4-11 Phase of Frequency Response Fuction

The frequency response can also be considered as the Laplace transform of the impulse response of the linear vibrating structure. Taking Laplace transforms on both sides of impulse response in Eqn. (2.4-45) and considering the convolution theorem of Laplace transform,

$$\int_0^\infty \mathbf{y}(t)e^{-st}dt = \int_o^\infty \left(\int_{-\infty}^t \mathbf{H}(t-\tau)\mathbf{f}(\tau)d\tau \right) e^{-st}dt. \tag{2.4-72}$$

That is

$$\mathbf{y}(s) = \mathbf{H}(s)\mathbf{f}(s). \tag{2.4-73}$$

Hence the impulse response matrix $\mathbf{H}(t)$ is the inverse Laplace transform of the transfer function matrix $\mathbf{H}(s)$ and

$$\mathbf{H}(t) = \mathbf{C}\exp[\mathbf{A}t]\mathbf{B} \tag{2.4-74}$$

or

$$\mathbf{H}(t) = \mathbf{C}\boldsymbol{\Psi}\exp[\boldsymbol{\Lambda}t]\boldsymbol{\Psi}^T\mathbf{D}. \tag{2.4-75}$$

The element of the impulse response function matrix is

$$h_{jk}(t) = \sum_{r=1}^{2n} e^{\lambda_r t}{}_r A_{jk}. \tag{2.4-76}$$

Eqns. (2.4-74) or (2.4-75) and (2.4-76) will play important roles in the time domain modal identification.

§ 2.5 SUMMARY

This chapter discusses the general theory of vibrating structures and develops the structural model, modal model and response model of a linear vibrating structure.

These models form the theoretical fundamentals of the structural and modal identification of the vibrating structure. They will be referred in the later chapters and hence are listed as follows.

1. Structural model:

In configurational form

$$\mathbf{M}_0\ddot{\mathbf{y}}(t) + \mathbf{C}_0\dot{\mathbf{y}}(t) + \mathbf{K}_0\mathbf{y}(t) = \mathbf{f}(t). \tag{2.5-1}$$

In state variable representation,

$$\mathbf{M}^*\dot{\mathbf{x}}(t) + \mathbf{K}^*\mathbf{x}(t) = \mathbf{D}\mathbf{f}(t) \tag{2.5-2}$$

or

$$\dot{\mathbf{x}}(t) = \mathbf{A}\mathbf{x}(t) + \mathbf{B}\mathbf{f}(t). \tag{2.5-3}$$

2. Modal model:

For undamped structure

$$\mathbf{K}_0\boldsymbol{\phi} = \lambda\mathbf{M}_0\boldsymbol{\phi} \tag{2.5-4}$$

with $\lambda = -\omega^2$. ω is the natural frequency and $\boldsymbol{\phi}$ represents the mode shapes of the vibrating structure.

For damped structure configurational representation

$$[\lambda^2 \mathbf{M}_0 + \lambda \mathbf{C}_0 + \mathbf{K}_0]\boldsymbol{\phi} = \mathbf{0}, \tag{2.5-5}$$

state representation

$$\lambda \mathbf{M}^* \boldsymbol{\psi} + \mathbf{K}^* \boldsymbol{\psi} = \mathbf{0} \tag{2.5-6}$$

or

$$\mathbf{A}\boldsymbol{\psi} = \lambda \boldsymbol{\psi}. \tag{2.5-7}$$

λ is the complex eigenvalue of the linear vibrating structure and may be expressed in terms of natural frequency ω and damping ratio η of the structure as

$$\lambda = -\eta\omega \pm \omega\sqrt{1-\eta^2} \tag{2.5-8}$$

$\boldsymbol{\phi}$ is the complex mode shape of the structure and is related to the eigenvector $\boldsymbol{\psi}$ of Eqn. (2.5-6) by

$$\boldsymbol{\psi}_i = \begin{Bmatrix} \boldsymbol{\phi}_i \\ \lambda_i \boldsymbol{\phi}_i \end{Bmatrix}. \tag{2.5-9}$$

Important orthogonal relationship

Following ***important orthogonal relationships*** will also often be used in this thesis.

For undamped structure

$$\boldsymbol{\Phi}^T \mathbf{M}_0 \boldsymbol{\Phi} = \mathbf{I} \tag{2.5-10}$$

and

$$\mathbf{\Phi}^T \mathbf{K}_0 \mathbf{\Phi} = \mathbf{\Lambda}. \tag{2.5-11}$$

For damped structure

$$\mathbf{\Psi}^T \mathbf{M}^* \mathbf{\Psi} = \mathbf{I} \tag{2.5-12}$$

and

$$\mathbf{\Psi}^T \mathbf{K}^* \mathbf{\Psi} = \mathbf{\Lambda}. \tag{2.5-13}$$

3. Response model

Response model may be expressed in frequency domain or time domain.

Frequency domain response model

For undamped structure

$$\mathbf{y}(\omega) = \mathbf{H}(\omega)\mathbf{f}(\omega) \tag{2.5-14}$$

and the frequency response matrix is

$$\mathbf{H}(\omega) = \mathbf{\Phi} diag[\omega_r^2 - \omega^2]^{-1} \mathbf{\Phi}^T. \tag{2.5-15}$$

In element form it will be

$$h_{jk}(\omega) = \sum_{r=1}^{n} \frac{{}_r\phi_j \, {}_r\phi_k}{\omega_r^2 - \omega^2} = \sum_{r=1}^{n} \frac{{}_rA_{jk}}{\omega_r^2 - \omega^2}. \tag{2.5-16}$$

For damped structure

$$\mathbf{y}(s) = \mathbf{H}(s)\mathbf{f}(s) \tag{2.5-17}$$

or

$$\mathbf{y}(\omega) = \mathbf{H}(\omega)\mathbf{f}(\omega) \tag{2.5-18}$$

and the transfer function matrix is

$$\mathbf{H}(s) = \mathbf{C}\boldsymbol{\Psi} diag[s - \lambda_r]^{-1}\boldsymbol{\Psi}^T\mathbf{D} \tag{2.5-19}$$

and the frequency response function matrix is

$$\mathbf{H}(\omega) = \mathbf{C}\boldsymbol{\Psi} diag[i\omega - \lambda_r]^{-1}\boldsymbol{\Psi}^T\mathbf{D}. \tag{2.5-20}$$

The element of the frequency response function matrix, $h_{jk}(\omega)$, may then be written as

$$h_{jk}(\omega) = \sum_{r=1}^{2n} \frac{{}_rA_{jk}}{i\omega - \lambda_r}. \tag{2.5-21}$$

Time Domain Response Model

Impulse response model

$$\mathbf{y}(t) = \int_{-\infty}^{t} \mathbf{H}(t-\tau)\mathbf{f}(\tau)d\tau \tag{2.5-22}$$

where

$$\mathbf{H}(t-\tau) = \begin{bmatrix} h_{11}(t-\tau) & h_{12}(t-\tau) & \cdots & h_{1n}(t-\tau) \\ h_{21}(t-\tau) & h_{22}(t-\tau) & \cdots & h_{2n}(t-\tau) \\ \vdots & \vdots & & \vdots \\ h_{n1}(t-\tau) & h_{n2}(t-\tau) & \cdots & h_{nn}(t-\tau) \end{bmatrix}. \tag{2.5-23}$$

The impulse response function matrix can be expressed in terms of modal parameters of the structure.

$$\mathbf{H}(t) = \mathbf{C}\boldsymbol{\Psi}\exp[\boldsymbol{\Lambda}t]\boldsymbol{\Psi}^T\mathbf{D}. \tag{2.5-24}$$

The element of the impulse response function matrix is

$$h_{jk}(t) = \sum_{r=1}^{2n} e^{\lambda_r t}{}_r A_{jk}. \tag{2.5-25}$$

Time domain free response model

Free response can be expressed as

$$\mathbf{x}(t) = \sum_{i=1}^{2n} e^{\lambda_i t} \boldsymbol{\psi}_i. \tag{2.5-26}$$

Time domain Forced response model

Forced response can be expressed in continuous time domain as

$$\mathbf{x}(t) = \mathbf{T}(t)\mathbf{x}(0) + \int_0^t \mathbf{T}(t-\tau)\mathbf{B}\mathbf{f}(\tau)d\tau, \tag{2.5-27}$$

in the discrete or discretized time domain

$$\mathbf{x}(k+1) = \mathbf{T}(T)\mathbf{x}(k) + \boldsymbol{\Delta}(T)\mathbf{f}(k) \qquad (k = 0, 1, 2, \cdots) \tag{2.5-28}$$

or

$$\mathbf{x}(k+i) = \mathbf{T}^i\mathbf{x}(k) + \sum_{l=0}^{i-1} \mathbf{T}^{i-1-l}\boldsymbol{\Delta}\mathbf{f}(k+i). \tag{2.5-29}$$

Chapter 3

A REVIEW OF MODAL IDENTIFICATION

By a fiction as remarkable as any to be found in law, what has once been published, even though it be in the Russian language, is spoken of as known, and it is too often forgotten that the rediscovery in the library may be a more difficult and uncertain process than the first discovery in the laboratory.

- Lord Rayleigh

§ 3.1 GENERAL VIEW

In many cases, the excessive vibration causes hazardous situations for human lives and structures and is one of main sources of design limitation. There is an even wider set of structures for which vibration is directly related to performance, either

by virtue of causing temporary malfunction during excessive motion or by creating disturbance or discomfort. Therefore, it is important that the vibration levels encountered in service or operation be anticipated and brought under satisfactory control. Besides, the structural integrity is required for structures even under extreme loading such as strong wave and earthquake loadings and hence it is essential to know the dynamic properties of structures. However, because the complexity of structures, the limitation of knowledge and experience of the designer as well as the likely variation during manufacture and construction, the analytical dynamic model may not represent the actual structural dynamic model adequately. The above mentioned vibration problem may not be solved satisfactorily by using the analytical dynamic model. Therefore, identification of the modal parameters of a vibrating structure, such as natural frequencies, damping ratios and mode shapes, and the structural parameters such as mass, stiffness and damping contribution is desirable. In addition to the direct identification of the structure's mass, stiffness and damping distributions using excitation and response data, modal parameters identified in the vibration tests can be used for indirect identification of structural parameters. Further, the modal identification can provide a better understanding the dynamic behavior of a structure. These identified modal parameters such as natural frequencies, damping ratios and mode shapes are directly related to the structure's physical parameters and are very useful in applications such as response predictions, input load identification, trouble shooting excessive vibrations, stability analyses and control system design, verification and/or modification of analytical dynamic models, structural integrity monitoring and incipient failure detection, among others, as mentioned in Chapter 1.

Although methods for modal identification have been attracting researchers' attentions, its principles are not new. A significant breakthrough occurred in modal

identification, when Kennedy and Pancu (1947) published a paper presenting a method for modal identification, which was a major leap in analytic power. They suggested that the comparison of real vs imaginary parts of the frequency response provided far more discrimination than observation of magnitude. The method could be applied in accurate determination of natural frequencies and damping levels in aircraft structures and was not out-dated until the rapid advance of measurement and analysis techniques in the 1960s. Bishop and Gladwell (1963) described the state of theory of single degree of freedom approximation testing which, at that time, was considerably in advance of its practical implementation. Since then, the principle has been refined by Skingle (1966) who proposed the use of correlation to separate desired modal response from interference during rapid sweeps. Smith and Woods (1972) introduced the concept of local and overall energy for discrimination and refined global frequency and damping estimation. Sloane and McKeever (1975) improved discrimination of closely coupled modes by converting frequency response data along the $j\omega$ axis to pole location in the s-plane, with a numerical Laplace transform making it possible to distinguish resonances in two dimensions instead of only one. McKenzie (1974) reported successful Laplace transform modal analysis of a flexural beam in preparation for B-1 flight tests.

Many advantages can be listed about these methods. They are economical since only one shaker is need. They are fairly straightforward and almost automatic test procedures. Most of the art is confined to the analysis stage which means improvements in the techniques seldom require expensive changes or additions to the test laboratory or equipment. As resonant frequencies get closer to each other, however, analytic and/or curve fitting techniques become more difficult since modes are allowed to superimpose in arbitrary combination.

Another type of method was first introduced by Lewis and Wrisley (1950) who suggested a technique with multiple shakers. With this method, a forcing vector is generated in such a fashion as to excite a normal mode of the structure. Since the structure is being excited into a single mode, the amplitude of the vibration measured at the various test points on the structure is a measure of modal coefficients. In such a test, parameter identification often is not required. The method is a relatively non-analytical approach to the interpretation of measured data, but demands more user attention and experience than today's computer-assisted automation for the same task.

By 1970 there had been major advances in transducers, electronics, digital analyzers and computers. These provided strong tools for establishing more advanced methods in modal identification. Many versions of multiple degree of freedom methods in frequency domain were developed to deal with situations of extremely light damping and very heavy damping (Klosterman, 1971; Richardson, 1974; Ramsey, 1975; Allemang, 1980; Brown, 1977; Ewins, 1982).

On one hand, most frequency domain methods are relatively easy to use and visualize, and in many cases reliable. On the other hand, the limitation of these methods is that they are not capable of identifying the very closely spaced frequencies. The reason for the limitation is essentially modal interference and hence some individual modes and natural frequencies cannot be observed separately. Although some multiple degree of freedom methods in the frequency domain have been introduced to deal with modal interference, they have the disadvantage that it must be determined in advance whether special attention is required. To avoid the limitation with frequency domain analysis, some time domain methods for modal identification have also been developed since the later 1960s because the computer,

particularly desk-top computer, has been advanced and the system theory has been developed and applied to the modal identification area.

The pioneers for the time domain method of modal identification are Spitznogle el al (1971). They used the Prony method with $4n$ pieces of information to determine the $4n$ unknowns. Their method is referred to as the Complex Exponential algorithm. It is a very simple technique to implement and has the advantage of fitting most individual measurements, however it computes different eigenvalues for each measurement and this has limited its applicability for modal measurements. This technique is also rather sensitive to noise since it has no inherent smoothing. For single measurements it works very well, and it appears to be generally useful for single-input and single-output system.

Gersch and Luo (1972) introduced an ARMA model to represent a vibrating structure system for modal identification. The random response of the structure to a white noise excitation was used to estimate the coefficients of the ARMA model by means of a two stage least squares estimation algorithm. The coefficients were then applied to compute the natural frequency and damping ratio. The coefficients of the ARMA model were also estimated using maximum likelyhood estimation method by Gersch, Nielsen and Akaite (1973). The method was extended to the case of multiple response observations by Gersch and Yonemoto (1977) and later by Pandit and Wu (1983). This method had potential as a promising procedure, however, it was confined in the identification of natural frequency and damping ratio. Another disadvantage is that only white noise was considered. This is not always realistic and is not applicable in the cases of the other types of excitations. Wang and Fang (1986) further improved Gersch's method by application of the method into identification of mode shapes. Unfortunately, the limitation that only white noise

excitation can be used still remained and observation noise was not considered in the identification procedure.

Ibrahim and Mikulcik (1973) developed a time domain method to use free decay response data for the modal identification. That is the so-called Ibrahim Time Domain (ITD) method. The concept of an oversized response model was introduced. Conversion of the identification to a eigenvalue problem is also an important feature of the method and "Modal Confidence Factors" were used to separate the structural modes and computational modes. The ITD method has been successfully used in some applications of aerospace testing. However, this method can only be used with free decay vibration data.

The Poly Reference time domain method was introduced by Vold et al (1977). The algorithm was aimed at reduction of computation requirements in order to bring time domain modal identification to on-site applications using small computers. This algorithm also uses free decay responses obtained from inverse FFT of the transfer functions. This takes advantage of the possible averaging of the FFT function, thus reducing the noise levels in the computed time functions. Such reduction in noise levels will require smaller identification models and, in turn, less computer storage and execution time. To conserve memory, only the eigenvalues are computed. The mode shapes are then calculated from the free response model in Eqn. (2.5-26) by use of the classical least squares method. Because the transfer functions are transformed from the time domain response by FFT, and this method uses the inverse FFT of the transfer function, the response data are transformed twice. Errors arising from such transformations need to be investigated. For the same reason, effects of leakage and frequency resolution on the identification results should also be studied.

Juang and Pappa (1985) presented the Eigensystem Realization Algorithm for the modal parameter identification and system model reduction. Their method uses singular value decomposition of a block matrix of the impulse response or free decay responses. Two accuracy indicators, i.e., the modal amplitude coherence and modal phase collinearity, were developed to quantify the structural and noise modes. An oversized identification model is also used. However, this method needs much more computer storage and execution time. Like the ITD method and Poly Reference algorithm, the method cannot deal with general excitation and response data.

Leuridan et al. (1985) developed the Direct Parameter Model Identification method. They used a difference equation as the discrete time representation for a multiple dimension system. In form, the difference equation representation is similar to the ARMA model, however, while the MA part of ARMA model represents the unknown random noise, the input part of the difference equation represents the known control input. The coefficient matrices of the difference equation are estimated using the least squares estimate method. On the basis of the impulse response function, the relationship of these coefficient matrices to the modal parameters of the dynamic structure were established. Consequently, the modal parameters are calculated through this relationship.

Hoshiya and Saito (1984) included the parameters to be identified as an additional state vector using Kalman extended filter to identify these parameters. A weight was used to accelerate the processing and an objecting function was introduced to minimize the difference between observations and corresponding estimates. This is an iterative algorithm and identified parameters can be improved as the new state is estimated using the measured data. The order of the vibrating structure must, however, be known in advance. This is usually unrealistic.

The different methods associated with modal identification as mentioned above are further reviewed in detail in the remainder of this chapter. The basic principles and implementation are described and the advantages and disadvantages of these methods discussed. § 3.2 is devoted to the single degree of freedom methods in the frequency domain. In § 3.3, the multiple degree of freedom methods in the frequency domain are introduced. In the § 3.4, the variety of time domain methods are further discussed.

§ 3.2 SINGLE DEGREE OF FREEDOM METHODS IN FREQUENCY DOMAIN

In the frequency domain, most methods for identification of modal parameters consist of two parts: (1) identification of eigenvalues, from which natural frequencies and damping ratios can be determined; (2) identification of eigenvectors, from which the modal coefficients can be determined. The solution for the eigenvalues from measured frequency response information is mathematically a nonlinear process which, in general, greatly complicates the parameter identification schemes.

The single degree of freedom modal identification methods surveyed in this section were historically used with swept sine testing techniques utilizing analog data analysis equipment. With the advent of mini-computer systems it is possible to measure frequency response information and computationally determine the modal parameters simultaneously. As a result of this improved computational capability, a large number of computational algorithms has been developed for computing modal information. Particularly, the advent of the dual channel Fast Fourier Transformation analyzer made these methods much easier to implement. In this sections each method will be reviewed as to its implementation, advantages and disadvantages.

Amplitude Response

The simplest method for modal identification in the frequency domain is the peak-amplitude method. The implementation of this method is as follows.

(a) The natural frequency is identified using the frequency response function plot, as shown in Fig. 3.2-1, and the frequency of maximum response is taken as the natural frequency of each mode(ω_r).

(b) The damping can be estimated by a number of different techniques, the most common one is the half power points. The half power points can be determined by the frequency bandwidth $\Delta\omega$ for a response level of $|h(\omega)|/\sqrt{2}$. The damping of the mode can be calculated as

$$\zeta_r = \frac{2(\omega_a^2 - \omega_b^2)}{\omega_r^2} \approx \frac{2\Delta\omega}{\omega_r} \quad \text{and} \quad \Delta\omega = \omega_a - \omega_b \tag{3.2-1a}$$

(c) An estimation of the modal coefficient of the mode can be obtained by assuming that the total response in this resonant region is attributed to a single term of the general frequency response function series such as

$$|_rA| = 2\zeta_r\omega_r|h(\omega_r)| \tag{3.2-1b}$$

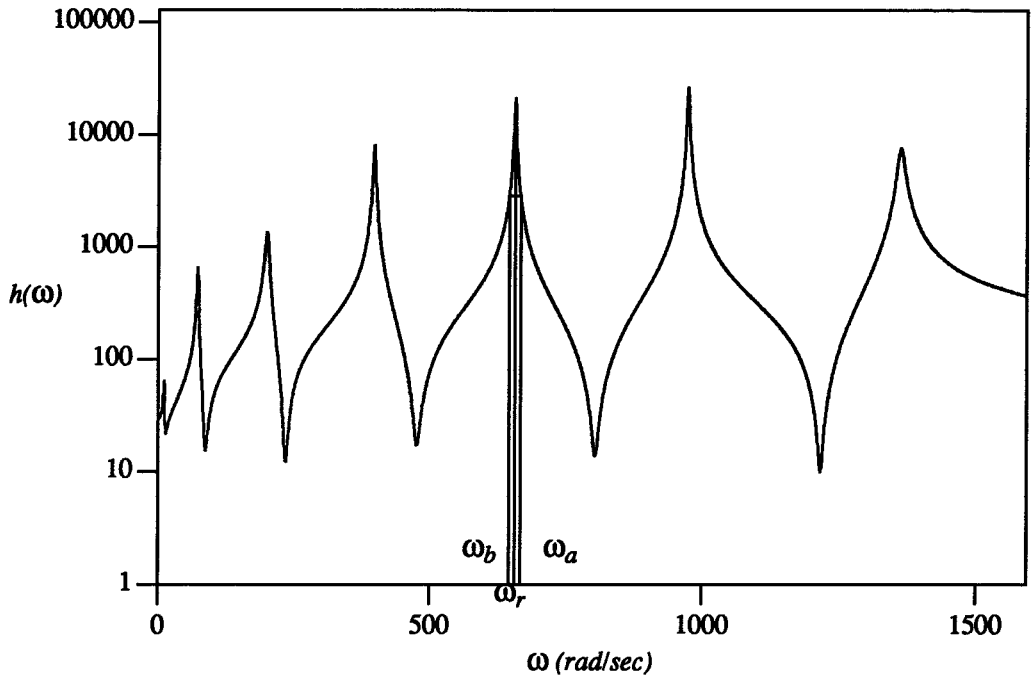

Fig. 3.2-1 Frequency Response Function

This method works adequately for structures whose frequency response functions exhibit well separated modes which are not so lightly-damped that accurate measurements at resonance are difficult to obtain but which, on the other hand, are not so heavily damped that the response at a resonance is strongly influenced by more than one mode. Apart from its simplicity, the advantage of this method is that a minimum amount of equipment can be used. If the structure is excited with a sine wave at the frequency of the resonance being investigated and the resulting response is filtered to eliminate any harmonic distortion then a simple voltmeter can be used to measure the modal coefficient. An oscilloscope can be used to determine the phase.

The main disadvantages are that the estimates of both damping and modal coefficient depend heavily on the accuracy of the maximum frequency response function level.

This is not however, a quantity which is readily measured with great accuracy, since most of the errors in measurement are concentrated around the resonant frequencies. The second disadvantage is that the single-mode assumption is not strictly applicable in many cases. Even with well-separated modes, it is often found that the neighboring modes do contribute a noticeable amount to the total response at the resonance of the mode being analyzed.

Circle Fit

Kennedy and Pancu(1947) developed the first version of the approach for the Circle Fit method for the structure with hysteretic damping characteristics. Klosterman (1971) further developed this method. As is later shown, the method can be extended to viscous damping cases and can also be extended to include complex modes by using Eqn. (2.4-71) with the following assumptions

1. The modes are only weakly coupled in the range where one mode is predominant. The contribution of lower and higher modes can be approximated by a complex constant $(R + iI)$.

2. The structure is relatively lightly damped.

The frequency response of the structure in the frequency range where the r-th mode is predominant can be obtained from Eqn. (2.4-71) as

$$h_{jk}(\omega) = \frac{{}_rU_{jk} + i\ {}_rV_{jk}}{-\zeta_r\omega_r + i(\omega - \omega_{dr})} + R + iI \tag{3.2-2}$$

where $R + iI$ includes the contribution of the term associated with the conjugated eigenvalue. ω_{dr} is the damped natural frequency and $\omega_{dr} = \omega_r\sqrt{1-\eta^2}$. It can be

proved that the real part and imaginary part of the frequency response $h_{jk}(\omega)$ form a circle. The following relations can be obtained from Eqn. (3.2-2)

$$\mathrm{Re}(h_{jk}(\omega)) = R + \frac{-{}_rU_{jk}\zeta_r\omega_r + {}_rV_{jk}(\omega - \omega_{dr})}{(\omega - \omega_{dr})^2 + (\zeta_r\omega_r)^2} \tag{3.2-3}$$

and

$$\mathrm{Im}(h_{jk}(\omega)) = I - \frac{{}_rV_{jk}\zeta_r\omega_r + {}_rU_{jk}(\omega - \omega_{dr})}{(\omega - \omega_{dr})^2 + (\zeta_r\omega_r)^2}. \tag{3.2-4}$$

Hence

$$\left[\mathrm{Re}(h_{jk}(\omega)) - (R - \frac{{}_rU_{jk}}{2\zeta_r\omega_r})\right]^2 + \left[\mathrm{Im}(h_{jk}(\omega)) - (I - \frac{{}_rV_{jk}}{2\zeta_r\omega_r})\right]^2$$

$$= \left[\frac{\sqrt{{}_rU_{jk}^2 + {}_rV_{jk}^2}}{2\zeta_r\omega_r}\right]^2. \tag{3.2-5}$$

The contribution of one dominant mode to general response is then represented in the Argand plane as a circle, as shown in Fig. 3.2-2. The coordinates of the center is

$$\left[R - \frac{{}_rU_{jk}}{2\zeta_r\omega_r},\ I - \frac{{}_rV_{jk}}{2\zeta_r\omega_r}\right] \tag{3.2-6}$$

and the diameter is

$$d = \frac{\sqrt{{}_rU_{jk}^2 + {}_rV_{jk}^2}}{\zeta_r\omega_r} \tag{3.2-7}$$

The complex modal coefficient expands or reduces the diameter and rotates the circle

in the Argand plane. On the other hand, the complex constant $(R + iI)$ will translate the center of the circle in the Argand plane, as shown in Fig. 3.2-2.

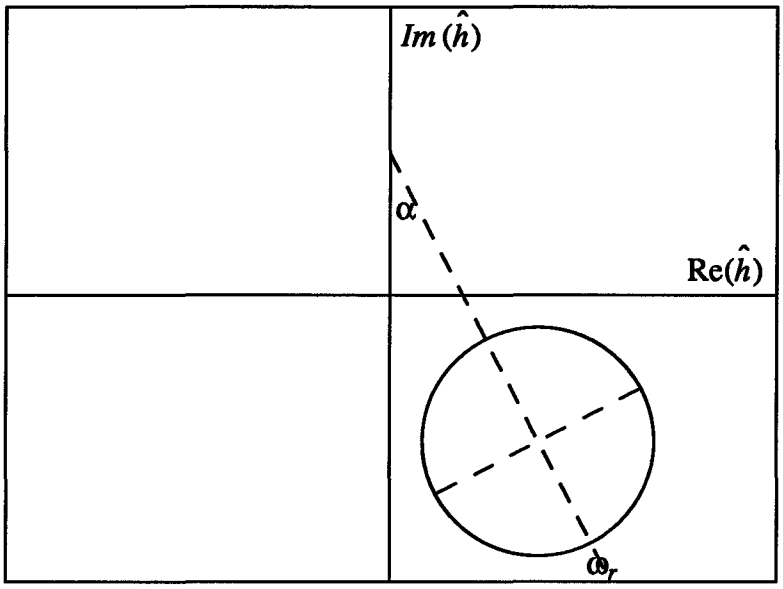

Fig. 3.2-2 Characteristics of Kennedy-Pancu Circle Fit

Using the least squares Circle Fit algorithm, a circle can be interactively fitted to the measured frequency response data at the designated natural frequency. The resonance frequency is determined by the sweep rate of the phase angle as a function of frequency. Where the rate reaches its maximum is the location of the resonance frequency. The damping ratio, as well as modal amplitude and phase, is defined by the location, diameter, and orientation of the circle.

This method is capable of separating coupled modes, but the solution may diverge and give very poor answers. The method is also fast and can be used to obtain complex modes but in order to get best possible results, should be used iteratively.

§ 3.3 MULTIPLE DEGREE OF FREEDOM METHODS IN FREQUENCY DOMAIN

The methods for single degree of freedom are straightforward and easy to implement. There are many cases however, where they cannot be applied to or do not give satisfactory results. The typical case is that modes are coupled and the single mode approximation is unreasonable. Very light damping may also cause inaccurate measurements at resonance. Therefore, methods for multiple degrees of freedom have been developed. There are many algorithms available for this task and are not described in this section individually. Instead, the different methods of frequency domain multiple curve fitting will be distinguished and their implementation will be explained. Eqn. (2.4-71) may act as the basis for development of a multiple degree of freedom method of modal identification. Continuous structures have an infinite number of degrees of freedom but, in general, only a finite number of modes can be used to describe the dynamic behavior of structures. The theoretical number of degrees of freedom can be reduced by using a finite frequency range (f_a, f_b). Consequently, the frequency response function can be broken into three partial sums, each covering the modal contribution corresponding to modes located in the frequency range (0, f_a), (f_a, f_b), (f_b, ∞) , as shown in Fig. 3.3-1.

In this case, Eqn. (2.4-71) can be rewritten as

$$h_{jk}(\omega) = \frac{y_j(\omega)}{f_k(\omega)} = -\frac{Y_{jk}}{\omega^2} + \sum_{r=r_a}^{r_b} \left(\frac{{}_rA_{jk}}{(i\omega - \lambda_r)} + \frac{{}_rA_{jk}^*}{(i\omega - \lambda_r^*)} \right) + Z_{jk} \qquad (3.3\text{-}1)$$

where

r_a = lower mode index of the frequency range of interest,

r_b = upper mode index of the frequency range of interest,

Y_{jk} = inertia restraint, and

Z_{jk} = residual flexibility.

The coefficients ${}_rA_{jk}$, ${}_rA^*_{jk}$, λ_r, λ^*_r, Y_{jk} and Z_{jk} need to be estimated using the measured frequency response data $h^m_{jk}(\omega_l)$.

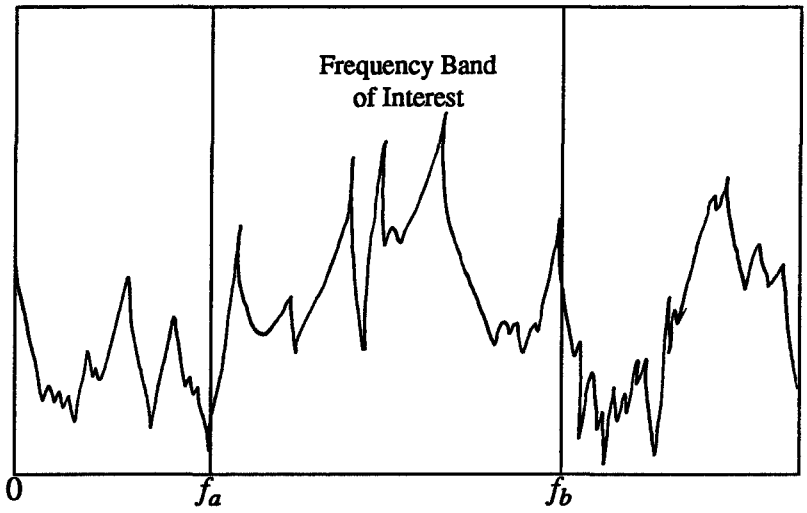

Fig. 3.3-1 Typical Frequency Response Measurement

The criterion is to minimize the error functional between the theoretical and experimental values of the frequency responses such as

$$\min[\sum_{l=1}^{N} | |h^m_{jk}(\omega_l) - h_{jk}(\omega_l)| |]. \tag{3.3-2}$$

A weighting factor w_l may be included in the criterion and

$$\min[\sum_{l=1}^{N} | |w_l(h^m_{jk}(\omega_l) - h_{jk}(\omega_l))| |] \tag{3.3-3}$$

If the derivatives of the error functional with respect to the unknowns are set to zero, a set of equations may be obtained to determine the abovementioned unknown parameters. The set of equations is nonlinear in λ_r and λ_r^* and cannot be solved directly by a linear least squares method. Therefore, algorithms have been developed to meet these needs. Mainly, there are two different procedures. The first procedure starts with fixed values of λ_r and λ_r^* that are obtained from other methods and remain unchanged throughout the procedure, the unknown modal coefficients ${}_rA_{jk}$ and ${}_rA_{jk}^*$, inertia restraint Y_{jk} and residual flexibility Z_{jk} are estimated by a linear least squares method. The second way is that an iterative least squares solution for all modal parameters is applied. These two ways may be described in more details as follows.

Linear Squares Estimation for Eigenvectors

When the eigenvalues are identified by other methods, the set of equations will be linear in the eigenvector and least squares estimation method can be used. Care has to be taken with weighting factors. The type of weighting depends on the characteristics of the measurements. For very lightly damped data , it is desirable to weight the off-resonance data because the amplitude is sharply peaked at the resonance and hence the most significant errors due to leakage and nonlinearity will occur at or near the resonances. Data near weak resonances may be more heavily weighted to help extract those modes. Areas of low coherence between excitation and response should be weighted very lightly.

To include local modes in those measurements where they are active, is essential. A local mode is a mode for which the modal displacement is nearly zero at all points on the structure except in a very small region. Because the eigenvalues are fixed in the estimation processing, the more accurate the eigenvalues are, the more accurately

will the eigenvectors be obtained.

Linearized Least Squares Algorithm

There are many cases that the eigenvalues cannot be obtained accurately by other frequency domain methods and they are allowed to change in the different measurement positions. The Gauss-Newton procedure may be used to linearize the estimation process. The frequency response function is expanded into a Taylor series and the higher-order terms are neglected, assuming that the changes in the parameters from their initial values will be small. The expansion is

$$h(\omega,e) = h(\omega,e_o) + \sum_{i=1}^{m} \frac{\partial h}{\partial e_i}(\omega,e_0)\Delta e_i \tag{3.3-4}$$

where e_0 is the vector of initial values of the modal parameters and Δe_i is the change in the i-th parameter.

The error functional to be minimized is

$$\sum_{k=1}^{N} \| h^m(\omega_k) - h(\omega,e_0) - \sum_{i=1}^{m} \frac{\partial h}{\partial e_i}(\omega_k,e_0)\Delta e_i \| . \tag{3.3-5}$$

By setting the derivatives of the functional with respect to e_i to zero, a set of linear equations for the values of Δe_i are obtained. These are solved at each iteration step, and the vector of initial values is updated,

$$e_1 = e_0 + \Delta e_i. \tag{3.3-6}$$

This processing is continued until the estimation satisfies some criteria. The

iteration procedure is devised so that any of the eigenvalues can be fixed and the remaining parameters iterated. If any mode starts to diverge, it can be fixed at the initial value or dropped from the list of eigenvalues. The most common form of divergence is for one mode to start to diverge. If this is allowed to continue, the whole process will diverge. The disadvantage of the method is that a very good set of initial values are needed and that measurement should have minimum distortion due to measurement errors.

The curve fitting method can also be applied to single mode approximation. In the case of single mode approximation, it is assumed near the resonance, the effect of all other modes could be represented by a constant. Thus the frequency response function may be written as

$$h_{jk}(\omega) = \frac{{}_{r_i}A_{jk}}{(i\omega - \lambda_{r_i})} + \frac{{}_{r_i}A^*_{jk}}{(i\omega - \lambda^*_{r_i})} - \frac{Y_{jk}}{\omega^2} + \sum_{r \neq r_i}^{r_b} \sum_{r=r_a} \left(\frac{{}_{r}A_{jk}}{(i\omega - \lambda_r)} + \frac{{}_{r}A^*_{jk}}{(i\omega - \lambda^*_r)} \right) + Z_{jk}. \tag{3.3-7}$$

If reasonably good estimates for the coefficients of the "second" term are obtained by other methods, for instance, the method described in § 3.2, then the assumption is not necessary because it can computed for each frequency.

When a set of measurement data $h^m_{jk}(\omega)$ near the resonance of ω_{r_i} is available, a true single degree of freedom behavior can be adjusted as

$$\frac{{}_{r_i}A_{jk}}{(i\omega - \lambda_{r_i})} + \frac{{}_{r_i}A^*_{jk}}{(i\omega - \lambda^*_{r_i})} = h^m_{jk}(\omega) - \left[-\frac{Y_{jk}}{\omega^2} + \sum_{r \neq r_i}^{r_b} \sum_{r=r_a} \left(\frac{{}_{r}A_{jk}}{(i\omega - \lambda_r)} + \frac{{}_{r}A^*_{jk}}{(i\omega - \lambda^*_r)} \right) + Z_{jk} \right]. \tag{3.3-8}$$

The methods described in § 3.2 may be used to obtain better estimates to the modal parameters for mode *r*. The procedure can be repeated iteratively for all the modes in the range of interest as many times as is necessary to obtain convergence to acceptable answers. In the case of strong coupling, the enhancement can be significant.

§ 3.4 TIME DOMAIN MODAL IDENTIFICATION METHODS

As mentioned in the general review, the frequency domain methods have the limitation that they cannot identify the very closely spaced modes, and they suffer from coupling of the modes which often occurs when the dampings are very heavy. To overcome these disadvantages, on one hand, the frequency domain methods have been used to attempt and overcome this problem. On the other hand, the time domain methods have developed rapidly because of computer advances. These time domain methods use time domain response data, or excitation and response data together to identify modal parameters. In contrast with the frequency domain methods, the emphasis of the time domain methods is more concentrated on the extraction computational procedures. The main time domain modal identification methods developed recently are discussed as follows.

Complex Exponential Algorithm

The time domain data for the complex exponential algorithm is a set of impulse response functions of a vibrating structure system. As indicated in Eqn. (2.5-25), the element of impulse response function matrix can be written as

$$h_{jk}(t) = \sum_{r=1}^{2n} e^{\lambda_r t}{}_r A_{jk} \tag{3.4-1}$$

where λ_r are the eigenvalues related to natural frequencies and damping ratios of a vibrating structure. ${}_rA_{jk}$ are the modal constants for the rth mode and t is the sampling time point. The basic equation for the complex exponential algorithm derived from the Prony method is

$$\sum_{r=0}^{2N} a_r h_{jk}(r) = 0 \tag{3.4-2}$$

where $a_{2N} = 1$ and a_r for $r = 0, 1, \cdots, 2N$ are to be determined.

Rearranging Eqn. (3.4-2) and collecting the impulse response functions for $t = 0, 1, 2, \cdots, 4N-1$, the full set of equations for the unknown a_r are obtained

$$\mathbf{Ha} = -\hat{\mathbf{h}} \tag{3.4-3}$$

where

$$\mathbf{H} = \begin{bmatrix} h_{jk}(0) & h_{jk}(1) & h_{jk}(2) & \cdots & h_{jk}(2N-1) \\ h_{jk}(1) & h_{jk}(2) & h_{jk}(3) & \cdots & h_{jk}(2N) \\ \vdots & \vdots & \vdots & \vdots & \vdots \\ h_{jk}(2N-1) & h_{jk}(2N) & h_{jk}(2N+1) & \cdots & h_{jk}(4N-2) \end{bmatrix} \tag{3.4-4}$$

$$\mathbf{a} = \begin{bmatrix} a_0 \\ a_1 \\ \vdots \\ a_{2N-1} \end{bmatrix} \tag{3.4-5}$$

and

$$\hat{\mathbf{h}} = \begin{bmatrix} h_{jk}(2N) \\ h_{jk}(2N+1) \\ \vdots \\ h_{jk}(4N-1) \end{bmatrix}. \tag{3.4-6}$$

This equation can be solved directly to determine the values of $a_0, a_1, \cdots, a_{2N-1}$ which are substituted into the polynomial equation to compute the poles α_i

$$a_0 + a_1\alpha + a_2\alpha^2 + \cdots + a_{2N-1}\alpha^{2N-1} = 0. \tag{3.4-7}$$

The equation is solved for the poles α_i which are used to compute the natural frequencies and damping ratios by equation $\alpha_i = e^{\lambda_i \Delta t}$.

Finally, the modal constants ${}_1A_{jk}, {}_2A_{jk}, \cdots, {}_{2N}A_{jk}$ can be calculated by the following equation

$$\mathbf{VA} = \mathbf{h} \tag{3.4-8}$$

where

$$\mathbf{V} = \begin{bmatrix} 1 & 1 & \cdots & 1 \\ \alpha_1 & \alpha_2 & \cdots & \alpha_{2N} \\ \alpha_1^2 & \alpha_2^2 & \cdots & \alpha_{2N}^2 \\ \vdots & \vdots & \vdots & \vdots \\ \alpha_1^{2N-1} & \alpha_2^{2N-1} & \cdots & \alpha_{2N}^{2N-1} \end{bmatrix}, \tag{3.4-9}$$

$$\mathbf{A} = \begin{bmatrix} {}_1A_{jk} \\ {}_2A_{jk} \\ {}_3A_{jk} \\ \vdots \\ {}_{2N}A_{jk} \end{bmatrix} \tag{3.4-10}$$

and

$$\mathbf{h} = \begin{bmatrix} h_{jk}(0) \\ h_{jk}(1) \\ h_{jk}(2) \\ \vdots \\ h_{jk}(2N-1) \end{bmatrix}. \tag{3.4-11}$$

To use this algorithm, it is necessary to have a set of impulse response data as indicated in Eqns. (3.4-4), (3.4-6) and (3.4-11) and the expected number of modes contained in these data. The advantage of the complex exponential method is that the nonlinear solution for the eigenvalues is obtained in a straightforward manner. The modal coefficients can be directly determined, as the case with frequency domain methods, when the eigenvalues are estimated.

The number of modes contained in the impulse data can be determined by computing the rank of the coefficient matrix used in calculating parameters a_r. Theoretically, when the specified number of modes exceeds the actual number of modes the matrix will be singular. However, because noise exists, the matrix will not be singular even though the specified number of modes exceeds the number of modes in the data. Hence, judgement must be used as to how the determinant of the matrix should be to zero. Despite this limitation, the procedure is a very useful one.

A further method to determine the number of modes is to use different segments of the impulse response to compute the mode constants. The variance between the computed modal constants can be used to distinguish the true modes from noise, or computational, modes.

The main disadvantage of this method is that a new set of eigenvalues is obtained for

every measurement, while in theory, the eigenvalues are the global properties of the structure. Any one of these sets will fit the data to close limits. From a plot of curve fit data, it may not be possible to distinguish the difference between the computed eigenvalues. Further, since the impulse response is the inverse Fourier transformation of the frequency response, the truncation of the frequency response may cause the distortion error in the impulse response data. It is also rather sensitive to noise since it has no inherent smoothing.

In order to overcome some shortcomings of the method, a least squares estimate version was developed. In this version, more measurements are taken into account in the computing process. Hence, Eqn. (3.4-3) can be solved by any least squares estimate method. When coefficients $a_1, a_2, \cdots, a_{2N-1}$ are computed, a set of impulse response functions at more time points is used and the least squares estimate method is also applied to Eqn. (3.4-8) to determine the modal constants ${}_1A_{jk}, {}_2A_{jk}, \cdots, {}_{2N}A_{jk}$.

The main advantage of this version is that it has the least squares elimination of noise and weighting can be associated with the least squares estimate. All of the measurements or any combination of measurements can be used to determine overall system modes by this version. In general, this version does a very good job of generating a set of eigenvalues for a structure. However, a different exciter position may generate a different set of eigenvalues and eigenvectors.

Ibrahim Time Domain Method

The Ibrahim Time Domain Method (ITD) uses free decay response as basic data to identify the modal parameters of a vibrating structure system. With consideration of measurement noise, the free decay response functions are linear combinations of the

modal parameters of the structure as shown in Eqn. (2.5-26)

$$\mathbf{y}(t) = \sum_{i=1}^{2n} e^{\lambda_i t}\boldsymbol{\psi}_i + \mathbf{w}(t) \tag{3.4-12}$$

where the $\boldsymbol{\psi}_i$ is the complex mode shape and λ_i is the eigenvalue which is related to the natural frequency and damping ratio of the vibrating structure under consideration, $\mathbf{w}(t)$ is the noise associated with the measurements.

In the ITD algorithm, two systems response matrices $\boldsymbol{\Phi}$ and $\hat{\boldsymbol{\Phi}}$ are formed such that

$$\boldsymbol{\Phi} = \begin{bmatrix} y_1(t_1) & y_1(t_2) & \cdots & y_1(t_{2r}) \\ y_2(t_1) & y_2(t_2) & \cdots & y_{2r}(t_{2r}) \\ \vdots & \vdots & \vdots & \vdots \\ y_{2n}(t_1) & y_{2n}(t_2) & \cdots & y_{2n}(t_{2r}) \end{bmatrix} = \boldsymbol{\Psi}\boldsymbol{\Lambda} \tag{3.4-13}$$

and

$$\hat{\boldsymbol{\Phi}} = \begin{bmatrix} y_1(t_1+\Delta t_1) & y_1(t_2+\Delta t_1) & \cdots & y_1(t_{2r}+\Delta t_1) \\ y_2(t_{1+}\Delta t_1) & y_2(t_2+\Delta t_1) & \cdots & y_{2r}(t_{2r}+\Delta t_1) \\ \vdots & \vdots & \vdots & \vdots \\ y_{2n}(t_1+\Delta t_1) & y_{2n}(t_2+\Delta t_1) & \cdots & y_{2n}(t_{2r}+\Delta t_1) \end{bmatrix} = \hat{\boldsymbol{\Psi}}\boldsymbol{\Lambda} \tag{3.4-14}$$

where $r > n$ and $y_i(t_j)$ is the free decay response of the i–th measurement at time t_j which is composed of n structural modes and their conjugates. Matrix $\hat{\boldsymbol{\Psi}}$ has the column vectors of $\hat{\boldsymbol{\psi}}_i = e^{\lambda_i \Delta t_1}\boldsymbol{\psi}_i$.

The two response matrices are then used in the equation

$$\mathbf{A}\boldsymbol{\Phi} = \hat{\boldsymbol{\Phi}} \tag{3.4-15}$$

to solve for **A**. When **A** is obtained, the eigenvalue problem

$$\mathbf{A}\boldsymbol{\psi} = \alpha\boldsymbol{\psi} \tag{3.4-16}$$

is then solved where the eigenvector $\boldsymbol{\psi}$ is the modal vector of the structure and the eigenvalue α can be related to the structure's eigenvalues λ by an exponential function $\alpha = e^{\lambda \Delta t_1}$. Finally the Mode Confidence Factors are computed and used to separate structural modes from noise, or computational, modes arising from use of an oversized identification model.

Poly Reference Method

The Poly Reference method also implements free decay responses but such responses are obtained from inverse FFT of the transfer functions. This algorithm was chosen to take advantage of the possible averaging of the FFT functions, thus reducing the noise levels in the computed time functions. Such reduction in noise level will require smaller identification models than the ITD method and, in turn, less computer storage and execution time. To conserve memory, only the eigenvalues are used to be computed from which the natural frequency and damping ratio are determined. The mode shape is calculated from the basic free decay response function in Eqn. (2.5-26) by a least squares estimation method. The polyreference method consists of the following steps.

1. The basic equation for the polyreference method is

$$\sum_{s=1}^{p} \mathbf{B}(s)\mathbf{F}(\exp(\mathbf{\Lambda}t))^{p-s} = \mathbf{0}. \tag{3.4-17}$$

In order to obtain the estimation of $\mathbf{B}(i)$, the following equation is formed

$$\mathbf{B}[\mathbf{T}_1 \ \cdots \ \mathbf{T}_i \ \cdots \ \mathbf{T}_m] = -[\mathbf{R}_1 \ \cdots \ \mathbf{R}_i \ \cdots \ \mathbf{R}_m] \tag{3.4-18}$$

where

$$\mathbf{R}_i = [\mathbf{y}_1(p) \ \ \mathbf{y}_2(p) \ \cdots], \tag{3.4-19}$$

$$\mathbf{T}_i = \begin{bmatrix} \mathbf{y}_i(p-1) & \mathbf{y}_i(p) & \cdots \\ \mathbf{y}_i(p-2) & \mathbf{y}_i(p-1) & \cdots \\ \vdots & \vdots & \vdots \\ \mathbf{y}_i(0) & \mathbf{y}_i(1) & \cdots \end{bmatrix} \tag{3.4-20}$$

and

$$\mathbf{B} = [\mathbf{B}(1) \ \ \mathbf{B}(2) \ \cdots \ \mathbf{B}(p)]. \tag{3.4-21}$$

The equation is usually overdetermined and thus its least squares solution can be obtained for $\mathbf{B}(i)$.

2. To determine the natural frequency and damping ratio, Eqn. (3.4-17) is multiplied by $\mathbf{e}_i$, the vector of all zeros except for a one in position i to obtain

$$\left[\sum_{s=0}^{p} \mathbf{B}(s)\alpha_i^{p-s}\right]\mathbf{F}_i = 0 \tag{3.4-22}$$

where $\alpha_i = e^{\lambda_i t}$ is the ith diagonal element of $\exp(\mathbf{\Lambda}t)$, and $\mathbf{F}_i$ is the ith row of $\mathbf{F}$.

3. A solution of the equation

$$\sum_{s=0}^{p} \mathbf{B}(s)\alpha_i^{p-s} = 0 \tag{3.4-23}$$

determines α_i. These α_i obtained are then substituted into Eqn. (3.4-22) and a complete set of mutually orthogonal vectors $\mathbf{F}_i$ can be found by solving Eqn. (3.4-22).

4. The natural frequency and damping ratio can be computed using the relation $\alpha_i = e^{\lambda_i t}$.

5. The mode shapes then can be found by solving the equation

$$\begin{bmatrix} \mathbf{y}_i(0) \\ \mathbf{y}_i(1) \\ \vdots \\ \mathbf{y}_i(j) \end{bmatrix} = \begin{bmatrix} \mathbf{F} \\ \mathbf{F}\exp(\Lambda t) \\ \vdots \\ \mathbf{F}\exp(\Lambda t)^j \end{bmatrix} \mathbf{S}\mathbf{x}_i(0) \tag{3.4-24}$$

where $\mathbf{x}_i(0)$ is the system state variable at time zero.

FFT algorithm transfers the time domain records into frequency domain data and these spectra are used to compute frequency response function. In the polyreference method, the frequency function is transformed back to the time domain. Errors arising from such transformation need to be investigated. Effects of leakage and frequency resolution on the identified results should also be studied.

Eigensystem Realization Algorithm

The Eigensystem Realization Algorithm was developed on the basis of the principles of minimal realization theory introduced by Ho and Kalman (1965). The basic formulation of the method is started with the state representation of a finite-dimensional, discrete time, linear, time-invariant vibrating structure as represented in Eqn. (2.5-28)

$$\mathbf{x}(k+1) = \mathbf{T}\mathbf{x}(k) + \mathbf{\Delta}\mathbf{f}(k) \tag{3.4-25}$$

and observation equation

$$\mathbf{y}(k) = \mathbf{C}\mathbf{x}(k). \tag{3.4-26}$$

Two special solutions to the state variable are the impulse response function

$$\mathbf{Q}(k) = \mathbf{C}\mathbf{T}^{k-1}\mathbf{\Delta} \tag{3.4-27}$$

and the initial state condition response

$$\mathbf{Q}(k) = \mathbf{C}\mathbf{A}^{k}[\mathbf{x}_1(0)\ \mathbf{x}_2(0)\ \cdots\ \mathbf{x}_m(0)]. \tag{3.4-28}$$

The minimal system realization is that when measurements $\mathbf{y}(k)$ are obtained, a set of constant matrices, [**T** **Δ** **C**], are constructed in terms of $\mathbf{y}(k)$ such that the identities of Eqn. (3.4-27) hold, and the order of **T** is a minimum.

The algorithm commences by forming the following $r \times s$ block matrix

$$\mathbf{H}_{rs}(k) = \begin{bmatrix} \mathbf{Q}(k) & \mathbf{Q}(k+t_1) & \cdots & \mathbf{Q}(k+t_{s-1}) \\ \mathbf{Q}(j_1+k) & \mathbf{Q}(j_1+k+t_1) & \cdots & \mathbf{Q}(j_1+k+t_{s-1}) \\ \vdots & \vdots & \vdots & \vdots \\ \mathbf{Q}(j_{r-1}+k) & \mathbf{Q}(j_{r-1}+k+t_1) & \cdots & \mathbf{Q}(j_{r-1}+k+t_{s-1}) \end{bmatrix}. \tag{3.4-29}$$

From the state representation and observation equations,

$$\mathbf{H}_{rs}(k) = \mathbf{V}_r \mathbf{T}^k \mathbf{W}_s^T \tag{3.4-30}$$

with

$$\mathbf{V}_r = \begin{bmatrix} \mathbf{C} \\ \mathbf{C}\mathbf{T}^{j_1} \\ : \\ : \\ \mathbf{C}\mathbf{T}^{j_{r-1}} \end{bmatrix} \tag{3.4-31}$$

and

$$\mathbf{W}_s^T = [\boldsymbol{\Delta} \;\; \mathbf{T}^{t_1}\boldsymbol{\Delta} \;\; \cdots \;\; \mathbf{T}^{t_{s-1}}\boldsymbol{\Delta}]. \tag{3.4-32}$$

$\mathbf{V}_r$ and $\mathbf{W}_s^T$ are the observability and controllability matrices, respectively.

The implementation of the method is as follows.

1. Factorize the block data matrix for k=1 using singular value decomposition

$$\mathbf{H}(0) = \mathbf{P}_N \mathbf{D}_N \mathbf{A}_N^T \tag{3.4-33}$$

where the columns of $\mathbf{P}_N$ and $\mathbf{A}_N^T$ are orthonormal and $\mathbf{D}_N$ is diagonal

$$\mathbf{D}_N = \begin{bmatrix} d_1 & \cdots & 0 & 0 & 0 \\ \vdots & \vdots & \vdots & \vdots & \vdots \\ 0 & \cdots & d_n & 0 & 0 \\ 0 & \cdots & 0 & d_{n+1} & 0 \\ \vdots & \vdots & \vdots & \vdots & \vdots \\ 0 & \cdots & 0 & 0 & d_N \end{bmatrix} \tag{3.4-34}$$

with monotonically non-increasing d_i (i=1, 2, ···, N)

$$d_1 \geq d_2 \geq \cdots \geq d_n \geq d_{n+1} \geq \cdots \geq d_N \geq 0. \tag{3.4-35}$$

2. $\mathbf{D}_N$ is replaced by a diagonal matrix $\mathbf{D}_n$ that differs from $\mathbf{D}_N$ only by truncation on d_{n+1}, ···, d_N. Correspondingly, matrices $\mathbf{P}_n$ and $\mathbf{A}_n$ are obtained by deleting the last $N-n$ columns of $\mathbf{P}_N$ and $\mathbf{A}_N$, respectively. The matrix $\mathbf{P}_n\mathbf{D}_n\mathbf{A}_n^T$ is the closest one to $\mathbf{H}(0)$ in the sense of maximal signal to noise ratio.

3. The reduced order realization of dimension n can be constructed by

$$\mathbf{T}^k = \mathbf{D}_n^{\frac{1}{2}} \mathbf{P}_n^T \mathbf{H}(k) \mathbf{A}_n \mathbf{D}_n^{-\frac{1}{2}}, \tag{3.4-36}$$

$$\mathbf{\Delta} = \mathbf{D}_n^{\frac{1}{2}} \mathbf{A}_n^T \mathbf{E}_{m1} \tag{3.4-37}$$

and

$$\mathbf{C} = \mathbf{E}_{p1}^T \mathbf{P}_n \mathbf{D}_n^{\frac{1}{2}} \tag{3.4-38}$$

where $\mathbf{E}_{m1}^T = [\mathbf{I}_m \ \mathbf{0}]$ and $\mathbf{E}_{p1}^T = [\mathbf{I}_p \ \mathbf{0}]$ with $\mathbf{I}_m$ and $\mathbf{I}_p$ being identity matrices of order m, and p and $\mathbf{0}$ a null matrix of appropriate dimensions.

The advantage of this method is that it permits the inclusion of only good and stringently measured signals without losing capability. The usefulness of this capability is the potential to minimize the distortion of the identified parameters caused by noise. Apart from this, a judicious choice of data and their proper arrangement in the block matrix $\mathbf{H}(0)$ can also be used to minimize the computational requirements of the method. These efforts could substantially reduce the order of the matrix for a numerically large problem.

Direct Parameter Model Identification Method

The Direct Parameter Model Identification Method was developed by J. M. Leuridan et al. (1985). This method starts with a higher order matrix differential equation describing the forced response of a linear viscous damped vibrating structure

$$[\mathbf{I}(\frac{d}{dt})^{2n} + \mathbf{D}_1(\frac{d}{dt})^{2n-1} + \cdots + \mathbf{D}_{2n}]\mathbf{y}(t) = [\mathbf{Q}_0(\frac{d}{dt})^{2n-2} + \cdots + \mathbf{Q}_{2n-2}]\mathbf{f}(t). \qquad (3.4\text{-}39)$$

$\mathbf{f}(t)$ represents the force excitation at the n_i excitation locations and $\mathbf{y}(t)$ the response, in the presence of random uncorrelated noise, at the n_o response locations. The matrices $\mathbf{D}_i$ and $\mathbf{Q}_i$ have appropriate dimensions.

Eqn. (3.4-39) is then discretized to yield the following difference equation

$$\mathbf{y}_k - \mathbf{A}_1\mathbf{y}_{k-1} - \cdots - \mathbf{A}_{2n}\mathbf{y}_{k-2n} = \mathbf{B}_0\mathbf{f}_k + \mathbf{B}_1\mathbf{f}_{k-1} + \cdots + \mathbf{B}_{2n-1}\mathbf{f}_{k-2n+1}. \qquad (3.4\text{-}40)$$

Eqn. (3.4-40) is rewritten as

$$\mathbf{XC} = \mathbf{F} + \mathbf{W} \tag{3.4-41}$$

where

$$\mathbf{C}^T = [\mathbf{C}_0 \;\; \mathbf{C}_1 \;\; \cdots \;\; \mathbf{C}_{2n-1}] \tag{3.4-42}$$

with

$$\mathbf{C}_i = [\mathbf{A}_{i+1} \;\; \mathbf{B}_i], \tag{3.4-43}$$

$$\mathbf{X}^T = \begin{bmatrix} \mathbf{z}_{n_b} & \mathbf{z}_{n_b+1} & \cdots & \mathbf{z}_{n_e} \\ \mathbf{z}_{n_b-1} & \mathbf{z}_{n_b} & \cdots & \mathbf{z}_{n_e-1} \\ \vdots & \vdots & \vdots & \vdots \\ \mathbf{z}_{n_b-2n+1} & \mathbf{z}_{n_b-2n} & \cdots & \mathbf{z}_{n_e-2n+1} \end{bmatrix} \tag{3.4-44}$$

with

$$\mathbf{z}_i = \begin{Bmatrix} \mathbf{y}_{i-1} \\ \mathbf{f}_i \end{Bmatrix}, \tag{3.4-45}$$

$$\mathbf{F}^T = [\mathbf{f}_{n_b} \;\; \mathbf{f}_{n_b+1} \;\; \cdots \;\; \mathbf{f}_{n_e}] \tag{3.4-46}$$

and

$$\mathbf{W}^T = [\mathbf{w}_{n_b} \;\; \mathbf{w}_{n_b+1} \;\; \cdots \;\; \mathbf{w}_{n_e}]. \tag{3.4-47}$$

The coefficient matrices $\mathbf{C}_i$ can be estimated by any least squares estimate method from measurements $\mathbf{f}_i$ and $\mathbf{y}_i$ using Eqn. (3.4-41). When impulse response function data are used, the following equation is used to represent the impulse response

$$[z\mathbf{I}-\mathbf{A}]\mathbf{E}(z)\mathbf{G}(z)=\mathbf{B}(z) \tag{3.4-48}$$

with

$$\mathbf{A}=\begin{bmatrix}\mathbf{A}_1 & \mathbf{A}_2 & \cdots & \mathbf{A}_{2n}\\ \mathbf{I} & \mathbf{0} & \cdots & \mathbf{0}\\ \mathbf{0} & \mathbf{I} & \cdots & \mathbf{0}\\ \vdots & \vdots & \vdots & \vdots\\ \mathbf{0} & \mathbf{0} & \cdots & \mathbf{I}\end{bmatrix} \tag{3.4-49}$$

$$\mathbf{E}(z)=\begin{bmatrix}z^{2n-1}\mathbf{I}\\ z^{2n-2}\mathbf{I}\\ \vdots\\ \mathbf{I}\end{bmatrix} \quad \mathbf{B}(z)=(\Delta t)^{-1}\begin{bmatrix}z^{2n}\mathbf{B}_0+\cdots+z\mathbf{B}_{2n-1}\\ \mathbf{0}\\ \vdots\\ \mathbf{0}\end{bmatrix}. \tag{3.4-50}$$

The mode shapes and eigenvalues can be computed as follows

$$\mathbf{A}\boldsymbol{\Psi}=\boldsymbol{\Psi}\mathbf{Z} \tag{3.4-51}$$

and the mode participated coefficients can be obtained as

$$\boldsymbol{\phi}_i=\lim_{z\to z_i}(z^{-1}\,|\boldsymbol{\Psi}^{-1}\mathbf{B}(z)|_i). \tag{3.4-52}$$

On the basis of the above theory, the implementation of the method is

1. Determine the rank r of sampled correlation matrix $\mathbf{R}_{yy}(0)$ by a singular value decomposition such as

$$\mathbf{R}_{yy}(0) = \mathbf{U}\mathbf{S}\mathbf{U}^T. \tag{3.4-53}$$

2. Using original or enhanced data sequences to estimate the coefficients matrices $\mathbf{A}_i$ and $\mathbf{B}_i$. The enhanced data sequences $\mathbf{H}_k^e$ may be transformed from original data $\mathbf{H}_k$ as

$$\mathbf{H}_k^e = \mathbf{U}_r\mathbf{H}_k \tag{3.4-54}$$

where $\mathbf{U}_r$ is the first r rows of matrix $\mathbf{U}$.

3. The modal parameters are calculated from the estimated matrices by Eqns. (3.4-47), (3.4-51) and (3.4-52).

4. Structural modes are separated from the noise and computation modes by inspection of damping values, maximum residues and validity of reciprocity.

Extended Kalman Filter - Weighted Global Iteration Procedure

The basic algorithm for this procedure is a recursive process for estimating the optimal state of the structure, and the identified modal parameters are included in the state variable. The procedure may be summarized as follows.

A general vibrating structure can be described by

$$\mathbf{x}(t) = \mathbf{f}(\mathbf{x}, t) + \mathbf{w}(t) \tag{3.4-55}$$

with observation at time $t = k\Delta t$,

$$\mathbf{y}(k) = \mathbf{C}\mathbf{x}(k) + \mathbf{v}(k) \tag{3.4-56}$$

where

$\mathbf{x}(k)$ = state vector at $t = k\Delta t$

$\mathbf{y}(k)$ = observation vector at $t = k\Delta t$;

$\mathbf{v}(k)$ = observation noise vector;

$\mathbf{w}(t)$ = system noise vector and

$\mathbf{C}$ = matrix associated with the observation.

Then, the state vector $\mathbf{x}(k+1)$ and its error covariance matrix $\mathbf{P}(k+1)$ at time $t = (k+1)\Delta t$ can be estimated recursively in light of $\mathbf{y}(k)$ as follows;

$$\hat{\mathbf{x}}(k+1) = \hat{\mathbf{x}}(k) + \int_{k\Delta t}^{(k+1)\Delta t} \mathbf{f}(\hat{\mathbf{x}}(i), t)dt + \mathbf{K}(k)[\mathbf{y}(k) - \mathbf{C}\hat{\mathbf{x}}(k)] \tag{3.4-57}$$

where the Kalman gain matrix $\mathbf{K}(k)$ is

$$\mathbf{K}(k) = \mathbf{P}(k)\mathbf{C}^T[\mathbf{C}\mathbf{P}(k)\mathbf{C}^T + \nabla_v]^{-1} \tag{3.4-58}$$

and

$$\mathbf{P}(k+1) = \mathbf{T}(k)[\mathbf{I} - \mathbf{K}(k)\mathbf{C}]\mathbf{P}(k)\mathbf{T}^T(k) + \nabla_w. \tag{3.4-59}$$

The state transition matrix $\mathbf{T}(k)$ can be evaluated approximately by

$$\mathbf{T}(k) \approx \mathbf{I} + \Delta t[\frac{\partial f(\mathbf{x}, t)}{\partial \mathbf{x}_j}]_{\mathbf{x} = \hat{\mathbf{x}}(k)}. \tag{3.4-60}$$

The extended Kalman filter algorithm starts with the initial conditions, $\hat{\mathbf{x}}(t_0)$ and $\mathbf{P}(t_0)$, to obtain $\hat{\mathbf{x}}(t_s)$ and $\mathbf{P}(t_s)$. Then $\mathbf{x}(t_0)$ and $\mathbf{P}(t_0)$ are replaced by $\hat{\mathbf{x}}(t_s)$ and $\mathbf{P}(t_s)$ and multiplied by a weight, $\mathbf{W}$, and the algorithm is iterated until the values become stable. The stability and convergency of the estimated parameters are also estimated by the nature of the objective function, θ. The objective function is defined as

$$\theta = [\sum_{i=1}^{N} (\gamma_i - \bar{\beta})^2]^{1/2} \tag{3.4-61}$$

and

$$\bar{\beta} = \frac{1}{N} \sum_{i=1}^{N} \gamma_i \qquad \gamma_i = \frac{\sum_{k=1}^{s} z_i^2(k)}{\sum_{k+1}^{s} y_i^2(k)} \tag{3.4-62}$$

$$z_i(k) = y_i(k) - f_i[\hat{x}(t_{k)}, \ t_k] \tag{3.4-63}$$

where

s = number of sampling points of observations,

N = dimension of observation vector $\mathbf{y}(k)$,

$\hat{x}_i$ = the ith component of the state vector $\hat{\mathbf{x}}$and

y_i = the ith component of observation vector $\mathbf{y}$.

The method can be used for the case of nonlinear structures and heavily corrupted observation data. The convergence for a nonlinear-hysteretic restoring force model was reported to be good by Hoshiya and Saito (1984). However, the degree of freedom of the structure being excited has to be decided in advance so that the Kalman filter performs well. The reasonably accurate initial estimates of the modal

parameters are essential for the method. Weight matrix **W** is important for accelerating the estimation process and reaching a stable state. To determine the weight matrix **W** requires, however, the user's judgement and experience.

Time Series Methods

Time series methods for modal identification have been studied by many researchers. The basic idea is that the discrete time series sequence of uniformly spaced samples of a scalar white noise excited stationary linear differential equation can be represented as an auto-regressive and moving average model. That is, the model such as

$$\sum_{i=0}^{2n} \alpha_i y_{t-i} = \sum_{i=0}^{2n} \beta_i e_{t-i}\,, \qquad \alpha_0 = \beta_0 = 1 \tag{3.4-64}$$

can represent an n-degree of freedom structural system that is representable by a set of ordinary differential equations excited by a vector white noise force.

In Eqn. (3.4-64) the coefficients $\alpha_1, \cdots, \alpha_{2n}$ are the coefficients of a characteristic polynomial of the discrete time system. They are related to the damping and natural frequencies η_i and ω_i $j = 1, \cdots, n$ of the structural system by

$$\sum_{i=0}^{2n} \alpha_i \xi^{2n-i} = \sum_{i=1}^{n} (\xi - \xi_i)(\xi - \xi_i^*) \tag{3.4-65}$$

and

$$\xi_i,\ \xi_i^* = \exp(-\eta_i \omega_i T \pm i\omega_i \sqrt{1-\eta_i^2}\, T) \tag{3.4-66}$$

where the ξ_i are the eigenvalues of the structure.

The two stage least squares procedures are used to estimate the $2n$ AR and $2n$ MA parameters for the ARMA model, $\alpha_1, \cdots, \alpha_{2n}, \beta_1, \cdots, \beta_{2n}$. The ARMA model can be written

$$\mathbf{y} = \mathbf{X}\boldsymbol{\theta} + \mathbf{e} \tag{3.4-67}$$

with

$$\mathbf{y} = \begin{bmatrix} y_{2n+1} \\ y_{2n+2} \\ \vdots \\ y_{2n+N} \end{bmatrix} \qquad \mathbf{e} = \begin{bmatrix} e_{2n+1} \\ e_{2n+2} \\ \vdots \\ e_{2n+N} \end{bmatrix} \tag{3.4-68}$$

$$\mathbf{X} = \begin{bmatrix} -y_{2n} & \cdots & -y_1 & -e_{2n} & \cdots & -e_1 \\ -y_{2n+1} & \cdots & -y_2 & -e_{2n+1} & \cdots & -e_2 \\ \cdots & \cdots & \cdots & \cdots & \cdots & \cdots \\ -y_{2n+N-1} & \cdots & -y_n & -e_{2n+N-1} & \cdots & -e_n \end{bmatrix} \tag{3.4-69a}$$

$$\boldsymbol{\theta} = \begin{bmatrix} \alpha_1 \\ \vdots \\ \alpha_{2n} \\ \beta_1 \\ \vdots \\ \beta_{2n} \end{bmatrix}. \tag{3.4-69b}$$

The estimate $\hat{\boldsymbol{\theta}}$, of $\boldsymbol{\theta}$, can be written as

$$\hat{\boldsymbol{\theta}} = [\mathbf{X}^T\mathbf{X}]^{-1}\mathbf{X}^T\mathbf{y}. \tag{3.4-70}$$

The covariances $C_{yy}(k)$, $C_{ee}(k)$, $C_{ye}(k)$ and $C_{ey}(k)$ are required for the solution of Eqn. (3.4-70). The value of $C_{yy}(k)$ for the observation data with noise may be written $C_{yy}(k) = C_{yy}(k) + \sigma_n^2\delta_k$. That is, the influence of the noise variation only changes the value of $C_{yy}(k)$ in the $C_{yy}(0)$ term.

As the first least squares stage, a "long" but finite AR time series model approximation to the y_t data in the ARMA model can be written in the form

$$\sum_{i=0}^{p}\bar{\alpha}_i y_{t-i} = e_t, \quad \bar{\alpha}_0 = 1, \quad E\{e_t\} = 0 \quad E\{e_t e_s\} = \sigma_e^2\delta_{t,s}. \tag{3.4-71}$$

The values of σ_e^2 and $\bar{\alpha}_i$, $i = 1, \cdots, p$ may be computed by solving the linear set of Yule-Walker equations

$$\sum_{i=0}^{p}\bar{\alpha}_i C_{yy}(k-i) = 0, \quad k=1, \cdots, p \tag{3.4-72}$$

and

$$\sigma_e^2 = \sum_{i=0}^{p}\bar{\alpha}_i C_{yy}(i).$$

The coefficients of the impulse response model corresponding to the "long" AR model satisfy the recursive formula

$$h_i = -\sum_{j=1}^{p}\bar{\alpha}_j h_{i-j}, \quad i=1, \cdots, 2n, \tag{3.4-73}$$

with $h_0 = 1$ and $h_i = 0$ for $i < 0$.

Finally, the $\sigma_{ye}(k)$ will be calculated by

$$C_{ye}(k) = \sigma_e^2 h_k \qquad k \geq 0 \tag{3.4-74}$$

with $h_k = 0$ for $k < 0$.

For the white noise excitation, $C_{ee}(k) = \sigma_e^2 \delta_k$. Since σ_e^2 is computed in fitting the "long" AR model in Eqn. (3.4-71), $C_{ey}(k) = C_{ye}(-k)$ is available from Eqn. (3.4-47) and $C_{yy}(k)$ is given, all the information required for the computation of the ARMA parameters α_i, β_i, $(i = 1, \cdots, 2n)$ in the second least squares stage can thus be computed via the first least squares stage.

As the second least squares stage, these covariances will be used in Eqn. (3.4-67) to estimate the parameters $\alpha_1, \cdots, \alpha_{2n}, \beta_1, \cdots, \beta_{2n}$.

Chapter 4

MODAL IDENTIFICATION OF VIBRATING STRUCTURES

One service mathematics has rendered the human race; it has put common sense back where it belongs, on the topmost shelf next to the dusty cannister labeled "discarded nonsense".

E. T. Bell

§ 4.1 INTRODUCTION

This chapter investigates the modal identification of a linear damped vibrating structure using response and/or excitation data in the time domain. The basic equations for the theoretical modal analysis with consideration of nonproportional

damping are Eqns. (2.3-26) and (2.3-28)

$$[\lambda^2\mathbf{M}_0 + \lambda\mathbf{C}_0 + \mathbf{K}_0] = \mathbf{0} \tag{4.1-1}$$

and

$$\lambda = -\eta\omega \pm i\omega\sqrt{1-\eta^2} \tag{4.1-2}$$

In the modal analysis, the matrices $\mathbf{M}_0$, $\mathbf{C}_0$ and $\mathbf{K}_0$ are used to calculate the eigenvalues and eigenvectors and thus the natural frequencies ω_i and damping ratios η_i. In the modal identification, the matrices $\mathbf{M}_0$, $\mathbf{C}_0$ and $\mathbf{K}_0$ are not known. The modal parameters of the structure have to be identified from vibration test data in terms of responses $\mathbf{y}(t)$ of the structure and excitations $\mathbf{f}(t)$. For the task of modal identification, models describing the relationship of excitations, initial conditions and responses of the structure are needed. As mentioned in chapter 3, the use of different descriptions of the motion of the structure will lead to different methods of the modal identification. In this study, use is made of the ARMAX model (autoregressive and moving average with control excitation model) of a vibrating structure for the modal identification in the time domain. The ARMAX model may be represented by the following equation

$$\begin{aligned}&\mathbf{y}(k) + \mathbf{G}_s\mathbf{y}(k-1) + \cdots + \mathbf{G}_1\mathbf{y}(k-s)\\ &= \mathbf{R}_m\mathbf{f}(k-1) + \cdots + \mathbf{R}_1\mathbf{f}(k-m) + \mathbf{e}(k) + \mathbf{S}_p\mathbf{e}(k-1) + \cdots + \mathbf{S}_1\mathbf{e}(t-p)\end{aligned} \tag{4.1-3}$$

This model describes the relationship of excitation $\mathbf{f}(k)$, response $\mathbf{y}(k)$ and noise $\mathbf{e}(k)$ in the time domain and thus may be used for the modal identification in the time domain. Using the ARMAX model to identify the modal parameters of a vibrating

structure consists of two main steps. First, the coefficient matrices $\mathbf{G}_i$ are determined using observed responses $\mathbf{y}(k)$ and/or excitations $\mathbf{f}(k)$ in the time domain. Second, the modal parameters are extracted through the relationship of these matrices $\mathbf{G}_i$ with the modal parameters. Matrices $\mathbf{G}_i$ may be estimated by numerical estimation methods using test data. For the different situation, different numerical method should be used. In this chapter, the least squares estimation method is used to illustrate the calculation of matrices $\mathbf{G}_i$. The major part of this chapter is devoted to establishing the relationships between the ARMAX model and other models of a vibrating structure and to develop two new methods for the modal identification based on these relationships.

The first method uses the estimated matrices $\mathbf{G}_i$ from the ARMAX model to form the following matrix

$$\mathbf{G} = \begin{bmatrix} \mathbf{0} & \mathbf{I} & \cdots & \mathbf{0} \\ \mathbf{0} & \mathbf{0} & \cdots & \mathbf{0} \\ \cdot\cdot & \cdot\cdot & \cdots & \cdot\cdot \\ \mathbf{0} & \mathbf{0} & \cdots & \mathbf{I} \\ \mathbf{G}_s & \mathbf{G}_{s-1} & \cdots & \mathbf{G}_1 \end{bmatrix} \tag{4.1-4}$$

The eigenvalue problem of the matrix $\mathbf{G}$ is solved and the modal parameters of the vibrating structure are derived from the eigenvalues and eigenvectors of the matrix $\mathbf{G}$.

The second method is also based on the ARMAX model of a vibrating structure. The mode shapes are identified separately from identification of the natural frequencies and damping ratios. The natural frequencies and damping ratios are identified through the transfer function of a univariate ARMAX model of the vibrating structure. Once the coefficients G_i of the univariate ARMAX model of the

vibrating structure are determined, the transfer function of the ARMAX model is obtained as

$$G(z) = 1 + G_{2n}z^{-1} + \cdots + G_1 z^{-2n} \tag{4.1-5}$$

The zeros of the transfer function are used to calculate the natural frequencies and damping ratios of the vibrating structure. The impulse response function matrix sequence is obtained from the multivariate ARMAX model. The mode shapes of the vibrating structure are derived from the impulse response function matrices with the identified natural frequencies and damping ratios. For the different character of excitations, the impulse response matrices may be obtained form different formulations describing the relationship of the impulse response function matrices with the coefficient matrices of the corresponding model of the vibrating structure.

For convenience, the first method is called the direct method, while the second method is referred to as the indirect method in this thesis. Some types of excitation techniques, including controlled deterministic excitation, controlled random excitation and random ambient excitation, can be used with the both methods. Both methods are also suitable to the free decay response data, which is often used in the free vibration modal testing.

The main advantages of both direct and indirect methods are as follows

1. They are very flexible and may be used with free decay response test, control excitation test and ambient excitation test. Either deterministic or stochastic excitations may be used.

2. The computation time may be saved, in particular, for the direct method.

3. The direct method is a general method and can be reduced to most present modal identification methods in the time domain.

4. Closely spaced frequencies can be identified.

The organization of this chapter is as follows. In § 4-2, an ARMAX model of a linear vibrating structure is developed from the response model of the structure in the time domain. The relationship of the coefficient matrices of the ARMAX model to the state transition matrix and output matrix of the structure is derived. § 4-3 is devoted to the development of the direct method for modal identification. The relationship between the eigen parameters of the structure and coefficient matrices of the ARMAX model is derived. This relationship forms the basis on which the modal parameters of the structure are identified. In § 4-4 the sampling impulse response model of a vibrating structure is introduced. The indirect method for modal identification is developed in § 4.5. The relationship between the eigenvalues of the structure and zeros of the transfer function of the ARMAX model is derived. The relationship of an AR model of the vibrating structure and its sampling impulse response model is also developed. The coefficient matrices of the AR model are identified using time domain data. These coefficient matrices are then used for the calculation of the impulse function matrices which are in turn used with the identified frequencies and damping ratios to determine the mode shapes of the vibrating structure. One of difficulties in modal identification is that the number of the modes of a vibrating structure which are excited in a test are not known in advance. § 4-6 discusses the methods for determination of the number of the modes being excited in a test from the observation data. In addition, some aspects related to the application of the proposed methods are also discussed. In § 4-7 numerical examples are presented to illustrate the implementation and usefulness of both developed methods. Finally, in § 4-8, a short summary is presented.

§ 4.2 ARMAX MODEL OF A DAMPED VIBRATING STRUCTURE

§ 4.2.1 Background

In order to identify the modal parameters of a linear damped vibrating structure using its ARMAX model, the ARMAX model needs first to be derived. The forced response model of a vibrating structure expressed in Eqn. (2.4-34) is used to achieve this goal. Generally excitation between the sampling intervals is unknown, therefore to calculate the integral in Eqn. (2.4-34) some approximations must be used. In this account the simplest assumption used is that the excitations remain constant during the interval, having a value between $\mathbf{f}(kt)$ and $\mathbf{f}((k+1)t)$

$$\mathbf{f}(kt+\tau) = m\mathbf{f}((k+1)t) + (1-m)\mathbf{f}(kt) \qquad 0 \le m < 1$$

Inserting $m = 0$ in the above equation

$$\mathbf{f}(kT+\tau) = \mathbf{f}(kT)$$

and Eqn. (2.4-44) can then be used and rewritten for the convenience of derivation

$$\mathbf{x}(k+1) = \mathbf{T}\mathbf{x}(k) + \Delta\mathbf{f}(k) \tag{4.2-1a}$$

$$\mathbf{x}(k+i) = \mathbf{T}^i\mathbf{x}(k) + \sum_{l=0}^{i-1}\mathbf{T}^{i-l-1}\Delta\mathbf{f}(k+l) \tag{4.2-1b}$$

where $\mathbf{x}(k)$ is a $2n$ state vector of the vibrating structure, $\mathbf{f}(k)$ is a p excitation vector, and $\mathbf{T}(t)$ is a $2n \times 2n$ state transition matrix of the vibrating structure.

$\mathbf{T}(t) = \exp(\mathbf{A}t)$ and $\Delta(t)$ is a $2n \times p$ matrix with

$$\Delta(t) = \int_0^t \mathbf{T}(t-\tau)\mathbf{B}d\tau$$

where **A** is the system matrix of the vibrating structure and **B** is the input matrix

$$\mathbf{A} = \begin{bmatrix} \mathbf{0} & \mathbf{I} \\ -\mathbf{M}_0^{-1}\mathbf{K}_0 & -\mathbf{M}_0^{-1}\mathbf{C}_0 \end{bmatrix} \quad \text{and} \quad \mathbf{B} = \begin{bmatrix} \mathbf{0} \\ \mathbf{M}_0^{-1}\mathbf{D}_0 \end{bmatrix} \tag{4.2-1c}$$

When the excitations are generated by digital generator, the above assumption about the excitation is accurate. The other kind of approximation of excitation can also be used. It is noted that the different approximations of the excitation does not affect the identification of modal parameters.

In practice, not all the state variables can be measured. Thus a measurement equation describing the relationship between measured responses and state variables is introduced. It is assumed that the first r displacements of the structure are measured and that the measurement is subject to measurement noise that also affects the measurements. It is assumed such effects can be lumped into an additive term $\mathbf{n}(k)$ at the output

$$\mathbf{y}(k) = \mathbf{C}\mathbf{x}(k) + \mathbf{n}(k) \tag{4.2-2}$$

where $\mathbf{y}(k)$ is the measured response, $\mathbf{y}(k) \in R^r$, and $\mathbf{n}(k)$ is the measurement noise, $\mathbf{n}(k) \in R^r$ at time $t = kT$. The noise $\mathbf{n}(k)$ is assumed to be independent of $\mathbf{x}(k)$ and have zero mean $E[\mathbf{n}(t)] = \mathbf{0}$ and finite covariance matrix $E[\mathbf{n}(t)\mathbf{n}^T(t-j)] = \nabla\delta_{tj} \neq \mathbf{0}$. ∇ is an $r \times r$ real positive definite matrix, and δ_{tj} is the Kronecker symbol. Both $\mathbf{x}$ and $\mathbf{n}(k)$ are unmeasurable. The measurement matrix $\mathbf{C}$ is an r ($mu\,2n$ matrix and has the rank of r

$$\mathbf{C} = [\ \mathbf{I}\ \mathbf{0}\ ] \tag{4.2-3}$$

where $\mathbf{I}$ is a $r \times r$ unit matrix and $\mathbf{0}$ is an $r \times (2n-r)$ null matrix.

There are many sources and causes for the noise term in Eqn. (4.2-2). Basically they are measurement noise because the sensors that measure the signals are subject to noise or drift.

Uncontrollable excitation that the structure is subject to is signals that have the character of excitation, but not controllable by the user, for example the ambient excitation to buildings. This uncontrollable excitation occurs in an unpredictable manner. The noise may in some case be separately measurable, but in the typical situation they are not noticeable only via their effect on the observed output. The assumption that the noise enters additively to the output implies some restriction. There is possibility that at times the measurements of input to the structure may also be noise corrupted. In such cases, the measured excitation values are regarded as the actual excitation, and their deviations from the true stimuli will be propagated through the structure and lumped into disturbance $\mathbf{n}(k)$.

A further assumption is that the vibrating structure is completely observable and controllable. The conditions are that the observability matrix

$$\mathbf{L}_{2n} = \begin{bmatrix} \mathbf{C} \\ \mathbf{CT} \\ \mathbf{CT}^2 \\ \vdots \\ \mathbf{CT}^{2n-1} \end{bmatrix} \tag{4.2-4}$$

has the rank of $2n$ and that the controllability matrix has the rank of $2n$

$$\mathbf{M}_{2n} = [\ \Delta\ \mathbf{T}\Delta\ \cdots\ \mathbf{T}^{2n-1}\Delta\ ]. \tag{4.2-5}$$

§ 4.2.2 Free Response Case

It is convenient to assume first that the structure is freely vibrating and that there is no observation noise. The corresponding free response expression and observation equation are

$$\mathbf{x}(k+1) = \mathbf{T}\mathbf{x}(k) \quad \text{and} \quad \mathbf{y}(k) = \mathbf{C}\mathbf{x}(k)$$

In this case, a $2n$ vector of augmented observations is defined as

$$\underline{\mathbf{y}}(s) = \begin{bmatrix} \mathbf{y}(k+1) \\ \mathbf{y}(k+2) \\ \vdots \\ \mathbf{y}(k+s) \end{bmatrix}$$

with $r \times s = 2n$.

The above free response and noise-free measurement expressions are inserted into this vector to obtain

$$\underline{\mathbf{y}}(s) = \begin{bmatrix} \mathbf{y}(k+1) \\ \mathbf{y}(k+2) \\ \vdots \\ \mathbf{y}(k+s) \end{bmatrix} = \begin{bmatrix} \mathbf{CT} \\ \mathbf{CT}^2 \\ \vdots \\ \mathbf{CT}^s \end{bmatrix} \mathbf{x}(k) = \mathbf{L}\mathbf{T}\mathbf{x}(k), \qquad \begin{bmatrix} \mathbf{C} \\ \mathbf{CT} \\ \vdots \\ \mathbf{CT}^{s-1} \end{bmatrix} \tag{4.2-6}$$

In a similar fashion,

$$\underline{\mathbf{y}}(s+1) = \begin{bmatrix} \mathbf{y}(k+2) \\ \mathbf{y}(k+3) \\ \vdots \\ \mathbf{y}(k+s+1) \end{bmatrix} = \begin{bmatrix} \mathbf{C}\mathbf{T}^2 \\ \mathbf{C}\mathbf{T}^3 \\ \vdots \\ \mathbf{C}\mathbf{T}^{s+1} \end{bmatrix} \mathbf{x}(k) = \mathbf{L}\mathbf{T}^2\mathbf{x}(k) \tag{4.2-7}$$

Since $\mathbf{L}$ is nonsingular, its inverse exists. Replacing $\mathbf{I}$ by $\mathbf{L}^{-1}\mathbf{L}$, $\underline{\mathbf{y}}(s+1)$ can be expressed in terms of $\underline{\mathbf{y}}(s)$

$$\underline{\mathbf{y}}(s+1) = \mathbf{L}\mathbf{T}^2\mathbf{x}(k) = \mathbf{L}\mathbf{T}\mathbf{L}^{-1}\mathbf{L}\mathbf{T}\mathbf{x}(k) = \mathbf{L}\mathbf{T}\mathbf{L}^{-1}\underline{\mathbf{y}}(s) \tag{4.2-8}$$

By defining

$$\mathbf{G} = \mathbf{L}\mathbf{T}\mathbf{L}^{-1} \tag{4.2-9}$$

Eqn. (4.2-8) becomes

$$\underline{\mathbf{y}}(s+1) = \mathbf{G}\underline{\mathbf{y}}(s) \tag{4.2-10}$$

It is important to note, regardless of $\mathbf{T}$, matrix $\mathbf{G}$ has the form

$$\mathbf{G} = \begin{bmatrix} \mathbf{0} & \mathbf{I} & \cdots & \mathbf{0} \\ \mathbf{0} & \mathbf{0} & \cdots & \mathbf{0} \\ \cdot\cdot & \cdot\cdot & \cdots & \cdot\cdot \\ \mathbf{0} & \mathbf{0} & \cdots & \mathbf{I} \\ \mathbf{G}_s & \mathbf{G}_{s-1} & \cdots & \mathbf{G}_1 \end{bmatrix} \tag{4.2-11}$$

This can be directly proved from the definition of the matrix $\mathbf{G}$ in Eqn. (4.2-9)

$$\mathbf{G} = \mathbf{LTL}^{-1} = \begin{bmatrix} \mathbf{C} \\ \mathbf{CT} \\ : \\ \mathbf{CT}^{s-1} \end{bmatrix} \mathbf{T} \begin{bmatrix} \mathbf{C} \\ \mathbf{CT} \\ : \\ \mathbf{CT}^{s-1} \end{bmatrix}^{-1} \tag{4.2-12}$$

Eqn. (4.2-12) can be rewritten as

$$\mathbf{G} = \mathbf{LTL}^{-1} = \begin{bmatrix} \mathbf{C} \\ \mathbf{CT} \\ : \\ \mathbf{CT}^{s-1} \end{bmatrix} \mathbf{I} \begin{bmatrix} \mathbf{CT}^{-1} \\ \mathbf{C} \\ : \\ \mathbf{CT}^{s-2} \end{bmatrix}^{-1} . \tag{4.2-13}$$

By assuming

$$\mathbf{D} = \begin{bmatrix} \mathbf{C} \\ \mathbf{CT} \\ : \\ \mathbf{CT}^{s-2} \end{bmatrix}, \tag{4.2-14}$$

$$\mathbf{E} = \mathbf{CT}^{s-1} \tag{4.2-16}$$

and

$$\mathbf{F} = \mathbf{CT}^{-1}, \tag{4.2-17}$$

Eqn. (4.2-13) can be written as

$$\mathbf{G} = \begin{bmatrix}\mathbf{D}\\ \mathbf{E}\end{bmatrix}\begin{bmatrix}\mathbf{F}\\ \mathbf{D}\end{bmatrix}^{-1} . \tag{4.2-17}$$

Letting

$$\begin{bmatrix}\mathbf{F}\\ \mathbf{D}\end{bmatrix}^{-1} = [\ \mathbf{F}_{-1}\ \ \mathbf{D}_{-1}\ ] , \tag{4.2-18}$$

then

$$\begin{bmatrix}\mathbf{F}\\ \mathbf{D}\end{bmatrix}[\ \mathbf{F}_{-1}\ \ \mathbf{D}_{-1}\ ] = \mathbf{I}. \tag{4.2-19}$$

That is

$$\mathbf{F}\mathbf{F}_{-1} = \mathbf{I} \qquad \mathbf{F}\mathbf{D}_{-1} = \mathbf{0} \tag{4.2-20}$$

and

$$\mathbf{D}\mathbf{F}_{-1} = \mathbf{0} \qquad \mathbf{D}\mathbf{D}_{-1} = \mathbf{I}. \tag{4.2-21}$$

Substituting Eqn. (4.2-18) into Eqn. (4.2-17) and considering Eqns. (4.2-20) and (4.2-21) yield

$$\mathbf{G} = \begin{bmatrix}\mathbf{D}\\ \mathbf{E}\end{bmatrix}[\ \mathbf{F}_{-1}\ \ \mathbf{D}_{-1}\ ] = \begin{bmatrix}\mathbf{D}\mathbf{F}_{-1} & \mathbf{D}\mathbf{D}_{-1}\\ \mathbf{E}\mathbf{F}_{-1} & \mathbf{E}\mathbf{D}_{-1}\end{bmatrix}. \tag{4.2-22}$$

That is

$$\mathbf{G} = \begin{bmatrix} \mathbf{0} & \mathbf{I} \\ \mathbf{EF}_{-1} & \mathbf{ED}_{-1} \end{bmatrix} = \begin{bmatrix} \mathbf{0} & \mathbf{I} & \cdots & \mathbf{0} \\ \mathbf{0} & \mathbf{0} & \cdots & \mathbf{0} \\ \cdot\cdot & \cdot\cdot & \cdots & \cdot\cdot \\ \mathbf{0} & \mathbf{0} & \cdots & \mathbf{I} \\ \mathbf{G}_s & \mathbf{G}_{s-1} & \cdots & \mathbf{G}_1 \end{bmatrix}. \tag{4.2-23}$$

Introducing the observation noise, Eqns. (4.2-6) and (4.2-7) are rewritten as

$$\underline{\mathbf{y}}(s) = \mathbf{LTx}(k) + \underline{\mathbf{n}}(s) \tag{4.2-24}$$

and

$$\underline{\mathbf{y}}(s+1) = \mathbf{LT}^2\mathbf{x}(k) + \underline{\mathbf{n}}(s+1) \tag{4.2-25}$$

with

$$\underline{\mathbf{n}}(s) = \begin{bmatrix} \mathbf{n}(k+1) \\ \mathbf{n}(k+2) \\ \vdots \\ \mathbf{n}(k+s) \end{bmatrix} \quad \text{and} \quad \underline{\mathbf{n}}(s+1) = \begin{bmatrix} \mathbf{n}(k+2) \\ \mathbf{n}(k+3) \\ \vdots \\ \mathbf{n}(k+s+1) \end{bmatrix} \tag{4.2-26}$$

Thus Eqn. (4.2-10) becomes

$$\underline{\mathbf{y}}(s+1) = \mathbf{G}\underline{\mathbf{y}}(s) + \underline{\mathbf{n}}(s+1) - \mathbf{G}\underline{\mathbf{n}}(s) \tag{4.2-27}$$

In matrix form, Eqn. (4.2-27) is written

$$\begin{bmatrix} \mathbf{y}(k+2) \\ \mathbf{y}(k+3) \\ \vdots \\ \mathbf{y}(k+s) \\ \mathbf{y}(k+s+1) \end{bmatrix} = \begin{bmatrix} \mathbf{0} & \mathbf{I} & \cdots & \mathbf{0} \\ \mathbf{0} & \mathbf{0} & \cdots & \mathbf{0} \\ \cdots & \cdots & \cdots & \cdots \\ \mathbf{0} & \mathbf{0} & \cdots & \mathbf{I} \\ \mathbf{G}_s & \mathbf{G}_{s-1} & \cdots & \mathbf{G}_1 \end{bmatrix} \begin{bmatrix} \mathbf{y}(k+1) \\ \mathbf{y}(k+2) \\ \vdots \\ \mathbf{y}(k+s-1) \\ \mathbf{y}(k+s) \end{bmatrix} + \begin{bmatrix} \mathbf{n}(k+2) \\ \mathbf{n}(k+3) \\ \vdots \\ \mathbf{n}(k+s) \\ \mathbf{n}(k+s+1) \end{bmatrix}$$

$$- \begin{bmatrix} \mathbf{0} & \mathbf{I} & \cdots & \mathbf{0} \\ \mathbf{0} & \mathbf{0} & \cdots & \mathbf{0} \\ \cdots & \cdots & \cdots & \cdots \\ \mathbf{0} & \mathbf{0} & \cdots & \mathbf{I} \\ \mathbf{G}_s & \mathbf{G}_{s-1} & \cdots & \mathbf{G}_1 \end{bmatrix} \begin{bmatrix} \mathbf{n}(k+1) \\ \mathbf{n}(k+2) \\ \vdots \\ \mathbf{n}(k+s-1) \\ \mathbf{n}(k+s) \end{bmatrix} \tag{4.2-28}$$

Expanding the equation and extracting the last row yield

$$\mathbf{y}(k+s+1) = \mathbf{G}_s\mathbf{y}(k+1) + \cdots + \mathbf{G}_1\mathbf{y}(k+s) + \mathbf{n}(k+s+1) - \mathbf{G}_s\mathbf{n}(k+1) - \cdots - \mathbf{G}_1\mathbf{n}(k+s) \tag{4.2-29a}$$

Without loss of generality, k can be assumed to be zero and hence

$$\mathbf{y}(s+1) = \mathbf{G}_s\mathbf{y}(1) + \cdots + \mathbf{G}_1\mathbf{y}(s) + \mathbf{n}(s+1) - \mathbf{G}_s\mathbf{n}(1) - \cdots - \mathbf{G}_1\mathbf{n}(s) \tag{4.2-29b}$$

Generally, Eqn. (4.2-29b) can be written as

$$\mathbf{y}(k+s+1) = \mathbf{G}_s\mathbf{y}(k+1) + \cdots + \mathbf{G}_1\mathbf{y}(k+s) + \mathbf{n}(k+s+1) + \mathbf{S}_s\mathbf{n}(k+1) + \cdots + \mathbf{S}_1\mathbf{n}(k+s) \tag{4.2-30a}$$

or dropping k

$$\mathbf{y}(s+1) = \mathbf{G}_s\mathbf{y}(1) + \cdots + \mathbf{G}_1\mathbf{y}(s) + \mathbf{n}(s+1) + \mathbf{S}_s\mathbf{n}(1) + \cdots + \mathbf{S}_1\mathbf{n}(s) \tag{4.2-30b}$$

This model is called the auto-regressive and moving average (ARMA) model of the vibrating structure.

Assuming

$$\mathbf{e}(s+1) = \mathbf{n}(s+1) + \mathbf{S}_1\mathbf{n}(s) + \cdots + \mathbf{S}_s\mathbf{n}(1) \tag{4.2-31}$$

then Eqn. (4.2-30b) can be written in more compact form

$$\mathbf{y}(s+1) = \mathbf{G}_1\mathbf{y}(s) + \cdots + \mathbf{G}_s\mathbf{y}(1) + \mathbf{e}(s+1) = \hat{\mathbf{G}}\hat{\mathbf{y}} + \mathbf{e}(s+1) \tag{4.2-32}$$

where

$$\hat{\mathbf{G}} = [\ \mathbf{G}_s\ \ \mathbf{G}_{s-1}\ \cdots\ \mathbf{G}_1\ ] \quad \text{and} \quad \hat{\mathbf{y}} = [\ \mathbf{y}^T(1)\ \ \mathbf{y}^T(2)\ \cdots\ \mathbf{y}^T(s)\ ]^T$$

The form in Eqn. (4.2-32) is not convenient for using different groups of data and can be transformed into the following form by the Kronecker multiplication and column operation on matrices

$$\mathbf{y}(s+1) = \mathbf{Y}^T(s)\boldsymbol{\theta} + \mathbf{e}(s+1) \tag{4.2-33}$$

where $\mathbf{Y}(s)$ is a $(2n \times r) \times r$ matrix

$$\mathbf{Y}(s) = \begin{bmatrix} \mathbf{y}(1) \\ \vdots \\ \mathbf{y}(s) \end{bmatrix} \otimes \mathbf{I}_r \tag{4.2-34}$$

and $\boldsymbol{\theta} \in R^{2n \times r}$, $\quad \boldsymbol{\theta} = column\ [\ \mathbf{G}_s\ \ \mathbf{G}_{s-1}\ \cdots\ \mathbf{G}_1\ ]$

The operator ⊗ is the Kronecker multiplication of matrices and the operator *column* indicates the column operation on a matrix. The details of their definition may be referred to Appendix 4A.

§ 4.2.3 Forced Response Case

When control forces or ambient disturbances are applied to the vibrating structure, the forced response model of the structure in Eqns. (4.2-1a) and (4.2-1b) is used directly to derive the ARMAX model of the vibrating structure for modal identification. To this end, it is convenient to assume the system is noise free and only control forces are applied to it. Thus the following augmented vectors are obtained

$$\underline{\mathbf{y}}(s) = [\ \mathbf{y}^T(k+1)\ \mathbf{y}^T(k+2)\ \cdots\ \mathbf{y}^T(k+s)\ ]^T,$$

$$\underline{\mathbf{y}}(s+1) = [\ \mathbf{y}^T(k+2)\ \mathbf{y}^T(k+3)\ \cdots\ \mathbf{y}^T(k+s+1)\ ]^T,$$

$$\underline{\mathbf{f}}(s) = [\ \mathbf{f}^T(k+1)\ \mathbf{f}^T(k+2)\ \cdots \mathbf{f}^T(k+s)\ ]^T,$$

$$\underline{\mathbf{f}}(s-1) = [\ \mathbf{f}^T(k)\ \mathbf{f}^T(k+1)\ \cdots\ \mathbf{f}^T(k+s-1)\ ]^T, \tag{4.2-35}$$

where $\mathbf{y}(i) \in R^r$, $\mathbf{f}(i) \in R^p$, $\underline{\mathbf{y}}(s) \in R^{s \times r}$ and $\underline{\mathbf{f}}(s) \in R^{s \times p}$.

Considering Eqns. (4.2-1a) and (4.2-2) $\underline{\mathbf{y}}(s)$ and $\underline{\mathbf{y}}(s+1)$ may be expressed as

$$\underline{\mathbf{y}}(s) = \mathbf{L}\mathbf{T}\mathbf{x}(k) + \mathbf{Q}\underline{\mathbf{f}}(s-1) \tag{4.2-36}$$

where $\mathbf{Q}$ is an $(s \times r) \times (s \times p)$ lower triangular matrix

$$\mathbf{Q} = \begin{bmatrix} \mathbf{C\Delta} & \mathbf{0} & \cdots & \mathbf{0} \\ \mathbf{CT\Delta} & \mathbf{C\Delta} & \cdots & \mathbf{0} \\ \cdots & \cdots & \cdots & \cdots \\ \mathbf{CT}^{s-1}\mathbf{\Delta} & \mathbf{CT}^{s-2}\mathbf{\Delta} & \cdots & \mathbf{C\Delta} \end{bmatrix} \tag{4.2-37}$$

and

$$\underline{\mathbf{y}}(s+1) = \mathbf{LT}^2\mathbf{x}(k) + \mathbf{D}\begin{bmatrix} \mathbf{f}(k) \\ \underline{\mathbf{f}}(s) \end{bmatrix} \tag{4.2-38}$$

where $\mathbf{D}$ is an $(s \times r) \times ((s+1) \times p)$ matrix

$$\mathbf{D} = \begin{bmatrix} \mathbf{CT\Delta} & \mathbf{C\Delta} & \mathbf{0} & \cdots & \mathbf{0} \\ \mathbf{CT}^2\mathbf{\Delta} & \mathbf{CT\Delta} & \mathbf{C\Delta} & \cdots & \mathbf{0} \\ \cdots & \cdots & \cdots & \cdots & \cdots \\ \mathbf{CT}^s\mathbf{\Delta} & \mathbf{CT}^{s-1}\mathbf{\Delta} & \mathbf{CT}^{s-2}\mathbf{\Delta} & \cdots & \mathbf{C\Delta} \end{bmatrix} = [\ \mathbf{LT\Delta}\ \ \mathbf{Q}\ ] \tag{4.2-39}$$

with $(\mathbf{LT\Delta})$ being an $(s \times r) \times p$ matrix

$$\mathbf{LT\Delta} = \begin{bmatrix} \mathbf{CT\Delta} \\ \mathbf{CT}^2\mathbf{\Delta} \\ \cdots \\ \mathbf{CT}^s\mathbf{\Delta} \end{bmatrix}. \tag{4.2-40}$$

The relationship between augmented vectors $\underline{\mathbf{y}}(s+1)$ and $\underline{\mathbf{y}}(s)$ can be derived as follows

$$\begin{aligned}\underline{\mathbf{y}}(s+1) &= \mathbf{LT}^2\mathbf{x}(k) + \mathbf{LT}\Delta\mathbf{f}(k) + \mathbf{Q}\underline{\mathbf{f}}(s) \\ &= \mathbf{LTITx}(k) + \mathbf{LT}\Delta\mathbf{f}(k) + \mathbf{Q}\underline{\mathbf{f}}(s)\end{aligned} \tag{4.2-41}$$

Since the observability matrix $\mathbf{L}$ is nonsingular, $\mathbf{I}$ is to be replaced by $\mathbf{L}^{-1}\mathbf{L}$ and Eqn. (4.2-41) becomes

$$\begin{aligned}\underline{\mathbf{y}}(s+1) &= \mathbf{LTL}^{-1}\mathbf{LTx}(k) + \mathbf{LT}\Delta\mathbf{f}(k) + \mathbf{Q}\underline{\mathbf{f}}(s) \\ &= \mathbf{GLTx}(k) + \mathbf{LT}\Delta\mathbf{f}(k) + \mathbf{Q}\underline{\mathbf{f}}(s)\end{aligned} \tag{4.2-42}$$

where $\mathbf{G} = \mathbf{LTL}^{-1}$ as defined in Eqn. (4.2-9). From Eqn. (4.2-36)

$$\mathbf{LTx}(k) = \underline{\mathbf{y}}(s) - \mathbf{Q}\underline{\mathbf{f}}(s-1) \tag{4.2-43}$$

Inserting Eqn. (4.2-43) into Eqn. (4.2-42) yields

$$\begin{aligned}\underline{\mathbf{y}}(s+1) &= \mathbf{G}\underline{\mathbf{y}}(s) - \mathbf{GQ}\underline{\mathbf{f}}(s-1) + \mathbf{LT}\Delta\mathbf{f}(k) + \mathbf{Q}\underline{\mathbf{f}}(s) \\ &= \mathbf{G}\underline{\mathbf{y}}(s) - \mathbf{GQ}\underline{\mathbf{f}}(s-1) + \mathbf{GL}\Delta\mathbf{f}(k) + \mathbf{Q}\underline{\mathbf{f}}(s) \\ &= \mathbf{G}\underline{\mathbf{y}}(s) - \mathbf{G}(\mathbf{Q}\underline{\mathbf{f}}(s-1) - \mathbf{L}\Delta\mathbf{f}(k)) + \mathbf{Q}\underline{\mathbf{f}}(s)\end{aligned} \tag{4.2-44}$$

The expression $\mathbf{Q}\underline{\mathbf{f}}(s-1)$–$\mathbf{L}\Delta\mathbf{f}(k)$ in the parenthesis of the second term of Eqn. (4.2-44) can be written

$$\begin{bmatrix} \mathbf{C}\Delta & \mathbf{0} & \cdots & \mathbf{0} \\ \mathbf{CT}\Delta & \mathbf{C}\Delta & \cdots & \mathbf{0} \\ \cdots & \cdots & \cdots & \cdots \\ \mathbf{CT}^{s-1}\Delta & \mathbf{CT}^{s-2}\Delta & \cdots & \mathbf{C}\Delta \end{bmatrix} \begin{bmatrix} \mathbf{f}(k) \\ \mathbf{f}(k+1) \\ \cdots \\ \mathbf{f}(k+s-1) \end{bmatrix} - \begin{bmatrix} \mathbf{C}\Delta & \mathbf{0} & \cdots & \mathbf{0} \\ \mathbf{CT}\Delta & \mathbf{0} & \cdots & \mathbf{0} \\ \cdots & \cdots & \cdots & \cdots \\ \mathbf{CT}^{s-1}\Delta & \mathbf{0} & \cdots & \mathbf{C}\Delta \end{bmatrix} \begin{bmatrix} \mathbf{f}(k) \\ \mathbf{f}(k+1) \\ \cdots \\ \mathbf{f}(k+s-1) \end{bmatrix}$$

$$= \begin{bmatrix} 0 & 0 & 0 & \cdots & 0 \\ 0 & C\Delta & C\Delta & \cdots & 0 \\ \cdots & \cdots & \cdots & \cdots & \cdots \\ 0 & CT^{s-2}\Delta & CT^{s-3}\Delta & \cdots & C\Delta \end{bmatrix} \begin{bmatrix} f(k) \\ f(k+1) \\ \cdots \\ f(k+s-1) \end{bmatrix}$$

$$= \begin{bmatrix} 0 & 0 & \cdots & 0 & 0 \\ C\Delta & C\Delta & \cdots & 0 & 0 \\ \cdots & \cdots & \cdots & \cdots & \cdots \\ CT^{s-2}\Delta & CT^{s-3}\Delta & \cdots & C\Delta & 0 \end{bmatrix} \begin{bmatrix} f(k+1) \\ f(k+2) \\ \cdots \\ f(k+s) \end{bmatrix} \tag{4.2-45}$$

The coefficient of the second term of Eqn. (4.2-44) can then be written as

$$G \begin{bmatrix} 0 & 0 & \cdots & 0 & 0 \\ C\Delta & C\Delta & \cdots & 0 & 0 \\ \cdots & \cdots & \cdots & \cdots & \cdots \\ CT^{s-3}\Delta & CT^{s-4}\Delta & \cdots & 0 & 0 \\ CT^{s-2}\Delta & CT^{s-3}\Delta & \cdots & C\Delta & 0 \end{bmatrix}$$

$$= \begin{bmatrix} 0 & I & \cdots & 0 \\ 0 & 0 & \cdots & 0 \\ \cdots & \cdots & \cdots & \cdots \\ 0 & 0 & \cdots & I \\ G_s & G_{s-1} & \cdots & G_1 \end{bmatrix} \begin{bmatrix} 0 & 0 & \cdots & 0 & 0 \\ C\Delta & C\Delta & \cdots & 0 & 0 \\ \cdots & \cdots & \cdots & \cdots & \cdots \\ CT^{s-3}\Delta & CT^{s-4}\Delta & \cdots & 0 & 0 \\ CT^{s-2}\Delta & CT^{s-3}\Delta & \cdots & C\Delta & 0 \end{bmatrix}$$

$$= \begin{bmatrix} C\Delta & 0 & \cdots & 0 & 0 \\ CT\Delta & C\Delta & \cdots & 0 & 0 \\ \cdots & \cdots & \cdots & \cdots & \cdots \\ CT^{s-2} & CT^{s-3}\Delta & \cdots & C\Delta & 0 \\ \sum_{j=1}^{s-1} G_j CT^{s-j-1}\Delta & \sum_{j=1}^{s-2} G_j CT^{s-j-2}\Delta & \cdots & G_1 C\Delta & 0 \end{bmatrix} \tag{4.2-46}$$

Combining the coefficient expressed in Eqn. (4.2-46) and that of the third term

expressed in Eqn. (4.2-37), Eqn.(4.2-44) becomes

$$\underline{\mathbf{y}}(s+1) = \mathbf{G}\underline{\mathbf{y}}(s) + \mathbf{R}\underline{\mathbf{f}}(s) \tag{4.2-47}$$

where $\mathbf{R}$ is an $(s \times r) \times (s \times p)$ matrix

$$\mathbf{R} = \begin{bmatrix} \mathbf{0} & \mathbf{0} & \cdots & \mathbf{0} \\ \cdots & \cdots & \cdots & \cdots \\ \mathbf{0} & \mathbf{0} & \cdots & \mathbf{0} \\ \mathbf{R}_s & \mathbf{R}_{s-1} & \cdots & \mathbf{R}_1 \end{bmatrix} \tag{4.2-48}$$

with $\mathbf{R}_i$ being $r \times p$ matrix and

$$\mathbf{R}_1 = \mathbf{C}\Delta$$

$$\mathbf{R}_i = \mathbf{C}\mathbf{T}^{i-1}\Delta - \sum_{j=1}^{i-1} \mathbf{G}_j \mathbf{C}\mathbf{T}^{i-j-1}\Delta \qquad \text{for } i = 1, 2, \cdots, s.$$

Expanding Eqn. (4.2-47) and considering the last row of the expansion, an ARX model of the linear vibrating structure is obtained

$$\mathbf{y}(k+s+1) = \mathbf{G}_s\mathbf{t}(k+1) + \cdots + \mathbf{G}_1\mathbf{y}(k+s) + \mathbf{R}_s\mathbf{f}(k+1) + \cdots + \mathbf{R}_1\mathbf{f}(k+s) \tag{4.2-49}$$

for $s = 1, 2, \cdots, N$.

Shifting the observation starting time to $k = 0$, k is eliminated and the ARX model in Eqn. (4.2-49) is thus rewritten as

$$\mathbf{y}(s+1) = \mathbf{G}_s\mathbf{y}(1) + \cdots + \mathbf{G}_1\mathbf{y}(s) + \mathbf{R}_s\mathbf{f}(1) + \cdots + \mathbf{R}_1\mathbf{f}(s) \tag{4.2-50}$$

for $s = 1, 2, \cdots, N$.

When the observation noise is included, the following model can be derived in a similar way to the case of free response

$$\mathbf{y}(s+1) = \mathbf{G}_s\mathbf{y}(1) + \cdots + \mathbf{G}_1\mathbf{y}(s) + \mathbf{R}_s\mathbf{f}(1) + \cdots + \mathbf{R}_1\mathbf{f}(s) + \mathbf{e}(s+1). \tag{4.2-51}$$

In matrix form

$$\mathbf{y}(s+1) = \mathbf{Q}\mathbf{z}(s) + \mathbf{e}(s+1) \tag{4.2-52}$$

where

$$\mathbf{Q} = [\ \mathbf{G}_s\ \cdots\ \mathbf{G}_1\ \ \mathbf{R}_s\ \cdots\ \mathbf{R}_1\ ]$$

and

$$\mathbf{z}(s) = [\ \mathbf{y}^T(1)\ \cdots\ \mathbf{y}^T(s)\ \ \mathbf{f}^T(1)\ \cdots\ \mathbf{f}^T(s)\ ]^T$$

Eqn. (4.2-52) is not convenient form to use for different group of data and may be transformed into the following form by the Kronecker multiplication and column operation

$$\mathbf{y}(s+1) = \mathbf{Z}^T(s)\boldsymbol{\theta} + \mathbf{e}(s+1) \tag{4.2-53}$$

where $\mathbf{Z}(s)$ is a $(2n\times(r+p))\times r$ matrix

$$\mathbf{Z}(s) = \mathbf{z}(s) \otimes \mathbf{I}_r = \begin{bmatrix} \mathbf{y}(1) \\ \vdots \\ \mathbf{y}(s) \\ \mathbf{f}(1) \\ \vdots \\ \mathbf{f}(s) \end{bmatrix} \otimes \mathbf{I}_r$$

and $\boldsymbol{\theta} \in R^{2n\times(r+p)}$, $\qquad \boldsymbol{\theta} = column\ [\ \mathbf{G}_s \ \cdots\ \mathbf{G}_1\ \ \mathbf{R}_s \ \cdots\ \mathbf{R}_1\ ]$

§ 4.3 MODAL IDENTIFICATION - THE DIRECT METHOD

In this section, the direct method for modal identification is developed. This method solves the eigenvalue problem of the matrix **G** expressed in Eqn. (4.2-11) to determine the modal parameters of a vibrating structure. Hence the relationship of the eigen parameters of the matrix **G** and modal parameters of the vibrating structure is needed to be established, and in the first part of this section this relationship is derived. In the second part of the section the direct method for modal identification is developed. In the third part of this section the estimation of matrix **G** is discussed. In the last part of this section, the method is summarized in flow charts.

§ 4.3.1 Relationship of Matrix G and Modal Parameters

The derivation of the relationship of matrix **G** and modal parameters of a vibrating structure consists of three steps: (1) to establish the relationship between the eigenvalues and eigenvectors of the system matrix **A** and the modal parameters of the vibrating structure; (2) to establish the relationship between the state transition matrix **T** and the eigenvalues and eigenvectors of the system matrix **A**; (3) to derive the relationship between the eigenvalues and eigenvectors of matrix **G** and the modal parameters of the vibrating structure.

1. Relationship of Eigen Parameters of Matrix **A** *and Modal Parameters of a Vibrating Structure*

By letting $\boldsymbol{\Psi}$ and $\boldsymbol{\Lambda}$ be eigenvector matrix and eigenvalue matrix of the system matrix **A**,

$$\mathbf{A}\boldsymbol{\Psi} = \boldsymbol{\Psi}\boldsymbol{\Lambda}, \tag{4.3-1}$$

in which

$$\boldsymbol{\Lambda} = \begin{bmatrix} \lambda_1 & & 0 \\ & \lambda_2 & \\ & & \ddots \\ 0 & & \lambda_{2n} \end{bmatrix} \tag{4.3-2}$$

and

$$\boldsymbol{\Psi} = [\ \psi_1\ \ \psi_2\ \cdots\ \psi_{2n}\ ] \tag{4.3-2.b}$$

with λ_i and ψ_i are the *i*th eigenvalue and eigenvector of the system matrix **A**, respectively.

It has been shown in chapter 2 that the eigenvalue matrix $\boldsymbol{\Lambda}$ and eigenvector matrix $\boldsymbol{\Psi}$ may be related to the eigenvalues λ_i and eigenvectors $\boldsymbol{\phi}_i$ of the vibrating structure described

$$\boldsymbol{\Psi} = \begin{bmatrix} \boldsymbol{\Phi} \\ \boldsymbol{\Phi}\boldsymbol{\Lambda} \end{bmatrix}. \tag{4.3-3}$$

$\boldsymbol{\Phi}$ is the matrix with eigenvectors $\boldsymbol{\phi}_i$ being its column vectors. $\boldsymbol{\Lambda}$ is the matrix with the eigenvalues λ_i being its diagonal elements.

2. Relationship between State Transition Matrix T *and Eigen Parameters of Matrix* A

To determine the relationship of the state transition matrix **T** to the eigenvalue matrix **Λ**, and eigenvector matrix **Ψ** of the system matrix **A**, the transformation of variables are defined as

$$\mathbf{x}(t) = \mathbf{\Psi}\mathbf{z}(t). \tag{4.3-4}$$

Substituting this relationship into Eqn. (2.3-13) yields

$$\mathbf{\Psi}\dot{\mathbf{z}}(t) = \mathbf{A}\mathbf{\Psi}\mathbf{z}(t) + \mathbf{B}\mathbf{f}(t) \tag{4.3-5}$$

and

$$\dot{\mathbf{z}}(t) = \mathbf{\Psi}^{-1}\mathbf{A}\mathbf{\Psi}\mathbf{z}(t) + \mathbf{\Psi}^{-1}\mathbf{B}\mathbf{f}(t). \tag{4.3-6}$$

Similar to the solution of Eqn. (2.2-13), the solution of equation (4.3-6) can be written as

$$\mathbf{z}(t) = \exp(\mathbf{\Psi}^{-1}\mathbf{A}\mathbf{\Psi}t)\mathbf{z}(0) + \int_0^t \exp(\mathbf{\Psi}^{-1}\mathbf{A}\mathbf{\Psi}(t-\tau))\mathbf{\Psi}^{-1}\mathbf{B}\mathbf{f}(\tau)d\tau. \tag{4.3-7}$$

From equation (4.3-1)

$$\mathbf{\Psi}^{-1}\mathbf{A}\mathbf{\Psi} = \mathbf{\Lambda}. \tag{4.3-8}$$

Hence

$$\mathbf{z}(t) = \exp(\mathbf{\Lambda} t)\mathbf{z}(0) + \int_0^t \exp(\mathbf{\Lambda}(t-\tau))\mathbf{\Psi}^{-1}\mathbf{B}\mathbf{f}(\tau)d\tau. \tag{4.3-9}$$

Expanding $\exp(\mathbf{\Lambda} t)$ in the exponential series gives

$$\exp(\mathbf{\Lambda} t) = \mathbf{I} + \begin{bmatrix} \lambda_1 t & \cdots & 0 & \cdots & 0 \\ 0 & \cdots & \lambda_i t & \cdots & 0 \\ 0 & \cdots & 0 & \cdots & \lambda_{2n} t \end{bmatrix} + \begin{bmatrix} \frac{(\lambda_1 t)^2}{2!} & \cdots & 0 & \cdots & 0 \\ 0 & \cdots & \frac{(\lambda_i t)^2}{2!} & \cdots & 0 \\ 0 & \cdots & 0 & \cdots & \frac{(\lambda_{2n} t)^2}{2!} \end{bmatrix} + \cdots$$

$$= \begin{bmatrix} e^{\lambda_1 t} & \cdots & 0 & \cdots & 0 \\ 0 & \cdots & e^{\lambda_i t} & \cdots & 0 \\ 0 & \cdots & 0 & \cdots & e^{\lambda_{2n} t} \end{bmatrix}. \tag{4.3-10}$$

Considering transformation defined in equation (4.3-4),

$$\mathbf{x}(t) = \mathbf{\Psi}\exp(\mathbf{\Lambda} t)\mathbf{\Psi}^{-1}\mathbf{x}(0) + \int_0^t \mathbf{\Psi}\exp(\mathbf{\Lambda}(t-\tau))\mathbf{\Psi}^{-1}\mathbf{B}\mathbf{f}(\tau)d\tau. \tag{4.3-11}$$

By comparison of Eqn. (4.3-11) with Eqn. (2.4-34), the relationship of the state transition matrix $\mathbf{T}$ to the eigenvalue matrix $\mathbf{\Lambda}$ and eigenvectors $\mathbf{\Psi}$ of the system matrix $\mathbf{A}$ is established as

$$\mathbf{T}(t) = \mathbf{\Psi}\exp(\mathbf{\Lambda} t)\mathbf{\Psi}^{-1} \tag{4.3-12a}$$

Since matrix $\exp(\mathbf{\Lambda}t)$ is diagonal, the eigenvalue problem of the state transition matrix $\mathbf{T}(t)$ is

$$\mathbf{T}(t)\mathbf{\Psi} = \mathbf{\Psi}\exp(\mathbf{\Lambda}t) \tag{4.3-12b}$$

It means that the state transition matrix $\mathbf{T}(t)$ has the eigenvalues $e^{\lambda_i t}$ and the same eigenvectors as the system matrix **A**.

3. Relationship of Eigen Parameters of Matrix G *and Eigen Parameters of System Matrix* A

From Eqn. (4.2-9) $\mathbf{G} = \mathbf{L}\mathbf{T}\mathbf{L}^{-1}$,

$$\mathbf{G}\begin{bmatrix}\mathbf{C}\\ \mathbf{C}\mathbf{T}\\ ..\\ \mathbf{C}\mathbf{T}^{(s-1)}\end{bmatrix} = \begin{bmatrix}\mathbf{C}\\ \mathbf{C}\mathbf{T}\\ ..\\ \mathbf{C}\mathbf{T}^{(s-1)}\end{bmatrix}\mathbf{T}. \tag{4.3-13}$$

Combining Eqn. (4.3-12) with Eqn. (4.3-13), and considering $\mathbf{\Psi}^{-1}$ being nonsingular, the relationship of the matrix **G** to the eigenvalue matrix $\mathbf{\Lambda}$ and eigenvector matrix $\mathbf{\Psi}$ of the system matrix **A** can be expressed as

$$\mathbf{G}\begin{bmatrix}\mathbf{C}\mathbf{\Psi}\\ \mathbf{C}\mathbf{\Psi}exp(\mathbf{\Lambda}t)\\ ..\\ \mathbf{C}\mathbf{\Psi}exp((s-1)\mathbf{\Lambda}t)\end{bmatrix} = \begin{bmatrix}\mathbf{C}\mathbf{\Psi}\\ \mathbf{C}\mathbf{\Psi}exp(\mathbf{\Lambda}t)\\ ..\\ \mathbf{C}\mathbf{\Psi}exp((s-1)\mathbf{\Lambda}t)\end{bmatrix}exp(\mathbf{\Lambda}t). \tag{4.3-14}$$

Since $\exp(\mathbf{\Lambda}t)$ is diagonal, Eqn. (4.3-14) represents an eigenvalue problem of matrix **G**.

§ 4.3.2 Modal Identification

Eqn. (4.3-14) is the basis of the direct method for modal identification. It represents an eigenvalue problem for matrix **G**. The eigenvalues of matrix **G** are the same as those of the state transition matrix **T** in Eqn. (4.3-12b). Since **C** is an $r \times 2n$ matrix with the first r columns forming a unit matrix and $\boldsymbol{\Psi}$ is the eigenvector matrix of the system matrix **A**, the top sub-matrix $\mathbf{C}\boldsymbol{\Psi}$ of the eigenvector matrix in Eqn. (4.3-14) has the columns which are the vectors with the first r elements of the eigenvectors $\boldsymbol{\psi}_i$ of the system matrix **A**.

By considering the relationship of the eigen parameters of the system matrix **A** to the modal parameters of the vibrating structure in Eqn. (4.3-3), the top sub-matrix $\mathbf{C}\boldsymbol{\Psi}$ represents the first r elements of the eigenvector $\boldsymbol{\phi}_i$ of the vibrating structure. When the number of measurement stations is the same as the order of the vibrating structure, Eqn. (4.3-14) is reduced to

$$\mathbf{G}\begin{bmatrix}\boldsymbol{\Phi} \\ \boldsymbol{\Phi} exp(\boldsymbol{\Lambda} t)\end{bmatrix} = \begin{bmatrix}\boldsymbol{\Phi} \\ \boldsymbol{\Phi} exp(\boldsymbol{\Lambda} t)\end{bmatrix} exp(\boldsymbol{\Lambda} t). \tag{4.3-15}$$

The upper halves of the eigenvectors of the matrix **G** are the eigenvectors of the vibrating structure. The eigenvalues of the matrix **G** are $e^{\lambda_i T}$, from which the eigenvalues λ_i, and then natural frequencies ω_i and damping ratios η_i of the vibrating structure can be calculated. To this end, the eigenvalues $e^{\lambda_i T}$ are symbolically written as

$$\alpha_i = e^{\lambda_i T} = e^{(-\eta_i \omega_i \pm i\omega_i \sqrt{1-\eta_i^2})T}. \tag{4.3-16}$$

Thus

$$-\eta_i\omega_i = \frac{1}{2T}\ln(\alpha_i\alpha_i^*) \tag{4.3-17}$$

and

$$\omega_i\sqrt{1-\eta_i^2} = \begin{cases} \frac{1}{T}\tan^{-1}\left|\frac{\alpha_i-\alpha_i^*}{\alpha_i+\alpha_i^*}\right| & \text{for } \alpha_i+\alpha_i^* \geq 0 \\ \frac{1}{T}\left(\pi-\tan^{-1}\left|\frac{\alpha_i-\alpha_i^*}{\alpha_i+\alpha_i^*}\right|\right) & \text{for } \alpha_i+\alpha_i^* < 0 \end{cases} . \tag{4.3-18}$$

The natural frequencies and damping factors can be determined as follows,

$$\omega_i = \sqrt{(-\eta_i\omega_i)^2 + (\omega_i\sqrt{1-\eta_i^2})^2} \tag{4.3-19}$$

and

$$\eta_i = \frac{|-\eta_i\omega_i|}{\omega_i} . \tag{4.3-20}$$

The relationship of the eigenvalue problem of matrix **G** to the eigen parameters of the vibrating structure can also be proved using matrix similarity theory as follows.

From Eqn. (4.2-9)

$$\mathbf{G} = \mathbf{LTL}^{-1} . \tag{4.3-21}$$

The matrices **G** and **T** are called *similar* and the relationship between **G** and **T** is called that of similarity. The characteristic equation of **G** is

$$|\alpha\mathbf{I} - \mathbf{G}| = |\alpha\mathbf{I} - \mathbf{L}\mathbf{T}\mathbf{L}^{-1}| = 0 . \tag{4.3-22}$$

By replacing $\mathbf{I}$ by $\mathbf{L}\mathbf{L}^{-1}$ and factorizing inside the determinant sign:

$$|\mathbf{L}(\alpha\mathbf{I} - \mathbf{T})\mathbf{L}^{-1}| = 0 . \tag{4.3-23}$$

This equation can be further simplified as

$$|\mathbf{L}(\alpha\mathbf{I} - \mathbf{T})\mathbf{L}^{-1}| = |\mathbf{L}|\,|\alpha\mathbf{I} - \mathbf{T}|\,|\mathbf{L}^{-1}| = |\alpha\mathbf{I} - \mathbf{T}| = 0 \tag{4.3-24}$$

since $|\mathbf{L}^{-1}| = 1 / |\mathbf{L}|$. This shows the characteristic equations (4.3-22) and (4.3-24) of $\mathbf{G}$ and $\mathbf{T}$ are identical and matrices $\mathbf{G}$ and $\mathbf{T}$ have the same eigenvalues. Furthermore, if $\boldsymbol{\psi}_i$ are the eigenvectors of $\mathbf{T}$ then

$$\mathbf{G}(\mathbf{L}\boldsymbol{\psi}_i) = \mathbf{L}\mathbf{T}\mathbf{L}^{-1}(\mathbf{L}\boldsymbol{\psi}_i) = \mathbf{L}\mathbf{T}\boldsymbol{\psi}_i = \mathbf{L}\lambda_i\boldsymbol{\psi}_i = \lambda_i(\mathbf{L}\boldsymbol{\psi}_i) \tag{4.3-26}$$

This shows that the eigenvectors of $\mathbf{G}$ are $\mathbf{L}\boldsymbol{\psi}_i$, for $i = 1, 2, \cdots, 2n$ and is coincident with the result in Eqn. (4.3-14).

Once matrix $\mathbf{G}$ is found, the modal parameters of the vibrating structure can be extracted as indicated.

§ 4.3.3 Estimation of Matrix G

As previously discussed, the estimate of matrix $\mathbf{G}$ becomes very important for the modal identification of a vibrating structure and hence is briefly discussed in this section. There are some numerical estimation methods which can be used to evaluate the matrix $\mathbf{G}$, however in this section the least squares estimate method is

used to develop two algorithms for estimation of matrix **G**. The first algorithm uses the ARMAX model in Eqn. (4.2-53). The second algorithm uses the model in Eqn. (4.2-47).

Considering the first proposed algorithm, taking the observation at time $t = 1, 2, \cdots, N$ and assuming that the response and excitation data are recorded from $t = 0$, i.e., $k = 0$, Eqn. (4.2-53) becomes

$$\mathbf{y}(N) = \mathbf{Z}(N)\boldsymbol{\theta} + \mathbf{e}(N) \tag{4.3-27}$$

where $\mathbf{y}(N) \in R^{r\times N}$, $\mathbf{e}(N) \in R^{r\times N}$ and

$$\mathbf{y}(N) = [\ \mathbf{y}^T(s+1)\ \ \mathbf{y}^T(s+2)\ \cdots\ \mathbf{y}^T(s+N)\ ]^T$$

$$\mathbf{e}(N) = [\ \mathbf{e}^T(s+1)\ \ \mathbf{e}^T(s+2)\ \cdots\ \mathbf{e}^T(s+N)\ ]^T.$$

$\mathbf{Z}(N)$ is an $(r\times N)\times(2n\times(r+p))$ matrix and

$$\mathbf{Z}(N) = [\ \mathbf{Z}(s)\ \ \mathbf{Z}(s+1)\ \cdots\ \mathbf{Z}(s+N-1)\ ]^T$$

$\boldsymbol{\theta} \in R^{2n\times(r+p)}$ and $\boldsymbol{\theta} = column[\ \mathbf{G}_s\ \mathbf{G}_{s-1}\cdots\mathbf{G}_1\ \mathbf{R}_s\ \mathbf{R}_{s-1}\cdots\mathbf{R}_1\ ]$.

When the ordinary least squares estimate method is applied, the estimate $\hat{\boldsymbol{\theta}}$ of $\boldsymbol{\theta}$ in the least squares sense is

$$\hat{\boldsymbol{\theta}} = (\mathbf{Z}(N)^T\mathbf{Z}(N))^{-1}\mathbf{Z}(N)^T\mathbf{y}(N)\ . \tag{4.3-28}$$

The flow chart for the modal identification can then be summarized as follows.

Table 4.3-1 Flow Chart for the First Algorithm

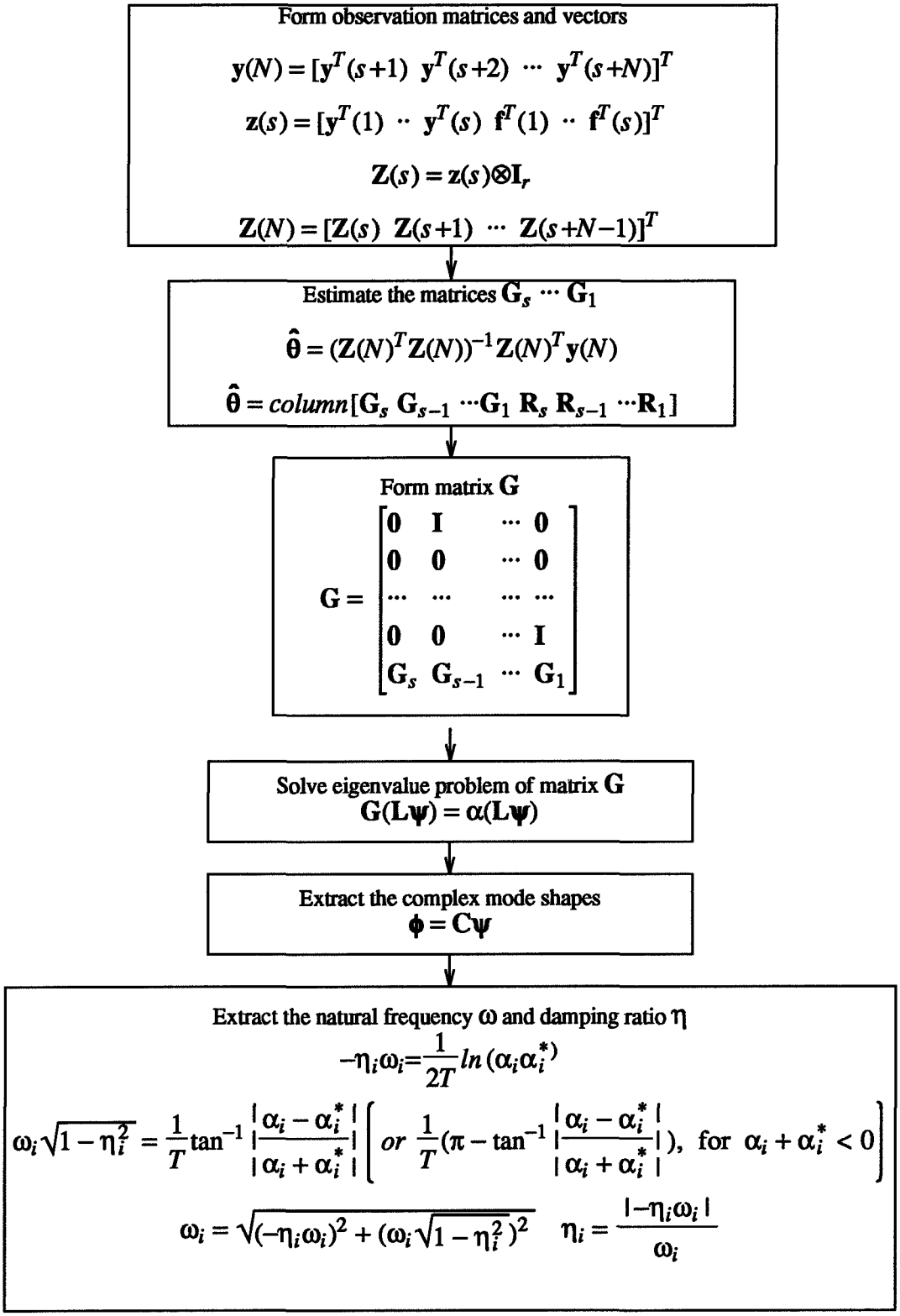

The second algorithm can be directly developed from Eqn. (4.2-47), which is rewritten as

$$\underline{\mathbf{y}}(s+1) = \mathbf{Z}^T(s)\boldsymbol{\theta} + \underline{\mathbf{e}}(s+1) \tag{4.3-29}$$

where $\mathbf{Z}(s)$ is a $(2n \times (2n+s \times p)) \times 2n$ matrix

$$\mathbf{Z}(s) = \begin{bmatrix} \underline{\mathbf{y}}(s) \\ \underline{\mathbf{f}}(s) \end{bmatrix} \otimes \mathbf{I}_{2n} \tag{4.3-30}$$

$$\boldsymbol{\theta} \in R^{2n \times (2n+r \times p)}$$

$$\boldsymbol{\theta} = column\ [\ \mathbf{G}\ \ \mathbf{R}\ ]\ . \tag{4.3-31}$$

Combining the observation at $k = 1, 2, \cdots, N$ yields

$$\underline{\mathbf{y}}(N) = \mathbf{Z}(N)\boldsymbol{\theta} + \underline{\mathbf{e}}(N) \tag{4.3-32}$$

where

$$\underline{\mathbf{y}}(N) = [\ \underline{\mathbf{y}}^T(s+1)\ \ \underline{\mathbf{y}}^T(s+2)\ \cdots\ \underline{\mathbf{y}}^T(s+N)\ ]^T$$

$$\underline{\mathbf{e}}(N) = [\ \underline{\mathbf{e}}^T(s+1)\ \ \underline{\mathbf{e}}^T(s+2)\ \cdots\ \underline{\mathbf{e}}^T(s+N)\ ]^T$$

and

$$\mathbf{Z}(N) = [\ \mathbf{Z}(s)\ \mathbf{Z}(s+1)\ \cdots\ \mathbf{Z}(s+N-1)\ ]^T$$

with N indicating the number of time data points.

When the least squares parameter estimation method is used

$$\hat{\boldsymbol{\theta}} = (\mathbf{Z}^T(N)\mathbf{Z}(N))^{-1}\mathbf{Z}^T(N)\mathbf{y}(N)\ . \tag{4.3-33}$$

In this case, the whole matrix **G** is estimated directly, while only the lower part of mathix **G** is estimated in the above algorithm. This algorithm is similar to the algorithm of the ITD method. In this algorithm matrix $\mathbf{Z}(n)$ consists of excitation and response data in the time domain, while in the ITD method this matrix consists of only free decay response data. If free decay response data is used with this algorithm, this algorithm will reduce to the algorithm of the ITD method.

The following scheme for this algorithm can then be obtained as in Table 4.3-2.

§ 4.4 SAMPLING IMPULSE RESPONSE

As mentioned in chapter 2, a linear damped vibrating structure can be described by its impulse response model in terms of impulse response function $\mathbf{H}(\tau)$ as follows

$$\mathbf{y}(t) = \int_{\tau=0}^{\infty} \mathbf{H}(\tau)\mathbf{f}(t-\tau)d\tau\ . \tag{4.4-1}$$

Knowing $\mathbf{H}(\tau)$ from $\tau = 0$ to ∞ and knowing $\mathbf{f}(s)$ for $s < t$, the corresponding response $\mathbf{y}(s)$ for $s < t$ can consequently be computed for any excitation. The impulse response is thus a complete characterization of the structure.

Table 4.3-2 Flow Chart for the Second Algorithm

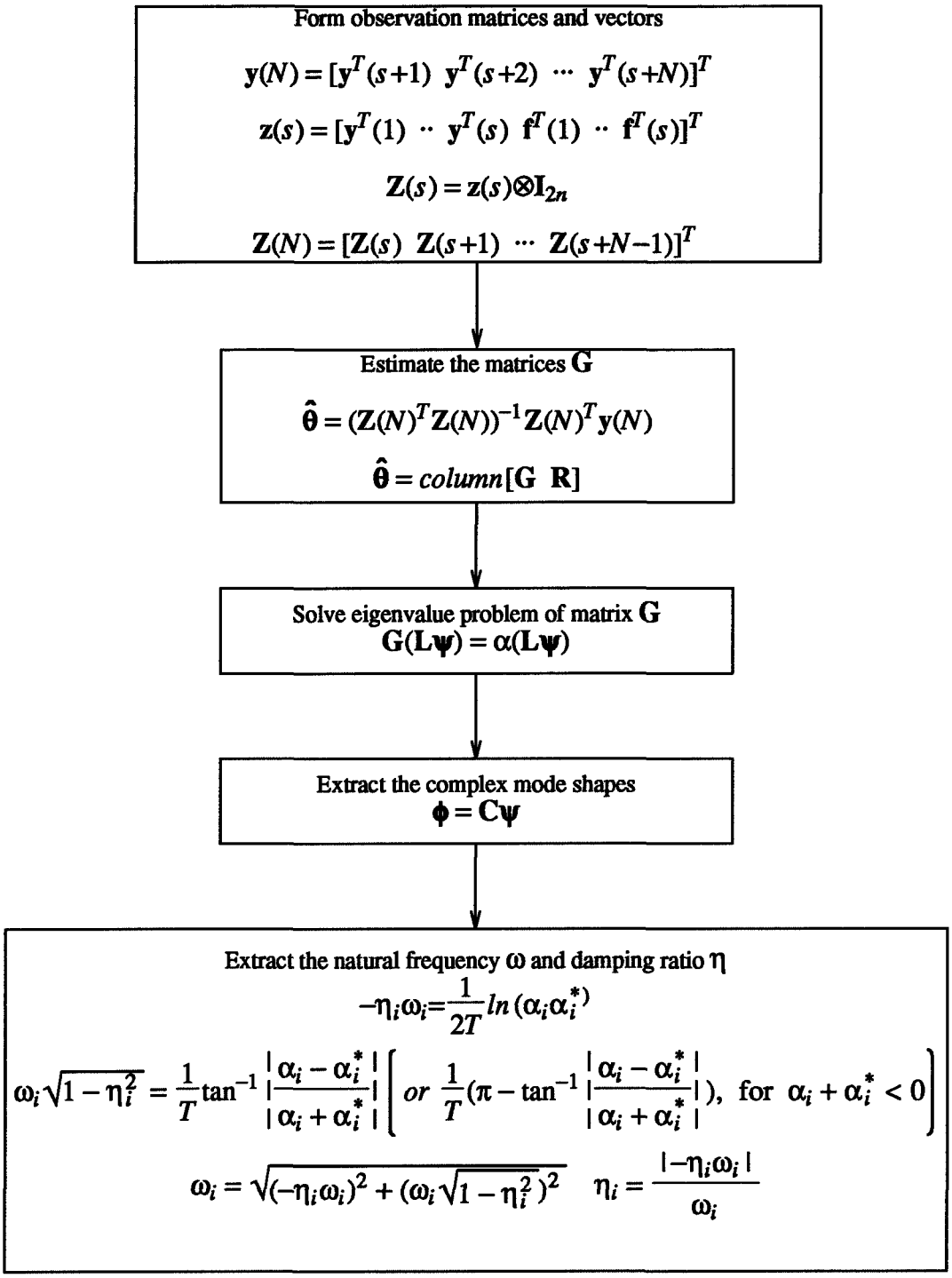

In the typical data-acquisition mode - discrete time form, the $\mathbf{y}(t)$ can be observed at the sampling instants $t_k = kT$, $k = 1, 2, \cdots$

$$\mathbf{y}(kT) = \int_{\tau=0}^{\infty} \mathbf{H}(\tau)\mathbf{f}(kT-\tau)d\tau \,. \tag{4.4-2}$$

The interval T is called the sampling interval. It is, of course, also possible to consider the situation where the sampling instants are not equally spread. Most often, in the computer or digital equipment control applications, the excitation signal $\mathbf{f}(t)$ is kept constant between the sampling instants:

$$\mathbf{f}(t) = \mathbf{f}_k, \qquad kT \le t < (k+1)T \,. \tag{4.4-3}$$

This is mostly done for practical implementation reasons, but it will also greatly simplify the analysis of the impulse response. Substituting Eqn. (4.4-3) into Eqn. (4.4-2) yields

$$\begin{aligned}\mathbf{y}(kT) &= \int_{\tau=0}^{\infty} \mathbf{H}(\tau)\mathbf{f}(kT-\tau)d\tau \\ &= \sum_{l=1}^{\infty} \int_{\tau=(l-1)T}^{lT} \mathbf{H}(\tau)\mathbf{f}(kT-\tau)d\tau \\ &= \sum_{l=1}^{\infty} \left[\int_{\tau=(l-1)T}^{lT} \mathbf{H}(\tau)d\tau\mathbf{f}_{k-l} \right] = \sum_{l=1}^{\infty} \mathbf{H}_T(l)\mathbf{f}_{k-l}\end{aligned} \tag{4.4-4}$$

where

$$\mathbf{H}_T(l) = \int_{\tau=(l-1)T}^{lT} \mathbf{H}(\tau)d\tau\,. \tag{4.4-5}$$

The expression in Eqn. (4.4-4) indicates the response at the sampling instants. Note that no approximation is involved in the excitation subject to the condition in Eqn. (4.4-3), and that it is sufficient to know the sequence $\mathbf{H}_T(l)$ from l=1 to ∞ in order to compute the response to the excitation. The relationship in Eqn. (4.4-4) describes a sampled-data model , and the matrix sequence $\mathbf{H}_T(l)$ from l=1 to ∞ is called the impulse response matrices of the structure.

Even if the excitation is not piecewise constant and subject to the condition in Eqn. (4.4-3), the representation in Eqn. (4.4-4) might still be a reasonable approximation, provided $\mathbf{f}(t)$ does not change too much during a sampling interval.

For convenience, Eqn. (4.4-4) is rewritten as

$$\mathbf{y}(t) = \sum_{k=1}^{\infty} \mathbf{H}(k)\mathbf{f}(t-k), \qquad t=0,\ 1,\ 2,\cdots, \qquad \textit{with}\ \ \mathbf{H}(0) = \mathbf{I} \tag{4.4-6}$$

When the excitation $\mathbf{f}(t)$ is the uncontrolled signal, the ARX model in Eqn. (4.2-50) becomes an AR model. By introducing a forward shift operator z and matrix polynomials

$$\mathbf{G}(z) = \mathbf{I} - \sum_{i=1}^{s} \mathbf{G}_i z^{-i}\,, \tag{4.4-7}$$

$$\mathbf{R}(z) = \sum_{i=1}^{s} \mathbf{R}_i z^{-i}, \qquad \text{and} \tag{4.4-8}$$

$$\mathbf{H}(z) = \mathbf{I} + \sum_{i=1}^{\infty} \mathbf{H}_i z^{-i}, \tag{4.4-9}$$

the AR model in Eqn. (4.2-50) and impulse response model in Eqn. (4.4-6) of the vibrating structure can be written as

$$\mathbf{G}(z)\mathbf{y}(k) = \mathbf{R}(z)\mathbf{f}(k) \tag{4.4-10}$$

and

$$\mathbf{y}(k) = \mathbf{H}(z)\mathbf{f}(k) \tag{4.4-11a}$$

or

$$\mathbf{y}(k) = \mathbf{H}(z)\mathbf{f}(k) + \boldsymbol{\varepsilon}(k) \tag{4.4-11b}$$

where the measurement noise $\boldsymbol{\varepsilon}(k)$ is involved.

Premultiplying both sides of Eqn. (4.4-10) by $\mathbf{R}^{-1}(z)$,

$$\mathbf{R}^{-1}(z)\mathbf{G}(z)\mathbf{y}(k) = \mathbf{f}(k) . \tag{4.4-12}$$

By defining $\mathbf{D}(z) = \mathbf{R}^{-1}(z)\mathbf{G}(z) = \mathbf{I} - \sum_{i=1}^{\infty} \mathbf{D}_i z^{-i}$, Eqn. (4.4-12) can be written as

$$\mathbf{D}(z)\mathbf{y}(k) = \mathbf{f}(k) . \tag{4.4-13}$$

Premultiplying both sides of Eqn. (4.4-11a) by $\mathbf{D}(z)$,

$$\mathbf{D}(z)\mathbf{y}(k) = \mathbf{D}(z)\mathbf{H}(z)\mathbf{f}(k)\,. \tag{4.4-14}$$

Comparing Eqn. (4.4-13) with Eqn. (4.4-14) yields

$$\mathbf{D}(z)\mathbf{H}(z) = \mathbf{I}. \tag{4.4-15}$$

By the convolution theorem, the time domain equivalent expression of Eqn. (4.4-15) is

$$\sum_{i=0}^{\infty} \mathbf{D}_i \mathbf{H}_{k-i} = \mathbf{I}\delta_k, \tag{4.4-16}$$

where δ_k is the Kronecker symbol. By considering $\mathbf{H}_0 = \mathbf{I}$ and directly evaluating Eqn. (4.4-16), the following recursive time domain relations are obtained for calculation of impulse response function matrix sequence $\mathbf{H}_k$ from the coefficient matrix sequence $\mathbf{D}_i$ of an AR model.

$$\mathbf{H}_0 = \mathbf{I}, \qquad \mathbf{H}_k = -\sum_{i=1}^{\infty} \mathbf{D}_i \mathbf{H}_{k-i} \quad \text{for } k = 1, 2, ,\cdots. \tag{4.4-17}$$

Once $\mathbf{D}_i$ are estimated from the AR model, the impulse response function $\mathbf{H}_k$ can be evaluated from the above recursive formulae. Note, since $\mathbf{H}_k = 0$ for $k < 0$, the sum in Eqn. (4.4-17) requires less than k terms for the computation. The impulse response model in Eqn. (4.4-11) and AR model in Eqn. (4.4-13) of a vibrating structure contain an infinite number of parameters. In practice, however, only a finite number of measured data will be available for the estimation of a finite number of parameters. By assuming their orders are M, $\mathbf{H}(z)$ in Eqn. (4.4-11) and $\mathbf{D}(z)$ in Eqn. (4.4-13) can rewritten as

$$\mathbf{H}(z) = \mathbf{I} + \sum_{i=1}^{M} \mathbf{H}_i z^{-i} \quad \text{and} \quad \mathbf{D}(z) = \mathbf{I} - \sum_{i=1}^{M} \mathbf{D}_i z^{-i}. \tag{4.4-18}$$

Therefore the estimation of the impulse response function is reduced to the estimation of the coefficient matrices of the AR model in Eqn. (4.4-13).

When the measurement noise is included, Eqn. (4.4-11b) becomes

$$\mathbf{y}(k) = \mathbf{H}(z)\mathbf{f}(k) + \boldsymbol{\varepsilon}(k) . \tag{4.4-19}$$

Correspondingly, Eqn. (4.4-13) can be written as

$$\mathbf{D}(z)\mathbf{y}(k) = \mathbf{f}(k) + \mathbf{D}(z)\boldsymbol{\varepsilon}(k) . \tag{4.4-20}$$

Similar procedures can be applied to Eqn. (4.4-20).

§ 4.5 INDIRECT METHOD FOR MODAL IDENTIFICATION

The indirect method for modal identification is presented in this section. This method consists of four main steps.

(i) estimation of the coefficient matrices of the AR model in Eqn. (4.4-13).

(ii) calculation of the impulse response function matrices from the estimated coefficient matrices of the AR model.

(iii) identification of the eigenvalues of the vibrating structure.

(iv) identification of the eigenvectors of the vibrating structure from the impulse response function matrices and eigenvalues.

§ 4.5.1 Estimation of Coefficient Matrices of AR Model

For the different excitations, different methods should be used to estimate the coefficient matrices of the AR model. Three cases of excitation are considered for the determination of the AR model: white noise excitation, general random excitation and control deterministic excitation.

1. White Noise Excitation

Some excitation such as ambient excitation can be considered as a white noise sequence. Assuming excitation $\mathbf{f}(k)$ is a multivariate white noise sequence independent of the response $\mathbf{y}(k)$ with zero mean and covariance matrix $\mathbf{\Omega}\delta_{ij}$, the coefficient matrix sequence $\mathbf{D}(k)$ of the AR model may then be estimated by solution of the Yule-Walker equation. Since the observation error $\boldsymbol{\varepsilon}(k)$ is white noise, $\mathbf{D}(z)\boldsymbol{\varepsilon}(k)$ can be expressed as another white noise sequence

$$\mathbf{D}(z)\boldsymbol{\varepsilon}(k) = \mathbf{e}(k). \tag{4.5-1}$$

The AR model in Eqn. (4.4-20) may then be written as

$$\mathbf{D}(z)\mathbf{y}(k) = \mathbf{w}(k), \qquad \mathbf{w}(k) = \mathbf{f}(k) + \mathbf{e}(k), \tag{4.5-2}$$

where $\mathbf{w}(k)$ is a white noise sequence. The solution is achieved by postmultiplying Eqn. (4.5-2) with $\mathbf{y}^T(k-j)$ and taking the ensemble average to obtain the important recursive relation for the correlation matrix $\mathbf{R}_k$

$$\mathbf{R}_k = \sum_{j=1}^{M} \mathbf{D}_j \mathbf{R}_{k-j}, \tag{4.5-3}$$

where $\mathbf{R}_k = E[\mathbf{y}(k)\,\mathbf{y}^T(k-j)]$, for $k = 1, 2, \cdots, M$

Eqn. (4.5-3) can be expressed in more compact block matrix form

$$\overline{\mathbf{R}} = \mathbf{R}\mathbf{D} \tag{4.5-4}$$

where

$$\mathbf{R} = \begin{bmatrix} \mathbf{R}_0 & \mathbf{R}_1 & \cdots & \mathbf{R}_{M-1} \\ \mathbf{R}_1^T & \mathbf{R}_0 & \cdots & \mathbf{R}_{M-2} \\ \vdots & \vdots & \vdots & \vdots \\ \mathbf{R}_{M-1}^T & \mathbf{R}_{M-2}^T & \cdots & \mathbf{R}_0 \end{bmatrix}, \tag{4.5-5}$$

$$\mathbf{D} = \begin{bmatrix} \mathbf{D}_1 \\ \mathbf{D}_2 \\ \vdots \\ \mathbf{D}_M \end{bmatrix}, \qquad \text{and} \tag{4.5-6}$$

$$\overline{\mathbf{R}} = \begin{bmatrix} \mathbf{R}_1 \\ \mathbf{R}_2 \\ \vdots \\ \mathbf{R}_M \end{bmatrix}. \tag{4.5-7}$$

Matrix $\mathbf{R}$ is positive definite, its inverse exists and the estimate of matrix $\mathbf{D}$ is

$$\hat{\mathbf{D}} = \mathbf{R}^{-1}\overline{\mathbf{R}}, \tag{4.5-8}$$

$$\mathbf{\Omega} = \mathbf{R}_0 - \sum_{i,j=1}^{M} \mathbf{D}_j \mathbf{R}_{i-j} \mathbf{D}_i^T. \tag{4.5-9}$$

In estimation, Eqn. (4.5-4) is usually not used, instead the Levinson algorithm is used since it is a fast algorithm and easy to use. The Levinson algorithm can be derived as follows, Eqn. (4.5-4) can be expressed as

$$\begin{bmatrix} \mathbf{R}_0 & \mathbf{R}_1 & \cdots & \mathbf{R}_{M-1} \\ \mathbf{R}_1^T & \mathbf{R}_0 & \cdots & \mathbf{R}_{M-2} \\ \vdots & \vdots & \vdots & \vdots \\ \mathbf{R}_{M-1}^T & \mathbf{R}_{M-2}^T & \cdots & \mathbf{R}_0 \end{bmatrix} \begin{bmatrix} \mathbf{D}_1^M \\ \mathbf{D}_2^M \\ \vdots \\ \mathbf{D}_M^M \end{bmatrix} = \begin{bmatrix} \mathbf{R}_1 \\ \mathbf{R}_2 \\ \vdots \\ \mathbf{R}_M \end{bmatrix}. \tag{4.5-10}$$

Eqn. (4.5-10) can be rewritten as

$$\begin{bmatrix} -\mathbf{R}_0 & -\mathbf{R}_1 & \cdots & -\mathbf{R}_M \\ -\mathbf{R}_1^T & \mathbf{R}_0 & \cdots & \mathbf{R}_{M-1} \\ -\mathbf{R}_2^T & \mathbf{R}_1^T & \cdots & \mathbf{R}_{M-2} \\ \vdots & \vdots & \vdots & \vdots \\ -\mathbf{R}_M^T & \mathbf{R}_{M-1}^T & \cdots & \mathbf{R}_0 \end{bmatrix} \begin{bmatrix} \mathbf{I} \\ \mathbf{D}_1^M \\ \mathbf{D}_2^M \\ \vdots \\ \mathbf{D}_M^M \end{bmatrix} = \begin{bmatrix} \mathbf{V}_M \\ \mathbf{0} \\ \mathbf{0} \\ \vdots \\ \mathbf{0} \end{bmatrix}. \tag{4.5-11}$$

Since $\mathbf{R}_i^T = \mathbf{R}_i$, the last M rows and M columns of Eqn. (4.5-11) are identical to Eqn. (4.5-10), while the first row is a definition of $\mathbf{V}_n$.

Suppose that Eqn. (4.5-11) has been solved for $\mathbf{D}_i^M$ and a solution for a higher order model in Eqn. (4.5-2) with order $M+1$ is sought. The estimates for $\mathbf{D}_i^{n+1}$ will then be defined analogously to Eqn. (4.5-11). To find this, it is noted

$$\begin{bmatrix} -\mathbf{R}_0 & -\mathbf{R}_1 & \cdots & -\mathbf{R}_M & -\mathbf{R}_{M+1} \\ -\mathbf{R}_1^T & \mathbf{R}_0 & \cdots & \mathbf{R}_{M-1} & \mathbf{R}_M \\ \vdots & \vdots & \vdots & \vdots & \vdots \\ -\mathbf{R}_M^T & \mathbf{R}_{M-1}^T & \cdots & \mathbf{R}_0 & \mathbf{R}_1 \\ -\mathbf{R}_{M+1}^T & \mathbf{R}_M^T & \cdots & \mathbf{R}_1^T & \mathbf{R}_0 \end{bmatrix} \begin{bmatrix} \mathbf{I} \\ \mathbf{D}_1^M \\ \vdots \\ \mathbf{D}_M^M \\ \mathbf{0} \end{bmatrix} = \begin{bmatrix} \mathbf{V}_M \\ \mathbf{0} \\ \vdots \\ \mathbf{0} \\ \mathbf{Q}_M \end{bmatrix}. \tag{4.5-12}$$

Here the first $M+1$ rows are identical to Eqn. (4.5-11), while the last row is a definition of $\mathbf{Q}_M$. The definition of $\hat{\mathbf{D}}_i^{M+1}$ looks quite like Eqn. (4.5-12), the only difference being that all but the first row of the right side should be zero. A moment's reflection on Eqn. (4.5-12) shows that it can be written as

$$\begin{bmatrix} -\mathbf{R}_0 & -\mathbf{R}_1 & \cdots & -\mathbf{R}_M & -\mathbf{R}_{M+1} \\ -\mathbf{R}_1^T & \mathbf{R}_0 & \cdots & \mathbf{R}_{M-1} & \mathbf{R}_M \\ \vdots & \vdots & \vdots & \vdots & \vdots \\ -\mathbf{R}_M^T & \mathbf{R}_{M-1}^T & \cdots & \mathbf{R}_0 & \mathbf{R}_1 \\ -\mathbf{R}_{M+1}^T & \mathbf{R}_M^T & \cdots & \mathbf{R}_1^T & \mathbf{R}_0 \end{bmatrix} \begin{bmatrix} \mathbf{0} \\ \mathbf{D}_M^M \\ \vdots \\ \mathbf{D}_1^M \\ \mathbf{I} \end{bmatrix} = \begin{bmatrix} \mathbf{Q}_M \\ \mathbf{0} \\ \vdots \\ \mathbf{0} \\ \mathbf{V}_M \end{bmatrix}. \tag{4.5-13}$$

By postmultiplying Eqn. (4.5-13) by $\mathbf{P}_M = -\mathbf{V}_M^{-1}\mathbf{Q}_M$ and adding to Eqn. (4.5-12) yields

$$\begin{bmatrix} -\mathbf{R}_0 & -\mathbf{R}_1 & \cdots & -\mathbf{R}_M & -\mathbf{R}_{M+1} \\ -\mathbf{R}_1^T & \mathbf{R}_0 & \cdots & \mathbf{R}_{M-1} & \mathbf{R}_M \\ \vdots & \vdots & \vdots & \vdots & \vdots \\ -\mathbf{R}_M^T & \mathbf{R}_{M-1}^T & \cdots & \mathbf{R}_0 & \mathbf{R}_1 \\ -\mathbf{R}_{M+1}^T & \mathbf{R}_M^T & \cdots & \mathbf{R}_1^T & \mathbf{R}_0 \end{bmatrix} \begin{bmatrix} \mathbf{I} \\ \mathbf{D}_1^M + \mathbf{D}_M^M \mathbf{P}_M \\ \vdots \\ \mathbf{D}_M^M + \mathbf{D}_1^M \mathbf{P}_M \\ \mathbf{P}_M \end{bmatrix} = \begin{bmatrix} \mathbf{V}_M + \mathbf{Q}_M \mathbf{P}_M \\ \mathbf{0} \\ \vdots \\ \mathbf{0} \\ \mathbf{0} \end{bmatrix}. \tag{4.5-14}$$

This is the defining relationship for $\hat{\mathbf{D}}_i^{M+1}$. Hence

$$\hat{\mathbf{D}}_k^{M+1} = \hat{\mathbf{D}}_k^M + \hat{\mathbf{D}}_{M-k+1}^M \hat{\mathbf{P}}_M, \quad k = 1, \cdots, M,$$
$$\hat{\mathbf{D}}_{M+1}^{M+1} = \hat{\mathbf{P}}_M,$$
$$\mathbf{V}_{M+1} = \mathbf{V}_M + \mathbf{Q}_M \hat{\mathbf{P}}_M, \tag{4.5-15}$$
$$\hat{\mathbf{P}}_M = -\mathbf{V}_M^{-1} \mathbf{Q}_M,$$
$$\mathbf{Q}_M = \sum_{k=1}^{M} (\mathbf{R}_{M+1-k})^T \hat{\mathbf{D}}_k - \mathbf{R}_{M+1}^T .$$

for $M = 1, 2, \cdots$

Starting with the initial conditions

$$\mathbf{V}_1 = -\mathbf{R}_1 \mathbf{R}_0^{-1} \mathbf{R}_1 - \mathbf{R}_0 \quad \text{and} \quad \hat{\mathbf{D}}_1^1 = \mathbf{R}_0^{-1} \mathbf{R}_1, \tag{4.5-16}$$

it is straightforward to compute $\hat{\mathbf{D}}_k^{M+1}$ from $\hat{\mathbf{D}}_k^M$.

2. General Random Excitation

In general, a random excitation is not a white noise sequence, hence the AR model in Eqn. (4.4-20) is not directly estimated by Levinson algorithm. In this case, the impulse response function matrix may be evaluated from the coefficient matrices of another modified AR model.

The following proper finite order impulse response model may be used in this case to approximate the infinite model in Eqn. (4.4-11b) with sufficient accuracy.

$$\mathbf{y}(k) = \mathbf{H}(z)\mathbf{f}(k) + \boldsymbol{\varepsilon}(k), \quad \mathbf{H}(z) = \mathbf{I} + \sum_{i=1}^{s} \mathbf{H}_i z^{-i}, \tag{4.5-17}$$

where $\boldsymbol{\varepsilon}(k)$ is an r-variate measurement noise sequence which is assumed to have a rational spectral density, and hence may be whitened by multivariate auto-regressive

form

$$\boldsymbol{\varepsilon}(k) = \mathbf{F}_1(z)\boldsymbol{\varepsilon}(k) + \mathbf{w}_1(k), \qquad \mathbf{F}_1(z) = \sum_{i=1}^{s} \mathbf{F}_{i1} z^{-i}. \tag{4.5-18}$$

$\mathbf{F}_{i1}$ are $r \times r$ coefficient matrices and $\mathbf{w}_1(k)$ is an $r \times 1$ white noise sequence with zero mean and covariance matrix $\boldsymbol{\Omega}_1$.

The excitation is assumed to be given by an AR model as

$$\mathbf{f}(k) = \mathbf{F}_2(z)\mathbf{f}(k) + \mathbf{w}_2(k), \qquad \mathbf{F}_2(z) = \sum_{i=1}^{s} \mathbf{F}_{i2} z^{-i}. \tag{4.5-19}$$

where $\mathbf{F}_{i2}$ are $p \times p$ coefficient matrices and $\mathbf{w}_2(k)$ is an $p \times 1$ white noise sequence with zero mean and covariance matrix $\boldsymbol{\Omega}_2$, representing the measurement noise for $\mathbf{f}(k)$.

Introducing augmented vectors

$$\mathbf{q}(k) = \begin{bmatrix} \mathbf{y}(k) \\ \mathbf{f}(k) \end{bmatrix}, \quad \mathbf{w}(k) = \begin{bmatrix} \mathbf{w}_1(k) \\ \mathbf{w}_2(k) \end{bmatrix}, \quad \boldsymbol{\xi}(k) = \begin{bmatrix} \boldsymbol{\varepsilon}(k) \\ \mathbf{f}(k) \end{bmatrix}, \tag{4.5-20}$$

Eqns. (4.5-17), (4.5-18) and (4.5-19) can be assembled into

$$\mathbf{q}(k) = \begin{bmatrix} \mathbf{0} & \mathbf{H}(z) \\ \mathbf{0} & \mathbf{0} \end{bmatrix} \mathbf{q}(k) + \boldsymbol{\xi}(k) \quad \text{and} \quad \boldsymbol{\xi}(k) = \begin{bmatrix} \mathbf{F}_1(z) & \mathbf{0} \\ \mathbf{0} & \mathbf{F}_2(z) \end{bmatrix} \boldsymbol{\xi}(k) + \mathbf{w}(k). \tag{4.5-21}$$

The covariance matrix of $\mathbf{w}(k)$ is then $\boldsymbol{\Omega} = \begin{bmatrix} \boldsymbol{\Omega}_1 & \mathbf{0} \\ \mathbf{0} & \boldsymbol{\Omega}_2 \end{bmatrix}$.

Premultiplying both sides of Eqn. (4.5-21) by $\left\{\mathbf{I}-\begin{bmatrix}\mathbf{F}_1(z) & \mathbf{0}\\ \mathbf{0} & \mathbf{F}_2(z)\end{bmatrix}\right\}$,

$$\mathbf{q}(k)=\begin{bmatrix}\mathbf{F}_1(z) & [\mathbf{I}-\mathbf{F}_1(z)]\mathbf{H}(z)\\ \mathbf{0} & \mathbf{F}_2(z)\end{bmatrix}\mathbf{q}(k)+\mathbf{w}(k). \tag{4.5-22}$$

Defining

$$\mathbf{D}(z)=\begin{bmatrix}\mathbf{F}_1(z) & [\mathbf{I}-\mathbf{F}_1(z)]\mathbf{H}(z)\\ \mathbf{0} & \mathbf{F}_2(z)\end{bmatrix}=\sum_{i=1}^{q}\mathbf{D}_i z^{-i}, \tag{4.5-23}$$

Eqn. (4.5-22) reduces to an AR model

$$\mathbf{q}(k)=\sum_{i=1}^{q}\mathbf{D}_i\mathbf{q}(k-i)+\mathbf{w}(k). \tag{4.5-24}$$

Since $\mathbf{q}(k)$ is measured, the coefficient matrix sequence $\mathbf{D}_i$ of the AR model in Eqn. (4.5-24) can be estimated by following the same procedure as in the case of white noise excitation, as discussed in the preceding section. Once the coefficient matrix sequence $\mathbf{D}_i$ is estimated, the impulse response function matrix sequence may be calculated using Eqn. (4.5-23). To this end, the matrix $\mathbf{D}_i$ is partitioned

$$\mathbf{D}_i=\begin{bmatrix}\mathbf{D}_{i11} & \mathbf{D}_{i12}\\ \mathbf{D}_{i21} & \mathbf{D}_{i22}\end{bmatrix}, \tag{4.5-25}$$

and compared with Eqn. (4.5-23),

$$\mathbf{F}_{i1} = \mathbf{D}_{i11}, \quad \mathbf{F}_{i2} = \mathbf{D}_{i22} \quad \text{and} \quad \mathbf{D}_{i12} = \mathbf{H}_i - \mathbf{F}_{i1}\mathbf{H}_i. \tag{4.5-26}$$

From Eqn. (4.5-26), the following recursive formulae is obtained

$$\mathbf{H}_i = \mathbf{D}_{i12} + \mathbf{D}_{i11}\mathbf{H}_i. \tag{4.5-27}$$

Eqn. (4.5-27) can also be written in element form such as

$$h_{ij}(k) = d_{i,j+s}(k) + \sum_{l=1}^{s}\sum_{m=1}^{s} d_{im}(l)h_{mj}(k-l). \tag{4.5-28}$$

As a result, the relationship in Eqn. (4.5-24) can be used to estimate the coefficient matrix sequence $\mathbf{D}_i$ and the recursive formulae Eqns. (4.5-27) or (4.5-28) may be used to calculate the impulse response function matrix sequence $\mathbf{H}_i$.

3. Control Excitation

In the case of control excitation and white noise observation error, the impulse response model with a finite number of parameters in Eqn. (4.5-17) can be used directly with the least squares estimate algorithm to determine the impulse functions $\mathbf{H}_i$. However, if the observation error is not white noise but has rational spectral density , the noise may be whitened as an AR process

$$\boldsymbol{\varepsilon}(k) = \mathbf{C}(z)\boldsymbol{\varepsilon}(k) + \mathbf{e}(k), \quad \mathbf{C}(z) = \sum_{i=1}^{s}\mathbf{C}_i z^{-i}. \tag{4.5-29}$$

Hence, $\mathbf{e}(k) = (\mathbf{I} - \mathbf{C}(z))\boldsymbol{\varepsilon}(k)$. The transfer function $\mathbf{I} - \mathbf{C}(z)$ implies the whitening filter for $\boldsymbol{\varepsilon}(k)$. Premultiplying this function on both sides of Eqn. (4.5-17) yields

$$\mathbf{y}(k) = \mathbf{C}(z)\mathbf{y}(k) + \mathbf{B}(z)\mathbf{f}(k) + \mathbf{e}(k), \tag{4.5-30}$$

$$\mathbf{B}(z) = (\mathbf{I} - \mathbf{C}(z))\mathbf{H}(z) = \sum_{i=0}^{m+s} \mathbf{B}_i z^{-i} \quad with \ \ \mathbf{B}_0 = \mathbf{0}.$$

The least squares estimate can be applied to Eqn. (4.5-30) to obtain $\mathbf{B}_i$ and $\mathbf{C}_i$ and the estimate $\mathbf{H}_i$ can be computed by using the following relation

$$\hat{\mathbf{H}}_1 = \hat{\mathbf{B}}_1 + \hat{\mathbf{C}}_1, \quad \hat{\mathbf{H}}_i = \hat{\mathbf{B}}_i + \hat{\mathbf{C}}_i + \sum_{l=1}^{i-1} \hat{\mathbf{C}}_l \hat{\mathbf{H}}_{i-l}, \quad i \geq 2. \tag{4.5-31}$$

§ 4.5.2 Identification of Natural Frequency and Damping Ratio

In § 4.3, an eigenvalue problem of matrix **G** was introduced for the modal identification

$$\mathbf{G}\boldsymbol{\phi} = \alpha\boldsymbol{\phi}. \tag{4.5-32}$$

The characteristic equation of matrix **G** is

$$\det(\alpha\mathbf{I} - \mathbf{G}) = 0 \tag{4.5-33}$$

Considering the structure of matrix **G** in Eqn. (4.2-11)

$$\mathbf{G} = \begin{bmatrix} \mathbf{0} & \mathbf{I} & \cdots & \mathbf{0} \\ \mathbf{0} & \mathbf{0} & \cdots & \mathbf{0} \\ : & : & : & : \\ \mathbf{0} & \mathbf{0} & \cdots & \mathbf{I} \\ \mathbf{G}_s & \mathbf{G}_{s-1} & \cdots & \mathbf{G}_1 \end{bmatrix}. \tag{4.5-34}$$

Eqn. (4.5-33) may be expanded as

$$\det(\mathbf{I} - \sum_{i=1}^{s} \alpha^{-i} \mathbf{G}_i) = 0 . \tag{4.5-35}$$

When there is one measurement station, the observation matrix $\mathbf{C}$ takes the form

$$\mathbf{C} = [\ 1\ 0\ 0\ \cdots\ 0\ ], \tag{4.5-36}$$

and the expansion in Eqn. (4.5-35) becomes

$$1 - \sum_{1}^{2n} \alpha^{-i} G_i = 0 . \tag{4.5-37}$$

On the other hand, the roots of the determinant of matrix polynomial $\mathbf{G}(z)$ are defined as the poles of the ARMA model. The characteristic equation of matrix polynomial $\mathbf{G}(z)$ is

$$\det(\mathbf{I} - \sum_{i=1}^{s} \mathbf{G}_i z^{-i}) = 0. \tag{4.5-38}$$

By comparison of Eqns. (4.5-35) and (4.5-38), the poles z of the ARMA model are equal to the eigenvalues α of matrix $\mathbf{G}$. The eigenvalues of matrix $\mathbf{G}$ can therefore be determined by the poles of the ARMA model. Once the eigenvalue α is identified, the eigenvalue of the vibrating structure can be calculated by equation $e^{\lambda T} = \alpha$. Assuming the order of the determinant of $\mathbf{G}(z)$ is $2n$, then $\det(\mathbf{G}(z))$ can be expanded as

$$\det(\mathbf{G}(z)) = 1 - G_1 z^{-1} - G_2 z^{-2} - \cdots - G_{2n} z^{-2n}. \tag{4.5-39}$$

From Eqn. (4.5-37) the det(G(z)) in Eqn. (4.5-39) is identical to the characteristic polynomial of the following matrix

$$\mathbf{G} = \begin{bmatrix} 0 & 1 & : & 0 & 0 \\ : & : & : & : & : \\ 0 & 0 & : & 0 & 1 \\ G_{2n} & G_{2n-1} & : & G_2 & G_1 \end{bmatrix}. \tag{4.5-40}$$

This means that $det(\mathbf{G}(z))$ is the determinant of the transfer function of a univariate ARMA model of the vibrating structure. In the case of white noise random excitation and white noise observation error, the univariate ARMA model can be written as

$$G(z)y(k) = F(z)u(k), \tag{4.5-41}$$

where

$$G(z) = 1 - \sum_{i=1}^{2n} G_i z^{-i} \quad \text{and} \quad F(z) = 1 + \sum_{i=1}^{2n} F_i z^{-i}. \tag{4.5-42}$$

$u(k)$ is a white noise process, the sum of white noise excitation and white noise measurement error.

Postmultiplying both sides of Eqn. (4.5-41) by $y(k-\tau)$ and taking the expectation for $k = 2n+1,\ 2n+2,\ \cdots,\ 2n+N$ and $N > 2n$ yields

$$\begin{bmatrix} R_y(2n) & R_y(2n-1) & \cdots & R_y(1) \\ R_y(2n+1) & R_y(2n) & \cdots & R_y(2) \\ .. & .. & \cdots & .. \\ R_y(2n+N-1) & R_y(2n+N-2) & \cdots & R_y(N) \end{bmatrix} \begin{bmatrix} G_1 \\ G_2 \\ : \\ G_{2n} \end{bmatrix} = \begin{bmatrix} R_y(2n+1) \\ R_y(2n+2) \\ : \\ R_y(2n+N) \end{bmatrix} \tag{4.5-43}$$

where $R_y(\tau)$ is the covariance function of the actual measurement $y(k)$ and the actual estimate of $R_y(\tau)$, based on N measurement data, can be calculated as

$$\hat{R}_y(\tau) = \frac{1}{N} \sum_{k=\tau}^{N+\tau-1} y(k)y(k-\tau). \tag{4.5-44}$$

In short form, Eqn. 4.5-43 becomes

$$\mathbf{Rg} = \mathbf{r}. \tag{4.5-45}$$

The least squares estimate of the AR part **g** is then obtained

$$\hat{\mathbf{g}} = (\mathbf{R}^T\mathbf{R})^{-1}\mathbf{R}^T\mathbf{r} \tag{4.5-46}$$

In the case of control excitation $f(k)$ and white noise error $w(k)$, det($\mathbf{G}(z)$) corresponds to the following univariate ARMA model

$$G(z)y(k) = E(z)f(k) + w(k), \qquad E(z) = \sum_{i=1}^{2n} E_i z^{-i}. \tag{4.5-47}$$

Assuming Assuming

$\boldsymbol{\theta} = [G_1 \ G_2 \ \cdots \ G_{2n} \ E_1 \ E_2 \cdots \ E_{2n}]^T$ and

$$\boldsymbol{\phi}(k) = [y(k-1)\, y(k-2) \cdots y(k-2n)\, f(k-1)\, f(k-2) \cdots f(k-2n)]^T, \tag{4.5-48}$$

Eqn. (4.5-47) in short form is

$$y(k) = \boldsymbol{\phi}^T(k)\boldsymbol{\theta} + w(k). \tag{4.5-49}$$

The least square estimate of the vector $\boldsymbol{\theta}$ is

$$\hat{\boldsymbol{\theta}} = \mathbf{R}^{-1}\mathbf{r} \tag{4.5-50}$$

where the $4n \times 4n$ matrix $\mathbf{R}$ and the $4n$-dimensional column vector $\mathbf{r}$ are

$$\hat{\mathbf{R}} = \begin{bmatrix} \hat{\mathbf{R}}_y & \hat{\mathbf{R}}_{yf} \\ \hat{\mathbf{R}}_{fy} & \hat{\mathbf{R}}_f \end{bmatrix} = \frac{1}{N}\sum_{k=1}^{N} \boldsymbol{\phi}(k)\boldsymbol{\phi}^T(k), \qquad \hat{\mathbf{r}} = \frac{1}{N}\sum_{k=1}^{N} \boldsymbol{\phi}(k)y(k). \tag{4.5-51}$$

The entries of $\hat{\mathbf{R}}_y$ and $\hat{\mathbf{r}}$ will be of form

$$\hat{R}_{ij} = \frac{1}{N}\sum_{k=1}^{N} y(k-i)y(k-j), \qquad 1 \le i,\ j \le 2n \tag{4.5-52}$$

and similar sums of $f(k-i)\cdot f(k-j)$ or $f(k-i)\cdot y(k-j)$ are used for the other entries of $\hat{\mathbf{R}}$. That is, they consist of the estimate of the correlation functions of $y(k)$ and $f(k)$.

The error of the estimate is

$$\hat{\boldsymbol{\theta}} - \boldsymbol{\theta} = \mathbf{R}^{-1}\frac{1}{N}\sum_{k=1}^{N} \boldsymbol{\phi}(k)w(k). \tag{4.5-53}$$

When $w(k)$ is a white noise sequence of independent random variables with zero mean values, then $w(k)$ does not depend on events up to time $k-1$, and hence $E(\boldsymbol{\phi}(k)w(k)) = \mathbf{0}$. $E(\boldsymbol{\phi}(k)\boldsymbol{\phi}^T(k)) = \mathbf{R}$ is positive definite and thus nonsingular. The estimate $\hat{\boldsymbol{\theta}}$ therefore converges to $\boldsymbol{\theta}$ as N tends to infinity.

Care needs to be exercised when the observation noise is not white. In this case, the least squares estimate will not converge to the true values of G_i and E_i. To deal with this problem, by assuming the observation noise has a rational spectral density, the noise can then be expressed by an AR process of order, say, r,

$$D(z)w(k) = e(k) \tag{4.5-54}$$

where $e(k)$ is a white noise sequence.

Premultiplying both sides of Eqn. (4.5-47) by $D(z)$ yields

$$D(z)G(z)y(k) = D(z)E(z)f(k)+e(k). \tag{4.5-55}$$

The least squares estimate algorithm can applied to Eqn. (4.5-55) to obtain estimates $D(z)G(z)$ and $D(z)E(z)$, and are consistent since $e(k)$ is white. However, $D(z)G(z)$ is of order $2n+r$ and thus has $2n+r$ roots, of which r roots belong to the AR process $D(z)$ of the colored noise. Since $D(z)G(z)$ and $D(z)E(z)$ have a common factor $D(z)$ of order r, they have r common roots. The roots of $D(z)E(z)$ are therefore also to be calculated and compared with those of $D(z)G(z)$. When some zeros of both parts are equal to each other, they are considered as roots of the noise AR part $D(z)$ and can be eliminated. Since exact "equality" is not a realistic comparison, then, when the values of some roots of the two groups are almost equal to each other, they may be expected to belong to excessive modes rather than the

actual structural modes and thus can be eliminated. The remaining roots of $D(z)G(z)$ will belong to $G(z)$ and be taken as the poles of the ARMA model of the vibrating structure.

For the free decay response data, a procedure similar to the case of white noise excitation and white noise observation error may be derived when the free decay response measurement errors can be considered as white noise sequence.

As previously mentioned in § 4.3, the eigenvalues of matrix **G** have the form of $e^{\lambda_i T}$, from which the eigenvalues, or natural frequencies, and critical damping factors of the original structure can be calculated by Eqns. (4.3-16) to (4.3-20).

§ 4.5.3 Identification of Eigenvectors

Sampling is performed in the discrete time, a linear vibrating structure's response to any excitation has the Z-domain relationship

$$\mathbf{y}(z) = \overline{\mathbf{H}}(z)\mathbf{f}(z) \tag{4.5-56}$$

where $\mathbf{y}(z)$ and $\mathbf{f}(z)$ are the Z-transform of the response and excitation sequences respectively. $\overline{\mathbf{H}}(z)$ is the system transfer function and can be expressed by the poles $e^{\lambda_i \Delta t}$ and residue matrix $\mathbf{U}_i$ such as

$$\overline{\mathbf{H}}(z) = \sum_{i=1}^{2n} \frac{\mathbf{U}_i}{1 - e^{\lambda_i \Delta t} z^{-1}}, \tag{4.5-57}$$

where matrix $\mathbf{U}_i = \boldsymbol{\psi}_i \boldsymbol{\psi}_i^T$ with λ_i and $\boldsymbol{\psi}_i$ being the eigenvalues and eigenvectors of the original structure, which are in general, complex. From discrete-time system theory, the corresponding impulse response function matrix sequence is the inverse Z-transform of the system transfer function, that is;

$$\mathbf{H}_k = \sum_{i=1}^{2n} \mathbf{U}_i (e^{\lambda_i \Delta t})^k = \sum_{i=1}^{2n} \mathbf{U}_i (\alpha_i)^k, \tag{4.5-58}$$

which, when extended to the full data set of N samples, gives

$$\begin{cases} \mathbf{H}_0 = \mathbf{U}_1 + \mathbf{U}_2 + \cdots + \mathbf{U}_{2n} \\ \mathbf{H}_1 = \alpha_1 \mathbf{U}_1 + \alpha_2 \mathbf{U}_2 + \cdots + \alpha_{2n} \mathbf{U}_{2n} \\ \cdots\cdots \\ \mathbf{H}_N = \alpha_1^N \mathbf{U}_1 + \alpha_2^N \mathbf{U}_2 + \cdots + \alpha_{2n}^N \mathbf{U}_{2n} \end{cases} \tag{4.5-59}$$

Eqn. (4.5-59) can be used to estimate residue matrix $\mathbf{U}_i$. In practice, only one column of each residue matrix needs to be identified and only one column of the impulse response function matrices for the different time instants is required for identification. The k-th column of matrices $\mathbf{H}_i$ and $\mathbf{U}_i$ is then considered and from Eqn. (4.5-59)

$$\mathbf{H} = \mathbf{U}\Gamma, \tag{4.5-60}$$

where

$$\Gamma = \begin{bmatrix} 1 & \alpha_1 & \alpha_1^2 & \cdots & \alpha_1^N \\ 1 & \alpha_2 & \alpha_2^2 & \cdots & \alpha_2^N \\ \cdots & \cdots & \cdots & \cdots & \cdots \\ 1 & \alpha_{2n} & \alpha_{2n}^2 & \cdots & \alpha_{2n}^N \end{bmatrix}, \tag{4.5-61}$$

$$\mathbf{H} = [\, \mathbf{h}_0^k \;\; \mathbf{h}_1^k \;\; \cdots \;\; \mathbf{h}_N^k \,] \tag{4.5-62a}$$

and

$$\mathbf{U} = [\, \mathbf{u}_1^k \;\; \mathbf{u}_2^k \;\; \cdots \;\; \mathbf{u}_{2n}^k \,]. \tag{4.5-62b}$$

The least square estimate of **U** is obtained as

$$\hat{\mathbf{U}} = \mathbf{H}\boldsymbol{\Gamma}^T(\boldsymbol{\Gamma}\boldsymbol{\Gamma}^T)^{-1}. \tag{4.5-63}$$

From the estimated residue $\hat{\mathbf{u}}_i^k = \hat{\boldsymbol{\psi}}_i\hat{\psi}_{ik}$, the eigenvector of the vibrating structure corresponding to the eigenvalue λ_i is $\hat{\boldsymbol{\psi}}_i = \hat{\mathbf{u}}_i^k/\hat{\psi}_{ik}$ with $\hat{\psi}_{ik} = \sqrt{\hat{u}_{ik}^k}$.

§ 4.6 SOME ASPECTS OF APPLICATION

§ 4.6.1 Determination of the Order of the Test Structure

Although it is known that the measured responses come from a linear vibrating structure, neither the parameters nor the degrees of freedom of the structure being excited are known. The first step for processing the identification of the modal parameters of a vibrating structure therefore is to determine the degrees of freedom of the structure being excited, which is equivalent to the rank of the response measurement matrix.

In order to achieve this goal, the following measurement matrix is formed

$$\bar{\mathbf{Q}}(s) = \begin{bmatrix} \mathbf{y}(1) & \mathbf{y}(2) & \cdots & \mathbf{y}(s-1) \\ \mathbf{y}(2) & \mathbf{y}(3) & \cdots & \mathbf{y}(s) \\ \vdots & \vdots & \cdots & \vdots \\ \mathbf{y}(N) & \mathbf{y}(N+1) & \cdots & \mathbf{y}(N+s-2) \end{bmatrix}. \tag{4.6-1}$$

There are three methods to be recommended for determination of the degrees of freedom of the structure by use of the measurement matrix. The first method is to

successively calculate the determinant of the matrix based on the properties of the matrix $\overline{\mathbf{Q}}^T\overline{\mathbf{Q}}$,

$$det(\overline{\mathbf{Q}}^T(k)\overline{\mathbf{Q}}(k)) \begin{Bmatrix} > \\ = \end{Bmatrix} 0 \text{ for } k \begin{Bmatrix} \leq \\ > \end{Bmatrix} m. \tag{4.6-2}$$

where k represents the momentary order of matrix $\overline{\mathbf{Q}}^T\overline{\mathbf{Q}}$ and m the exact order of the structure excited in the test. This can be done by successively calculating the determinant of matrix $\overline{\mathbf{Q}}^T\overline{\mathbf{Q}}$ by assuming k degrees of freedom with $k = 1, 2, \cdots$, until the determinant of the matrix becomes zero at $k = m + 1$. Then the real order of the structure will be m. Care should be taken about so called "zero". Exact zero is not a reasonable test, instead a near zero test should be performed by choosing a tolerance ε close to absolute precision of the number of the calculation. The determinant ratio can be calculated as

$$DV(k) = det(\overline{\mathbf{Q}}^T(k)\overline{\mathbf{Q}}(k)) \,/\, det(\overline{\mathbf{Q}}^T(k+1)\overline{\mathbf{Q}}(k+1)) \tag{4.6-3}$$

for succeeding orders $k = 1, 2, 3, \cdots$. If the value of the determinant ratio $DV(k)$ shows a distinct increase compared with previous value $DV(k-1)$, the value of k corresponds approximately to the real order m.

The second method is to perform the singular-value decomposition of matrix $\overline{\mathbf{Q}}^T\overline{\mathbf{Q}}$ such as

$$\overline{\mathbf{Q}}^T\overline{\mathbf{Q}} = \mathbf{U}\mathbf{S}\mathbf{U}^T. \tag{4.6-4}$$

$\mathbf{S}$ is a diagonal matrix with the singular values s_i in monotonic decreasing order and $\mathbf{U}$ is a orthogonal matrix.

For a tolerance ε, if

$$s_m/s_1 \geq \varepsilon > s_{m+1}/s_1, \tag{4.6-5}$$

the rank of matrix $\overline{\mathbf{Q}}^T\overline{\mathbf{Q}}$ will be *m*. The tolerance should be somewhat larger than the relative precision of the numbers of the calculation.

The third method is to perform an orthogonal-triangular decomposition. By permuting the columns of $\overline{\mathbf{Q}}^T\overline{\mathbf{Q}}$, the diagonal elements of **R** can be arranged to be monotonically decreasing, i.e., there is a permutation matrix **P** such that

$$\overline{\mathbf{Q}}^T\overline{\mathbf{Q}}\mathbf{P} = \mathbf{UR}. \tag{4.6-6}$$

U is an orthogonal matrix and **R** is an upper triangular matrix with diagonal elements $r_{11} \geq r_{22} \geq \cdots \geq r_{pp} \geq 0$. If $\overline{\mathbf{Q}}^T\overline{\mathbf{Q}}$ is of rank *m*, a sharp break after r_{mm} can be expected, that is,

$$r_{mm} \gg r_{ii} \quad when \quad i > m\ . \tag{4.6-7}$$

While the first two methods can detect well-defined rank of matrix $\overline{\mathbf{Q}}^T\overline{\mathbf{Q}}$, the third method may be conservative for determining the rank of matrix $\overline{\mathbf{Q}}^T\overline{\mathbf{Q}}$.

§ 4.6.2 The Number of Measurement Stations

The number of measurement stations depends on the purpose of a test, the degrees of freedom to be excited and accuracy requirement. From the above discussion and Eqns. (4.2-11) and (4.3-14), if only the frequencies and damping ratios need to be identified, a single measurement station with adequate time point data will be

enough for the identification. In this case, the matrix G becomes

$$\mathbf{G} = \begin{bmatrix} 0 & 1 & \cdot\cdot & 0 & 0 \\ \cdot\cdot & \cdot\cdot & \cdot\cdot & \cdot\cdot & \cdot\cdot \\ 0 & 0 & \cdot\cdot & 1 & 0 \\ 0 & 0 & \cdot\cdot & 0 & 1 \\ G_{2n} & G_{2n-1} & \cdot\cdot & G_2 & G_1 \end{bmatrix} \tag{4.6-8}$$

whose characteristic polynomial is

$$\sum_{i=0}^{2n} G_i \alpha^{2n-i} = \prod_{j=1}^{n} (\alpha - e^{\lambda_j T})\,(\alpha - e^{\lambda_j^* T}) \tag{4.6-9}$$

with $G_0 = 1$ and * representing the conjugate of a complex number.

It can also be seen from equation (4.3-14) that in order to identify the eigenvectors of a test structure, at least two measurement stations are required. However, in this case only two co-ordinates of each eigenvector can be identified. If more coordinates of each eigenvector are required to be identified, more measurement stations should be arranged. An alternative method is to arrange two measurement stations at each time and one measurement station is fixed in a series of tests as the reference measuring points. Other measurement stations can move each time in the series of tests.

§ 4.6.3 Numerical Computing

Matrix $\mathbf{Z}^T(N)\mathbf{Z}(N)$ in Eqns. (4.3-28) and (4.3-33) may be ill-conditioned, in particular when its dimension is high. There exists a method to find $\hat{\boldsymbol{\theta}}$ that is much better numerically behaved. The so called "square-root filtering algorithms" are recommended for use in the least squares estimation.

From Eqns. (4.3-28) and (4.3-33), it can be seen that only half of the number of the

parameters in Eqn. (4.3-28) compared with that of Eqn. (4.3-33), need to be estimated. This is one of the computation advantages of the direct method. In addition to this, the matrix for the eigenvalue problem in Eqn. (4.3-14) is a Hessenberg matrix, the eigenvalue problem of which is much easier to solve than that of the ITD method and computation time can be reduced in the solution of the eigenvalue problem of matrix **G**.

§ 4.6.4 Sampling Rate

The sampling rate will be dealt with in Chapter 6 in detail. However, for completeness, it is briefly discussed in this section. Through simple manipulations of trigonometric formulas, the sampling rate f_s should satisfy the following relationship

$$f_s > (\frac{2}{k+1}) f_{\max} \tag{4.6-10}$$

where $f_{\max}$ is the maximum frequency and can be identified by the sampling rate f_s, whilst k is determined according to the range of frequencies considered. For the range of 0 to $f_{\max}$, $k = 0$. For the range of $f_{\min} > 0$ to $f_{\max}$, $k = 0, 1, \cdots, p$ and $p < \frac{f_{\min}}{f_{\max} - f_{\min}}$. A frequency $f_N = f_s / 2$ is called *Nyquist* frequency. The information about frequencies higher than the Nyquist frequency will be lost.

When $f_{\max}$ is excessively high, the whole range of $(0 - f_{\max})$ requires an extremely high sampling rate which may present practical difficulties. In this case, there are two methods recommended to solve the problem. The first method is to divide the whole range of frequencies into some sub-range band. This approach allows smaller sampling rates to be used for each frequency band. Each frequency band must be

studied using response information which contains only frequency components in the range of interest (through filtering or other means). The second solution is to use a high recording speed tape recorder to record the signals and then play them back at a lower speed during the digitization process. The ratio of two speeds is used later as a correction factor to obtain the actual structural frequencies.

§ 4.6.5 Relationships of the Direct Method with Other Time Domain Methods

The direct method is a very general method, which can be reduced to some other time domain methods under certain circumstances. As mentioned in § 4.4, generally the response of a vibrating structure can be expressed in terms of the convolution product of the impulse function of the system and the excitations such as

$$\mathbf{y}(t) = \int_0^\infty \mathbf{H}(\tau)\mathbf{f}(t-\tau)d\tau. \tag{4.6-11}$$

$\mathbf{H}(\tau)$is the impulse function matrix of the structure and $\mathbf{H}(0) = \mathbf{I}$ without loss of generality, $\mathbf{y}(k)$ is the response vector and $\mathbf{f}(k)$ is the excitation vector. In discrete time form, Eqn. (4.6-11) can be written as

$$\mathbf{y}(k) = \sum_{i=0}^{\infty} \mathbf{H}_i \mathbf{f}(k-i). \tag{4.6-12}$$

The response takes a weighted sum of previous excitation measurements and the relationship (4.6-12) is the impulse response model of the vibrating structure.

On the other hand, assuming the excitations are applied to the structure until time $i = m$, the ARX model in Eqn. (4.2-50) becomes

$$\mathbf{y}(k) = \sum_{i=1}^{k-1} \mathbf{G}_i \mathbf{y}(k-i) + \sum_{i=1}^{m} \mathbf{R}_i \mathbf{f}(k-i). \tag{4.6-13}$$

By using the backward shift operator z, Eqns. (4.6-12) and (4.6-13) may be written as

$$\mathbf{y}(k) = \mathbf{H}(z)\mathbf{f}(k) \tag{4.6-14}$$

and

$$\mathbf{G}(z)\mathbf{y}(k) = \mathbf{R}(z)\mathbf{f}(k). \tag{4.6-15}$$

where

$$\mathbf{H}(z) = \mathbf{I} + \sum_{i=1}^{\infty} \mathbf{H}_i z^i, \tag{4.6-16}$$

$$\mathbf{G}(z) = \mathbf{I} - \sum_{i=1}^{k-1} \mathbf{G}_i z^i \tag{4.6-17}$$

and

$$\mathbf{R}(z) = \sum_{i=1}^{m} \mathbf{R}_i z^i. \tag{4.6-18}$$

From these two equations,

$$\mathbf{G}(z)\mathbf{H}(z) = \mathbf{R}(z). \tag{4.6-19}$$

Comparing the terms with the same power of z in both sides of Eqn. (4.6-19) yields

$$\mathbf{G}(z)\mathbf{H}_j = \mathbf{0} \qquad \text{for } j > m. \tag{4.6-20}$$

On recalling Eqn. (4.6-17) and the definition of backward shift operator z, Eqn. (4.6-

20) can be rewritten as

$$\mathbf{H}_j = \mathbf{G}_1\mathbf{H}_{j-1} + \mathbf{G}_2\mathbf{H}_{j-2} + \cdots + \mathbf{G}_s\mathbf{H}_{j-s}. \tag{4.6-21}$$

Eqn. (4.6-21) is the fundamental equation for the Poly Reference Time Domain method. When the parameters in Eqn. (4.6-21) are scalars, this equation becomes the fundamental equation for the Least Square Complex Exponential method.

When only free decay vibration data is used in the modal identification, Eqn. (4.2-47) will readily reduce to

$$\underline{\mathbf{y}}(s+1) = \mathbf{G}\underline{\mathbf{y}}(s) \tag{4.6-22}$$

which is the fundamental equation of the ITD method.

When one measurement station is used for identification of the natural frequencies and damping ratios, the ARMA model in Eqn. (4.2-30) will readily reduce to a univariate model, which is the fundamental of the mathematical model method.

§ 4.7 NUMERICAL EXAMPLES

This section is devoted to the illustration of the implementation and effectiveness of the methods presented in this chapter. The examples consist of two parts. The first part of this section is designed to demonstrate the direct method and is constituted by three simulated examples. In the second part of this section, two simple examples are used to illustrate the usefulness of the indirect method.

§ 4.7.1 Examples for the Direct Method

Three simulated experiments are used to illustrate the application and accuracy of the

direct method. The advantage of using the simulated experiments is that they can test the effectiveness of a method under controlled conditions. In the simulated experiment, a mathematical model of a structure is given and dynamic responses of the structure in the time domain are determined using conventional dynamic analytical methods. Eigenvectors, natural frequencies and damping ratios are identified from the excitation and response data. The eigenvectors, natural frequencies and damping ratios are calculated from the original mathematical model as the "exact" values. The identified modal parameters are then compared with those "exact" values to illustrate the effectiveness of the method.

The **first example** shown in Fig. 4.7-1 is a typical spring-mass-damper system with three degrees of freedom. This example is designed to illustrate the power of the direct method to identify very closely spaced frequencies and highly damping ratios using forced vibration data.

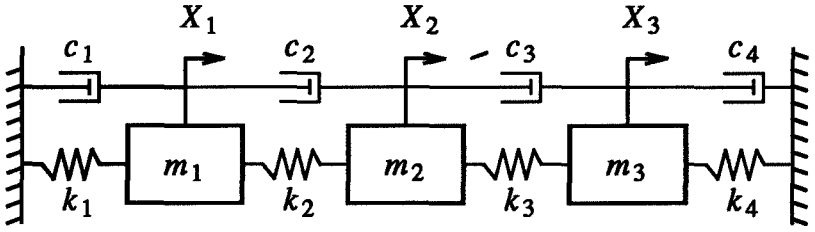

Fig. 4.7-1 Mass-Spring-Damper System of 3-Dof

The three cases in this example are considered for well spaced natural frequencies, very closely spaced natural frequencies and a highly damped structure, respectively.

The structural parameters of these three cases are listed in Table 4.7-1. The forced vibration data is used in the identification. A sampling interval of 0.55sec was used and 100 samples were recorded. In order to illustrate the process of the identification

of modal parameters, case 1 of this example proceeds in detail.

Table 4.7-1 Structure Parameters of the Three DOF of Spring-Mass-Damper System

	M			K			C		
CASE 1	25	0	0	251	-1	0	0.8	-0.1	0
	0	25	0	-1	5	-4	-0.1	0.2	-0.1
	0	0	25	0	-4	254	0	-0.1	0.8
CASE 2	25	0	0	300	-100	0	0.8	-0.1	0
	0	25	0	-100	300	-200	-0.1	0.2	-0.1
	0	0	25	0	-200	350	0	-0.1	0.8
CASE 3	25	0	0	300	-100	0	80	-10	0
	0	25	0	-100	300	-200	-10	90	-80
	0	0	25	0	-200	350	0	-80	100

For case 1, the general mass matrix is

$$\mathbf{M}^* = \begin{bmatrix} -\mathbf{K} & \mathbf{0} \\ \mathbf{0} & \mathbf{M} \end{bmatrix} = \begin{bmatrix} -251.0 & 1.0 & 0.0 & 0.0 & 0.0 & 0.0 \\ 1.0 & -5.0 & 4.0 & 0.0 & 0.0 & 0.0 \\ 0.0 & 4.0 & -254.0 & 0.0 & 0.0 & 0.0 \\ 0.0 & 0.0 & 0.0 & 25.0 & 0.0 & 0.0 \\ 0.0 & 0.0 & 0.0 & 0.0 & 25.0 & 0.0 \\ 0.0 & 0.0 & 0.0 & 0.0 & 0.0 & 25.0 \end{bmatrix}$$

The general stiffness matrix is

$$\mathbf{K}^* = \begin{bmatrix} \mathbf{0} & \mathbf{K} \\ \mathbf{K} & \mathbf{C} \end{bmatrix} = \begin{bmatrix} 0.0 & 0.0 & 0.0 & 251.0 & -1.0 & 0.0 \\ 0.0 & 0.0 & 0.0 & -1.0 & 5.0 & -4.0 \\ 0.0 & 0.0 & 0.0 & 0.0 & -4.0 & 254.0 \\ 251.0 & -1.0 & 0.0 & 0.8 & -0.1 & 0.0 \\ -1.0 & 5.0 & -4.0 & -0.1 & 0.2 & -0.1 \\ 0.0 & -4.0 & 254.0 & 0.0 & -0.1 & 0.8 \end{bmatrix}$$

The system matrix is then

$$\mathbf{A} = -\mathbf{M}^{*-1}\mathbf{K}^{*} = -\begin{bmatrix} -\mathbf{K} & \mathbf{0} \\ \mathbf{0} & \mathbf{M} \end{bmatrix}^{-1} \begin{bmatrix} \mathbf{0} & \mathbf{K} \\ \mathbf{K} & \mathbf{C} \end{bmatrix} = \begin{bmatrix} \mathbf{0} & \mathbf{I} \\ -\mathbf{M}^{-1}\mathbf{K} & -\mathbf{M}^{-1}\mathbf{C} \end{bmatrix}$$

$$= \begin{bmatrix} 0.00 & 0.00 & 0.00 & 1.00 & 0.00 & 0.00 \\ 0.00 & 0.00 & 0.00 & 0.00 & 1.00 & 0.00 \\ 0.00 & 0.00 & 0.00 & 0.00 & 0.00 & 1.00 \\ -10.04 & 0.04 & 0.00 & -0.032 & 0.004 & 0.00 \\ 0.04 & -0.20 & 0.16 & 0.004 & -0.008 & 0.004 \\ 0.00 & 0.16 & -10.16 & 0.00 & 0.004 & -0.032 \end{bmatrix}$$

The eigenvalue problem of the matrix A is solved

$$\mathbf{A}\lambda = \lambda\psi$$

The eigenvalues are

$\lambda_1, \lambda_1^* = -0.0039 \pm i\,0.444$

$\lambda_2, \lambda_2^* = 0.0160 \pm i\,3.169$

$\lambda_3, \lambda_3^* = -0.0161 \pm i\,3.188$

and eigenvectors are

$$\Psi = \begin{bmatrix} 1.000+i0.000 & 1.000+i0.000 & 1.000+i0.000 & 1.000+i0.000 & 1.000+i0.000 & 1.000+i0.000 \\ 245.7+i10.65 & 245.7-i10.65 & -0.004+i0.001 & -0.004-i0.001 & -2.787-i0.880 & -2.787+i0.880 \\ 3.947+i0.131 & 3.947-i0.131 & -0.005+i0.002 & -0.005-i0.002 & 168.5+i67.00 & 168.5-i67.00 \\ -0.004-i0.444 & -0.004+i0.444 & -0.016-i3.169 & -0.016+i3.169 & -0.016-i3.188 & -0.016+i3.188 \\ 3.766-i109.2 & 3.766+i109.2 & 0.004+i0.013 & 0.004-i0.013 & -2.761+i8.900 & -2.761-i8.900 \\ 0.043-i1.754 & 0.043+i1.754 & 0.007+i0.016 & 0.007-i0.016 & 210.9-i538.1 & 210.9+i538.1 \end{bmatrix}$$

The exact frequencies and damping ratios are

$\omega_1, \omega_1^* = 0.444 rad/sec$

$\omega_2,\ \omega_2^* = 3.169 rad/sec$

$\omega_3,\ \omega_3^* = 3.188 rad/sec$

$\eta_1,\ \eta_1^* = 0.008832$

$\eta_2,\ \eta_2^* = 0.005055$

$\eta_3,\ \eta_3^* = 0.005038$

The sampling interval is 0.55 sec and the system state transition matrix **T** is

$$\mathbf{T} = \Psi \exp(\Lambda T)\Psi^{-1}$$

$$= \begin{bmatrix} -0.1646+00 & 0.4594-02 & 0.3137-04 & 0.3082+00 & 0.1405-02 & 0.5066-05 \\ 0.3685-02 & 0.9701+00 & 0.1752-01 & 0.1405-02 & 0.5433+00 & 0.4230-02 \\ 0.2870-04 & 0.1837-01 & -0.1747+00 & 0.9249-05 & 0.4229-02 & 0.3058+00 \\ -0.3095+01 & 0.1205-01 & 0.1732-03 & -0.1745+00 & 0.5816-02 & 0.3685-04 \\ 0.7628-02 & -0.1079+00 & 0.4396-01 & 0.5816-02 & 0.9657+00 & 0.1956-01 \\ 0.1060-03 & 0.4809-01 & -0.3107+01 & 0.3859-04 & 0.1956-01 & -0.1845+00 \end{bmatrix}$$

The input force $\mathbf{f}(t)$ is simulated by

$$f_l(j\Delta t) = \sqrt{2}\sum_{i=1}^{N}[S_{f_i f_l}(i\Delta\omega)\Delta\omega]^{1/2}\cos(ij\Delta\omega\Delta t+\psi_i) \qquad (4.7\text{-}1)$$

where $l = 1$, 2 and 3; $S_{f_i f_l}(\omega)$ is one-sided spectral density of $f_l(t)$, ψ_i is statistically independent random phase angles uniformly distributed between 0 and 2π, and N is the number of data points. The input spectra that are used for simulation are shown in Fig. 4.7-2.

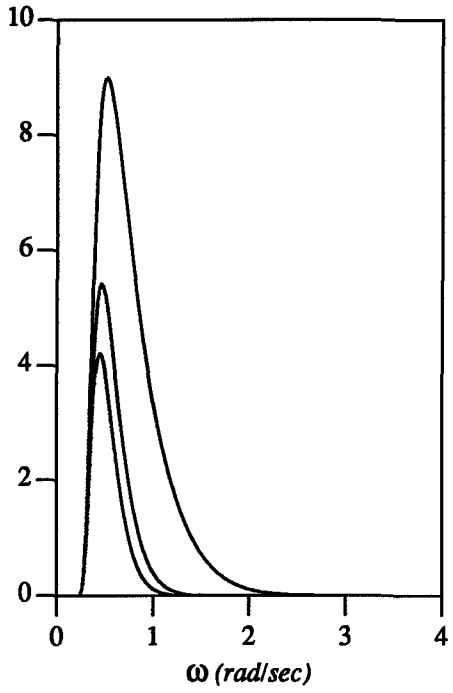

Fig. 4.7-2 Spectra of Input Excitations

Hence the excitation in the time domain calculated by Eqn. 4.7-1 using the spectra shown in Fig. 4.7-2, and

$$S_{f_i f_l}(\omega) = \frac{\alpha g^2}{\omega} e^{-\sigma(\frac{\omega_0}{\omega})^4 + \frac{2\omega^2 y_l}{g}}$$

where $\alpha = 0.0081$, $\sigma = 0.74$, g=32.6, and $\omega_0 = \frac{g}{75}$.

For the three spectra $S_{f_1 f_1}$, $S_{f_2 f_2}$ and $S_{f_3 f_3}$, $y_1 = 15$, $y_2 = 50$ and $y_3 = 70$ respectively. In this study, the frequency interval is $\Delta\omega = 0.02 rad/sec$, the time interval is $\Delta t = 0.55 sec$ and the number N is 2000. The excitation in the three stations for the first 40 seconds is obtained and shown as in Fig 4.7-3.

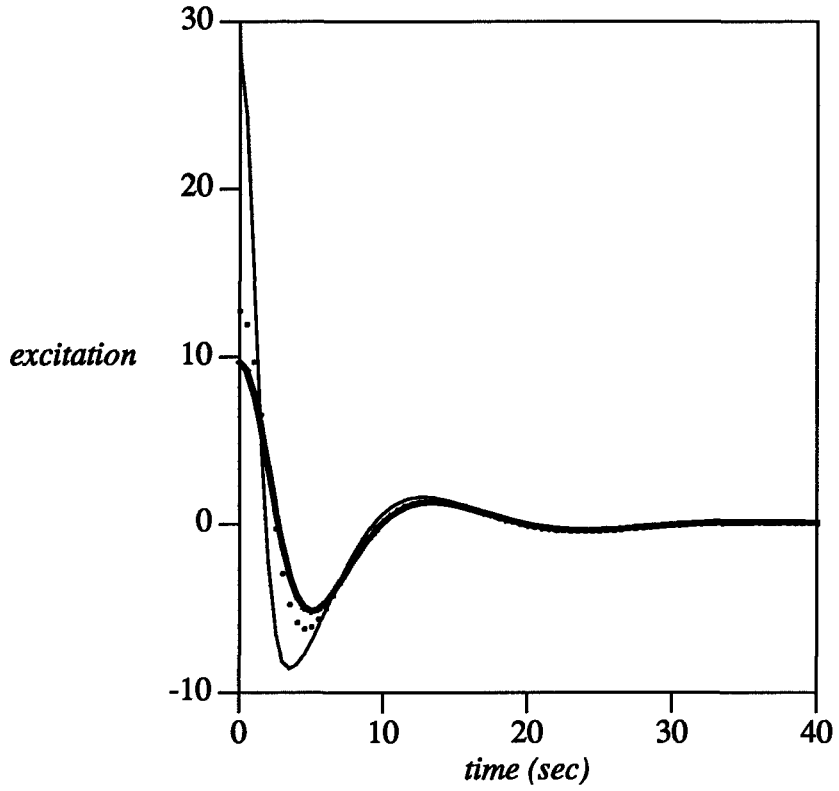

Fig. 4.7-3 Excitation History in Time Domain

The excitation in time domain will in turn be used for calculating the response of the three degree of freedom system. The responses are calculated by the state transition method and checked by the numerical intergration method. The time histories of response of three measurement stations to the three excitation points for the first 10 seconds are shown in Fig 4.7-4

These excitations and responses are used to estimate the coefficients of ARMAX model of the structure. Three different measurements are arranged: 1. three measurement stations, 2. two measurement stations, 3. single measurement station.

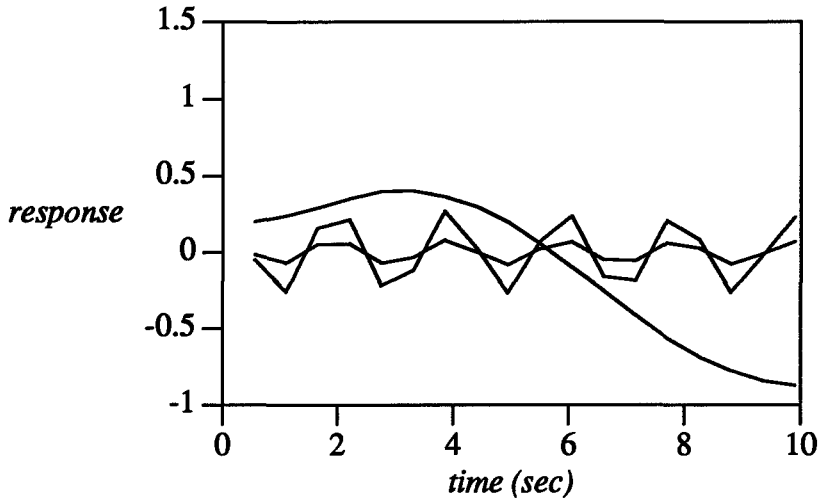

Fig. 4.7-4 Time Histories of Response of Three Measurement Stations

From the estimated results, matrix G for calculations of the identified eigenvalues and eigenvectors may be formed as follows

1. For three measurement stations

$$\begin{bmatrix} 0.00+0 & 0.00+0 & 0.00+0 & 0.10+1 & 0.00+0 & 0.00+0 \\ 0.00+0 & 0.00+0 & 0.00+0 & 0.00+0 & 0.10+1 & 0.00+0 \\ 0.00+0 & 0.00+0 & 0.00+0 & 0.00+0 & 0.00+0 & 0.10+1 \\ -0.98+0 & -0.17-2 & 0.25-5 & -0.34+0 & 0.11-1 & 0.71-4 \\ -0.29-2 & -1.00+0 & -0.29-2 & 0.87-2 & 0.19+1 & 0.36-1 \\ -0.29-4 & -0.17-2 & -0.98+0 & 0.57-4 & 0.38-1 & -0.36+0 \end{bmatrix}$$

2. For two measurement stations

$$\begin{bmatrix} 0.00+0 & 0.00+0 & 0.10+1 & 0.00+0 & 0.00+0 & 0.00+0 \\ 0.00+0 & 0.00+0 & 0.00+0 & 0.10+1 & 0.00+0 & 0.00+0 \\ 0.00+0 & 0.00+0 & 0.00+0 & 0.00+0 & 0.10+1 & 0.00+0 \\ 0.00+0 & 0.00+0 & 0.00+0 & 0.00+0 & 0.00+0 & 0.10+1 \\ 0.80+1 & -0.18+1 & 0.18+1 & -0.65+0 & 0.78+1 & -0.18+1 \\ 0.28+2 & -0.61+1 & 0.97+1 & -0.32+1 & 0.27+2 & -0.66+1 \end{bmatrix}$$

3. For single measurement station

$$\begin{bmatrix} 0.00+0 & 0.10+1 & 0.00+0 & 0.00+0 & 0.00+0 & 0.00+0 \\ 0.00+0 & 0.00+0 & 0.10+1 & 0.00+0 & 0.00+0 & 0.00+0 \\ 0.00+0 & 0.00+0 & 0.00+0 & 0.10+1 & 0.00+0 & 0.00+0 \\ 0.00+0 & 0.00+0 & 0.00+0 & 0.00+0 & 0.10+1 & 0.00+0 \\ 0.00+0 & 0.00+0 & 0.00+0 & 0.00+0 & 0.00+0 & 0.10+1 \\ -0.79+0 & 0.96+0 & -0.16+1 & 0.25+1 & -0.16+1 & 0.13+1 \end{bmatrix}$$

The eigenvalue problem of matrix **G** can be solved

$$\mathbf{G}\lambda_i = \lambda_i \boldsymbol{\psi}_i$$

The eigenvalues and eigenvectors obtained for cases with different number of measurement stations are as follows

1. For three measurement stations, the eigenvalues are

$\alpha_1, \alpha_1^* = 0.9682 \pm i0.2413$

$\alpha_2, \alpha_2^* = -0.1799 \pm i0.9746$

$\alpha_3, \alpha_3^* = -0.1696 \pm i0.9766$

and eigenvectors are

$$\boldsymbol{\Psi} = \begin{bmatrix} 1.000+i0.000 & 1.000+i0.000 & 1.000+i0.000 & 1.000+i0.000 & 1.000+i0.000 & 1.000+i0.000 \\ 245.7+i10.65 & 245.7-i10.65 & -2.769-i0.865 & -2.769+i0.865 & -0.004+i0.001 & -0.004-i0.001 \\ 3.947+i0.132 & 3.947-i0.132 & 167.4+i66.02 & 167.4-i66.02 & -0.005+i0.001 & -0.005-i0.001 \\ 0.968-i0.241 & 0.968+i0.241 & -0.180-i0.975 & -0.180+i0.975 & -0.170-i0.977 & -0.170-i0.977 \\ 240.5-i48.98 & 240.5+i48.98 & -0.345+i2.855 & -0.345-i2.855 & 0.002+i0.0037 & 0.002-i0.0037 \\ 3.854-i0.825 & 3.854+i0.825 & 34.23-i175.0 & 34.23+i175.0 & 0.002+i0.004 & 0.002-i0.004 \end{bmatrix}$$

The identified eigenvalues are

$\lambda_1, \lambda_1^* = -0.0039 \pm i0.4441$

$\lambda_2, \lambda_2^* = -0.0160 \pm i3.1690$

$\lambda_3, \lambda_3^* = -0.0161 \pm i3.1880$

The identified frequencies are

$\omega_1 = 0.444 rad/sec$

$\omega_2 = 3.169 rad/sec$

$\omega_3 = 3.188 rad/sec$

The identified damping ratios are

$\eta_1 = 0.008832$

$\eta_2 = 0.005055$

$\eta_3 = 0.005038$

2. For two measurement stations, the eigenvalues are

$\alpha_1, \alpha_1^* = 0.9595 \pm i0.2216$

$\alpha_2, \alpha_2^* = -0.1696 \pm i0.9766$

$\alpha_3, \alpha_3^* = -0.1799 \pm i0.9747$

and eigenvectors are

$$\Psi = \begin{bmatrix} 1.000+i0.000 & 1.000+i0.000 & 1.000+i0.000 & 1.000+i0.000 & 1.000+i0.000 & 1.000+i0.000 \\ 3.955+i0.122 & 3.955-i0.122 & -0.007+i0.001 & -0.007-i0.001 & 166.0+i74.34 & 166.0-i74.34 \\ 0.960-i0.222 & 0.960+i0.222 & -0.170-i0.977 & -0.170+i0.977 & -0.180-i0.975 & -0.180+i0.975 \\ 3.822-i0.759 & 3.822+i0.759 & 0.001+i0.007 & 0.001-i0.007 & 42.60+i175.2 & 42.60-i175.2 \\ 0.872-i0.425 & 0.872+i0.425 & 0.925+i0.331 & 0.925-i0.331 & -0.918-i0.351 & -0.918+i0.351 \\ 3.498-i1.575 & 3.498+i1.575 & 0.006-i0.003 & 0.006+i0.003 & -178.4-i10.01 & -178.4+i10.01 \end{bmatrix}$$

The identified eigenvalues are

$\lambda_1, \lambda_1^* = -0.0280 \pm i0.4126$

$\lambda_2, \lambda_2^* = -0.0160 \pm i3.1690$

$\lambda_3, \lambda_3^* = -0.0161 \pm i3.1880$

The identified frequencies are

$\omega_1 = 0.414 rad/sec$

$\omega_2 = 3.169 rad/sec$

$\omega_3 = 3.188 rad/sec$

The identified damping ratios are

$\eta_1 = 0.06768$

$\eta_2 = 0.00505$

$\eta_3 = 0.00504$

3. For one measurement station

The obtained eigenvalues are

$\alpha_1, \alpha_1^* = 0.9682 \pm i0.2413$

$\alpha_2,\ \alpha_2^* = -0.1418 \pm i0.8843$

$\alpha_3,\ \alpha_3^* = -0.1800 \pm i0.9747$

The identified eigenvalues are

$\lambda_1,\ \lambda_1^* = -0.0039 \pm i0.4441$

$\lambda_2,\ \lambda_2^* = -0.2004 \pm i\,3.1450$

$\lambda_3,\ \lambda_3^* = -0.0161 \pm i3.1880$

The identified frequencies are

$\omega_1 = 0.441 rad/sec$

$\omega_2 = 3.151 rad/sec$

$\omega_3 = 3.188 rad/sec$

The identified damping ratios are

$\eta_1 = 0.00883$

$\eta_2 = 0.0636$

$\eta_3 = 0.00506$

The comparison of the identified results with the different number of measurement stations for case 1 is shown in Table 4.7-2.

From Table 4.7-2, it can be seen that the frequencies may be identified with good accuracy for the different number of measurement stations. The damping ratios are not identified so well as the frequencies.

Table 4.7-2 Comparison of Identified Results for Different Measurement Stations

Three Degrees of Freedom System

	Frequency (rad/sec)			Damping Ratio		
Mode	First Mode	Second Mode	Third Mode	First Mode	Second Mode	Third Mode
Exact Value	0.4441	3.169	3.188	0.008832	0.005055	0.005038
Three Measuring Stations	0.4441	3.169	3.188	0.008832	0.005055	0.005038
Two Measuring Stations	0.4136	3.169	3.188	0.06768	0.005053	0.005044
One Measuring Station	0.4441	3.151	3.188	0.00883	0.0636	0.005063

Table 4.7-3 Identified Results for the System of Three Degree of Freedom

		Frequency (rad/sec)		Damping ratio		Mode	
		Original	Identified	Original	Identified	Original	Identified
CASE 1	mode 1	0.4441	0.4435	0.0088	0.0088	1 0.2457+3±0.1065+2 0.3947+1±0.1314+0	1 0.2457+3±0.1063+2 0.3947+1±0.1316+0
	mode 2	3.169	3.169	0.0051	0.0051	1 -0.3986-2±0.1217-2 -0.5189-2±0.2050-2	1 -0.3996-2±0.1226-2 -0.4520-2±0.1288-2
	mode 3	3.188	3.188	0.0050	0.0050	1 -0.2787+1±0.8800+0 0.1684+3±0.6698+2	1 -0.2769+1±0.8653+0 0.1674+3±0.6601+2
CASE 2	mode 1	1.946	1.946	0.3480-2	0.3475-2	1 0.2053+1±0.4987-2 0.1608+0±0.1848-3	1 0.2053+1±0.4985-2 0.1508+1±0.1869-3
	mode 2	3.521	3.521	0.4563-2	0.4562-2	1 -0.9921-1±0.2336-3 -0.4951+0±0.1531-3	1 -0.9921-1±0.2344-3 0.4951+0±0.1552-3
	mode 3	4.671	4.671	0.2818-2	0.2871-2	1 -0.2454+1±0.1808-1 0.2512+1±0.4126-2	1 -0.2454+1±0.1808-1 0.2512+1±0.4128-2
CASE 3	mode 1	2.002	1.996	0.1830	0.1843	1 0.2013+1±0.8489+0 0.1623+1±0.9140+0	1 0.2002+1±0.8425+0 0.1612+1±0.9083+0
	mode 2	3.497	3.496	0.4515	0.4511	1 -0.6461-1±0.6301-1 -0.2209+0±0.2748+0	1 -0.6538-1±0.6307-1 -0.2218+0±0.2759+0
	mode 3	4.570	4.565	0.7559	0.7550	1 -0.3607+1±0.4073+1 0.5680+0±0.4401+1	1 -0.5397+0±0.4041+1 0.7483+0±0.4350+1

The details for other two cases are similar. The identified results for the all three cases are shown in Table 4.7-3. The identified modal parameters given in this table indicate the direct method is capable of identification of the natural frequencies, damping ratios and eigenvectors with good accuracy even when the frequencies are very closely spaced and the damping of the system is heavy.

The **second example** is a marine riser with five clamps as shown in Fig. 4.7-5.

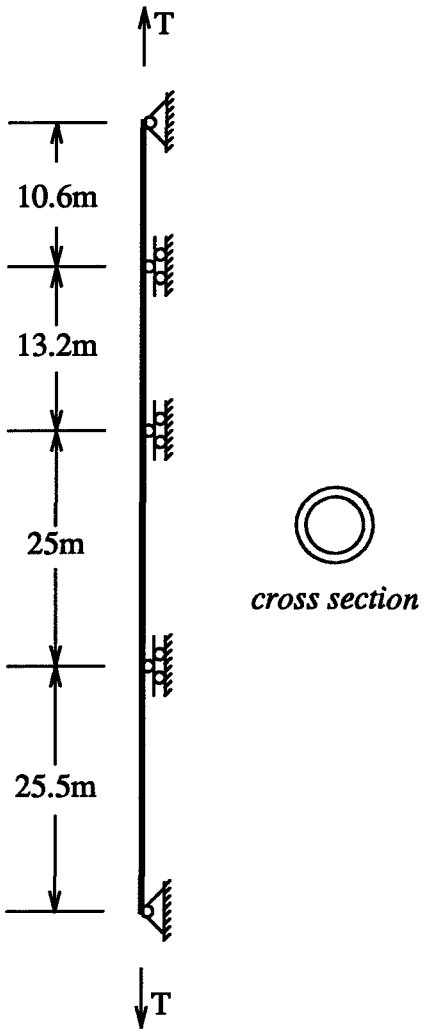

Fig. 4.7-5 Marine Riser

In this example, free decay vibration data will be used to identify the modal parameters of the marine riser. Thirty two normal modes were calculated by the finite element method. The first eight modes were used to generate a set of free decay response data. In order to illustrate the capability of identification of closely spaced frequencies, the frequencies calculated by finite element method are not used. Instead, the frequencies are arbitrarily assigned as 12, 12.5, 40, 48, 56, 72, 100 and 114 Hz with damping factor 0.02 for all modes.

Since the calculated modes are normal instead of complex, the following formula is used to compute the free decay response data.

$$\mathbf{q}(k) = \sum_{i=1}^{8} \boldsymbol{\phi}_i e^{(-\eta_i \omega_i)} cos\,(\omega_i \sqrt{1-\eta_i^2})$$

In practical observation, noise is inevitable, a set of random white noise of 15% RMS of the noise to signal ratio was added to simulate an actual situation. The free decay responses without noise and with noise are shown in Figs. 4.7-6 and 4.7-7.

Twenty four simulated measurement stations were arranged equally spaced along the riser. Sampling frequency was taken as 150Hz and 450 samples were recorded, corresponding to a recording of 3 seconds.

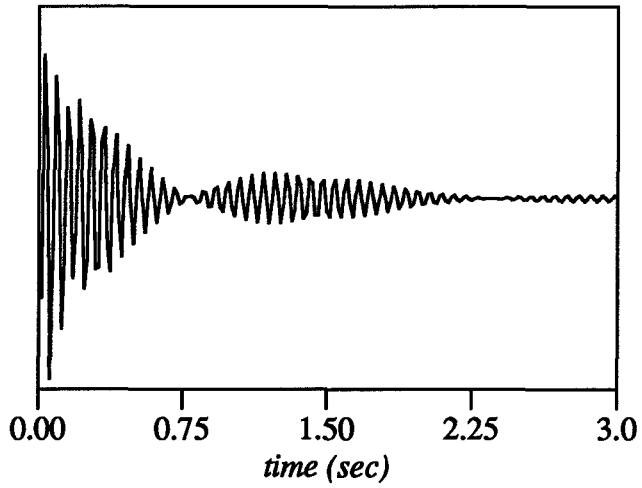

Fig. 4.7-6 Free Decay Responses Without Noise

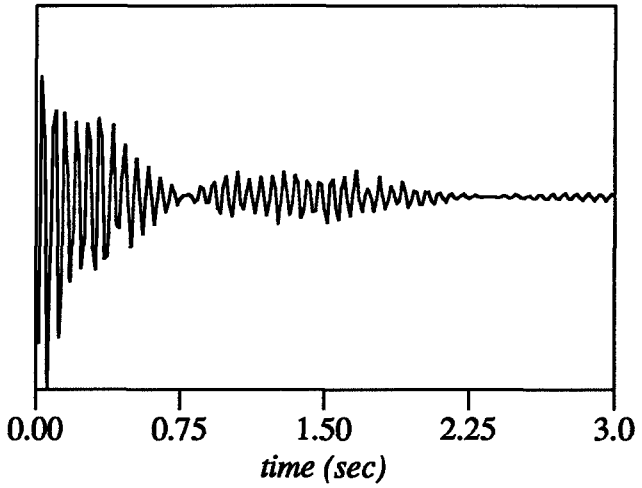

Fig. 4.7-7 Free Decay Responses With Noise

The corresponding Nyquist frequency is 150/2 = 75 Hz and the information about frequencies higher than 75 Hz is thus lost by sampling. When analyzing the free decay response data it will be assumed that the modal parameters which generate the data are not known. The measurement data matrix $\overline{\mathbf{Q}}$ was formed according to Eqn. (4.6-1). The rank of the matrix $\overline{\mathbf{Q}}^T\overline{\mathbf{Q}}$ was found to be six and six modes were identified. The identified modal parameters are given in Table 4.7-4.

Table 4.7-4 Identification Results for the Marine Riser for Six Modes, 25% Noise and 24 Degrees of Freedom

MODE No.	FREQUENCY (Hz)	DAMPING RATIO (%)	MSCC WITH INPUT MODE No 1	2	3	4	5	6
1	12.06	1.87	100	0	0	0	0	0
2	12.53	2.12	3	100	0	0	0	0
3	39.93	2.11	0	0	100	0	0	0
4	48.09	1.82	0	0	0	100	0	0
5	55.87	2.06	0	2	0	0	100	0
6	72.48	2.08	0	0	3	0	0	100

The called "Mode Shape Correlation Constant" (MSCC) was used to access the accuracy of identified mode shapes. The following equation is used to compute the MSCC

$$MSCC = \frac{|\phi_a^* \times \phi_b|^2}{[\phi_a^* \times \phi_a] \times [\phi_b^* \times \phi_b]} \times 100$$

where

ϕ_a is the assumed input mode:

ϕ_b is the identified mode;

* means the conjugate transpose of a vector.

$| \; |$ indicates the magnitude.

The accuracy of identified frequencies and damping factors were qualified by direct comparison. It is observed that the natural frequencies, damping ratios and eigenvectors were identified with reasonable accuracy even when the frequencies are very closely spaced.

The **third example** is a simulated fixed ended beam with impulse response data being used to identify the natural frequencies, damping ratios and mode shapes. The

impulse responses are generated according to the following equation

$$h_{jk} = \sum_{r=1}^{n} {}_r\phi_j \, {}_r\phi_k \, e^{-\eta_r \omega_r} \cos(\omega_i \sqrt{1-\eta_i^2})$$

The modes shapes of the beam used in generation of the impulse response data are given by

$$\phi_n(x) = A_n \left[(\frac{\alpha}{\beta})_n (\sinh a_n x - \sin a_n x) + \cosh a_n x - \cos a_n x \right]$$

where

$$(\frac{\alpha}{\beta})_n = \frac{\cos a_n l - \cosh a_n l}{\sinh a_n l - \sin a_n l}$$

and

$$a_n l = (n + \frac{1}{4})\pi.$$

The calculated frequencies were not used in generation of the impulse response data. Instead, the frequencies of the beam were assigned as 9, 25, 49, 81, 121, 169 Hz with damping factors of 0.02 for all modes.

Fourteen measurement stations, equally spaced along the beam, are used with two sets of test data. The first set of response data is evaluated from the first four modes of the beam while the second set of response data is calculated from the first six modes. In order to simulate an actual test, a set of randomly generated noise was

imposed on the response data to get two sets of measurements with 20% and 15% RMS of the noise to signal ratio respectively. Sampling frequencies of 200 Hz and 350 Hz were used and 150 and 200 samples have been recorded, respectively..

The identified frequencies and damping ratios, and MSCC of each mode are listed in Tables 4.7-5 and 4.7-6 for the four and six modes response cases respectively. The results indicate the frequencies are identified with good accuracy, damping ratios are identified with errors smaller than noise to signal ratios and the identified mode shapes have reasonable accuracy.

Table 4.7-5 Identification Results of Beam for Four Modes
30% Noise and 15 Degrees of Freedom

MODE	FREQUENCY	DAMPING RATIO	MSCC WITH INPUT MODE No			
No.	(Hz)	(%)	1	2	3	4
1	9.0212	1.86	100	0	0	0
2	25.0412	2.16	0	100	0	0
3	49.1360	2.07	0	0	100	0
4	81.1267	1.92	3	0	0	100

Table 4.7-6 Identification Results for the Beam for Six Modes
20% Noise and 15 Degrees of Freedom

MODE	FREQUENCY	DAMPING RATIO	MSCC WITH INPUT MODE No					
No.	(Hz)	(%)	1	2	3	4	5	6
1	8.9761	1.89	100	0	0	0	0	0
2	25.0626	2.18	0	100	0	0	0	0
3	49.2783	2.09	0	0	100	0	0	0
4	81.3849	1.87	0	0	0	100	0	0
5	122.0356	1.89	0	2	0	0	100	0
6	170.1217	2.04	0	0	3	0	0	100

§ 4.7.2 Examples for the Indirect Method

In this part, two digital simulation examples are used to investigate the efficiency

and accuracy of the indirect method. The first example is a three degrees of freedom structure, with structural parameters obtained from a tall building with two horizontal displacements and a torsional displacement being considered. The mass, stiffness and damping matrices are respectively given as follows,

$$\mathbf{M}_o = \begin{bmatrix} 0.1650+06 & 0.0000+00 & -0.1486+07 \\ 0.0000+00 & 0.1650+06 & 0.1486+07 \\ -0.1486+07 & 0.1486+07 & 0.3567+08 \end{bmatrix},$$

$$\mathbf{C}_o = \begin{bmatrix} 0.220+06 & 0.000+00 & -0.225+07 \\ 0.000+00 & 0.220+06 & -0.225+07 \\ -0.225+07 & -0.225+07 & 0.330+08 \end{bmatrix},$$

$$\mathbf{K}_o = \begin{bmatrix} 0.416750+09 & 0.000000+00 & -0.330066+10 \\ 0.000000+00 & 0.416750+09 & 0.330066+10 \\ -0.330066+10 & 0.330066+10 & 0.852170+11 \end{bmatrix}.$$

These structural parameters are used to calculate the "exact" modal parameters and to generate the response data to a pseudo random excitation. The simulated response data are then used to identify the modal parameters by the indirect method. The identified modal parameters are compared with the "exact" ones to illustrate the efficiency and accuracy.

The structure is considered to have non-proportional damping and hence its mode shapes are complex. The natural frequency of the twist motion is also very close to one of the flexural frequencies.

The excitation used for generation of the response is a three variate pseudo random white noise process with different covariance matrices in the different trials. These

excitations are applied to three "points" of the structure. The response data are calculated by mode superposition method. Numerical integration is also used to verify the response data. The verified response data are considered as "measured" responses. These data are then used with the indirect method to identify the natural frequencies, damping ratios and complex modes.

The sampling frequency of 50 Hz was used and 1200 samples were recorded. In order to obtain the stationary steady response data, the first 200 samples were discarded. The average identified modal parameters of 11 trials are shown in the Table 4.7-9.

The second example is a system with two degrees of freedom, whose mass, damping and stiffness matrices are

$$\mathbf{M}_o = \begin{bmatrix} 80 & 0 \\ 0 & 400 \end{bmatrix},$$

$$\mathbf{C}_o = \begin{bmatrix} 150 & -89 \\ -89 & 600 \end{bmatrix},$$

$$\mathbf{K}_o = \begin{bmatrix} 30000 & -30000 \\ -30000 & 100000 \end{bmatrix}.$$

The excitation sequence is a univariate white noise with different covariance matrices for different trials. The excitation was applied to a point of the system.

TABLE 4.7-9. - Comparison of Identified Results to the Exact Modal Parameters of 3 DOF System

Mode	Frequency (Hz)		Damping Factor		Mode Shape	
	Exact	Identified	Exact	Identified	Exact	Identified
Mode 1	7.708+0	7.698+0	0.5664-2	0.5522-2	1 -1.0195+1±*i*0.1052+0 0.0928+0±*i*0.0025+0	1 -1.0322+0±*i*0.1073+0 0.0986+0±*i*0.0028+0
Mode 2	7.999+0	7.976+0	0.1327-1	0.1524-1	1 -0.8110+0±*i*0.3173+0 0.0000+0±*i*0.0000+0	1 -0.8275+0±*i*0.3194+0 0.0000+0±*i*0.0000+0
Mode 3	10.044+0	10.020+0	0.6734-1	0.6655-1	1 -0.6123+0±*i*1.0281+0 -0.1294+0±*i*0.0819+0	1 --0.6147+0±*i*1.0314+0 -0.1306+0±*i*0.0835+0

Observation errors for the response were added as a chi-squared sequence. The average noise to signal ratio was taken 15% RMS. The sampling rate was 20 Hz and 1400 sample were recorded. The first 300 samples were not used in order to obtain the stationary response data. Since the observation errors were not white noise, an excessive eigenvalue was observed from the AR part of the univariate ARMA model of the system. This excessive eigenvalue was found by comparing the zeros of the AR part with those of the MA part. A zero of the AR part had almost the same value as one of the zeros of the MA part and thus this zero was considered to be excessive. This excessive mode may be caused by the non-white noise observation errors and hence is eliminated. Table 4.7-10 shows the comparison of the zeros of the AR and MA parts. The identified average results of five trials are listed in Table 4.7-11.

It is observed that the the natural frequencies, damping ratios and complex modes of the two examples were identified with adequate accuracy, even when two of the natural frequencies are very close to each other in the first example.

Table 4.7-10. - Zeros of AR and MA Parts

AR Part (1)	MA Part (2)
9.885-1 ±*i* 2.063-1	10.723-1 ±*i* 4.372-1
9.521-1 ±*i* 3.481-1	2.384+1
-3.372+1 ±*i* 5.364-1	-3.371+1 ±*i* 5.359-1

Table 4.7-11 - Comparison of Identified Results to the Exact Modal Parameters of 2 DOF System

	Frequency (Hz)		Damping Factor		Mode Shape	
Mode	Exact	Identified	Exact	Identified	Exact	Identified
Mode 1	1.839+0	1.967+0	0.5001-1	0.4744-1	1 0.6439+0±*i*0.8668-4	1 0.6227+0±*i*0.7885-4
Mode 2	3.528+0	3.349+0	0.5005-1	0.3897-1	1 -0.3106+0±*i*0.8021-4	1 -0.2976+0±*i*0.7803-4

§ 4.8 SUMMARY

Two time domain methods for modal identification of vibrating structures are developed in this chapter. The direct method is a general method which can use free response data, impulse response function and forced excitation and response data in time domain. This method can deal with deterministic and random vibration test. Under certain circumstances, the method may be reduced to the least squares complex exponential method, Polyreference Time Domain method, Ibrahim Time Domain method or time series method. The indirect method is able to deal with random vibration test, particularly, for the ambient vibration tests, in which the response may be treated as white noise random process. The indirect method also is able to find the false poles caused by the test noise or measurement errors.

For both direct and indirect methods, an improved modal model of a vibrating structure, including the highly coupled and closely spread modes, can be identified with satisfactory accuracy.

APPENDIX 4A KRONECKER PRODUCT AND COLUMN OPERATOR FOR A MATRIX

The Kronecker product of an $m \times n$ matrix $\mathbf{A}=[a_{ij}]$ and a $p \times r$ matrix $\mathbf{B}=[b_{ij}]$ is defined as

$$\mathbf{A} \otimes \mathbf{B} = \begin{bmatrix} a_{11}\mathbf{B} & a_{12}\mathbf{B} & \cdots & a_{1n}\mathbf{B} \\ a_{21}\mathbf{B} & a_{22}\mathbf{B} & \cdots & a_{2n}\mathbf{B} \\ \vdots & \vdots & \vdots & \vdots \\ a_{m1}\mathbf{B} & a_{m2}\mathbf{B} & \cdots & a_{mn}\mathbf{B} \end{bmatrix} \tag{4A.1}$$

This is an $(m \times p) \times (n \times r)$ matrix.

The operator "*column*" is defined as the operation to form a column vector out of a matrix by stacking its columns on top of each other

$$column\ \mathbf{B} = \begin{bmatrix} \mathbf{b}^1 \\ \mathbf{b}^2 \\ \vdots \\ \mathbf{b}^r \end{bmatrix} \tag{4A.2}$$

where $\mathbf{b}^j$ is the jth column of $\mathbf{B}$.

Chapter 5

MODAL IDENTIFICATION USING Z-TRANSFORMATION

The full area of ignorance is not mapped: We are at present only exploring its fringes.

- J.D. Bernal

§ 5.1 INTRODUCTION

The Fourier transformation is usually used with frequency domain methods for modal identification when the structure is considered as a continuous time system. The traditional way of performing a frequency analysis, however, is to pass the signal through a system consisting of filter, detector and recorder (or display). A digital filter is a calculation device which receives a sequence of digital value at its

input, operates on each sample in a defined manner, and outputs a sample of each input. The digital frequency analysis technique in common use, viz., FFT analysis, involves a direct evaluation of estimates of Fourier Transformation. The FFT algorithm is an efficient way of calculating so-called Discrete Fourier Transformation which is a discrete, finite approximation to the Fourier Transformation. In essence, therefore, frequency domain modal identification methods are discrete methods. In a practical vibration test, the measured data is generally sampled at discrete time instants. Most time domain methods use these discrete signals as basic data set for identification of modal parameters of a vibrating structure through a computer, which is also a discrete system, and only treats digital signals rather than continuous signals. Time domain methods are also essentially discrete modal identification methods. The Z-transformation is a transformation of a discrete-time signal defined as a power series in z^{-1} whose coefficients are the amplitudes of the discrete-time signals. Therefore the Z-transformation is suitable for the analysis of practical vibration test data and the identification of modal parameters of tested structures.

In this chapter the Z-transfer function of the vibrating structure is used to derive an auto-regressive and moving average (ARMA) model of the structure. The relationship between the eigenvalues of the structure and poles of the ARMA model is derived on the basis that the eigenvalues of the structure can then be determined through the identification of the poles of the ARMA model. A multivariate ARMA model is used with a multiple input and multiple output vibration test to identify the mode shapes as well as the natural frequencies and damping ratios. As will be discussed, the method can also be applied to the single point excitation modal testing and multiple shaker excitation modal testing.

§ 5.2 introduces the basic concept of the Z-transformation. The Z-transfer function of vibrating structures is discussed in § 5.3. Estimation of the Z-transfer function using response and excitation data in the time domain is tackled in § 5.4. The univariate and multivariate models are also discussed, respectively. § 5.5 is devoted to the derivation of technique for determination of modal parameters from the Z-transfer function of vibrating structures. Several numerical examples are given in § 5.6 to illustrate the implementation and effectiveness of the method. § 5.7 concludes this chapter with discussions of numerical computation and conclusions.

§ 5.2 Z-TRANSFORMATION

The Z-transformation of a discrete-time signal $f(n)$ which is identically zero for negative discrete time is defined as a power series in z^{-1} whose coefficients are the amplitudes of the discrete-time signal. That is,

$$Z[f(k)] = \hat{f}(z) = f(0) + \frac{f(1)}{z} + \frac{f(2)}{z^2} + \frac{f(3)}{z^3} + \cdots = \sum_{k=0}^{\infty} f(k) z^{-k} \tag{5.2-1}$$

The sampled sequence $\{f(n)\}$ is called the generating sequence of the Z-transformation.

The following four significant properties of Z-transformation are related to the present study of the modal determination.

1. Linearity Property

   If a sequence $f(k)$ is a linear combination of two other sequences, that is

$$f(k) = af_1(k) + bf_2(k) \qquad \text{for } k = 0, 1, 2, \cdots \tag{5.2-2}$$

where a and b are constants,

then

$$\hat{f}(z) = a\hat{f}_1(z) + b\hat{f}_2(z) \tag{5.2-3}$$

where

$$\hat{f}(z) = Z[f(k)], \quad \hat{f}_1(z) = Z[f_1(k)] \text{ and } \hat{f}_2(z) = Z[f_2(k)]$$

2. Right-Shifting Property

If $\hat{f}(z) = Z[f(k)] = \sum_{k=0}^{\infty} f(k)z^{-k}$, then

$$Z[f(k-m)] = z^{-m}\hat{f}(z) \tag{5.2-4}$$

3. Left-Shifting Property

$$Z[f(k+m)] = z^m\hat{f}(z) - \sum_{k=0}^{m-1} f(k)z^{m-k} \tag{5.2-5}$$

4. Convolution-Summation Property

The excitation and response can be related to one another through the convolution summation

$$\mathbf{y}(k) = \mathbf{H}(0)\mathbf{f}(k) + \mathbf{H}(1)\mathbf{f}(k-1) + \mathbf{H}(2)\mathbf{f}(k-2) + \cdots \tag{5.2-6}$$

where $\mathbf{H}(i)$ is the impulse response function matrix sequence of the vibrating structure, $\mathbf{y}(i)$ and $\mathbf{f}(i)$ are the response and excitation vectors respectively. The Z-transformation of the response is then equal to the product of the Z-

transformations of the excitation and the impulse response matrix sequence, that is,

$$\hat{\mathbf{y}}(z) = \mathbf{H}(z)\hat{\mathbf{f}}(z) \tag{5.2-7}$$

The Z-transformation provides a bridge between continuous- and discrete-time signal processing because the Laplace transformation $\hat{f}(s)$ of an ideal impulse sampled signal $f(t)$ is related to the Z-transform $\hat{f}(z)$ of the discrete-time signal $f(kT)$ by the transformation $z = e^{sT}$. This transformation maps the left half plane in the complex s-plane into the unit circle in the complex z-plane, as shown in Fig. 5.2-1. The interior of the unit circle, the unit circle, and the exterior of the unit circle in the z-plane have the similar meaning for discrete-time signals as the left half s-plane, $j\omega$ axis, and right s-plane for continuous-time signal. Here j indicates the imaginary unit.

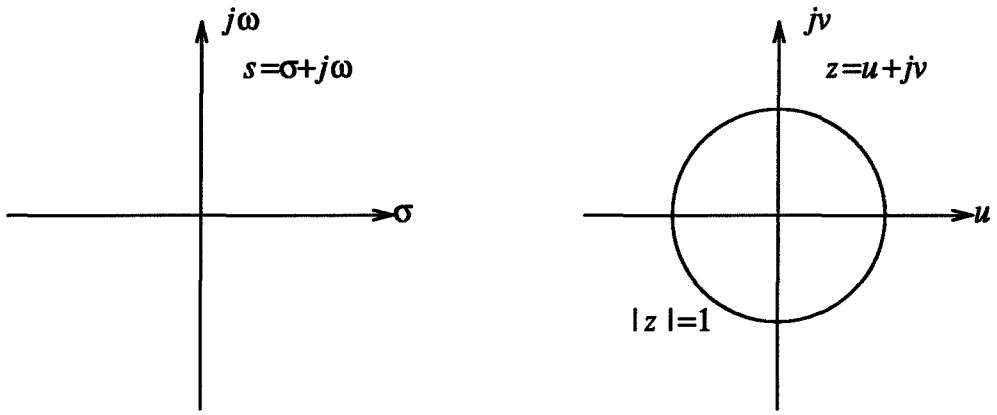

Fig. 5.2-1. Mapping induced by $z = e^{sT}$

§ 5.3 Z-TRANSFER FUNCTION OF A VIBRATING STRUCTURE

As discussed in chapter 2, A vibrating structure can be described in discrete form by

$$\mathbf{x}(k+1) = \mathbf{T}\mathbf{x}(k) + \mathbf{\Delta}\mathbf{f}(k), \tag{5.3-1}$$

$$\mathbf{y}(k) = \mathbf{C}\mathbf{x}(k) \tag{5.3-2}$$

where $\mathbf{f}(t)$ is assumed to be constant within the sampling interval $0 \le t \le T$, Hence,

$\mathbf{\Delta} = \mathbf{\Delta}(\tau) = \int_0^T \mathbf{T}(T-\tau)\mathbf{B}d\tau =$ constant matrix.

Eqn. (5.3-1) can also be considered as the state-space relationship of the vibrating structure in discrete time form. Taking the Z-transformation on each side of Eqns. (5.3-1) and (5.3-2) gives

$$z\hat{\mathbf{x}}(z) - z\mathbf{x}(0) = \mathbf{T}\hat{\mathbf{x}}(z) + \mathbf{\Delta}\hat{\mathbf{f}}(z) \tag{5.3-3}$$

$$\hat{\mathbf{y}}(z) = \mathbf{C}\hat{\mathbf{x}}(z). \tag{5.3-4}$$

Rearranging the terms of Eqn. (5.3-3) and premultiplying both sides of the equation by the inverse of matrix $[\, z\mathbf{I} - \mathbf{T}\,]$ yields an expression for Z-transformation of the state vector $\mathbf{x}(k)$ given by

$$\hat{\mathbf{x}}(z) = z[\, z\mathbf{I} - \mathbf{T}\,]^{-1}\mathbf{x}(0) + [\, z\mathbf{I} - \mathbf{T}\,]^{-1}\mathbf{\Delta}\hat{\mathbf{f}}(z). \tag{5.3-5}$$

On the other hand, from Eqn. (5.3-1)

$$\mathbf{x}(k) = \mathbf{T}^k\mathbf{x}(0) + \sum_{j=0}^{k-1}\mathbf{T}^{k-1-j}\Delta\mathbf{f}(j).$$

$$= \mathbf{T}(k)\mathbf{x}(0) + \sum_{j=0}^{k-1}\mathbf{T}(k-1-j)\Delta\mathbf{f}(j). \tag{5.3-6}$$

According to the convolution-summation property of the Z-transform, by comparing Eqn. (5.3-5) with Eqn. (5.3-6) and assuming the initial condition $\mathbf{x}(0) = \mathbf{0}$, the Z-transform of the transition matrix $\mathbf{T}(k)$ is given by

$$Z[\mathbf{T}(k)] = [\, z\mathbf{I} - \mathbf{T}]^{-1} \tag{5.3-7}$$

When matrix $\mathbf{A}$ is not defective (for example, the eigenvalues λ_i are distinct,) $\mathbf{T}(k) = \mathbf{\Psi}\exp[\mathbf{\Lambda}kT]\,\mathbf{\Psi}^{-1}$ and its Z-transformation is

$$Z[\mathbf{T}(k)] = \mathbf{\Psi}\, z\mathbf{I}[z\mathbf{I} - \exp[\mathbf{\Lambda}T]]^{-1}\,\mathbf{\Psi}^{-1} \tag{5.3-8}$$

From Eqn. (5.3-7) and Eqn. (5.3-8)

$$[z\mathbf{I} - \mathbf{T}]^{-1} = \mathbf{\Psi}\,[\mathbf{I} - z^{-1}\exp[\mathbf{\Lambda}T]]^{-1}\,\mathbf{\Psi}^{-1} \tag{5.3-9}$$

When the initial condition $\mathbf{x}(0) = 0$, From Eqns. (5.3-4) and (5.3-5),

$$\hat{\mathbf{y}}(z) = \mathbf{C}[z\mathbf{I} - \mathbf{T}]^{-1}\Delta\hat{\mathbf{f}}(z). \tag{5.3-10}$$

Denoting the Z-transfer function matrix of the vibrating structure by $\mathbf{H}(z)$, then

$$\hat{\mathbf{y}}(z) = \mathbf{H}(z)\hat{\mathbf{f}}(z). \tag{5.3-11}$$

Comparing this equation with Eqn. (5.3-10), the *Z*-transfer function matrix is given by

$$\mathbf{H}(z) = \mathbf{C}[z\mathbf{I} - \mathbf{T}]^{-1}\mathbf{\Delta} = \mathbf{C}\mathbf{\Psi}[\mathbf{I} - z^{-1}\exp[\mathbf{\Lambda}T]]^{-1}\mathbf{\Psi}^{-1}\mathbf{\Delta}. \tag{5.3-12}$$

From the previously defined values of $\mathbf{\Delta}$, and state transition matrix $\mathbf{T}(t)$,

$$\begin{aligned}\mathbf{\Delta} &= \int_0^T \mathbf{\Psi} exp\,[\mathbf{\Lambda}(T-\tau)]\mathbf{\Psi}^{-1}\mathbf{B}d\tau = \mathbf{\Psi}\mathbf{E}\mathbf{\Psi}^{-1}\mathbf{B} \\ &= \mathbf{\Psi}\mathbf{E}(\mathbf{\Psi}^T\begin{bmatrix}-\mathbf{K}_o & \mathbf{0}\\ \mathbf{0} & \mathbf{M}_o\end{bmatrix}\mathbf{\Psi})^{-1}\mathbf{\Psi}^T\mathbf{D}.\end{aligned} \tag{5.3-13}$$

where $\mathbf{E}$ is a diagonal matrix and

$$\mathbf{E} = diag[e_i] = diag[\,\lambda_i T - 1\,]$$

It has been shown in chapter 2 that the eigenvector matrix satisfies the following relationship

$$\mathbf{\Psi}^T\begin{bmatrix}-\mathbf{K}_o & \mathbf{0}\\ \mathbf{0} & \mathbf{M}_o\end{bmatrix}\mathbf{\Psi} = \mathbf{I}. \tag{5.3-14}$$

Substituting Eqn. (5.3-14) into Eqn.(5.3-13) yields

$$\mathbf{\Delta} = \mathbf{\Psi}\mathbf{E}\mathbf{\Psi}^T\mathbf{D} \tag{5.3-15}$$

It is known that the eigenvector ψ_i can also be related to the eigenvector ϕ_i of the original vibration equation

$$\mathbf{M}_o\ddot{\mathbf{y}}(t) + \mathbf{C}_o\dot{\mathbf{y}}(t) + \mathbf{K}_o\boldsymbol{\eta}(t) = \mathbf{f}(t) \tag{5.3-16}$$

by the expression

$$\boldsymbol{\Psi}_i = \begin{Bmatrix} \boldsymbol{\phi}_i \\ \lambda_i\boldsymbol{\phi}_i \end{Bmatrix}. \tag{5.3-17}$$

From Eqn. (5.3-12) and Eqn. (5.3-15),

$$\mathbf{H}(z) = \mathbf{C}\,\boldsymbol{\Psi}\,[\mathbf{I} - z^{-1}\exp[\boldsymbol{\Lambda}T]]^{-1}\,\mathbf{E}\,\boldsymbol{\Psi}^T\,\mathbf{D}. \tag{5.3-18}$$

Likewise by substituting Eqns. (5.3-15) and (5.3-17) into Eqn. (5.3-18),

$$\mathbf{H}(z) = \sum_{i=1}^{2n} \frac{\mathbf{A}_i}{1 - z^{-1}e^{\lambda_i T}}. \tag{5.3-19}$$

$\mathbf{A}_i$ is an $n \times n$ matrix called the modal constant matrix and $\mathbf{A}_i = e_i\lambda_i\boldsymbol{\phi}_i\boldsymbol{\phi}_i^T$. Since any linear combination of the eigenvectors corresponding to the eigenvalue λ_i, is also an eigenvector corresponding to λ_i. If the modal constant matrix $\mathbf{A}_i$ is written as

$$\mathbf{A}_i = \boldsymbol{\kappa}_i\boldsymbol{\kappa}_i^T \tag{5.3-20}$$

where $\boldsymbol{\kappa}_i = e_i^{\frac{1}{2}}\lambda_i^{\frac{1}{2}}\boldsymbol{\phi}_i$, then $\boldsymbol{\kappa}_i$ also is the eigenvector of the i-th mode of the vibrating structure. The eigenvalue of the vibrating structure and its modal constant matrix can then be determined by the Z-transfer function of the structure, as discussed next.

From matrix theory,

$$[z\mathbf{I}-\mathbf{T}]^{-1}=\frac{1}{\det[z\mathbf{I}-\mathbf{T}]}adj[z\mathbf{I}-\mathbf{T}]. \tag{5.3-21}$$

The determinant of the $2n\times 2n$ matrix $[z\mathbf{I}-\mathbf{T}]$ is a polynomial of degree $2n$ in complex variable z,

$$\det[z\mathbf{I}-\mathbf{T}]=z^{2n}+d_1z^{2n-1}+d_2z^{2n-2}+\cdots+d_{2n}, \tag{5.3-22}$$

where d_i is the coefficient of the polynomial while the adjoint matrix of $[z\mathbf{I}-\mathbf{T}]$ is a polynomial matrix and may be expressed as

$$adj[z\mathbf{I}-\mathbf{T}]=\mathbf{G}_1z^{2n-1}+\mathbf{G}_2z^{2n-2}+\mathbf{G}_3z^{2n-3}+\cdots+\mathbf{G}_{2n}. \tag{5.3-23}$$

$\mathbf{G}_i$ is the $2n\times 2n$ coefficient matrix of the polynomial matrix. It follows that from Eqns. (5.3-12) and (5.3-21) the Z-transfer function of the vibrating structure can be expressed as

$$\mathbf{H}(z)=\frac{\mathbf{C}adj[z\mathbf{I}-\mathbf{T}]\boldsymbol{\Delta}}{\det[z\mathbf{I}-\mathbf{T}]} \quad or \tag{5.3-24a}$$

$$\mathbf{H}(z)=\frac{\mathbf{H}_1z^{2n-1}+\mathbf{H}_2z^{2n-2}+\mathbf{H}_3z^{2n-3}+\cdots+\mathbf{H}_{2n}}{z^{2n}+d_1z^{2n-1}+d_2z^{2n-2}+\cdots+d_{2n}} \tag{5.3-24b}$$

where $\mathbf{H}_i$ is $n\times n$ matrix and $\mathbf{H}_i=\mathbf{C}\mathbf{G}_i\boldsymbol{\Delta}$, which implies the assumption that $\mathbf{D}$ is an $n\times n$ matrix.

A procedure for the estimation of the Z-transfer function of a vibrating structure can then be derived from Eqn. (5.3-24).

§ 5.4 ESTIMATE OF THE Z-TRANSFER FUNCTION

From Eqns. (5.3-11) and (5.3-24)

$$\hat{\mathbf{y}}(z)(1+d_1z^{-1}+d_2z^{-2}+\cdots+d_{2n}z^{-2n})$$
$$=(\mathbf{H}_1z^{-1}+\mathbf{H}_2z^{-2}+\mathbf{H}_3z^{-3}+\cdots+\mathbf{H}_{2n}z^{-2n})\hat{\mathbf{f}}(z). \tag{5.4-1}$$

Applying the right-shifting property of the Z-transformation and taking the inverse transformation of Eqn. (5.4-1) yields the characterizing difference equation

$$\mathbf{y}(k)+d_1\mathbf{y}(k-1)+d_2\mathbf{y}(k-2)+\cdots+d_{2n}\mathbf{y}(k-2n)$$
$$=\mathbf{H}_1\mathbf{f}(k-1)+\mathbf{H}_2\mathbf{f}(k-2)+\mathbf{H}_3\mathbf{f}(k-3)+\cdots+\mathbf{H}_{2n}\mathbf{f}(k-2n). \tag{5.4-2}$$

This represents an auto-regressive and moving average (ARMA) model and forms the basis for the determination of the Z-transfer function matrix. The poles of the ARMA model are the poles of the Z-transfer function.

Several cases for the use of Eqn. (5.4-2) to determine the Z-transfer function matrix sequence are discussed as follows.

§ 5.4.1 Univariate Model

a. Single Point Excitation and Single Point Response

When a single excitation point and a single response point are arranged in a vibration modal test, only one component of the excitation $\mathbf{f}(k)$ and one component of response $\mathbf{y}(k)$ are measured. In this case, Eqn. (5.4-2) becomes a univariate ARMA model.

Without loss of generality, assuming the i-th component of the excitation vector and the j-th component of response vector are measured at time instant $k = 2n,\ 2n+1,\ \cdots,\ N$, Eqn. (5.4-2) becomes

$$y_i(k) + d_1 y_i(k-1) + d_2 y_i(k-2) + \cdots + d_{2n} y_i(k-2n)$$
$$= h_{ij}^{(1)} f_j(k-1) + h_{ij}^{(2)} f_j(k-2) + \cdots + h_{ij}^{(2n)} f_j(k-2n).$$

Further, by assembling all the measurement data for $k = 2n,\ 2n+1,\ \cdots,\ N$, the following equation is obtained

$$\hat{\mathbf{y}} = \mathbf{Q}\boldsymbol{\theta} \tag{5.4-3}$$

where

$$\hat{\mathbf{y}} = [y_j(2n)\ \ y_j(2n+1)\ \cdots\ y_j(N)]^T, \tag{5.4-4}$$

$$\boldsymbol{\theta} = [-d_1\ \ -d_2\ \cdots\ -d_{2n}\ \ h_{1i}^{(1)}\ \ h_{ji}^{(2)}\ \cdots\ h_{ji}^{(2n)}]^T \tag{5.4-5}$$

and $\mathbf{Q}$ is an $(N-2n+1)\times 4n$ matrix

$$\mathbf{Q} = \begin{bmatrix} y(2n-1) & y(2n-2) & \cdots & y(0) & f(2n-1) & f(2n-2) & \cdots & f(0) \\ y(2n) & y(2n-1) & \cdots & y(1) & f(2n) & f(2n-1) & \cdots & f(1) \\ \cdots & \cdots & \cdots & \cdots & \cdots & \cdots & \cdots & \cdots \\ y(N-1) & y(N-2) & \cdots & y(N-2n) & f(N-1) & f(N-2) & \cdots & f(N-2n) \end{bmatrix} \tag{5.4-6}$$

The superscript (k) of $h_{ji}^{(k)}$ indicates the element belongs to the k-th matrix $\mathbf{H}_k$ and subscript ji indicates the j-row and i-th column element of the matrix.

It is clear that the sampling number N should be larger than $6n-1$. The least square estimate of the parameter $\boldsymbol{\theta}$ can then be obtained as

$$\boldsymbol{\theta} = (\mathbf{Q}^T\mathbf{Q})^{-1}\mathbf{Q}^T\hat{\mathbf{y}} \tag{5.4-7}$$

The matrix $\mathbf{Q}^T\mathbf{Q}$ and vector $\mathbf{Q}^T\hat{\mathbf{y}}$ may also be assumed to approach asymptotically the auto-correlation and cross-correlation matrix, respectively. This will be so for responses from stationary random force inputs when the observation period is sufficiently long.

§ 5.4.2 Multivariate Model

In a practical modal test, the following methods are commonly used. A shaker vibrates the tested structure at a single point and responses are measured at multiple points. Another method measures the response at a single point as the tested structure is successively impacted at multiple points by an impactor or hammer. This section discusses the use of the Z-transformation with these test methods to identify the modal parameters. Application of the Z-transformation to the multiple excitation and multiple response testing is also discussed.

In order to derive suitable algorithms for the above test methods, the modal constant matrix has to be further discussed. From Eqn. (5.3-20), the modal constant matrix of the tested structure can be expressed in detail as

$$\mathbf{A}_l = \begin{bmatrix} a_{11}^l & a_{12}^l & : & a_{1i}^l & : & a_{1n}^l \\ a_{21}^l & a_{22}^l & : & a_{2i}^l & : & a_{2n}^l \\ : & : & : & : & : & : \\ a_{i1}^l & a_{i2}^l & : & a_{ii}^l & : & a_{in}^l \\ : & : & : & : & : & : \\ a_{n1}^l & a_{n2}^l & : & a_{ni}^l & : & a_{nn}^l \end{bmatrix} \tag{5.4-8}$$

The matrix $\mathbf{A}_l$ is symmetric and $a_{ij}^l = \kappa_i^l \kappa_j^l$. Considering κ_j^l or κ_i^l as a constant multiplier, either the i-th row or j-th column can be regarded as the l-th complex mode shape of the vibrating structure. The minimum data for deriving the l-th mode shape is therefore one column or one row of the l-th modal constant matrix. Accordingly, one column or one row of the coefficient matrix sequence $\mathbf{H}_i$ of the ARMA model in Eqn. (5.4-2) is needed to be identified for deriving the mode shape.

a. Single Point Excitation and Multiple Point Response

In case of the single point excitation testing, the excitation is applied at a single point while the responses are measured at several points on the structure. Accordingly, one column, for example the j–th column, of the matrix $\mathbf{A}_l$ is estimated. The j-th column vector $\mathbf{h}_j^{(i)}$ of matrix $\mathbf{H}_i$ replaces matrix $\mathbf{H}_i$ itself in Eqn. (5.4-2) and excitation vector $\mathbf{f}(k-i)$ is correspondingly replaced by its j-th component $f_j(k-i)$. Eqn. (5.4-2) then becomes

$$\begin{aligned} &\mathbf{y}(k) + d_1\mathbf{y}(k-1) + d_2\mathbf{y}(k-2) + \cdots + d_{2n}\mathbf{y}(k-2n) \\ &= \mathbf{h}_j^{(1)} f_j(k-1) + \mathbf{h}_j^{(2)} f_j(k-2) + \cdots + \mathbf{h}_j^{(2n)} f_j(k-2n) \end{aligned} \tag{5.4-9}$$

If n response measurement stations are arranged, this vector equation can be decoupled into n univariate ARMA models

$$y_i(k) + d_1 y_i(k-1) + d_2 y_i(k-2) + \cdots + d_{2n} y_i(k-2n)$$
$$= h_{ij}^{(1)} f_j(k-1) + h_{ij}^{(2)} f_j(k-2) + \cdots + h_{ij}^{(2n)} f_j(k-2n) \quad i = 1, 2, \cdots, n \tag{5.4-10}$$

where i indicates the i-th component of vectors $\mathbf{y}$ and $\mathbf{h}_j^{(k)}$. Being treated in the same way as for the univariate ARMA model previously discussed, $d_1, d_2, \cdots, d_{2n}$ and $h_{ij}^{(1)}, h_{ij}^{(2)}, \cdots, h_{ij}^{(2n)}$ for $i = 1, ,2, \cdots, n$ can be estimated. The final estimate of d_i can be taken as the average of all the individual estimates and the estimate of $\mathbf{h}_j^{(k)}$ is formed from n estimates of $h_{ij}^{(1)}$, $h_{ij}^{(2)}$, $\cdots$, $h_{ij}^{(2n)}$.

Another method to simultaneously estimate d_i and $\mathbf{h}_i$ is developed as follows. The estimated parameters are formed as;

$$\mathbf{d} = [\, d_1 \;\; d_2 \;\; d_3 \;\; \cdots \;\; d_{2n} \,]^T, \tag{5.4-11}$$

$$\bar{\mathbf{h}}_i = [\, h_{ij}^{(1)} \;\; h_{ij}^{(2)} \;\; \cdots \;\; h_{ij}^{(2n)} \,]^T \tag{5.4-12}$$

with $h_{ij}^{(k)}$ representing the i-th component of the the j-th column vector $\mathbf{h}_j^{(k)}$ of the coefficient matrix $\mathbf{H}_k$, and

$$\boldsymbol{\theta} = \begin{bmatrix} \mathbf{d} \\ \bar{\mathbf{h}}_1 \\ \bar{\mathbf{h}}_2 \\ \cdots \\ \bar{\mathbf{h}}_n \end{bmatrix}. \tag{5.4-13}$$

$\boldsymbol{\theta}$ is an $((n+1)\times 2n) \times 1$ column vector. The measured time domain data are formed as;

$$\bar{\mathbf{y}}_i(k) = [\, y_i(k-1)\ \ y_i(k-2)\ \cdots\ y_i(k-2n)\,], \tag{5.4-14}$$

$$\mathbf{f}_j(k) = [\, f_j(k-1)\ \ f_j(k-2)\ \cdots\ f_j(k-2n)\,] \tag{5.4-15}$$

and

$$\mathbf{Q}(k) = \begin{bmatrix} \bar{\mathbf{y}}_1(k) & \mathbf{f}_j(k) & \mathbf{0} & \cdots & \mathbf{0} \\ \bar{\mathbf{y}}_2(k) & \mathbf{0} & \mathbf{f}_j(k) & \cdots & \mathbf{0} \\ \vdots & \vdots & \vdots & \cdots & \vdots \\ \bar{\mathbf{y}}_n(k) & \mathbf{0} & \mathbf{0} & \cdots & \mathbf{f}_j(k) \end{bmatrix}. \tag{5.4-16}$$

$\mathbf{Q}(k)$ is an $n \times ((n+1)\times 2n)$ matrix. Then Eqn. (5.4-2) may be written in a compact form

$$\mathbf{y}(k) = \mathbf{Q}(k)\boldsymbol{\theta}. \tag{5.4-17}$$

Assembling the measurement data at time instant $k = 2n,\ 2n+1,\ \cdots,\ N$, the following equation can be obtained

$$\mathbf{u} = \mathbf{Q}\boldsymbol{\theta}, \tag{5.4-18}$$

where $\mathbf{u}$ is a $((N-2n+1)\times n))\times 1$ column vector with

$$\mathbf{u}=[y_1(2n)\, y_1(2n+1) \cdots y_1(N)\, y_2(2n) \cdots y_2(N) \cdots y_n(2n) \cdots y_n(N)]^T \tag{5.4-19}$$

and $\mathbf{Q}$ is a $((N-2n+1)\times n) \times ((n+1)\times 2n)$ matrix with

$$\mathbf{Q} = \begin{bmatrix} \bar{\mathbf{Y}}_1 & \bar{\mathbf{F}}_j & \mathbf{0} & \cdots & \mathbf{0} \\ \bar{\mathbf{Y}}_2 & \mathbf{0} & \bar{\mathbf{F}}_j & \cdots & \mathbf{0} \\ \vdots & \vdots & \vdots & \cdots & \vdots \\ \bar{\mathbf{Y}}_n & \mathbf{0} & \mathbf{0} & \cdots & \bar{\mathbf{F}}_j \end{bmatrix}. \tag{5.4-20}$$

with $\bar{\mathbf{Y}}_i$ and $\bar{\mathbf{F}}_i$ being $(N-2n+1) \times 2n$ matrices

$$\bar{\mathbf{Y}}_i = \begin{bmatrix} y_i(2n-1) & y_i(2n-2) & \vdots & y_i(0) \\ y_i(2n) & y_i(2n-1) & \vdots & y_i(1) \\ \vdots & \vdots & \vdots & \vdots \\ y_i(N-1) & y_i(N-2) & \vdots & y_i(N-2n) \end{bmatrix} \tag{5.4-21}$$

and

$$\bar{\mathbf{F}}_j = \begin{bmatrix} f_j(2n-1) & f_j(2n-2) & \vdots & f_j(0) \\ f_j(2n) & f_j(2n-1) & \vdots & f_j(1) \\ \vdots & \vdots & \vdots & \vdots \\ f_j(N-1) & f_j(N-2) & \vdots & f_j(N-2n) \end{bmatrix}. \tag{5.4-22}$$

The least square estimate of $\boldsymbol{\theta}$ is then

$$\boldsymbol{\theta} = (\mathbf{Q}^T\mathbf{Q})^{-1}\mathbf{Q}^T\mathbf{u} \tag{5.4-23}$$

The number of samples N must be taken such that $N \geq 4n+1$ and hence the least squares estimates exist.

b. Multiple Point Excitation and Single Point Response

In the case of single response testing, the excitation is applied to several points of the structure and response is picked up at a single point. Accordingly, one row of the

matrix $\mathbf{A}_i$ is estimated. The row vector $(\mathbf{h}_j^{(i)})^T$ of the matrix $\mathbf{H}_i$ replaces the matrix $\mathbf{H}_i$ itself and the response vector $\mathbf{y}(k)$ is replaced by the measured, for example, j-th element $y_j(k)$. Eqn. (5.4-2) becomes

$$y_j(k) + d_1 y_j(k-1) + d_2 y_j(k-2) + \cdots + d_{2n} y_j(k-2n)$$
$$= (\mathbf{h}_j^{(1)})^T \mathbf{f}(k-1) + (\mathbf{h}_j^{(2)})^T \mathbf{f}(k-2) + (\mathbf{h}_j^{(3)})^T \mathbf{f}(k-3) + \cdots + (\mathbf{h}_j^{(2n)})^T \mathbf{f}(k-2n) \quad (5.4\text{-}24a)$$

A similar procedure to the case of single excitation test can be applied to estimate coefficient d_i and row vector $(\mathbf{h}_j^{(i)})^T$.

In impact testing, the excitation is not applied simultaneously and Eqn. (5.4-2) has the following form in this case,

$$y_j(k) + d_1 y_j(k-1) + d_2 y_j(k-2) + \cdots + d_{2n} y_j(k-2n)$$
$$= h_{ji}^{(1)} f_i(k-1) + h_{ji}^{(2)} f_i(k-2) + \cdots + h_{ji}^{(2n)} f_i(k-2n) \quad (5.4\text{-}24b)$$

This equation represents the impact at i-th station and response at j-th station and is similar to Eqn. (5.4-10) and the same procedues can be used.

c. Multiple Point Excitation and Multiple Point Response

In the case of multiple point excitation and multiple point response modal testing, a univariate ARMA model can be developed for the i-th component of the response vector $\mathbf{y}(k)$ such as

$$y_i(k) + d_1 y_i(k-1) + d_2 y_i(k-2) + \cdots + d_{2n} y_i(k-2n)$$
$$= (\mathbf{h}_i^{(1)})^T \mathbf{f}(k-1) + (\mathbf{h}_i^{(2)})^T \mathbf{f}(k-2) + \cdots + (\mathbf{h}_i^{(2n)})^T \mathbf{f}(k-2n) \quad (5.4\text{-}25)$$

where $y_i(k)$ is the i-th component of the response vector $\mathbf{y}(k)$ and $(\mathbf{h}_i^{(k)})^T$ indicates

the i-th row of the coefficient matrix $\mathbf{H}_k$ in the ARMA model in Eqn. (5.4-2). The procedure for estimation of the coefficient d_i and coefficient vector $(\mathbf{h}_i^{(k)})^T$ can be individually performed for every component of the response $\mathbf{y}(k)$ as discussed above. All the individual estimates of d_i are averaged and the mean values are taken as the estimates of d_i. All the estimates of $(\mathbf{h}_i^{(k)})^T$ form the modal constant matrix $\mathbf{H}_k$.

Another procedure can also be developed to estimate d_i and $(\mathbf{h}_i^{(k)})^T$ simultaneously. Taking the transpose of both sides of Eqn. (5.4-25) yields

$$\begin{aligned} &y_i(k) + d_1 y_i(k-1) + d_2 y_i(k-2) + \cdots + d_{2n} y_i(k-2n) \\ &= \mathbf{f}^T(k-1)\mathbf{h}_i^{(1)} + \mathbf{f}^T(k-2)\mathbf{h}_i^{(2)} + \cdots + \mathbf{f}^T(k-2n)\mathbf{h}_i^{(2n)} \end{aligned} \tag{5.4-26}$$

Assuming

$$\bar{\mathbf{Y}}_i(k) = \begin{bmatrix} y_i(2n-1) & y_i(2n-2) & \cdots & y_i(0) \\ y_i(2n) & y_i(2n-1) & \cdots & y_i(1) \\ \cdots & \cdots & \cdots & \cdots \\ y_i(N-1) & y_i(N-2) & \cdots & y_i(N-2n) \end{bmatrix} \tag{5.4-27}$$

$$\underline{\mathbf{y}}_i = \begin{bmatrix} y_i(2n) \\ y_i(2n+1) \\ \vdots \\ y_i(N) \end{bmatrix},$$

$$\bar{\mathbf{f}}(k) = [\ \mathbf{f}(k-1)^T\ \ \mathbf{f}(k-2)^T\ \ \cdots\ \ \mathbf{f}(k-2n)^T\ ]$$

where $\bar{\mathbf{Y}}_i(k)$ is an $(N-2n+1) \times 2n$ matrix, $\underline{\mathbf{y}}_i$ is an $(N-2n+1) \times 1$ column vector and $\bar{\mathbf{f}}(k)$ is a $1 \times 2n^2$ row vector and the estimated parameters

$$\boldsymbol{\theta}=\begin{bmatrix}\mathbf{d}\\ \mathbf{h}_1^{(1)}\\ \mathbf{h}_2^{(1)}\\ ..\\ \mathbf{h}_n^{(1)}\\ \mathbf{h}_1^{(2)}\\ ..\\ \mathbf{h}_n^{(2)}\\ ..\\ \mathbf{h}_1^{(2n)}\\ ..\\ \mathbf{h}_n^{(2n)}\end{bmatrix} \qquad \mathbf{d}=\begin{bmatrix}d_1\\ d_2\\ :\\ :\\ d_{2n}\end{bmatrix} \tag{5.4-28}$$

with $\boldsymbol{\theta}$ being a $(2n\times(n^2+1))\times 1$ column vector, then the following equation can be obtained

$$\mathbf{u}=\mathbf{Q}\boldsymbol{\theta} \tag{5.4-29}$$

where $\mathbf{u}$ is an $((N-2n+1)\times n)\times 1$ column vector

$$\mathbf{u}=\begin{bmatrix}\underline{\mathbf{y}}_1\\ \underline{\mathbf{y}}_2\\ ..\\ \underline{\mathbf{y}}_n\end{bmatrix} \tag{5.4-30}$$

and $\mathbf{Q}$ is an $((N-2n+1)\times n)\times(2n\times(n^2+1))$ matrix.

$$\mathbf{Q} = \begin{bmatrix} \bar{\mathbf{Y}}_1 & \bar{\mathbf{F}} & \cdots & \mathbf{0} \\ \bar{\mathbf{Y}}_2 & \mathbf{0} & \cdots & \mathbf{0} \\ \vdots & \vdots & \cdots & \vdots \\ \bar{\mathbf{Y}}_n & \mathbf{0} & \cdots & \bar{\mathbf{F}} \end{bmatrix} \tag{5.4-31}$$

with

$$\bar{\mathbf{F}} = \begin{bmatrix} \bar{\mathbf{f}}(2n) \\ \bar{\mathbf{f}}(2n+1) \\ \cdots \\ \bar{\mathbf{f}}(N) \end{bmatrix}. \tag{5.4-32}$$

The least square estimate of $\boldsymbol{\theta}$ is

$$\boldsymbol{\theta} = (\mathbf{Q}^T\mathbf{Q})^{-1}\mathbf{Q}^T\mathbf{u}. \tag{5.4-33}$$

The number of samples N should be greater than $2n^2+2n+1$ so that the least squares estimates exist. The matrix $\mathbf{Q}^T\mathbf{Q}$ and vector $\mathbf{Q}^T\mathbf{u}$ in Eqns. (5.4-23) and (5.4-33) may be assumed to approach asymptotically the auto-correlation and cross-correlation, respectively. This will be true for responses from stationary random force inputs when the observation period is theoretically approaching infinite and practically of adequate length.

§ 5.5 DETERMINATION OF MODAL PARAMETERS

§ 5.5.1 Determination of Natural Frequencies and Damping Ratios

Once $\boldsymbol{\theta}$ has been estimated, the coefficients d_i can be determined and substituted into the determinant in Eqn. (5.3-22) to equate the determinant with zero and to solve the equation. The roots, z_i, of the equation are the poles of the ARMA model as well as

of the Z-transfer function matrix $\mathbf{H}(z)$ of the vibrating structure. It is well known that the eigenvalue λ_i of a vibrating structure is expressed as

$$\lambda_i = -\omega_i \eta_i \pm j\omega_i \sqrt{1-\eta_i^2}$$

where ω_i is the natural frequency of the vibrating structure and η_i is its damping ratio. j represents the imaginary unit. As noted, $z_i = e^{\lambda_i T}$, and since z_i are complex, it can be written

$$z_i = a_i + jb_i = e^{\lambda_i T} = e^{-\omega_i \eta_i T} e^{j\omega_{id} T} = c_i e^{j\theta_i}. \tag{5.5-1}$$

where ω_{id} is the damped natural frequency of the vibrating structure and

$$\omega_{id} = \omega_i \sqrt{1-\eta_i^2}$$

Hence

$$c_i = \sqrt{a_i^2 + b_i^2} = e^{-\omega_i \eta_i T} \tag{5.5-2}$$

and

$$\theta_i = \tan^{-1} \frac{b_i}{a_i} = \omega_{id} T. \tag{5.5-3}$$

The natural frequencies and damping ratios can therefore be obtained from the following two equations

$$\omega_i \eta_i = \frac{-\ln(a_i^2 + b_i^2)}{2T} \tag{5.5-4}$$

and

$$\omega_{id} = \omega_i \sqrt{1-\eta_i^2} = \frac{\tan^{-1}(b_i / a_i)}{T}. \tag{5.5-5}$$

§ 5.5.2 Determination of Mode Shapes

When either columns or rows of each matrix $\mathbf{H}_i$ are estimated, the mode shapes can be determined. A technique for determination mode shapes is recommended as follows.

From Eqn. (5.3-19) and $z_i = e^{\lambda_i T}$, Eqn. (5.3-24) can be expanded into a partial fraction summation

$$\mathbf{H}(z) = \sum_{i=1}^{2n} \frac{\mathbf{A}_i}{1 - z^{-1} z_i} \tag{5.5-6}$$

where $\mathbf{A}_i$ is the modal constant matrix.

To determine the values of the modal constant matrix, the following procedure is recommended. In order to evaluate $\mathbf{A}_1$, it will be expedient to multiply each side of Eqn. (5.5-6) by $(1 - z^{-1} z_1)$. Then

$$(1 - z^{-1} z_1)\mathbf{H}(z) = \mathbf{A}_1 + \sum_{i=2}^{2n} \frac{(1 - z^{-1} z_1)\mathbf{A}_i}{1 - z^{-1} z_i}. \tag{5.5-7}$$

Since the relationship is to be true for all values of z, it certainly must hold for $z = z_1$ where each term on the right side is zero except $\mathbf{A}_1$. Hence, evaluating the above expression at $z = z_1$ significantly eases the determination of $\mathbf{A}_1$ and results in

$$\mathbf{A}_1 = (1 - z^{-1} z_1)\mathbf{H}(z)\,|_{z=z_1}. \tag{5.5-8}$$

It is clear that this procedure can be used in finding the remaining values of the modal constant matrix, that is

$$\mathbf{A}_i = (1 - z^{-1} z_i)\mathbf{H}(z)\,|_{z=z_i} \quad \text{for} \quad i = 1, 2, \cdots, 2n. \tag{5.5-9}$$

The denominator of $\mathbf{H}(z)$ in Eqn. (5.3-24b) is factorized into $(z - z_1)(z - z_2)\cdots(z - z_{2n})$ and $\mathbf{A}_i$ is then calculated using Eqn. (5.5-9) for each poles z_i.

Considering a constant multiplier, any column or row of the matrix $\mathbf{A}_i$ will represent the i-th mode of the vibrating structure. Similarly, in the case of single point excitation modal testing, a column modal shape vector will be determined by the following expression

$$\mathbf{a}_i = (1 - z^{-1} z_i)\mathbf{h}(z)\,|_{z=z_i} \quad \text{for} \quad i = 1, 2, \cdots, 2n. \tag{5.5-10}$$

The case of multiple shaker and one response measuring point modal testing or impact testing, the row modal shape vector can be evaluated in much the same way

$$\mathbf{a}_i^T = (1 - z^{-1} z_i)\mathbf{h}^T(z)\,|_{z=z_i} \quad \text{for} \quad i = 1, 2, \cdots, 2n. \tag{5.5-11}$$

§ 5.6 NUMERICAL EXAMPLES

Some digital computer simulated tests are presented to demonstrate the application and efficiency of the present method. The assumed structure is a cantilevered beam with mass density of $7.85\,t/m^3$, elasticity modulus of $200 \times 10^3\,MPa$ and dimensions of $14mm \times 25mm \times 1000mm$. The cantilever can be depicted as in Fig. 5.6-1.

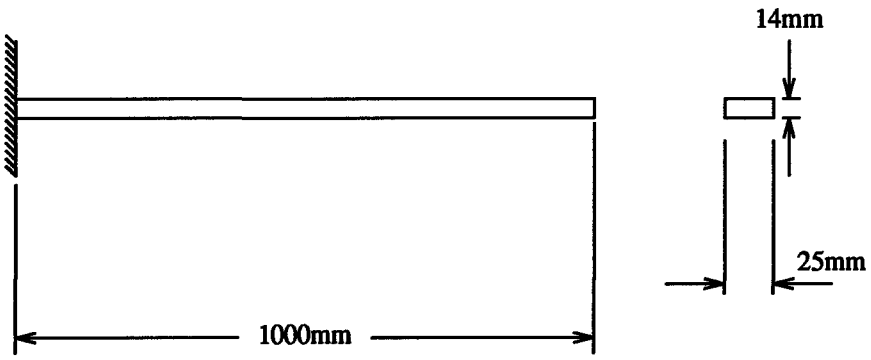

Fig. 5.6-1 Geometry of Cantilever Beam

The first five modal parameters, including natural frequencies and mode shapes were calculated by the finite element method. These calculated modal parameters are considered as "exact" values, which are compared with the identified results to assess the accuracy of identification. All the modes were assigned the same damping ratio of 0.02.

The excitation signals were treated as accurate without corrupted noise. The responses were evaluated by mode superposition method and checked by a numerical integration technique. In order to simulate the actual test, some level of corrupted noise was added into the responses.

Two types of simulating vibration tests were performed. The first digital test simulated the single point excitation modal test. The excitation point was arranged at the tip of the cantilever and six response points were equally spaced from the tip to the support as shown in Fig. 5.6-2. The response data were randomly added with noise of 15% RMS of the noise to signal ratio. Sampling rate was 1400 Hz and 1600 samples were evaluated.

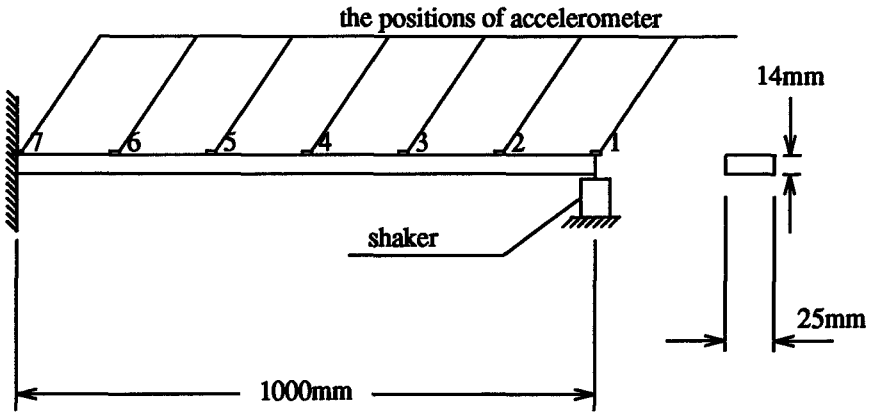

Fig. 5.6-2 Simulation of Single Shaker Test

The excitation is simulated by

$$f(j\Delta t) = \sqrt{2}\sum_{i=1}^{N}[S_{ff}(i\Delta\omega)\Delta\omega]^{1/2}\cos(ij\Delta\omega\Delta t + \psi_i) \tag{5.6-1}$$

$S_{ff}(\omega)$ are one-sided spectral density of the excitation $f(t)$; ψ_i is a statistically independent random phase angle uniformly distributed between 0 and 2π; and N is the number of data points. The spectra of excitation used for simulation is shown in Fig. 5.6-3.

The spectrum is calculated by the following formula

$$S_{ff}(\omega) = \frac{\alpha g^2}{\omega} e^{-(\sigma(\frac{\omega_0}{\omega})^4 + \frac{2\omega^2 y}{g})} \tag{5.6-2}$$

where α=0.0081, g=32.6, σ=0.74, $\omega_0=\frac{g}{75}$ and y=5.0.

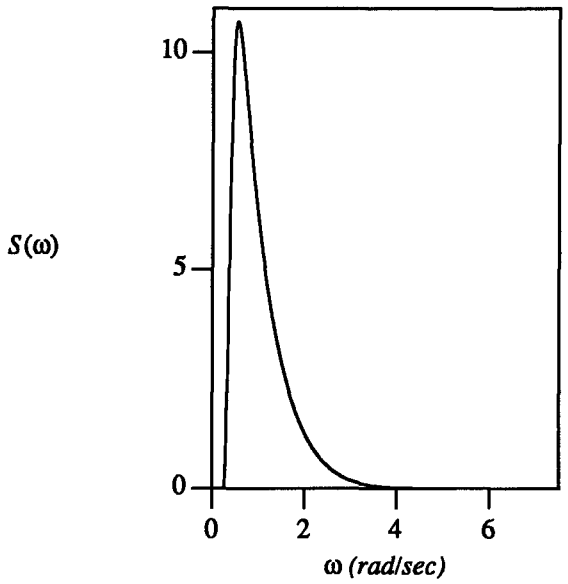

Fig. 5.6-3 Spectra of Input Excitations

The response is computed by means of numerical integration using the assumed structural parameters and the simulated excitation, the measurements of response are then generated by adding noise to the response, as shown in Figures. 5.6-4 to 5.6-6.

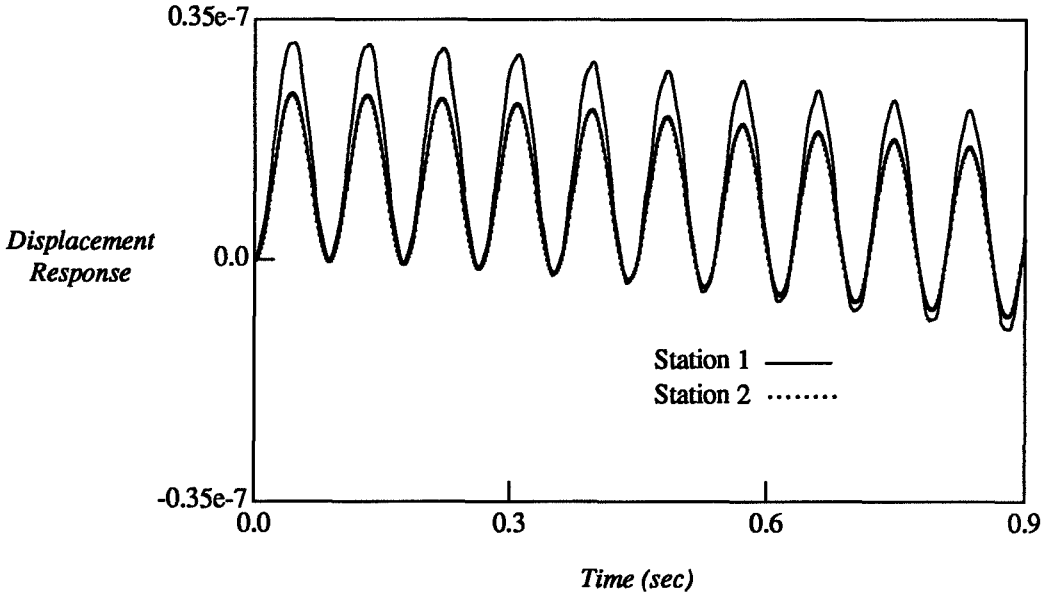

Fig. 5.6-4 Response History in Time Domain at Station 1 and 2

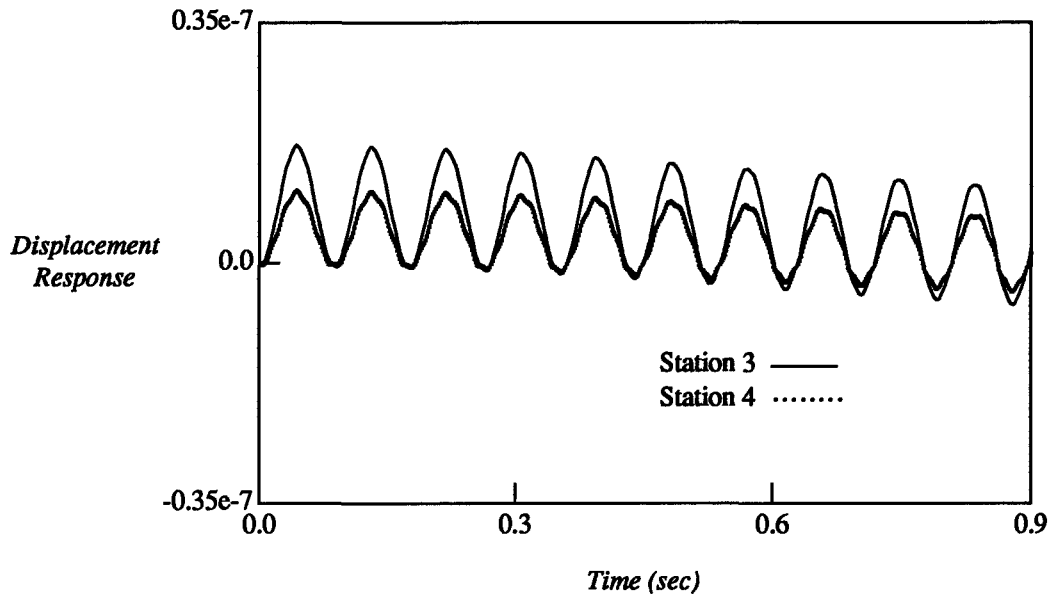

Fig. 5.6-5 Response History in Time Domain at Station 3 and 4

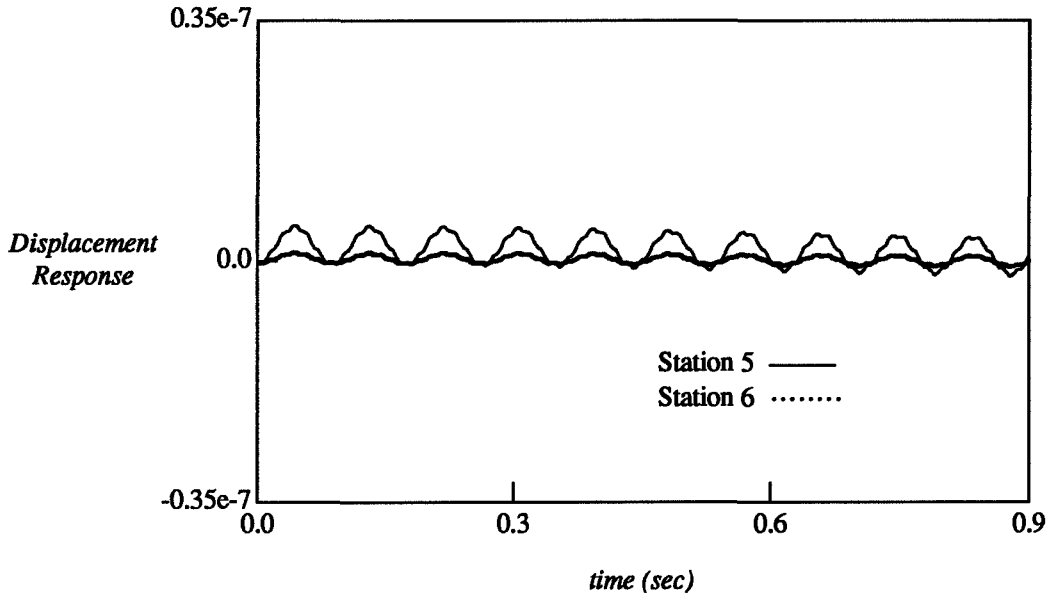

Fig. 5.6-6 Response History in Time Domain at Station 5 and 6

The modal parameters can now be estimated on the basis of the excitation and response measurements.

The second digital test simulated the single response measurement point and multiple impact excitation modal testing. In the test, a response measurement point was placed at the tip of the cantilever while six impact positions were arranged along the cantilever with equal spaces, as shown in Fig. 5.6-7.

In practical experiments, the transient excitation can be generated by an impact, which may be implemented with a hammer or similar impacting device which is not permanently attached to the structure or model.

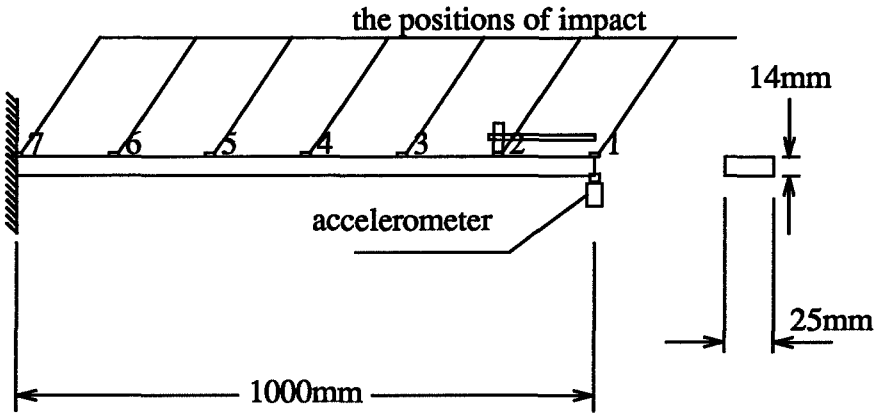

Fig. 5.6-7 Simulation of Single Impact Test

The hammer impact will produce an impulse excitation. The mathematical definition of the unit impulse is

$$\delta(t-\tau)=0, \quad t\neq\tau \qquad \int_{-\infty}^{\infty}\delta(t-\tau)dt=1 \tag{5.6-3}$$

and the unit impulse has units $time^{-1}$. The unit impulse excitation can be shown as in Fig. 5.6-8.

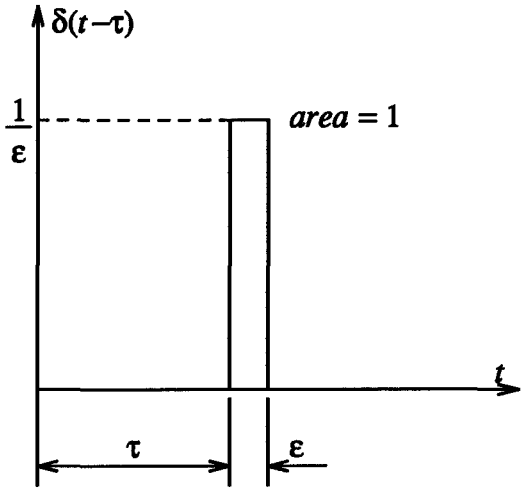

Fig. 5.6-8 Unit Impulse

The responses to the unit impulse applied to the six stations are shown in Fig. 5.6-9 to 5.6-14.

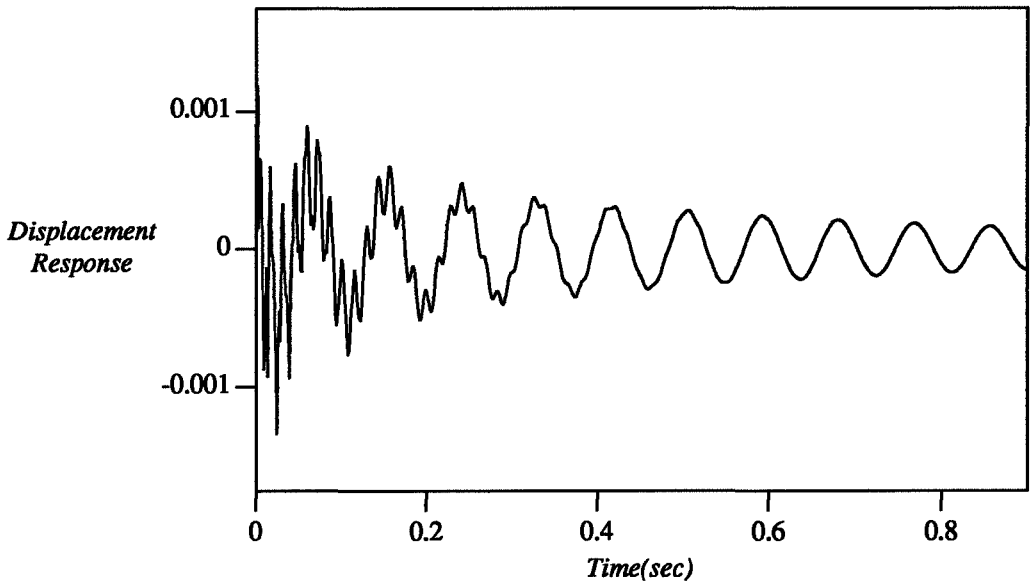

Fig. 5.6-9 Responses to Impact on Station 1

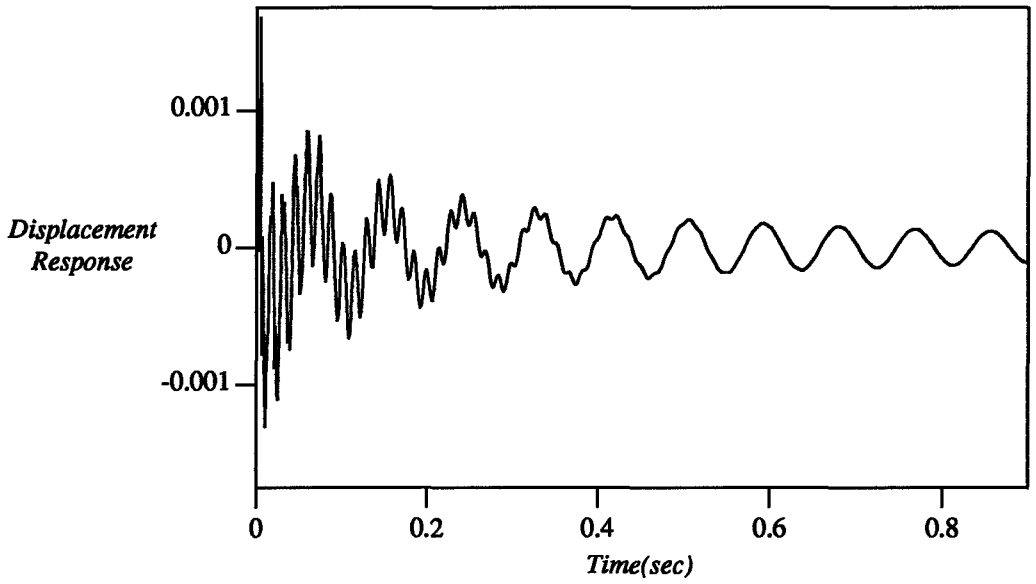

Fig. 5.6-10 Responses to Impact on Station 2

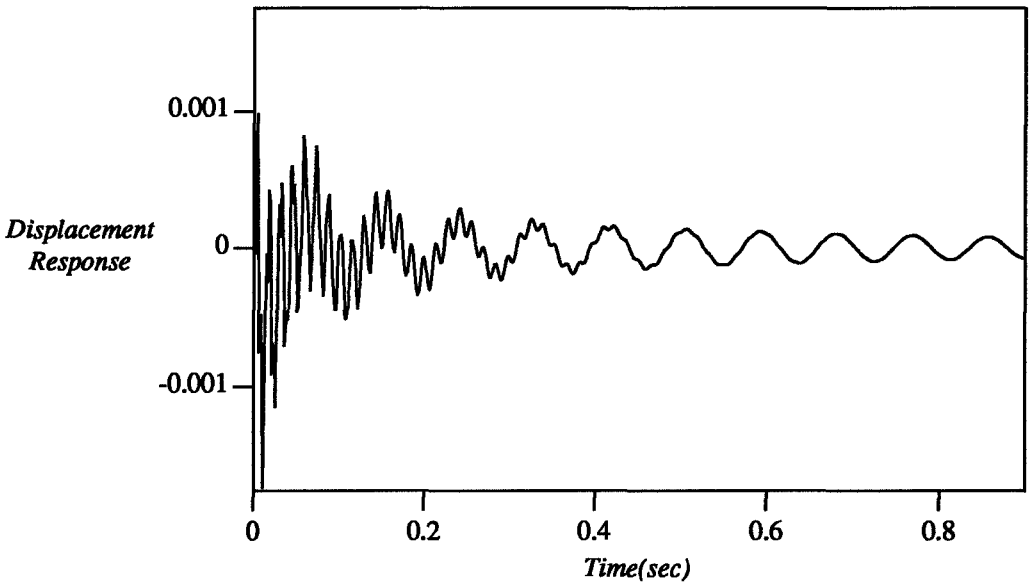

Fig. 5.6-11 Responses to Impact on Station 3

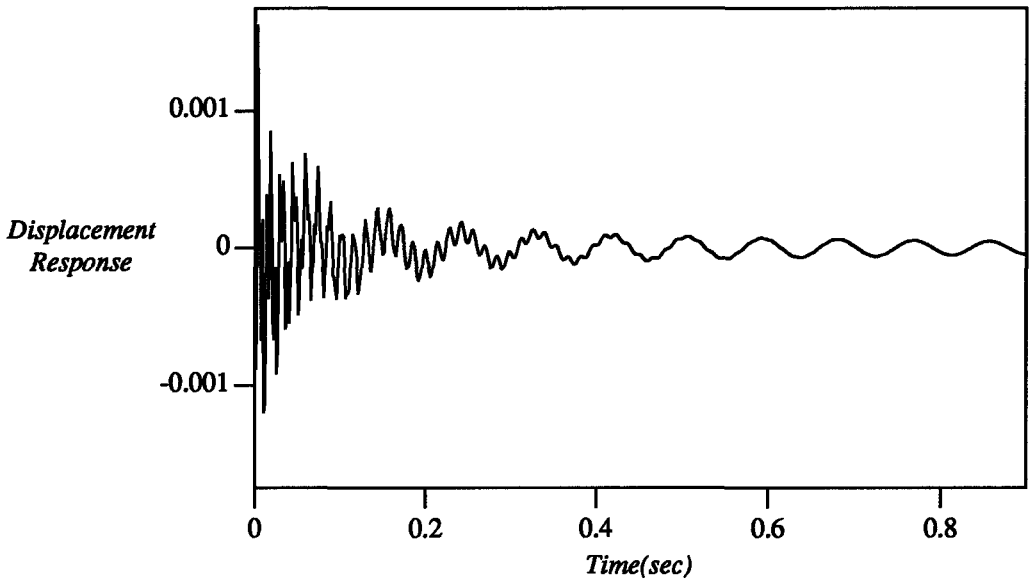

Fig. 5.6-12 Responses to Impact on Station 4

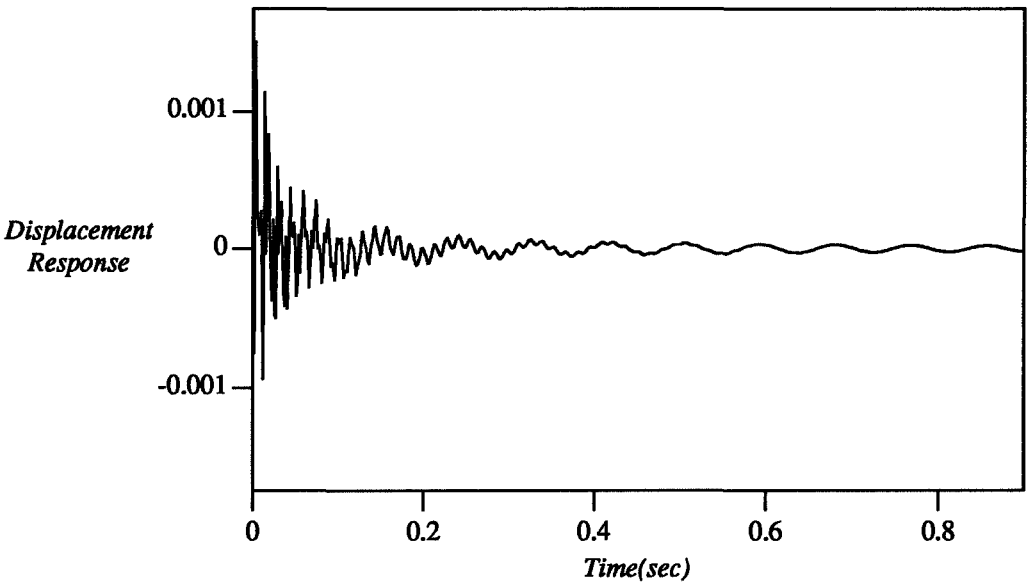

Fig. 5.6-13 Responses to Impact on Station 5

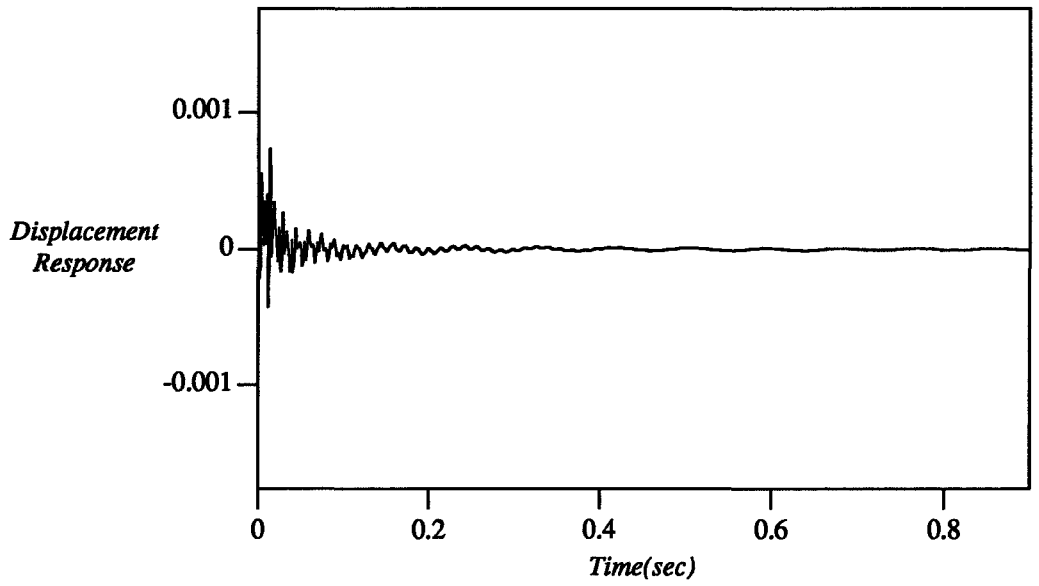

Fig. 5.6-14 Responses to Impact on Station 6

A noise with a level 15% RMS of noise to signal ratio was randomly added to the calculated responses. The sampling frequency was 1500 Hz and 1200 samples were evaluated.

All the simulated excitation and response data were used with the corresponding method developed in this chapter to determine the modal parameters of the cantilever including natural frequencies, damping ratios and mode shapes. The results and comparisons with the "exact" modal parameters are shown in Tables 5.6-1 and 5.6-2.

The accuracies of the frequencies and damping ratios are judged directly. The accuracies of the mode shapes are assessed by Mode Shape Correlation Constant, as mentioned in chapter 4. The results indicate that the present method can determine the modal parameters of a vibrating structure with adequate accuracy.

Table 5.6-1 Identified Results by Simulating Single Point Excitation and Comparison with the "Exact" Modal Parameters

MODE No	FREQUENCY (Hz)		DAMPING RATIO (%)		MSCC WITH INPUT MODE No				
	Exact	Identified	Exact	Identified	1	2	3	4	5
1	11.39	11.31	0.02	0.031	100	0	4	0	0
2	71.53	72.31	0.02	0.027	0	100	0	0	6
3	200.38	200.32	0.02	0.024	4	0	100	0	0
4	393.15	397.65	0.02	0.040	0	6	0	100	0
5	652.01	656.65	0.02	0.034	0	0	5	0	100

Table 5.6-2 Identified Results by Simulating Impact Excitation and Comparison with the "Exact" Modal Parameters

MODE No	FREQUENCY (Hz)		DAMPING RATIO (%)		MSCC WITH INPUT MODE No				
	Exact	Identified	Exact	Identified	1	2	3	4	5
1	11.39	11.27	0.02	0.034	100	0	4	2	0
2	71.53	71.51	0.02	0.024	0	100	0	0	5
3	200.38	200.32	0.02	0.024	4	0	100	2	0
4	393.15	398.03	0.02	0.035	0	6	0	100	4
5	652.01	657.25	0.02	0.036	0	0	6	0	100

§ 5.7 DISCUSSIONS AND CONCLUSIONS

From the above discussion, it can be seen that in a single excitation and single response test only the frequencies and damping ratios can be identified. In order to obtain the complex modes, at least two response points should be observed in the case of single excitation test or two excitation points should arranged in the case of single response test.

Another important point is that the number of degrees of freedom of a tested structure is unknown in advance. It must be determined according to observation

data. There are many procedures which have been used, as discussed in § 4.6. The methods recommended in that section may be used with the proposed method in this chapter as well.

The accuracy of identified modal parameters depends on the accuracy of the estimate method of the coefficients d_i and matrices $\mathbf{H}_i$. The estimates of these coefficients and matrices are obtained by least squares estimates in Eqns. (5.4-7), (5.4-23) or (5.4-33). However, the matrix $\mathbf{QQ}^T$ in these equations may be ill conditioned, in particular if its dimension is high. Therefore, the least squares estimation problem is not necessarily solved in a straightforward manner. There exist methods to find $\hat{\boldsymbol{\theta}}$ that are much better numerically behaved, which do not have the normal equations as a starting point. This has been extensively studied in other literature on the numerical analysis of least squares estimation. The underlying idea in these methods is that the matrix $\mathbf{QQ}^T$ is not formed. Instead, an orthonormal transformation is performed on the matrix $\mathbf{QQ}^T$. Consider Eqn. (5.4-7) as an example. Assume $\mathbf{T}$ is an $(N-2n+1) \times 4n$ orthonormal matrix .i.e, $\mathbf{TT}^T = \mathbf{I}$. Choose $\mathbf{T}$ such that

$$\mathbf{QT} = [\mathbf{S} \mid \mathbf{0}] \tag{5.7-1}$$

where $\mathbf{S}$ is a $4n$ upper triangular matrix. Since $\mathbf{T}$ is orthonormal,

$$\mathbf{Q} = \mathbf{T}^T[\mathbf{S} \mid \mathbf{0}] \tag{5.7-2}$$

which is a *QR* factorization of $\mathbf{Q}$. There exist several numerically good methods for *QR* factorization.

Let

$$\mathbf{yT} = [\mathbf{a} \mid \mathbf{b}] \tag{5.7-3}$$

where **a** is a $1\times 4n$ row vector and **b** is a $1\times(N-6n+1)$ row vector.

The least squares criterion becomes

$$|[\mathbf{a} \mid \mathbf{b}] - \boldsymbol{\theta}[\mathbf{S} \mid \mathbf{0}]|^2 = |\mathbf{a} - \boldsymbol{\theta}\mathbf{S}|^2 + |\mathbf{b}|^2 \tag{5.7-4}$$

which is minimized for

$$\boldsymbol{\theta}\mathbf{S} = \mathbf{a} \tag{5.7-5}$$

giving minimization

$$min(|[\mathbf{a} \mid \mathbf{b}] - \boldsymbol{\theta}[\mathbf{S} \mid \mathbf{0}]|^2) = |\mathbf{b}|^2 \tag{5.7-6}$$

It can be noticed

$$\mathbf{SS}^T = \mathbf{QTT}^T\mathbf{Q}^T = \mathbf{Q}^T \tag{5.7-7}$$

The conditioning number of **S** is thus the square root of conditioning number of $\mathbf{QQ}^T$. Therefore, the linear system (5.7-5) is much better conditioned than its counterpart (5.4-7). The described procedure for solving least squares estimation is consequently preferred. However, it should also be said that the straightforward solution Eqn. (5.4-7) in many cases gives reasonably acceptable accuracy, if the dimension of $\boldsymbol{\theta}$ is not too large.

Estimation of $\boldsymbol{\theta}$ with any of the described methods requires arithmetic operations, for

example in Eqn. (5.4-7), proportional to $(N-2n+1)(4n)^2+(4n)^3$. Then no advantage is taken of the possible internal structure of **Q**. Consequently, the individual estimation model for the multivariate case in Eqns. (5.4-9) and (5.4-10) or (5.4-24) and (5.4-25) are numerically preferred. In the case of single point excitation test, for example, when individual estimation model is used, the arithmetic operations are proportional to $((N-2n+1)\times(4n)^2 + (4n)^3)\times n$. However, when multiple simultaneous estimation model in Eqn. (5.4-18) is used, it requires arithmetic operations proportional to $(N-2n+1)\times(2n^2+2n)^2 + (2n^2+2n)^3$.

The following conclusions can then be obtained. The application of *Z*-transformation in the modal identification is investigated in this chapter. The *Z*-transformation is used to develop an ARMA model with all the coefficients of the denominator and numerator of the *Z*-transfer function of the dynamic structure, as its coefficients. The time domain excitation and response data are used to estimate the coefficients of the ARMA model and the modal parameters are determined from all the coefficients. The *Z*-transformation can be used in both the single point excitation modal testing and multiple excitation - multiple response modal testing to extract the modal parameters of a tested vibrating structure. A new technique for derivation of mode shapes from *Z*-transfer function of a vibrating structure is presented. Numerical example is given to demonstrate the effectiveness and accuracy of the application of *Z*-transformation in modal identification.

Chapter 6

LABORATORY TESTING AND EXPERIMENTAL TECHNIQUES

Approach your problems from the right end and start with the solutions. Then, perhaps, one day you will find the final question.

- R. H. Van Gulik

§ 6.1 INTRODUCTION

The principal reason for developing methods for modal identification is to apply these methods in analysis of modal test data to obtain the modal parameters. The accuracy of the identified modal parameters depends on both the analysis method used and test data obtained. The better the test data is, the more is the acuuracy of the

identified modal parameters. It is therefore necessary to use appropriate experimental techniques in the modal testing in order to get the best possible data. The procedure in applying the identification methods, developed in the preceding chapters, to the experimental environment is also important for identification of good modal parameters. This chapter is then devoted to the following two main practical problems: experimental techniques for the modal test of a vibrating structure, and the application of the developed methods in this thesis for modal identification with the modal testing. For completeness, some techniques developed by others, which are useful for modal testing, are also included in this chapter.

No excitation signal type is universally applicable to all structural testing situations but the majority of cases is optimally covered by transient or random signals. § 6.2 discusses a number of excitation signals and driving units with their advantages and disadvantages described. Accurate measurement of responses is most important for the success of identification of modal parameter. In § 6.3, the techniques of measuring the response are dealt with. Since modal testing is usually conducted using electronic equipment, it is difficult to avoid information loss during the test because of the incorrect sampling rate used. § 6.4 studies the sampling rate in order to minimize these losses. The collected data in an experiment is not always good enough for identification algorithms and needs to be pretreated as discussed in § 6.5. When modal parameters of a structure are identified, the number of degrees of freedom contained in the test data must be first determined and § 6.6 is devoted to the investigation of the methods for assessing this. Before modal testing is performed, it is necessary to consider the type of excitation signal and determine the spectrum bandwidth of the signal most suitable to the structure modal test. Further, the techniques of performing the modal testing are also of practical importance and are studied in § 6.7. Application of the methods for modal identification in this

thesis to the modal tests was conducted in the Laboratory of Structural Engineering at The University of New South Wales. § 6.8 concentrates on the description and discussion of the tests and results. § 6.9 discusses some special techniques in modal testing and a short summary is given in § 6.10 to conclude this chapter.

§ 6.2 EXCITATION TECHNIQUES

In most applications of structure testing, it is necessary to excite the structure with a well controlled and measurable excitation. A number of different types of excitation signals are available for this testing, each having its own advantages and disadvantages. The method of excitation must be simple, economical and practical. Moreover, in the present study, the exciter must have a spectral density of excitation with sufficiently large components to drive the structure through the whole range of the frequencies over which the vibration characteristics of the structure need to be identified. In this section, the most common types of excitation techniques will be described and discussed. The types of driving unit described here are the impact hammer and the shaker. The excitation signals described are (1) impact impulse, (2) step, (3) sine, (4) random (5) pseudo-random, and (6) periodic random.

It should first be considered if multi-exciters are needed to drive the structure or if a single exciter is sufficient. Multi-exciters were first suggested by Lewis and Wrisley (1950) to produce a single mode response in a heavily damped structure. Although theoretically an infinite number of drivers is required, a limited number must be used to drive a real structure. An experimentally iterative process of adjusting the forces produced by the exciters is used in the sophisticated technique advocated by Smith and Wood (1972) for each specific mode of the structure, as there are needs to be a unique force distribution for each mode to be separately excited. Since the present study deals with situations in which a number of different modes may be present it is

not necessary to use more than a single exciter. This makes the exciting system simpler and contributes to more accurate results as an experimental iterative process of testing is not involved.

The second consideration is the choice of the driving unit itself. It is possible to use either an impact hammer or a shaker.

Using a hammer to impact a structure into vibration is a simple method of excitation. When the structure is excited by the hammer, energy is transferred to the structure in a very short period of time giving a typical input force signal impulse to the structure as shown in Fig. 6.2-1.

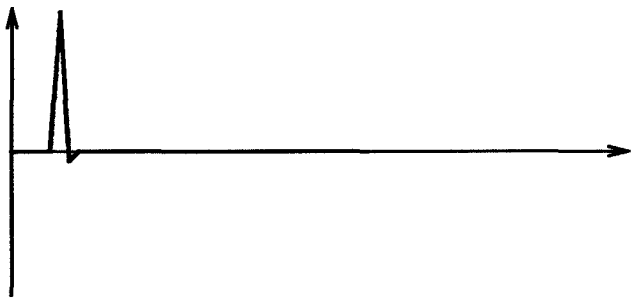

Fig. 6.2-1 A Typical Impulse Excitation

Basically, the shape of this force signal depends upon the type of the hammer tip, mass of the hammer and the dynamic characteristics of the structure under investigation. The magnitude of the impact is determined by the mass of the hammer head and the velocity of the hammer when it hits the structure. The frequency range, which is effectively excited by this type of device, is determined by the length of the signal which is controlled by the stiffness of the contacting surfaces and the mass of the hammer head. There is system resonance at a frequency given by

$$\left(\frac{contact\ \ stiffness}{hammer\ \ head\ \ mass}\right)^{1/2} \tag{6.2-1}$$

Further, it is also difficult to deliver energy into the test structure. The stiffer the material of the hammer head, the shorter is the signal and the higher is the frequency range covered by the impact. Hence, a set of different hammer tips and heads is used to permit the regulation of the frequency range to be encompassed in a test. A hammer with a hard head can be used to excite higher frequency modes, whereas a hammer with a softer head can be used to concentrate more energy at lower frequencies. Similarly, the lighter the head mass the higher the effective frequency range. A hammer is a very simple driver and produces the transient impulse excitation which is suitable for a wide variety of engineering structures. The method for excitation is fast and particularly convenient when testing is conducted in the field. However, the bandwidth of the power spectrum of the input force is not easily controlled and there is no guarantee that all natural frequencies in the entire range of interest are well excited. On the other hand, using a stiffer tip than necessary will result in energy being input to vibrations outside the range of interest at the sacrifice of those inside that range. The impulse also has a high crest factor (i.e. high amplitude but low root mean squares value) which can force some structures into non-linearity and is therefore not suitable for non-linear structures.

According to experience gained in testing at the University of New South Wales, the difficulties of applying the hammer impact are: 1. it is difficult to impact the structure with the same magnitude, position and orientation at each impact. 2. it requires practice to make the impact without multiple impacts or "hammer bounce".

Electromagnetic shakers are the most common type of exciter, and are formed by a coil and magnet assembly which represent the simplest suitable driver for use with

the present study. The frequency and amplitude of excitation are controlled independently of each other, giving more operational flexibility. The shaker takes any input signal from a signal generator required to drive the system and is able to input an adequate level of energy throughout the whole range of frequencies of interest. The electromagnetic shaker can also be easily used to excite free vibrations. Disconnecting the magnetic coil from the exciting circuit provides a time marker for the instant at which the excitation force is removed and the structure begins its free vibration response. This instant can readily be determined and the recording unit can be signaled to begin recording the response signal.

Care should be exercised about the measurement of the force applied to the structure. Although it may appear that the difference between the force generated with shaker and that applied to the structure is likely to be small, it must be noted that just near resonance very little force is required to produce a large response and what usually happens is that without altering the settings on the power amplifier or signal generator, there is a marked reduction in the force level at frequencies adjacent to the structure's natural frequencies. As a result, the true force applied to the structure becomes the difference between the force generated in the exciter and inertia force required to move the drive rod and shaker and is, in fact, much smaller than either.

Consider as an example a plate subject to a vibration test. Where the excitation and response are measured at the same point and in the immediate vicinity of the first natural frequency of the plate, the plate behaves very similar to a single degree of freedom oscillator with an apparent mass of m_{s1} and apparent stiffness k_{s1}. Assume the mass of moving parts of the shaker and connection to the structure is m_m. If the force generated by the shaker is F_m and the acceleration of the structure is $\ddot{x}$, the force F_s applied to the structure will be

$$F_s = F_m - m_m \ddot{x} \tag{6.2-2}$$

There is need for a direct measurement of the force applied to the structure as close to the surface of the structure as possible in order to obtain a reliable and accurate indication of the excitation level. A possible arrangement of force measurement is shown in Fig. 6.2-2.

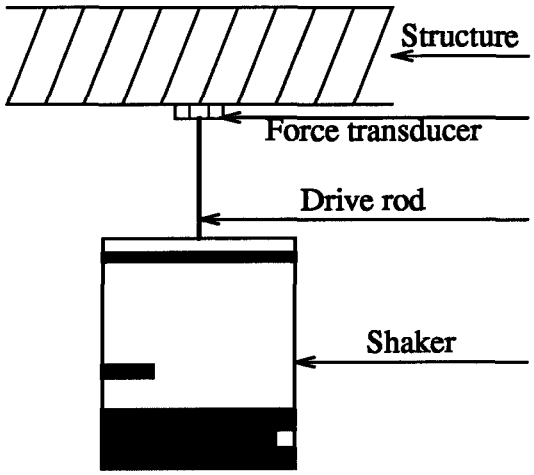

Fig. 6.2-2 Arrangement of Force Measurement

Generally, the larger the shaker, the greater the force which may be generated for exciting the structure. However, besides the obvious penalty of expense incurred by using too large an exciter, there is usually a limitation imposed on the working frequency range.

A shaker can be used with a number of generator signals, such as a step input, step relaxation input, sinusoidal input, sweep sinusoidal input, pure random input, pseudo-random input, periodic impulse and periodic random excitation.

A step input has a uniform spectral density over the entire frequency range and is theoretically an ideal method to excite all the modes of a structure. However in

practice, it is usually unattainable.

The step relaxation excitation can be used in free vibration test. To generate the step relaxation excitation, a lightweight cable is attached to the structure and used to preload the system to some allowable force level or deflection. The structure vibrates when the cable is severed. This method is capable of putting a great deal more energy into the structure, especially in the lower modes.

Sinewave excitation has been the traditional input signal in modal analysis for many years and is still widely used. The sinewave can be either stepped or swept through the frequency range of interest. The sinusoidal excitation offers some advantages over other forms of input. The advantages include (1) the frequency range of the excitation, and consequently the response, can readily be controlled, and (2) a large amount of energy can be concentrated and input to the structure within the range of frequencies required. This results in relatively high signal-to-noise ratios.

Random excitation as shown in Fig. 6.2-3 is a continuous type of signal which never repeats itself and whose amplitudes can only be predicted in terms of statistical parameters. It can be described in terms of its power spectral density. The main characteristic of the random estimates for each recorded data block is that they have random amplitudes and random phases. In practice, the random signal is often found to be a Gaussian random signal.

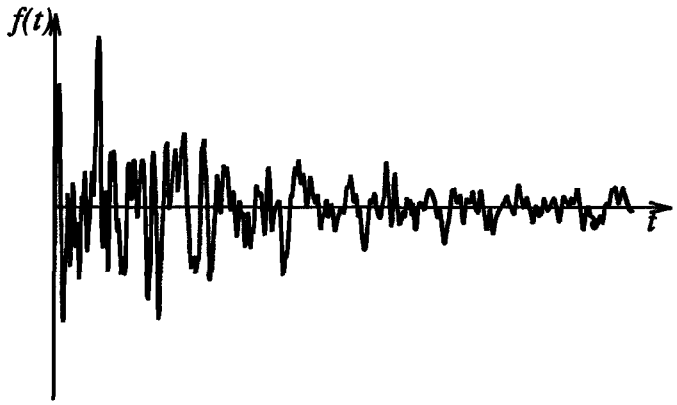

Fig. 6.2-3 Random Noise Signal

It is usual for random excitation to be applied through an attached shaker. The random signal can provide wide frequency spectra, e.g. a white noise signal has a constant power spectral density over the entire frequency range. The random signal can be band-limited to the frequency range of interest by filtering and modulating the original broad band white noise signal. Thus excitation of frequencies outside this band is avoided and a better dynamic range in the analysis can be obtained. Random excitation is the best excitation method for non-linear structures. To increase the accuracy, an averaging process for the results of different data sets can be carried out through repeatedly recording the measurement after each period of excitation. As different excitation signals are used in each case, different response records are expected according to the instant at which the excitation signal was started and stopped. This averaging enables the reduction of non-linear effects, noise, and distortion in the measurements by taking an increasing number of averages of the results. The disadvantage of this approach is that the signal averaging is needed. In addition to this, there may be leakage problems.

The pseudo-random signal, as indicated in Fig. 6.2-4, is made up of a segment of random signal of certain length of period, which is generated for the period of time and then repeated, which offers a high level of energy of excitation for the modes

affected by the signal and can provide reduction of the noise-to-signal ratio in the recorded response. The pseudo-random signal is designed in such a way that each frequency component has the same amplitude in the frequency range of interest. The phase angle between the different components, however, is random.

The main advantage in using pseudo-random excitation is that no leakage in the analysis occurs, the spectrum can therefore be shaped to only frequencies in the range of interest, and hence only a few averages are required. The most serious disadvantage of this pseudo-random method of excitation is that if the same repeated excitation function is used for every response data record taken, non-linearities and distortion cannot be removed from the measurements by ensemble averaging since they are excited equally each time and not according to random criteria.

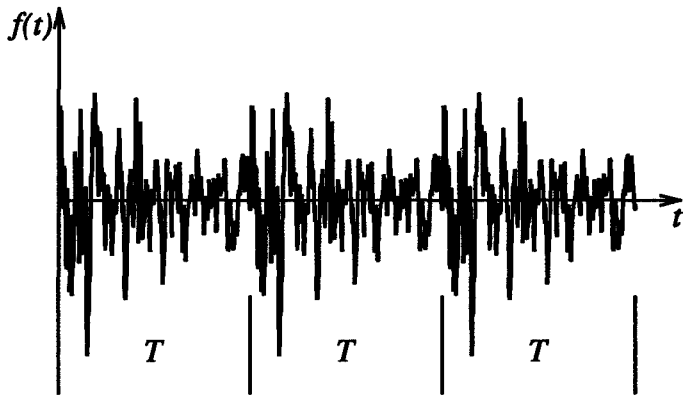

Fig. 6.2-4 Example of a Pseudo-Random Signal

Periodic random excitation can also be used with the present study. This type of excitation, as shown in Fig. 6.2-5, is the combination of pseudo-random and true random.

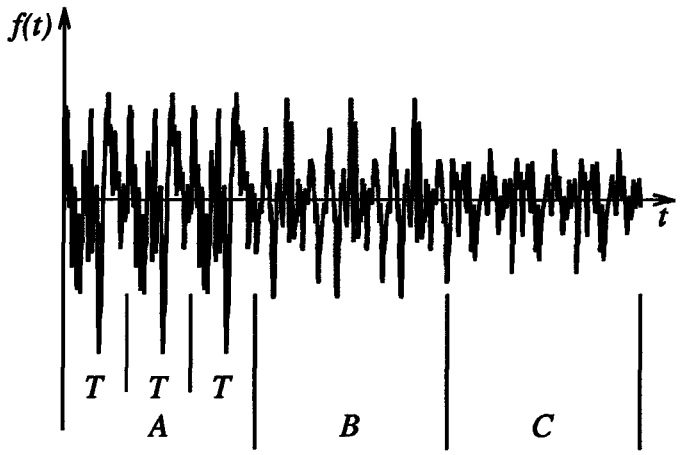

Fig. 6.2-5 Periodic Random Excitation Signal

In the periodic random process, a pseudo-random excitation is generated and after a few cycles, a measurement of the input and the now steady-state response is made. A different pseudo-random sequence is then generated, the procedure is repeated and the result treated as the second sample in what will develop to be an ensemble of random samples. The advantage over the simple random excitation is that due to the essential periodic nature of each of the periodic random samples, there are no leakage or bias errors in any of the measurements. However, the cost is an increase in the measurement time since 2/3 or 3/4 of the data available is unused while steady response conditions are awaited for each new sample.

§ 6.3 MEASURING THE RESPONSE

Measuring the response is an important step in the modal testing. It is generally necessary to consider and deal with a certain level of noise arising from the experimental measurements.

Different types of transducer are used to measure different structural responses. Ammong the other transducer, accelerometers such as those of piezoelectric type can be most conveniently used with the present study because of their sensitivity, wide

frequency range, small size and ease of mounting on the structure. Accelerometers have been used in the field of structural dynamics for a long time, and are well developed and easy to use. The response of a very light structure may be affected significantly by the mass of an accelerometer or there may even be space restrictions which do not permit the mounting of an accelerometer. In such cases, non-contact velocity, displacement or strain transducers, or contacting electrical strain gauges may be used instead of accelerometers. However, the accuracy and sensitivity of these instruments are much lower than that of accelerometers.

The correct location and installation of transducers, especially accelerometers, is important. There are various means of fixing the transducers to the surface of the test structure, some more convenient than others. These fixing methods range from a threaded stud, which requires the appropriate modification of the test structure, through to various adhesives in conjunction with a stud, to the use of a small magnet plate or wax, which is simplest and easiest to use.

Another consideration when attaching the transducer is the extent of local stiffening which is introduced by its addition to the structure. If this is being fixed to a relatively flexible plate-like surface, then there is a distinct possibility that local stiffness will be increased considerably. The only solution to this difficulty is to move the transducer to the another more substantial part of the structure.

The connection of the exciter to the structure must be carefully considered. Most practical structures have generally complex and multidimensional movements. When pushed in one direction, the structure responds not only in that direction but also in others. Hence it is possible that it can give rise to a secondary form of excitation if the shaker is not correctly connected with the structure. A possible solution to this problem is to connect the exciter with the structure by a connecting rod. The advantages of such connecting rod are its very high axial stiffness but very low

bending stiffness. Hence moment excitation and rotational inertial loading would not be induced. Further this connection can protect the shaker and transducer and help the positioning of the shaker.

§ 6.4 CHOICE OF SAMPLING RATE AND PRESAMPLING FILTERS

Data sampling from a test is performed with electronic equipment-based data-acquisition system. It is inevitable that such sampling leads to information losses, and it is therefore important to select proper sampling rate so that these losses are minimized. In this section, it is assumed that the sampling is carried out with equal sampling intervals.

Suppose that a signal $f(t)$ is sampled with the sampling interval T and

$$f_k = f(kT), \quad k = 1, 2, \cdots \tag{6.4-1}$$

By denoting the sampling frequency by $\omega_s = 2\pi/T$, then $\omega_N = \omega_s/2$ is the *Nyquist frequency*. A signal with frequency higher than ω_N cannot, when sampled, be distinguished from one in the interval $[-\omega_N, \omega_N]$. It follows from simple manipulations with trigonometric formulas that with $|\omega| > \omega_N$, there exists a $\bar{\omega}$ and $-\omega_N < \bar{\omega} < \omega_N$ so that

$$\begin{aligned} \cos(\omega KT) &= \cos(\bar{\omega} KT) \\ \sin(\omega KT) &= \sin(\bar{\omega} KT) \end{aligned} \quad k = 0, 1, 2, \cdots \tag{6.4-2}$$

Consequently, the part of the signal spectrum that corresponds to frequencies higher than ω_N will be interpreted as contributions from lower frequencies. This is the *alias* phenomenon; the frequency appears under an assumed mode. It also means that the

spectrum of the sampled signal will be a superposition of different parts of the original spectrum:

$$\Phi_T(\omega) = \sum_{r=-\infty}^{\infty} \Phi_c(\omega + r\omega_u) \tag{6.4-3}$$

Here $\Phi_c(\omega)$ is the spectrum of the continuous-time spectrum, defined as

$$R_c(\tau) = \bar{E}f(t)f(t+\tau) = \lim_{L\to\infty} \frac{1}{L}\int_0^L Ef(t)f(t+\tau)dt \tag{6.4-4a}$$

$$\Phi_c(\omega) = \int_{-\infty}^{\infty} R_c(\tau)e^{-i\omega\tau}d\tau \tag{6.4-4b}$$

and $\Phi_T(\omega)$ is the spectrum of the sampled signal

$$R_T(l\cdot T) = \bar{E}f_k f_{k+l} = \lim_{N\to\infty} \frac{1}{N}\sum_{k=1}^{N} Ef(kT)f(kT+lT) \tag{6.4-5a}$$

$$\Phi_T(\omega) = T\sum_{l=-\infty}^{\infty} R_T(l\,T)e^{i\omega lT} \tag{6.4-5b}$$

The effect of Eqn. (6.4-3) is called folding: the original spectrum is folded (and added) to give the sampled spectrum.

The information regarding frequencies higher than the Nyquist frequency is thus lost by sampling. It is then important not to allow the folding effect to distort the component of the spectrum below the Nyquist frequency. This is achieved by a presampling filter $\kappa(p)$

$$f_F(t) = \kappa(p) f(t) \tag{6.4-6}$$

where p is the differentiation operation. The spectrum of the filtered signal $f_F(t)$ will therefore, be

$$\Phi_c^F(\omega) = |\kappa(i\omega)|^2 \Phi_c(\omega) \tag{6.4-7}$$

Ideally, $\kappa(i\omega)$ should have a characteristic so that

$$\begin{aligned} |\kappa(i\omega)| &= 1 \quad \omega \le \omega_N \\ |\kappa(i\omega)| &= 0 \quad \omega > \omega_N \end{aligned} \tag{6.4-8}$$

This can be realized only approximately. In the ideal case,

$$\Phi_c^F(\omega) = \begin{cases} \Phi_c(\omega) & \omega \le \omega_N \\ 0 & \omega > \omega_N \end{cases} \tag{6.4-9}$$

which means that the signal

$$f_k^F = f_F(kT) \tag{6.4-10}$$

will have a spectrum from Eqn. (6.4-3)

$$\Phi_T^F(\omega) = \Phi_c(\omega) \tag{6.4-11}$$

With the filter in Eqns. (6.4-6) and (6.4-8) a sampled spectrum with no alias effects is obtained. Therefore this filter is called an antialiasing filter. Such a filter should be applied before sampling if the signal is suspected to have non-negligible energy above the Nyquist frequency.

A typical situation occurring in data sampling is that the signal consists of a useful component and disturbance component, and the spectrum band of the disturbances is greater than that of the signal. The sampling rate is then usually chosen so that most of the spectrum of useful part is below ω_N. The antialiasing filter essentially cuts away high-frequency noise contributions.

Consider

$$f(t) = p(t) + v(t) \tag{6.4-12}$$

where $p(t)$ is the useful signal and $v(t)$ is the noise. Let $\Phi_c^v(\omega)$ be the spectrum of $v(t)$. The sampled, prefiltered signal then is

$$f_k^F = p_k^F + v_k^F \qquad f_k^F = f_F(kT) \tag{6.4-13}$$

where the variance of the noise is

$$E(v_k^F)^2 = \int_{-\omega_N}^{\omega_N} \Phi_T^{v_F}(\omega + r\omega_s)d\omega \tag{6.4-14}$$

From this expression it can be seen that the noise effects from the higher frequencies are folded into the region $[-\omega_N, \omega_N]$ and are thus contributing to the noise power. By eliminating the high-frequency noise by an antialiasing filter, the variance of the v_k^F is reduced by the term

$$\sum_{r\neq 0} \int_{-\omega_N}^{\omega_N} \Phi_c^v(\omega + r\omega_N)d\omega = \int_{|\omega|>\omega_N} \Phi_c^v(\omega)d\omega \tag{6.4-15}$$

compared to the condition with no presampling filter. This is a significant noise reduction if the noise spectrum has considerable energy above the Nyquist frequency.

If the input is band limited and has no energy above the cutoff frequency ω_B, all useful information in the output also lies below ω_B. An antialiasing filter with cutoff frequency ω_B and sample with interval $T = \pi/\omega_B$ is then applied with no loss of information. If the input is not band limited, the antialiasing filter will destroy useful information at the same time as the noise is reduced. If T is so chosen that the Nyquist frequency(= the cutoff frequency for the filter) is above the bandwidth of the system, the loss of information is not significant. In this case the antialiasing filter should be also applied to the input signal.

If the input is piecewise constant over the sampling interval, the sampled input equals the constant value and no presampling filtering should be applied to this sequence. The stepwise changes in the process input do, though, contain high frequencies that could travel through the process to the output. An antialiasing filter applied to the process output could thus distort useful information. There are three ways to handle this problem:

1. Sample fast enough that the process is well damped above the Nyquist frequency. The high frequency components in the output that originate from input are then insignificant.

2. Consider the antialiasing output filter as part of the process and model the system from input to filtered output.

3. Since the antialiasing filter is known, include it as a known part of the model and let the predicted output pass through the filter before being used in the

identification.

If the frequency of interest is too high, it may give rise to a practical difficulty of sampling with very high sampling rate. Fortunately, there is a way to overcome this difficulty. In the case of a high frequency of interest, the whole range of frequencies can be divided into some sub-ranges and testing can be carried out for these sub-ranges which may have lower limit greater than zero.

The minimum sampling rate can be derived as follows. From Eqn. (4.3-18),

$$\omega_d = \omega\sqrt{1-\eta^2} = \frac{1}{T}\arctan\left|\frac{\alpha-\alpha^*}{\alpha+\alpha^*}\right| \tag{6.4-16}$$

The inverse trigonometric function arc tan$x$ is not single valued, the principal value for arc tan$x$ is defined as

$$y = Arc\ \tan x \qquad -\frac{\pi}{2} < y < \frac{\pi}{2} \tag{6.4-17}$$

The inverse trigonometric function arc tan$x$ can then be written in terms of its principal value as

$$y = \arctan x = Arc\ \tan x + K\pi \qquad K = 0,\ 1,\ 2,\cdots,\ n \tag{6.4-18}$$

Eqn. (6.4-16) can then expressed as

$$\omega_d = \frac{1}{T}\left(Arc\ \tan\left|\frac{\alpha-\alpha^*}{\alpha+\alpha^*}\right| + K\pi\right) \tag{6.4-19}$$

From Eqn. (6.4-19), for any value of K, the value of damped natural frequency ω_d should have a single value and satisfy the following

$$\frac{1}{T}K\pi < \omega_d < \frac{1}{T}(K+1)\pi \tag{6.4-20}$$

that is

$$\frac{1}{T}K\pi < 2\pi f_d < \frac{1}{T}(K+1)\pi \tag{6.4-21}$$

$\frac{1}{T}$ is the sampling rate and denoted as f_s and hence the minimum sampling rate $(f_s)_{\min}$ is determined as

$$(f_s)_{\min} > \frac{2f_{\max}}{K+1}, \quad K = 0,\ 1,\ 2,\ \cdots,\ L \tag{6.4-22}$$

where f_s is the sampling rate, $f_{\max}$ is the maximum frequency of interest and K an integer.

For K values different from zero, there is a minimum limit on the natural frequency which can be determined by

$$f_{\min} > \frac{K(f_s)_{\max}}{2}, \quad K = 0,\ 1,\ 2,\ \cdots,\ L \tag{6.4-23}$$

where $f_{\min}$ is the minimum frequency of interest.

This yields the maximum value of K which can be used for any band of frequencies

of interest ($f_{\min}$, $f_{\max}$) and which is determined by

$$K_{\max} < \frac{f_{\min}}{f_{\max} - f_{\min}} \tag{6.4-24}$$

Therefore, there are two alternatives available, if there is a wide range of frequencies of interest.

1. The entire range can be covered at once with $K = 0$. However, this might need an excessively high sampling rate and/or an extremely large mathematical model size.

2. The entire range is subdivided into several narrower ranges, each to be covered separately by using recorded data which contains frequency contributions inside this range only. This approach allows smaller sampling rates to be used with each frequency band, and the number of modes included in data will be less than if the entire range is used. The resulting mathematical model size will be smaller, allowing smaller memory requirements for computation and less round-off error in the results.

In general, it is recommended to use the minimum possible value of K which the recording unit can handle.

For example, if there is a range of frequencies of $0 - 3000Hz$, the minimum sampling rate is $2 \times 3000 = 6000Hz$ when the range of frequencies is considered as a whole. Alternatively, the range of frequencies can be divided into four bands: $0 - 800Hz$, $800 - 1400Hz$, $1400 - 2200Hz$ and $2200Hz - 3000Hz$. The sampling rates for each band can be determined as follows.

For $0 - 800Hz$, from Eqn. (6.4-24) the maximum value of K is

$$K \leq L = \frac{0}{800 - 0} = 0 \tag{6.4-25}$$

K is then taken to be 0 and the minimum sampling rate is determined from Eqn. (6.4-22)

$$(f_s)_{\min} > \frac{2 \times f_{\max}}{0+1} = \frac{2 \times 800}{1} = 1600Hz \tag{6.4-26}$$

For the band of $800 - 1400Hz$, the maximum values of K are determined by

$$K \leq L = \frac{800}{1400 - 800} = 1.33 \tag{6.4-27}$$

then K will take the values of 0 or 1. When $K = 1$, the minimum sampling frequency is

$$(f_s)_{\min} > \frac{2 \times 1400}{1+1} = 1400Hz \tag{6.4-28}$$

and from Eqn. (6.4-23) the maximum sampling frequency is

$$(f_s)_{\max} > \frac{2 \times 800}{1} = 1600Hz \tag{6.4-29}$$

Hence the sampling rate should be

$$1400Hz < f_s < 1600Hz \tag{6.4-30}$$

The sampling rates for the remaining bands can be obtained in the similar manner.

§ 6.5 PRETREATMENT OF TEST DATA

When the data has been collected from the identification experiment, it is unlikely to be in a satisfactory condition for immediate use in identification algorithms. There are several possible deficiencies in the data that should be considered

1. High-frequency disturbances in the data record above the frequency of interest of the structure under test.

2. Drift and offset, and low-frequency-disturbances with a possible periodic character.

It is important therefore to polish the data so as to avoid problems in the identification.

If any high-frequency disturbances are detected, they indicate that the choice of sampling rate and presampling filter were not suitable. If, after the test, the sampling rate was found to be unnecessarily high, the data must be resampled and a digital antialias filter must be applied before the resampling, in the same manner as previously discussed.

Single erroneous or highly disturbed values of the measured data, such as from bursts, may have a very substantial influence on the resulting estimate. It is thus necessary to protect the estimate from corrupted data.

§ 6.6 ESTIMATION OF THE ORDER OF THE TESTING STRUCTURE

The order of a linear structure excited in a test must be determined before the modal

parameters can be identified. There are many different ways to estimate the order of a test structure based on a preliminary data analysis. Some methods have already been discussed in chapters 4 and 5. The following preliminary data analysis techniques are often used and hence discussed briefly.

1. Testing ranks in sample covariance matrices
2. Correlating variables
3. Examining the information matrix.

These are discussed as follows.

1. ***Testing ranks in covariance matrices:***

   Consider the true structure being described by

$$y(t) + a_1 y(t-1) + \cdots + a_n y(t-n) = \qquad (6.6\text{-}1)$$
$$b_1 f(t-1) + b_2 f(t) + \cdots + b_n f(t-n) + v_0(t)$$

   for some noise sequence $[v_0(t)]$. Consider also that n is the smallest number for which this holds, i.e., n is the true order. As usual, it can be assumed

$$\mathbf{q}_s(t) = [-y(t-1) \cdots -y(t-n)\, f(t-1) \cdots f(t-n)]^T \qquad (6.6\text{-}2)$$

   Suppose first that $v_0(t) = 0$, then Eqn. (6.6-1) implies that the matrix

$$\mathbf{R}^s(N) = \frac{1}{N}\sum_{t=1}^{N} \mathbf{q}_s(t)\mathbf{q}_s^T(t) \qquad (6.6\text{-}3)$$

   will be nonsingular for $s \leq n$ and singular for $s \geq n+1$. The determinant $\kappa(s) = det(\mathbf{R}^s(N))$, could thus be used as a test quantity for the model order.

For a noise $[v_0(t)]$ present in Eqn. (6.6-1), Eqn. (6.6-2) can still be used with a suitable threshold, provided the signal-to-noise ratio is high. If this is not the case, the enhanced matrix can be used

$$\hat{\mathbf{R}}^s(N) = \mathbf{R}^s(N) - \hat{\sigma}^2\mathbf{R}_v \tag{6.6-4}$$

where $\hat{\sigma}^2\mathbf{R}_v$ is the estimated influence of $v_0(t)$ on $\mathbf{R}^s(N)$. A better alternative, when the influence of $v_0(t)$ is not negligible, is to use other correlation vectors. If noise sequence $[v_0(t)]$ and excitation sequence $[f(t)]$ are uncorrelated,

$$\zeta_s = [y(t-1)\, y(t-2) \cdots y(t-2s)] \tag{6.6-5}$$

and

$$\bar{\mathbf{R}}^s_\zeta = \bar{E}\mathbf{q}_s(t)\zeta_s^T(t). \tag{6.6-6}$$

Eqn. (6.6-6) is nonsingular for $s \leq n$ and singular for $s \geq n+1$. Replacing $\bar{E}$ by sample mean gives a usable test quantity. If sequence $[v_0(t)]$ is known to be a moving average of order r, so that $y(t-r-1)$ and $v_0(t)$ are uncorrelated,

$$\zeta_s(t) = \mathbf{q}_s(t-r) \tag{6.6-7}$$

can be used in Eqn. (6.6-6).

2. ***Correlating variables:***

The order-determination problem is to include one more variable in a model structure or not. This variable could be $y(t-n-1)$ in Eqn.(6.6-1) or a measured possible disturbance variable $w(t)$. In either case, the question is whether this new variable can contribute when explaining the response variable $y(t)$ and can be measured by the correlation between $y(t)$ and $w(t)$.

However, to discount the possible relationship between $y(t)$ and $w(t)$, already accounted for by the smaller model structure, the correlation should be measured between $w(t)$ and remaining residual $\varepsilon(t, \hat{\theta}_N) = y(t) - \hat{y}(t \mid \hat{\theta}_N)$.

3. ***The information matrix:***

If the order of a test structure is overestimated, global and local identifiability will be lost. It means that

$$\mathbf{g}(t, \theta) = \frac{d\hat{\mathbf{y}}(t \mid \theta)}{d\theta}$$

will not have full rank at $\theta = \theta^*$ and hence the information matrix

$$\mathbf{M}_N = \frac{1}{\kappa_0} \sum_{t=1}^{N} E\mathbf{g}(t, \theta_0)\mathbf{g}^T(t, \theta_0)$$

will be singular. Since the Gauss-Newton search algorithm uses the inverse of the information matrix, a natural test quantity to determine the model order will be the conditioning number of this matrix.

Techniques 1 and 2 were recommended in chapter 4.

§ 6.7 EXCITATION BANDWIDTH AND ANALYSIS OF TEST DATA

§ 6.7.1 Excitation Bandwidth Consideration

Three alternative input-output arrangements have been investigated to assess their suitability for the proposed methods in this thesis.

The first alternative is to excite a structure by a signal which has a sufficiently large frequency spectrum of excitation and is filtered so as to excite the structure only within the range of interest.

The second alternative is to generate the excitation signal with the range of interested frequencies directly.

In these two cases, the exciting signal contains all the frequencies of interest, but there is no guarantee that only those modes of the structure which have natural frequencies within the range will be excited. Due to an impedance mismatch between the structure and the exciter, or due to the initial transient excitation, the structure may be excited with a spectrum having appreciable amplitudes outside the frequency range of interest.

The third alternative would not filter the excitation signal, instead the response signal is filtered to exclude any components outside the range of frequencies of interest. This arrangement guarantees both that the excitation covers the frequency range of interest and that the response data covers only this range. Preliminary experimental work indicated that the third alternative could be best controlled and hence was used in the subsequent experimental measurements.

§ 6.7.2 Analysis of Test Data

After all the excitation and response data have been recorded, the next step is to analyze the test data so that the modal parameters of the tested structure could be identified. Usually, the following procedure is necessary to reach the goal.

1. Using Eqn. (6.4-18), the maximum value of K is determined according to the range of frequencies of interest.

2. The suitable sampling rate will be computed by Eqns. (6.4-16) and (6.4-17) using a K value as low as possible. The sampling rate determined in such a manner is the best practical value to be used. However, care must be exercised in determining the range of interested frequencies. If the range is too large, it may require division into some sub-range to lower the sampling rates.

3. When test data has been collected from the identification experiment, it is unlikely to be ready for immediate use in any of the proposed identification methods. The data must be checked to determine if there are high-frequency disturbances, occasional bursts or drift, offset or low-frequency-disturbances. If possible, the data should then be polished. If not, the data must be resampled. Meanwhile, a digital antialias filter must be applied before any resampling, as discussed in § 6.4.

4. When the testing data is considered good enough, the order of the tested structure must be determined so that the proposed mathematical model of the tested structure can be used to identify its modal parameters.

5. For each method of modal identification, the corresponding matrices required by the method are constructed from test data.

6. Using an appropriate proposed methods, the modal parameters of the tested structure are determined.

7. Since time domain methods suffer greatly from contamination of the data by extraneous noise, it is appropriate to carry out an averaging process in an attempt to obtain better results. Taking more and more averages of results may reduce noise, distortion and non-linear effects. On the other hand, too many averages require more computer time and increase the round-off errors. Usually, there are three stages at which the data can be averaged: (1) the data obtained after the above step 3, (2) intermediate results which are used to compute the eigenvalue and eigenvectors, (3) the resulting eigenvalues and eigenvectors. Experience indicates using the averages of the intermediate results would give better results.

§ 6.8 EXPERIMENTAL WORK AND RESULTS

The experimental work has been conducted in the Structural Engineering Laboratory at The University of New South Wales to investigate the application of modal test techniques and the proposed methods in this thesis to the laboratory experimental environment. This section is devoted to the description of the experimental work and the results. Some of experience gained from testing is also mentioned.

The apparatus used in the experimental work is broadly divided into two main separate systems: namely, the excitation system and the data recording system.

§ 6.8.1 Excitation System

As discussed in § 6.2, there are two kinds of excitation system used in the test:

hammer system and exciter system. The arrangement of the hammer exciting system is shown in the block diagram in Fig. 6.8-1.

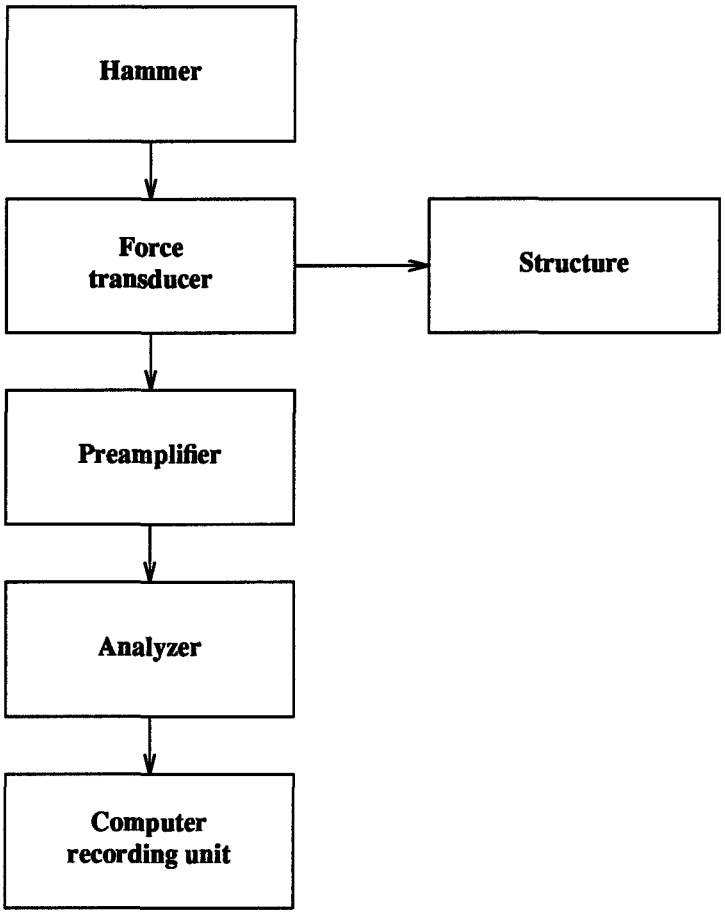

Fig. 6.8-1 Diagram of Hammer Exciting System in Test

A hammer of Bruel & Kjaer type 8202 is used to input the impact force on the testing structures. The hammer has a force transducer of Bruel & Kjaer type 8200 built into the tip to register the force input. A tip with the hammer imparts a pulse with a broad frequency range to the test structure and a blow from this hammer will simultaneously excite all the modes of vibration. The resulting vibrational motion is registered by a response pickup accelerometer mounted on the structure. Hammer

excitation requires less equipment than any other excitation method; only the instrumented hammer and one response accelerometer is needed. The signals picked up by the force transducer and accelerometer are transferred by a line drive preamplifier for Bruel & Kjaer type 2644 to the analyzer.

The line-drive preamplifier type 2644 is able to drive very long cables without losses and can withstand much more severe environmental conditions than normal preamplifiers. The 2644 has two other special benefits: (1) It can be used being mounted directly on the top face of accelerometers or force transducers fitted with top connectors, and (2) its line-drive power-supply system uses only one coaxial cable for power and signal transmission. The amplified signal is then transferred into a Bruel & Kjaer analyzer type 2034. The signal is filtered through the filter in the analyzer and is transferred to the computer and recorded in the disc as the excitation data.

The second excitation approach used in the tests is an exciter capable of generating pseudo-random signal. The excitation system of this kind is shown in Fig. 6.8-2. The pseudo-random signal is originally generated by the Bruel & Kjaer analyzer type 2034 and transferred to a power amplifier type 2706 of Bruel & Kjaer which in turn amplifies the signal before transferring it to the exciter of Bruel & Kjaer type 4809. The exciter is connected with a Bruel & Kjaer type 8200 force transducer through a flexible rod with a force transducer attached to the proper location to be excited on the structure. The flexible rod has good stiffness in its axial direction but relatively flexible in the other five directions ensuring the driving force from the exciter is applied to the structure along the axis of the rod.

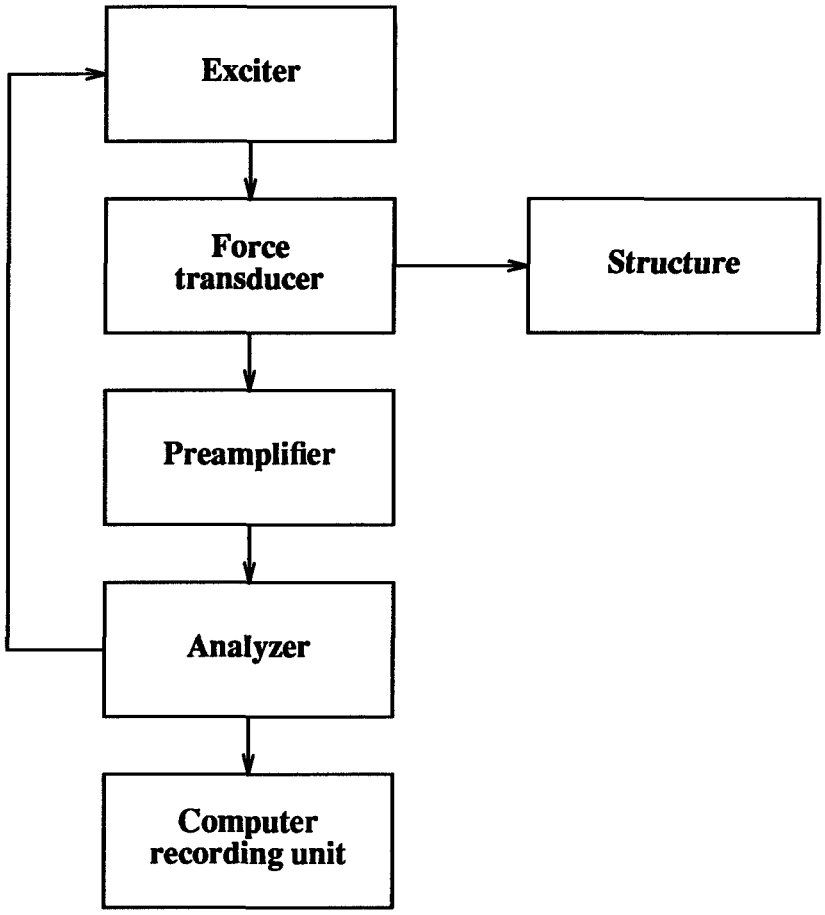

Fig. 6.8-2 Diagram of Exciter Exciting System in Test

However, if the drive rod is made too long, or too flexible, then the rod can begin to introduce the effects on its own resonances into the measurements and these can be very difficult to extricate from the genuine data. The exciter is indirectly fixed to the ground or solid isolated base.

The signal generated from the crystal in the accelerometer is transferred into the charge amplifier of Bruel & Kjaer 2635 which in turn converts the high impedance output from piezoelectric accelerometer to a lower impedance suiting the measuring/analyzing equipment. The charge amplifier has additional signal-conditioning facilities, for example, integration to velocity and displacement, frequency-band-limiting filters, transducer-sensitivity conditioning, and selectable

unified output levels. The signal from the amplifier is transmitted to the analyzer to be filtered again, and then transmitted to the computer and recorded in the disc as response data.

§ 6.8.2 Response Measurement System

The measurement response arrangement which was used for the experimental work is shown in the diagram in Fig. 6.8-3.

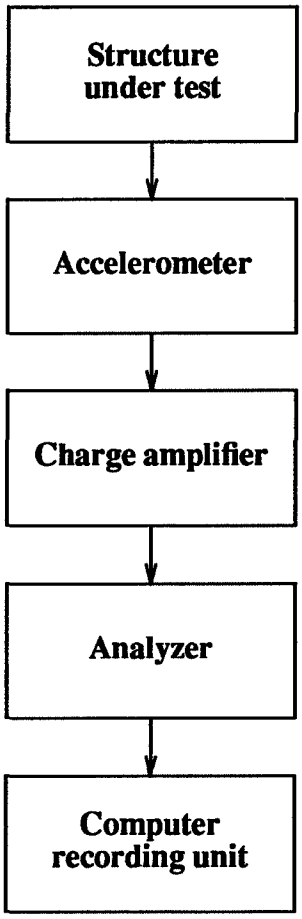

Fig. 6.8-3 Diagram of Response Measurement System in Test

Two types of piezoelectric accelerometers are used: (a) Bruel & Kjaer type 4384 and (b) Bruel & Kjaer type 4370. The first type weighs 11 *g* and has sensitivity of

8.35 mV/g which is better for testing light structures where mass loading may be a problem. The second type weighs 54 g and has sensitivity of 80 mV/g which is suitable for heavier and stiffer structures because of its higher sensitivity.

Since the signal from the accelerometer is small, it is entered into a charge amplifier (Bruel & Kjaer 2635). To limit each experimental response data set to the selected frequency range, the charge amplifier output signal is processed through a band pass filter in the Bruel & Kjaer type 2034 analyzer. Although filtering guarantees that the final response signal does not include contributions of the modes outside the range of testing, it tends to increase the noise-to-signal ratio of the response.

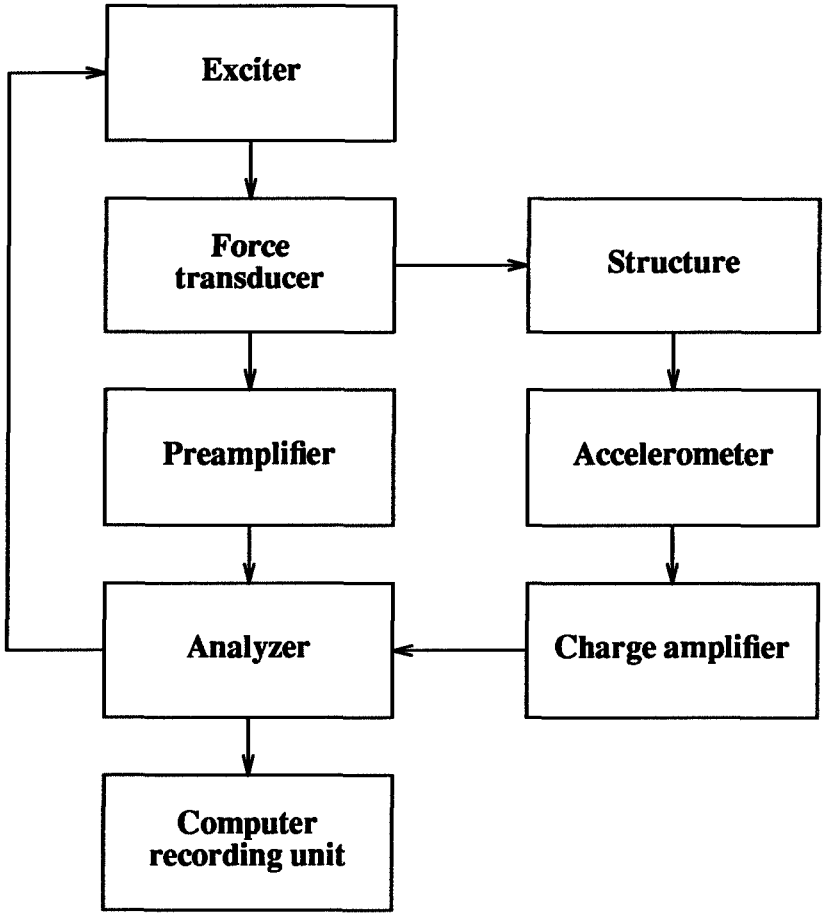

Fig. 6.8-4 Diagram of Typical Testing Arrangement

The filtered response signal then enters the computer to be recorded as response data at the proper sampling rate.

The complete testing arrangement is diagrammatically shown in Fig. 6.8-4.

§ 6.8.3 Experimental Procedures

The experimental setups for hammer impact testing and shaker excitation testing are shown in Figs. 6.8-5 and 6.8-6, respectively.

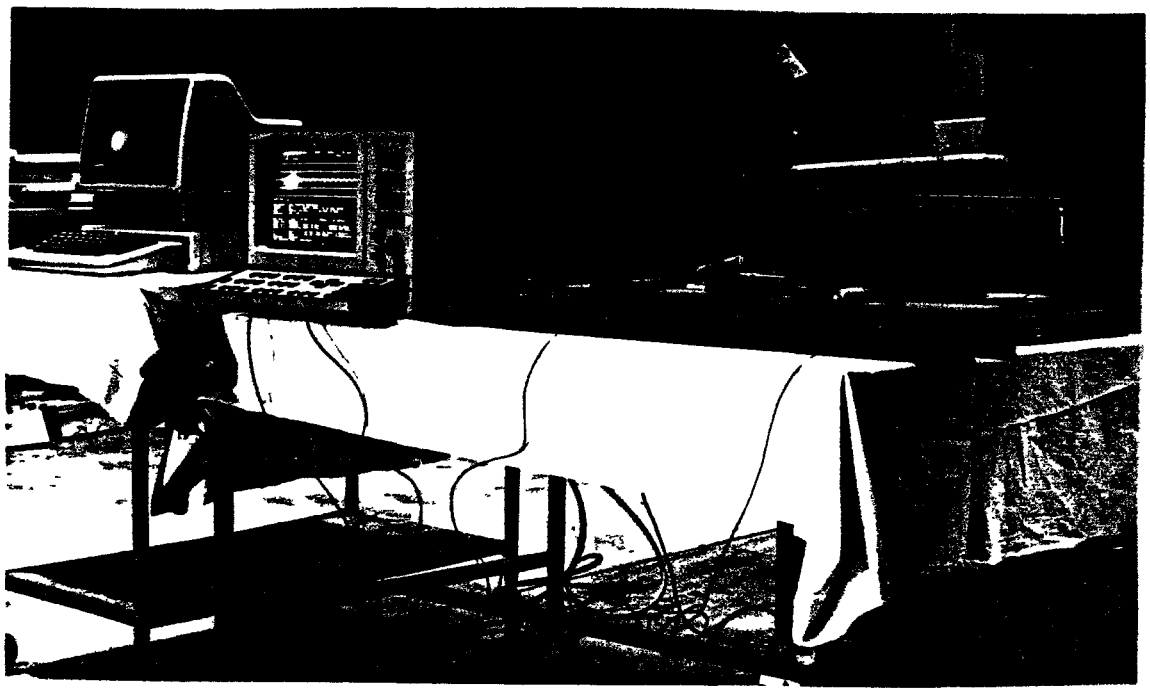

Fig. 6.8-5 The Equipment Assembly for Hammer Impact Testing

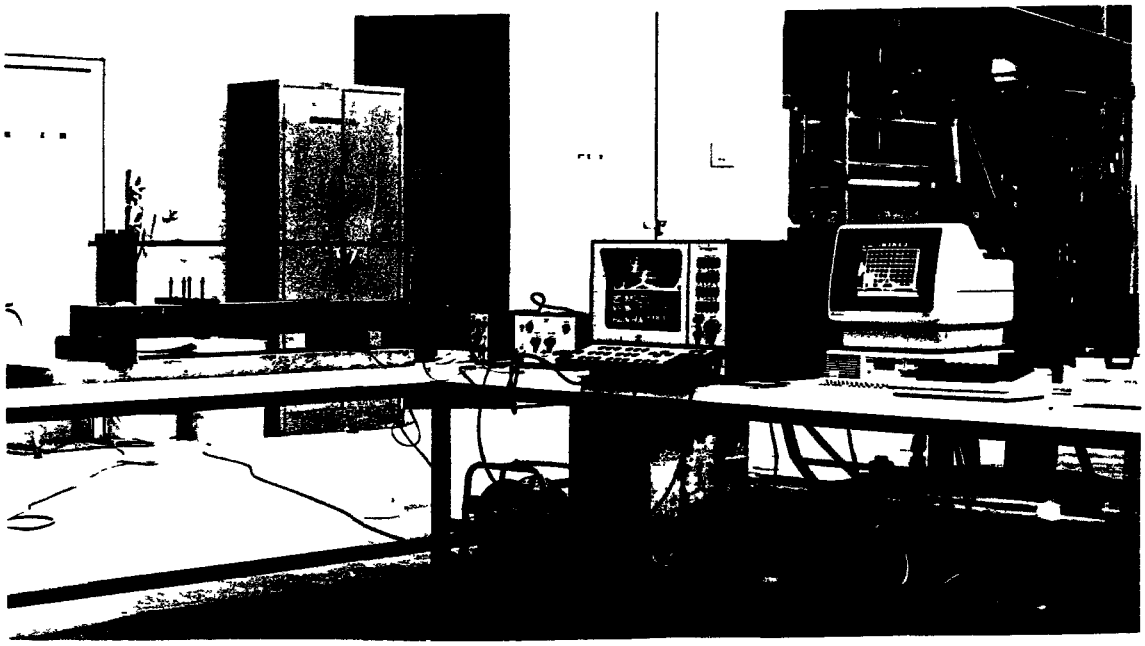

Fig. 6.8-6 The Testing Rig for Shaker Excitation Testing

In case of hammer impact testing, the impact impulse signal is entered into channel A of analyzer 2034 through line drive amplifier as time domain excitation. The response is picked up by accelerometer and also transferred into channel B of analyzer 2034. Both impulse and response signals are filtered by a filter in the analyzer and then transferred to computer to be recorded. The computer used for these tests was a HP 2000 series PC.

In case of shaker excitation testing, a pseudo-random signal is generated by the analyzer 2034, amplified by the power amplifier 2706 and then input to the shaker. The excitation signal from shaker is then applied to the structure. There is a force transducer attached to the structure to pick up the excitation. Signals picked up by the force transducer are entered into the charge amplifier to be amplified and filtered, and then input to the channel A of analyzer 2034. The response signals are picked up by the accelerometer, amplified by line drive amplifier, and then input to channel B of the analyzer. Both excitation and response signals are filtered in the analyzer by a filter and then fed into a computer to be recorded.

There are two structural models to be used in the laboratory for modal testing: a cantilevered beam, as shown in Fig. 6.8-7, and a 15 storey high rise building model, as shown in Fig. 6.8-8.

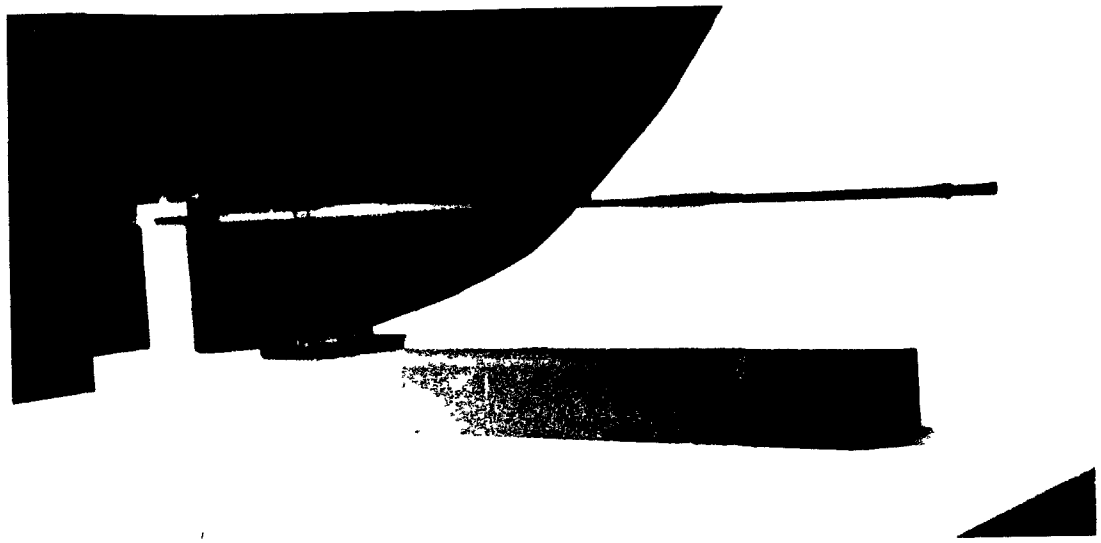

Fig. 6.8-7 A Cantilevered Beam Model

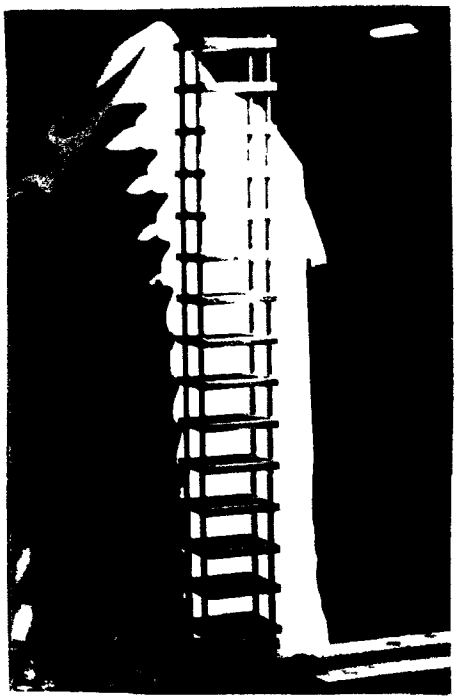

Fig. 6.8-8 A 15 Storey High Rise Building Model

The cantilevered beam has widely spaced natural frequencies and very low level of damping. The beam is made of steel. The results from both the theoretical solution and finite element analysis are available for the comparison with the experimental results. The high rise building model has dimensions such that it has closely spaced natural frequencies.

§ 6.8.4 Test Results for the Cantilevered Beam

Three types of testing were conducted on the cantilevered beam: impact excitation, shaker forced excitation, and free decay vibration. For impact testing, a total of 50 experimental data sets were recorded, for shaker forced excitation testing a total of 70 experimental data sets were recorded and for the free decay response testing, a total of 65 experimental data sets were recorded. All this test data is processed by using the proposed methods in chapters 4 and 5. For comparison, all this data is also processed by the circle fit method. The dimensions of the cantilevered beam are shown in Fig. 6.8-9.

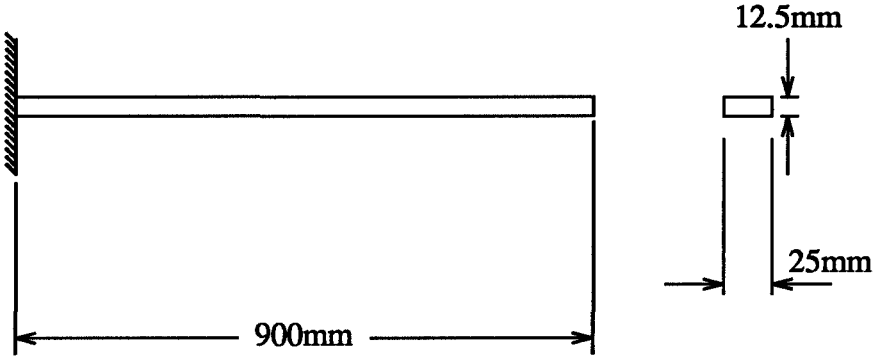

Fig. 6.8-9 Dimension of the cantilever beam

In the shaker forced excitation testing, the excitation applied to the cantilever was the pseudo random signals generated by an exciter which was located at 10 mm from the free end of the cantilever.

Seven measurement stations for the responses were arranged along the cantilever equally spaced as shown in Fig. 6.8-10. To limit the range of frequencies of interest, the accelerometer outputs were filtered to eliminate frequency components higher than 800Hz. The sampling rate was 1600Hz. The recording time was 1.5sec and 2400 samples were recorded.

The free decay responses were generated after sudden termination of excitation of the cantilever. To minimize the bias in the data, the excitation was set to a constant value for a reasonable long time before it was terminated. The measurement arrangement was the same as in the forced excitation testing.

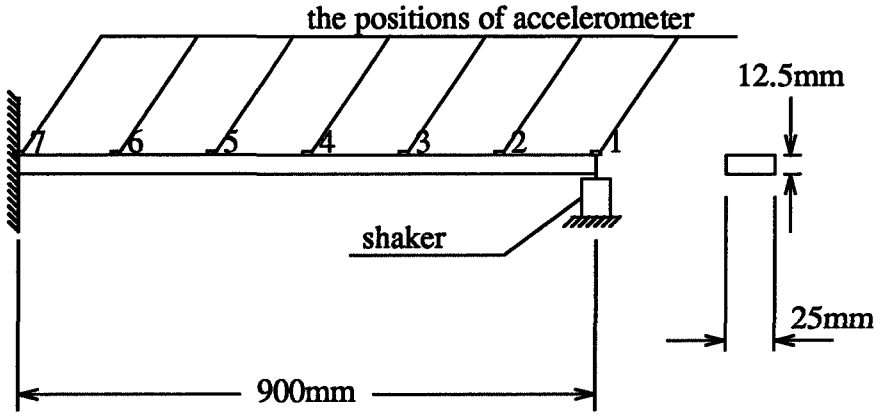

Fig. 6.8-10 Single Shaker Test for the Cantilevered Beam

The first four mode shapes identified by the direct method and circle fit method are compared with the finite element results in Figs. 6.8-11 to 6.8-14.

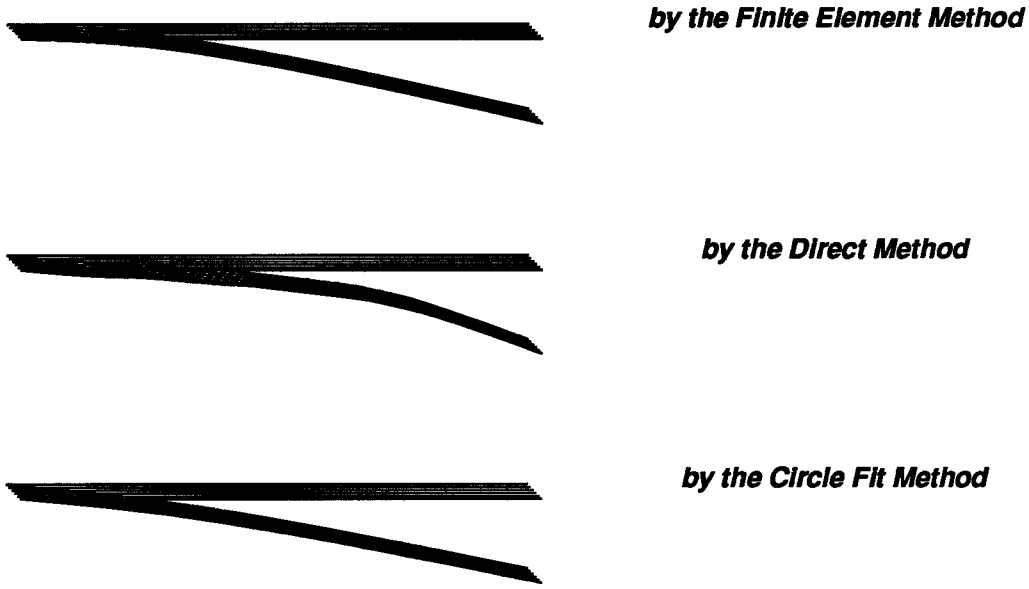

Fig. 6.8-11 Comparison of the First Mode

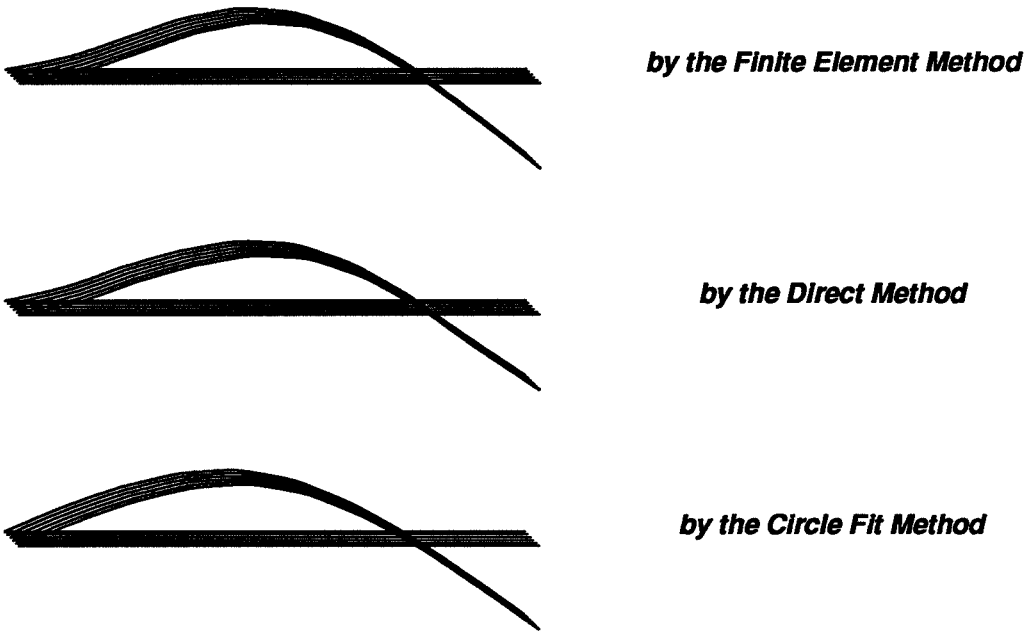

Fig. 6.8-12 Comparison of the Second Mode

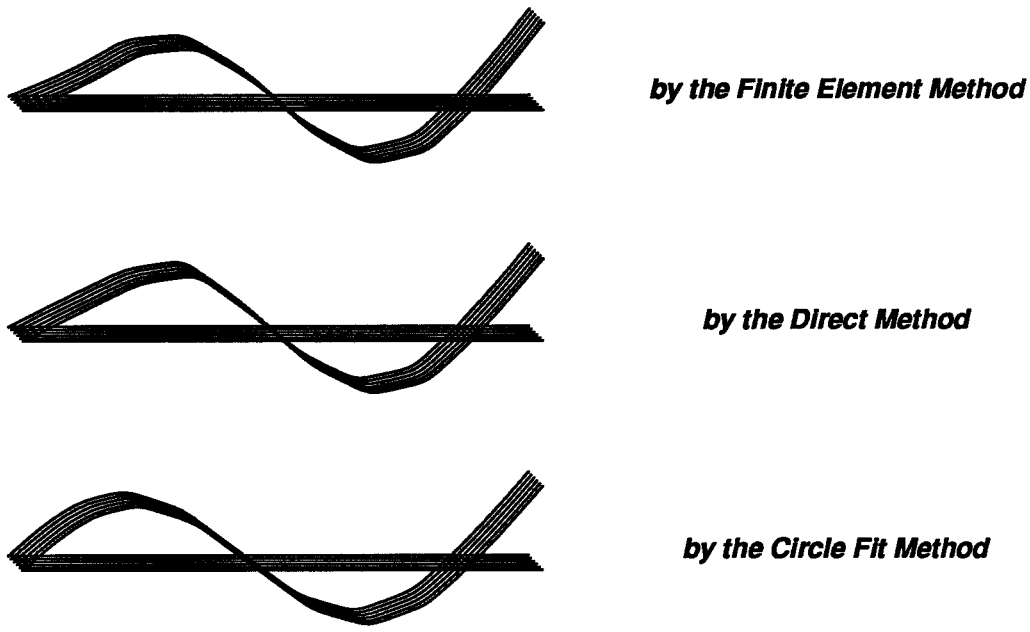

Fig. 6.8-13 Comparison of the Third Mode

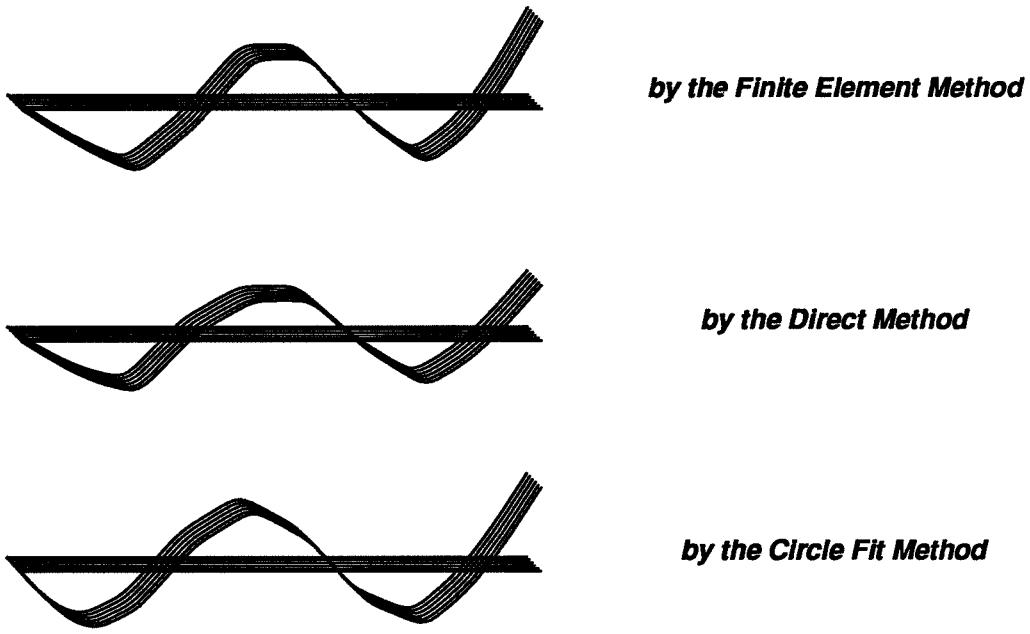

Fig. 6.8-14 Comparison of the Fourth Mode

It can be seen from these figures that the direct method is able to identify the mode

shapes as accurately as the circle fit method. The identified results by both methods are very close to the results by finite element method. The frequency response functions regenerated from the identified modal parameters by both the direct method and the circle fit method are presented in Figs. 6.8-15 to 6.8-18. In the figures, the dotted lines indicate the regenerated frequency response functions from the identified modal parameters by the circle fit method while the solid line indicate the regenerated frequency response functions from the modal parameters by the direct method. Fig. 6.8-15 shows the magnitudes of the frequency response function, while Fig. 6.8-18 gives the phases of the frequency response function. The real part of the response function is indicated in Fig. 6.8-16, and the imaginary part of the response function is shown in Fig. 6.8-17. These figures indicate that the frequency response functions generated from the identified modal parameters by both methods are very close to each other.

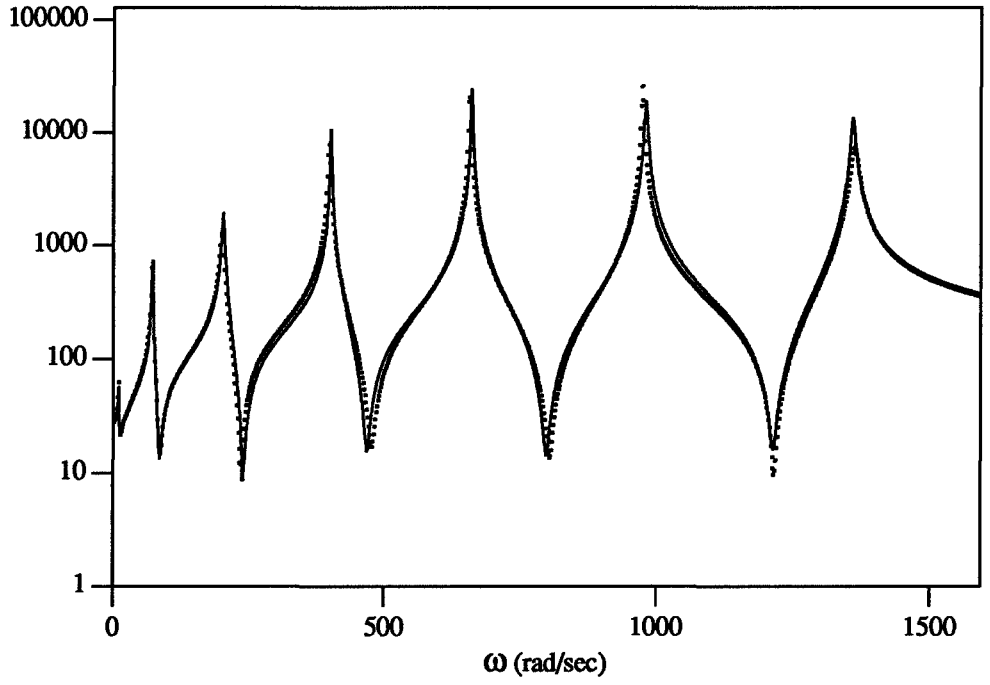

Fig. 6.8-15 Frequency Response Function in Magnitude

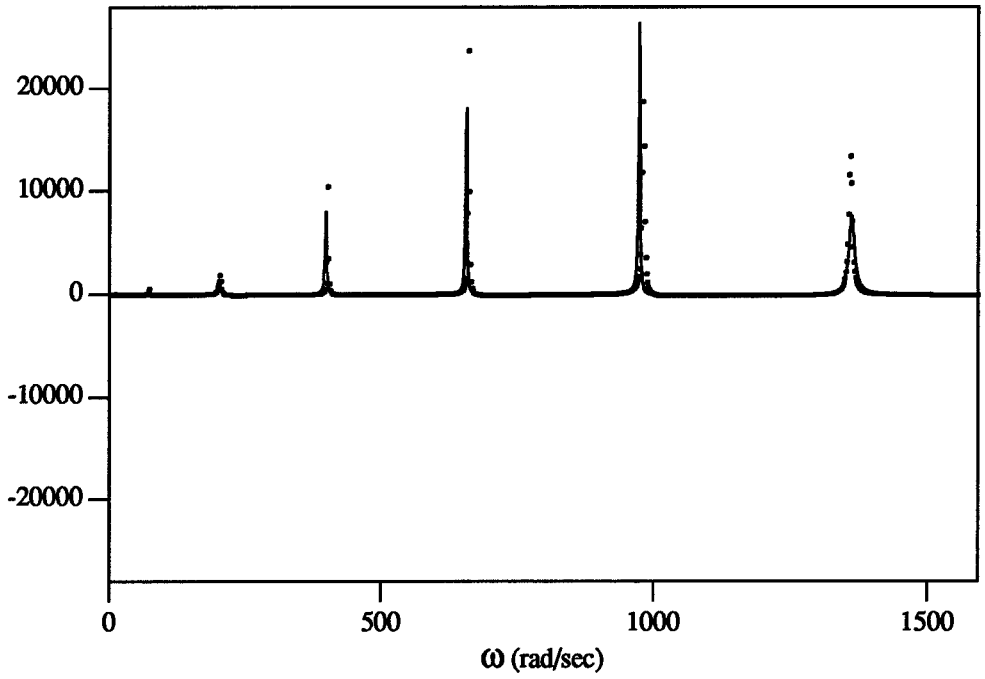

Fig. 6.8-16 Frequency Response Function (Real)

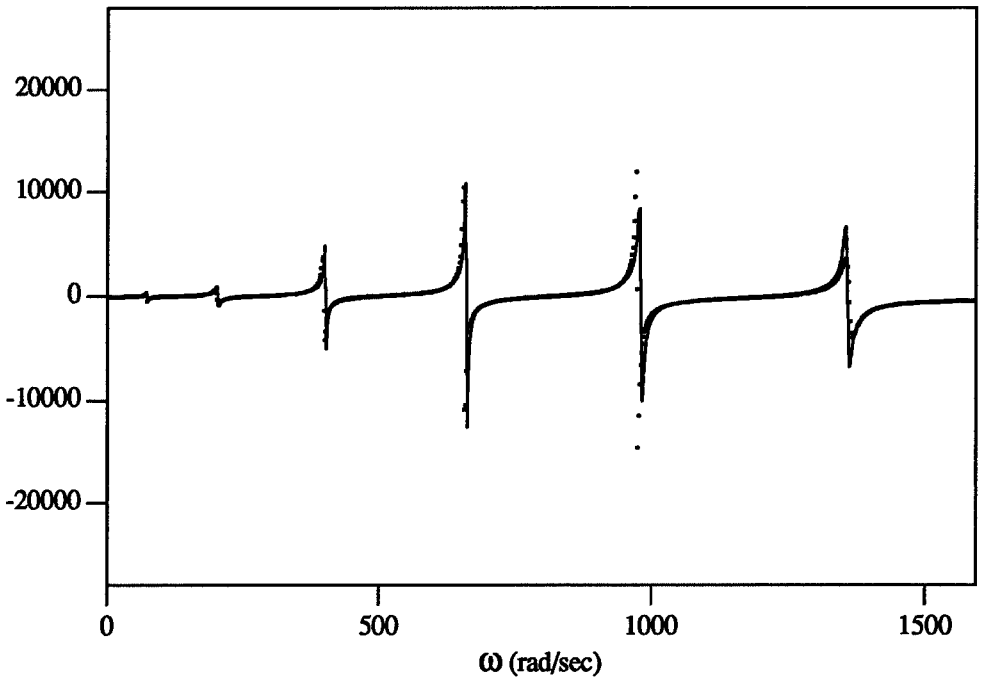

Fig. 6.8-17 Frequency Response Function (Imaginary)

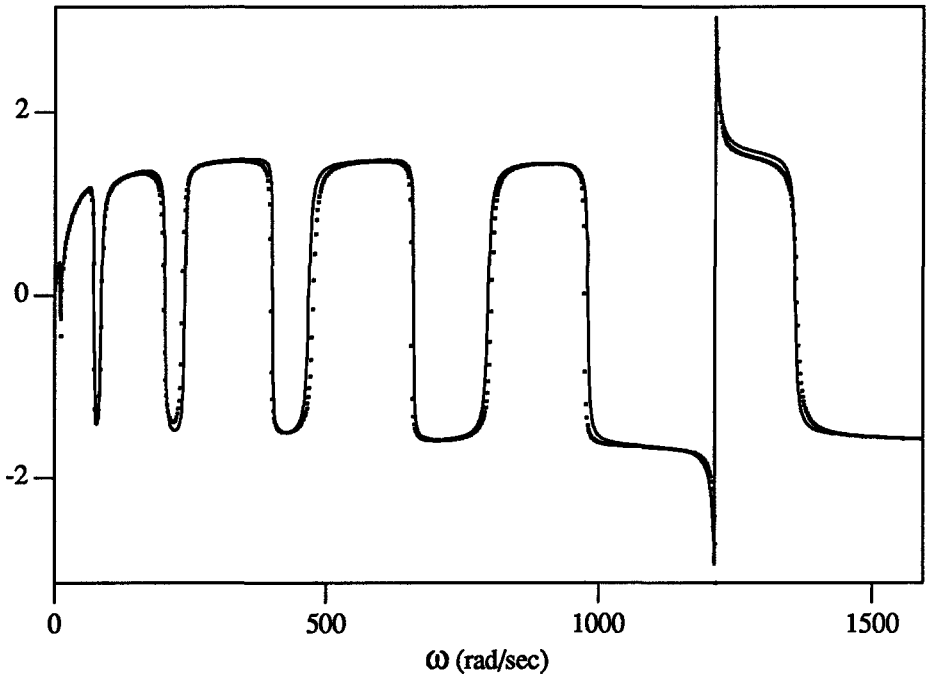

Fig. 6.8-18 Frequency Response Function (Phase)

The arrangement of the excitation stations for the impact testing are shown in Fig. 6.8-19. An accelerometer is located 10 mm from the tip of the cantilever.

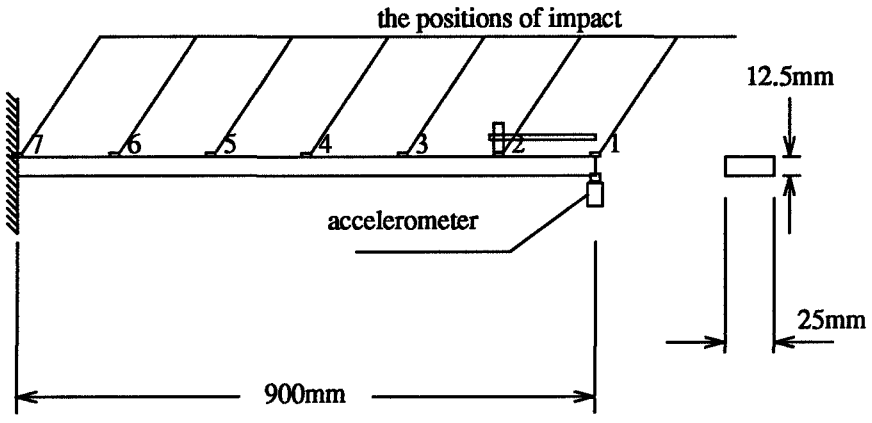

Fig. 6.8-19 Impact Testing for the Cantilevered Beam

A sample of the results of the identification test is given in Tables 6.8-1 and 6.8-2. Table 6.8-1 shows only the mode shapes identified by the first proposed method in

chapter 4. Table 6.8-2 shows the identified frequencies and damping ratios by all the proposed methods in chapters 4 and 5. It is observed that all the proposed methods can identify frequencies and dampings with reasonable accuracies. For comparison, the test results by a frequency method-circle fit are listed in Tables 6.8-1 and 6.8-2, too. The pseudo-random signal was used for the forced testing of the beam. The free response signal depends on the level of excitation of the cantilever before the excitation is removed, as well as on the position of the measurement station. The greater the free response signal, the better the results. However, excessive excitation may cause structural non-linearities.

Table 6.8-1 Identified Modes for the Cantilever

	Complex mode		Normal Mode
	Direct method	Circle fit method	FEM method
Mode 1	1.000	1.000	1.000
	0.732+i0.008	0.709+i0.005	0.862
	0.584+i0.221	0.539+i0.187	0.725
	0.462-i0.063	0.410-i0.028	0.590
Mode 2	1.000	1.000	1.000
	0.482+i0.010	0.450+i0.007	0.515
	0.091+i0.021	0.082+i0.017	0.055
	-0.564+i0.010	-0.539+i0.006	-0.336
Mode 3	1.000	1.000	1.000
	0.094+i0.002	-0.089+i0.015	0.001
	-0.676-i0.023	-0.637-i0.015	-0.429
	-0.778+i0.009	-0.748+i0.007	-0.684
Mode 4	1.000	1.000	1.000
	-0.332-i0.021	-0.309-i0.018	-0.095
	-0.868-i0.031	-0.837-i0.026	-0.684
	-0.151-i0.002	-0.147-i0.001	-0.398
Mode 5	1.000	1.000	1.000
	-0.667-i0.032	-0.647-i0.027	-0.353
	-0.591+i0.005	-0.575+i0.004	-0.623
	0.763+i0.015	0.741+i0.011	0.271

Table 6.8-2 Identified Frequencies and Damping Ratios for the Cantilever

Mode	Experimental Results										Theoretical Results	
	Direct method		Indirect method		Impact excitation		Single Exciter		Circle fit method		Analytical	Finite element
	Frequency (Hz)	Damping ratio	Frequency (Hz)	Damping ratio	Frequency (Hz)	Damping ratio	Frequency (Hz)	Damping ratio	Frequency (Hz)	Damping ratio	Frequency (Hz)	Frequency (Hz)
1	11.03	0.068	11.24	0.071	11.83	0.073	11.13	0.071	11.27	0.069	12.55	12.44
2	71.63	0.016	72.03	0.021	72.12	0.022	71.93	0.019	71.51	0.017	79.22	77.85
3	200.25	0.015	200.42	0.017	200.81	0.018	199.24	0.014	200.32	0.008	220.06	218.10
4	395.75	0.004	396.21	0.006	396.43	0.008	395.85	0.004	398.07	0.004	431.31	427.95
5	652.25	0.002	653.31	0.003	653.52	0.003	652.36	0.002	657.25	0.003	712.99	709.67

Note:

Direct method is referred as to the first method in chapter 4.

Indirect method is referred as to the second method in chapter 4.

Impact excitation is referred as to the method developed in § 5.4-2, a.

Single exciter is referred as to the method developed in § 5.4-2, b.

From the testing, it was found that increasing the number of degrees of freedom in the mathematical model, by adding extra modes, improves the results for the identified modes. It appears that the results for extra modes may include a large the effect of the random noise in the data and that the "real" modes appear to come from the data with a smaller noise to signal ratio. It is also found that the proposed methods are not sensitive to the nodal points.

The results obtained by placing the accelerometers very close to one of the nodal points of an excited mode were analyzed. The natural frequency of that mode can be identified but a higher percentage of error was evident. This is because it is difficult to place the accelerometer exactly at the nodal point, and that mode still has small contribution to the response data.

§ 6.8.5 Experimental Results for a 15 Storey Building Model

The 15 storey building tested model was made of steel with dimensions shown in Fig. 6.8-20. The model is fixed on the ground. Impact and shaker forced excitation testing were performed on this model with pseudo-random signal being used as the excitation in the shaker excitation testing. The testing was conducted along the planes as shown in Fig. 6.8-20(a) and 20(b). Both bending and torsional modes were identified. Since the frequencies of these modes are closely spaced, the response data was filtered so that only the desired modes would be included in the response signals. Optimal sampling 120 *Hz* was used according to the range of frequencies.

For impact testing, 50 data sets were taken, while for the shaker forced testing, 70 data sets were recorded for different conditions of excitation and response measurements. The 15 storey building model is a symmetric structure which has

almost repeated shear vibration frequencies and very close torsional vibration frequency. This fact makes the identification of the frequencies of the model very difficult. In order to identify these repeated and very closely spaced frequencies, the model is modified to be asymmetric using some studs. The tests were conducted in two orthogonal shear vibration directions and the excitation is not applied along the symmetric axes. The test data was analyzed by the direct and indirect methods in chapter 4 and by the methods developed in chapter 5. The results for the identified natural frequencies of the first five modes are listed in Table 6.8-3, and indicate the proposed methods can identify very closely spaced frequencies.

Table 6.8-3 Identified Natural Frequencies of the 15 Storey Building Model

	Identified Frequencies (Hz)			
	Direct method	Indirect method	Impact test	Shaker test
Mode 1	16.27	16.39	16.47	16.32
Mode 2	17.35	17.46	17.62	17.51
Mode 3	17.40	17.59	17.78	17.64
Mode 4	49.38	49.64	49.77	49.59
Mode 5	52.12	52.25	52.37	52.22

♣ The impact test means the method developed in chapter 5 using impact test data,

♦ The shaker test means the method developed in chapter 5 using shaker test data.

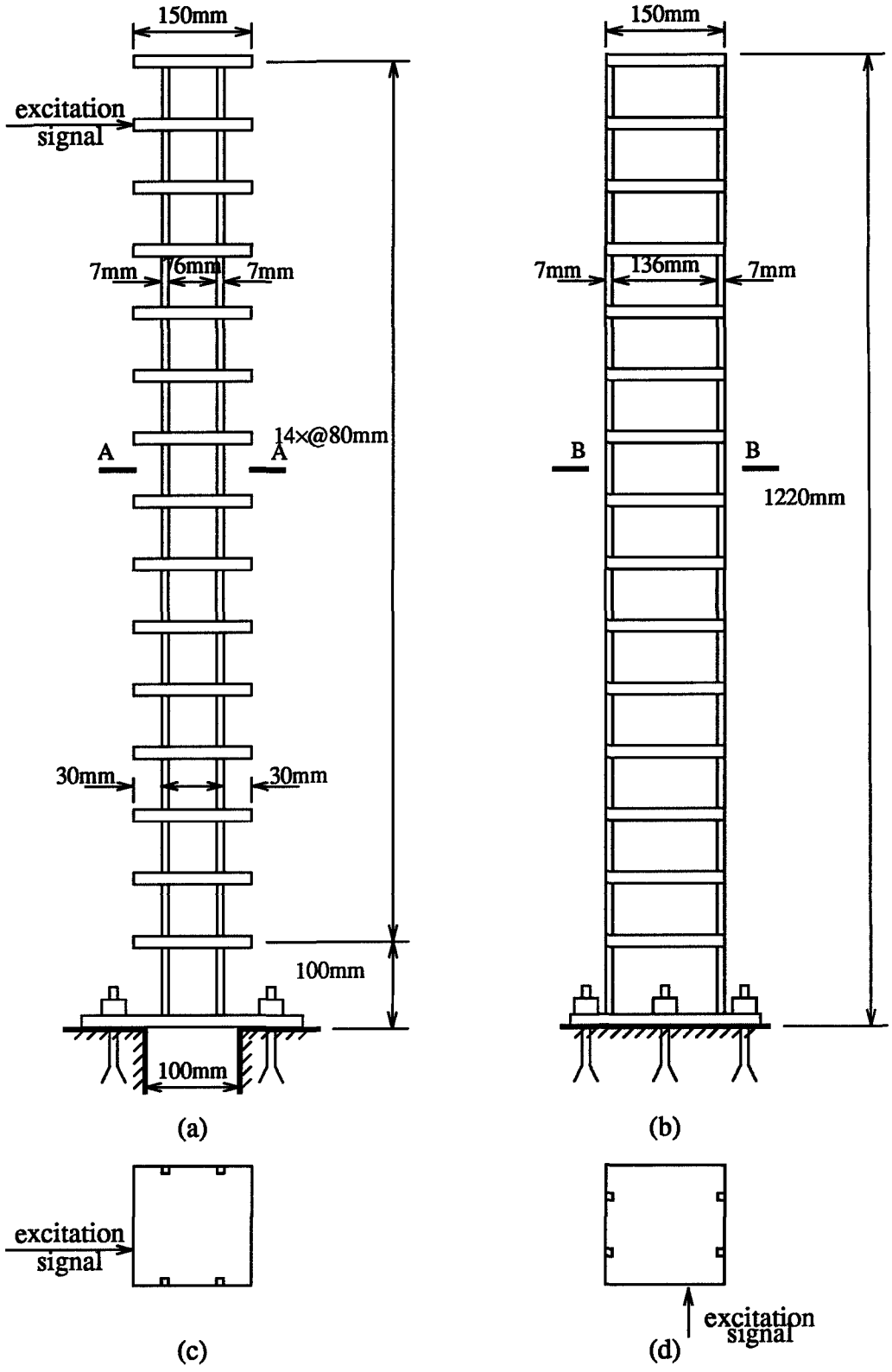

Fig. 6.8-20 Dimensions of the 15 Storeys Building Model

§ 6.9 SOME ASPECTS OF MODAL TESTING

This section is intended to address a few of the common errors in the modal identification test.

§ 6.9.1 Mode Shape Aliasing

The error of mode shape aliasing is fairly common among some users of modal analysis. The term aliasing generally refers to a sampled data phenomena where the number of samples is insufficient to accurately describe the data, and the "higher frequency" data has not been removed prior to sampling. As the name implies, there are too few measurement points on the structure being tested to define an accurate shape. Fig. 6.9-1 illustrates the phenomenon on a test of a simply supported beam.

Assume that there are five measurement stations equally spaced along the beam as shown in Fig. 6.9-1(a). In Fig. 6.9-1(b), there are sufficient measurement stations to correctly obtain the mode shape of the first mode of the beam. In Fig. 6.9-1(c), the solid line indicates the correct third mode while the dashed line indicates the wrong third mode because of insufficient measurement stations. In some cases, for a higher mode, however, an insufficient number of measurements causes the mode shape to appear to be a lower mode and is consequently in error. If only two measurement stations are equally spaced along the beam, the third mode would not be identified since these station points are the nodes of the third mode.

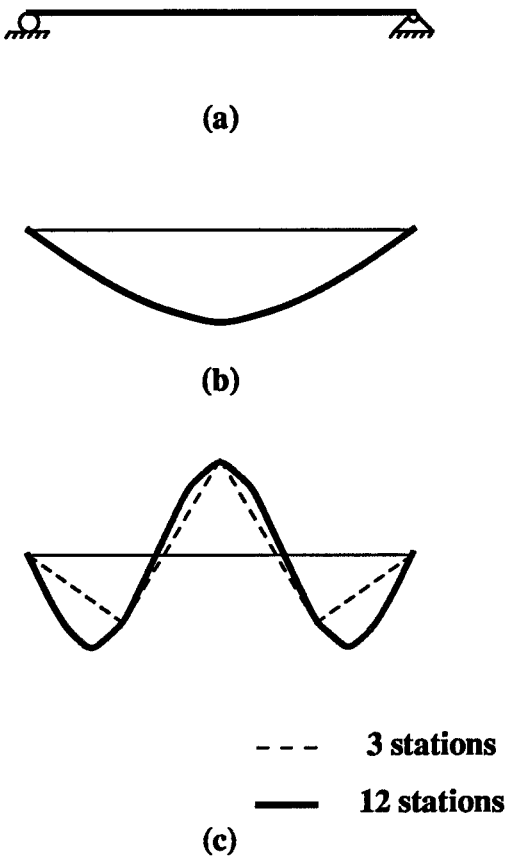

Fig. 6.9-1 Mode Aliasing Phenomenon

§ 6.9.2 Mode Shapes on Symmetric Structures

If the tested structure is symmetric, it often appears as though the mode shapes measured depend on the position of the transducer. It is known, however, that mode shapes of linear structures are independent of response or excitation measurement locations. The presence of the accelerometer however can create an asymmetrical condition in an otherwise symmetric structure, and a node point is usually found to pass close to or through the reference location. In cases where the response measurement station is moved around the structure and the excitation point is fixed, the node point is essentially pulled around the structure with the transducer, and some misleading shapes can be generated, depending on the number of measurements made around the structure.

The above phenomena are because of the fact that there are close spaced or repeated frequencies of the structure. This means simply that there are two resonances at exactly the same frequency having the same shapes, but the two shapes have their axes orthogonal to each other and they can occur often in symmetric structures such as the 15 storey building model.

One method of dealing with this situation experimentally is to make a minor modification to the structure, intentionally causing it to be slightly asymmetric so that the two resonances will split apart. They will have similar mode shapes and can be easily identified by the proposed methods in this thesis even though the two frequencies are numerically very close.

§ 6.9.3 The Force Correction due to Mass of Measuring Instrument

The force measured by the force transducer is not the "exact" force applied to the structure due to the mass of the measuring instrument such as hammer or exciter and the tip mass of the force transducer. Minor mass correction is required to determine the actual excitation. Fig. 6.9-2 shows the correction required.

Suppose the mass of the tip of the force transducer is m, the mass of the shaker or hammer is M and the force measured by the force transducer is F_m, the actual force applied to the structure can be computed by

$$F_s = (m + M)\ddot{x}$$

$$F_m = M\ddot{x}$$

$$F_s = F_m \frac{m + M}{M}$$

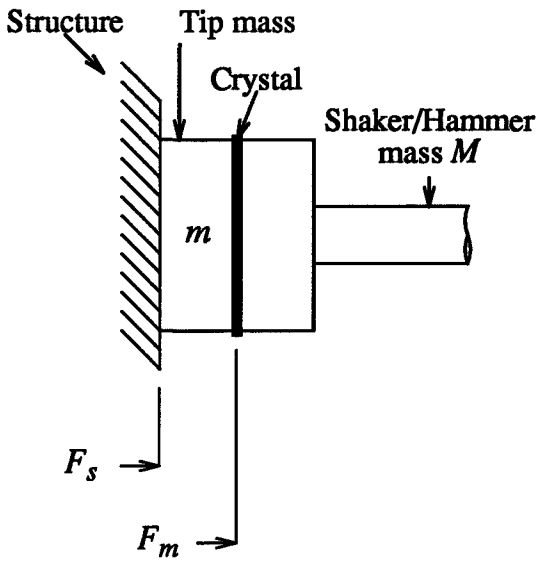

Fig. 6.9-2 Correction of the Applied Force

§ 6.9.4 Calibration

During the test, the calibration provides the overall sensitivity of the complete instrumentation system without examining the performance of individual elements. This overall sensitivity can be obtained by a calibration process since an independent measurement of the ratio of response and force can be made. By assuming the response is acceleration and excitation is force, the ratio of the acceleration and force will be $\frac{1}{mass}$, a quantity which can readily be measured by independent means. If measurement is performed on a simple rigid mass-like structure, the result will be a constant magnitude over the frequency range at a value equal to the reciprocal of the mass of the calibration block and this can be accurately determined by weighing.

A typical calibration block which can be used is shown in Fig. 7.9-3 and the result from a calibration measurement, indicating the overall system calibration factor, which is then used to convert the measured values of (volts/volt) to those of (acceleration/force).

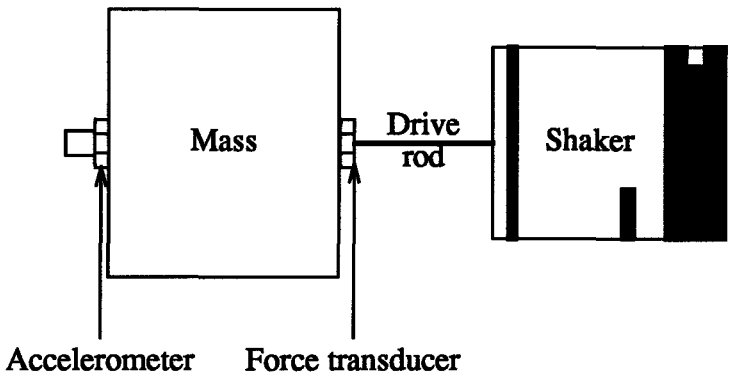

Fig. 6.9-3 Mass Calibration Procedure

§ 6.10 SUMMARY

This chapter discusses the modal testing techniques and applications of the proposed methods to the modal testing. As well it discusses the importance of using correct application techniques to obtain meaningful test data.

To use the proposed methods one requires excitation and response data, or response data only in case of free vibration testing. Digitizing the measured data, with an appropriate sampling rate, provides the data set for analysis. Computer analysis of the digital data produces the final results in the form of natural frequencies, damping ratios and mode shapes for all modes contributing to the measured data.

A complex structure can be identified in steps by the proposed technique according to different range of frequencies of interest. In each step a certain selected band of frequencies is covered. The same procedure can be used for identifying high frequencies or in situation where data storage capacity is limited. The choice of sampling rates can be optimized, depending on the particular experiment.

The experimental work has established that the proposed methods in this thesis are

not sensitive to measurement noise. They are therefore promising methods for dynamic structural testing and identification. These methods also preserve the advantage of time domain methods by being capable of identifying closely spaced frequencies.

Chapter 7

IDENTIFICATION OF STRUCTURAL PARAMETERS

It isn't that they can't see the solution. It is that they can't see the problem.

G. K. Chesterton

§ 7.1 INTRODUCTION

As discussed in Chapter 1, structural system identification is the process of determining parameters in the equations of motion of a structure from test data. For identification of structural parameters there are usually two classes of techniques: modal techniques and non-modal techniques. Modal techniques use modal test data, i.e. frequencies, damping ratios and mode shapes of a vibrating structure to

determine its structural parameters.

The modal parameters can be classified as measurable quantities, since they are properties of the structure and not dependent on the analytical formulation. The modal parameters, however, as previously discussed, are not directly measurable but are identified from response and/or excitation measurements. Using modal test data to improve the analytical model of a vibrating structure and hence obtain an improved description of a structure is discussed in this chapter. Methods have been developed to deal with some form of this identification task, however, the majority of these methods deal only with structural systems with no damping or with proportional damping. In reality, however, a lot of vibrating structures have nonproportional damping. Another deficiency of these methods is that they require the measured modes to satisfy the theoretical requirement of orthogonality with respect to the mass and stiffness matrices. Such a requirement can only be satisfied when the structure has no daming or possesses proportional damping. It is true that for simple structures with only small amounts of damping, the measured modes (complex modes) are very close to the normal modes. For more complex structures, however, complex modes can be very much different from the normal modes. Attempts to use these complex modes as normal modes for satisfying the orthogonality requirement may lead to adverse effects on the process of identification. In particular for structures with non-proportional damping, it is extremely difficult to measure normal modes. Measured modes are complex. The procedure of using these measured modes directly, for the analysis and identification as normal modes, can result in large errors in the off-diagonal terms of the system matrices.

In this chapter, a method is presented to overcome these problems. The method is a

direct identification method which can be used to obtain mass, damping and stiffness matrices from the measured eigenvalues and eigenvectors. This method is based on the minimum of parameter changes, in which the Euclidian norm of all parameter changes should be minimized, and uses the measured test values of complex eigenvalues and eigenvectors directly, rather than using the complex eigenvectors as normal modes. The advantage of the method is to improve mass, stiffness and damping matrices simultaneously as well as being capable of assessing the quality of test modal data. The method can, therefore, be applied to identification of a vibrating structure with general damping.

As discussed in chapter 2, if complete set of modal vectors, damped natural frequencies and damping ratios of a vibrating structure can be obtained from modal test, then

$$\mathbf{\Psi}^T\mathbf{M}^*\mathbf{\Psi} = \mathbf{I} \tag{7.1-1}$$

$$\mathbf{\Psi}^T\mathbf{K}^*\mathbf{\Psi} = \mathbf{\Lambda} \tag{7.1-2}$$

and the structural parameters of the structure can be determined by

$$\mathbf{M}^* = (\mathbf{\Psi}^T)^{-1}\mathbf{\Psi}^{-1} \tag{7.1-3}$$

$$\mathbf{K}^* = (\mathbf{\Psi}^T)^{-1}\mathbf{\Lambda}\mathbf{\Psi}^{-1} \tag{7.1-4}$$

Unfortunately, test modal data is in general incomplete. The number of modes obtained from any test is usually less than the number of model degrees of freedom of the structure. In order to use the incomplete modal data to identify the structural

parameters, the theory of generalized inverse of a rectangular matrix can be applied in identification of the structural parameters using this incomplete modal test data.

Given good test data and a reasonable but not necessarily precise, analytical model, the method will yield an improved model which is compatible with the test. The basic requirements for the method are a set of measured complex eigenvectors and eigenvalues from modal test.

This chapter is organized as follows. A brief review of the main methods for structural identification is given in § 7.2. In § 7.3, the theoretical background is briefly introduced so that the proposed method is developed on the basic theory of structural dynamics. The proposed method is developed in § 7.4 by minimization of an Euclidian norm. § 7.5 is devoted to the application of pseudo-inverse of the matrix in the structural identification. Usually not all coordinates of the analytical model are measured in a vibration test and the full mode, including the unmeasured coordinates, needs to be computed, and this is considered in § 7.6. In order to illustrate the proposed method, two simulated examples are given in § 7.7. The discussions in § 7.7 concentrate on the comparison of the proposed method with AMI method. The last section, § 7.8, will conclude the chapter with some remarks. Appendix A gives the definition of the pseudo inverse of a matrix, while in Appendices B and C, the algorithms for computing full modes and pseudo-inverse of a matrix are presented.

§ 7.2 STRUCTURAL IDENTIFICATION METHODS

There are numerous methods for the structural identification. The common starting point for structural identification is the modal survey. Having a set of test modes,

some methods can be used with the mode data to identify the structural parameters. Collins, Hart, Hasselman and Kennedy (1974) developed statistical structural identification method using a linear Taylor's series expansion of the modal parameters about the prior estimate of the structural parameters. Essentially, this method is the Bayesian technique and requires a prior estimate of the structural parameters. The modes from modal testing are frequently corrected to enforce orthogonality to an analytical mass matrix using a technique such as Gram-Schmidt orthogonalization, or the Targoff method (1976). In this method, the analytical mass matrix is assumed correct and the corrected modes are taken as linear combinations of test modes. Baruch (1978), Berman (1979) and Wei (1980) developed a method called by Berman as Automated Model Improvement method which can also be used to generate an improved analytical mass and stiffness matrices by minimizing changes in a weighted least squares sense. The improved mass and stiffness matrices exactly reproduces the measured mode shapes and frequencies. This procedure has been applied in many cases with considerable success. A disadvantage of the method is that it produces off-tridiagonal elements in both mass and stiffness matrices representing the physically unconnected degrees of freedom. Since the method reproduces exact test modes regardless of good or corrupted modal data, it would not improve the analytical model in the case of heavily corrupted modal data.

A method was developed by Kabe (1985) to improve the stiffness matrix without changing its topology. The method uses the test modes orthogonalized to the analytic mass matrix. The disadvantage of the method is that it requires very large computational efforts and hence is not applied in practice.

All these methods tackle the structural identification of the structures without consideration of nonproportional damping.

Caravani, Watson and Thomson (1977) presented a time domain recursive least squares method to identify the general damping. Yun and Shinozuka (1980) used a nonlinear Kalman filtering approach to the problem. Beliveau (1976) developed a Bayesian method to identify the viscous damping using a modified Newton-Raphson scheme and perturbation of eigenvalues and eigenvectors. Hanagud, Meyyappa, Cheng and Craig (1984) were tackling the identification of structural system with nonproportional damping assuming some or all of the elements of the mass matrix are known. All the unknown parameters including mass, stiffness and damping are determined by minimizing the Euclidean norm of a matrix that assures the satisfaction of the equations of the eigenvalue problem and the appropriate orthogonality conditions. The method developed in this chapter while inspired by AMI method avoids the disadvantage of reproducing test modes even using heavily corrupted modal data. Further, identification of structures with non-proportional damping is mainly considered by this method.

§ 7.3 THEORETICAL BACKGROUND

As discussed in chapter 2, a dynamic structural system of n degrees of freedom can be described by the state equation in the $2n$ space as follows.

$$\mathbf{M}^*\dot{\mathbf{x}}(t) + \mathbf{K}^*\mathbf{x}(t) = \mathbf{r}(t)\,. \tag{7.3-1}$$

For the convenience of derivation of the algorithm for identification of structural parameters, matrices $\mathbf{M}^*$ and $\mathbf{K}^*$ are rearranged as

$$\mathbf{M}^* = \begin{bmatrix} \mathbf{0} & \mathbf{M} \\ \mathbf{M} & \mathbf{C} \end{bmatrix} \tag{7.3-2}$$

$$\mathbf{K}^* = \begin{bmatrix} -\mathbf{M} & \mathbf{0} \\ \mathbf{0} & \mathbf{K} \end{bmatrix} \tag{7.3-3}$$

$$\mathbf{r}(t) = \begin{Bmatrix} \mathbf{p}(t) \\ \mathbf{0} \end{Bmatrix}. \tag{7.3-4}$$

The associated eigenvalue problem becomes

$$\mathbf{K}^* \boldsymbol{\psi} = -\lambda \mathbf{M}^* \boldsymbol{\psi}. \tag{7.3-5}$$

where $\boldsymbol{\psi}$ is eigenvector; λ the eigenvalue.

If the eigenvectors are normalized, the following relationships are held.

$$\boldsymbol{\Psi}^T \mathbf{M}^* \boldsymbol{\Psi} = \mathbf{I} \tag{7.3-6}$$

and

$$\boldsymbol{\Psi}^T \mathbf{K}^* \boldsymbol{\Psi} = \boldsymbol{\Lambda} \tag{7.3-7}$$

in which

$$\boldsymbol{\Lambda} = diag\,(\lambda_1, \lambda_2, \cdots, \lambda_m)$$

It is assumed that only m modes are known and $\boldsymbol{\Psi}$ is an $n \times m$ matrix. $\boldsymbol{\Lambda}$ is then an $m \times m$ diagonal matrix with the eigenvalues λ_i being its diagonal.

Eqns. (7.3-5), (7.3-6) and (7.3-7) are three basic theoretical relationships which apply to linear, general damped structures represented as finite element models. The proposed method in this chapter is based on these three equations.

§ 7.4 DEVELOPMENT OF THE PROPOSED METHOD

Minimizing the changes of structural parameters can be obtained mathematically by minimization of the Euclidian norm

$$\varepsilon = \| \mathbf{W}(\mathbf{M}^* - \mathbf{M}_A^*)\mathbf{W} \| + \| \mathbf{W}(\mathbf{K}^* - \mathbf{K}_A^*)\mathbf{W} \| \tag{7.4-1}$$

$\mathbf{W}$ is a weighting matrix, $\mathbf{M}^*$ and $\mathbf{K}^*$ are the unknown improved matrices and $\mathbf{M}_A^*$ and $\mathbf{K}_A^*$ are the given analytical matrices. Minimizing the norm (7.4-1) minimizes the relative changes in the elements of the matrices.

Defining Lagrangian multipliers, χ_{ij} and ξ_{ij}, for each element in Eqn. (7.3-13) and Eqn. (7.3-14), respectively, and introducing

$$\alpha_{ij} = \chi_{ij}(\mathbf{\Psi}^T(\mathbf{M}^* - \mathbf{M}_A^*)\mathbf{\Psi} - \mathbf{I} + A_a)_{ij} \tag{7.4-2}$$

and

$$\beta_{ij} = \xi_{ij}(\mathbf{\Psi}^T(\mathbf{K}^* - \mathbf{K}_A^*)\mathbf{\Psi} - \mathbf{\Lambda} + B_a)_{ij} \tag{7.4-3}$$

the following Lagrangian function may be written,

$$\theta = \varepsilon + \sum_{i=1}^{m}\sum_{j=1}^{m}(\alpha_{ij} + \beta_{ij}) \tag{7.4-4}$$

where $A_a = \mathbf{\Psi}^T\mathbf{M}_A^*\mathbf{\Psi}$, $\quad B_a = \mathbf{\Psi}^T\mathbf{K}_A^*\mathbf{\Psi}$,

$$\mathbf{\Psi}^T(\mathbf{M}^* - \mathbf{M}_A^*)\mathbf{\Psi} - \mathbf{I} + A_a = \mathbf{0} \tag{7.4-5}$$

and

$$\boldsymbol{\Psi}^T(\mathbf{K}^* - \mathbf{K}_A^*)\boldsymbol{\Psi} - \boldsymbol{\Lambda} + B_a = \mathbf{0} \tag{7.4-6}$$

which are, in fact, the constraints (7.3-13) and (7.3-14). Differentiating equation (7.4-4) with respect to each element of matrices $\mathbf{M}^*$ and $\mathbf{K}^*$ and equating these results to $\mathbf{0}$ will satisfy the minimization of equation (7.4-1), provided the constraints (7.3-13) and (7.3-14) are also satisfied. This process results in the matrix equations

$$2\mathbf{W}^2(\mathbf{M}^* - \mathbf{M}_A^*)\mathbf{W}^2 + \boldsymbol{\Psi}\mathbf{X}\boldsymbol{\Psi}^T = \mathbf{0} \tag{7.4-7}$$

and

$$2\mathbf{W}^2(\mathbf{K}^* - \mathbf{K}_A^*)\mathbf{W}^2 + \boldsymbol{\Psi}\boldsymbol{\Xi}\boldsymbol{\Psi}^T = \mathbf{0} \tag{7.4-8}$$

or

$$\mathbf{M}^* - \mathbf{M}_A^* = -\frac{1}{2}(\mathbf{W}^2)^{-1}\boldsymbol{\Psi}\mathbf{X}\boldsymbol{\Psi}^T(\mathbf{W}^2)^{-1} \tag{7.4-9}$$

and

$$\mathbf{K}^* - \mathbf{K}_A^* = -\frac{1}{2}(\mathbf{W}^2)^{-1}\boldsymbol{\Psi}\boldsymbol{\Xi}\boldsymbol{\Psi}^T(\mathbf{W}^2)^{-1} \tag{7.4-10}$$

where $\mathbf{X}$ and $\boldsymbol{\Xi}$ are square matrices of χ_{ij} and ξ_{ij}, respectively.

Substituting Eqns. (7.4-9) and (7.4-10) into Eqns. (7.3-11) and (7.3-12) yields the solutions for $\mathbf{X}$ and $\boldsymbol{\Xi}$

$$\mathbf{X} = -2\mathbf{R}^{-1}(\mathbf{I} - A_a)\mathbf{R}^{-1} \tag{7.4-11}$$

and

$$\Xi = -2\mathbf{R}^{-1}(\mathbf{\Lambda} - B_a)\mathbf{R}^{-1} \tag{7.4-12}$$

These expressions are then substituted into Eqns. (7.4-9) and (7.4-10) to obtain

$$\mathbf{M}^* = \mathbf{M}_A^* + (\mathbf{W}^2)^{-1}\mathbf{\Psi}\mathbf{R}^{-1}(\mathbf{I} - A_a)\mathbf{R}^{-1}\mathbf{\Psi}^T(\mathbf{W}^2)^{-1} \tag{7.4-13}$$

and

$$\mathbf{K}^* = \mathbf{K}_A^* + (\mathbf{W}^2)^{-1}\mathbf{\Psi}\mathbf{R}^{-1}(\mathbf{\Lambda} - B_a)\mathbf{R}^{-1}\mathbf{\Psi}^T(\mathbf{W}^2)^{-1} \tag{7.4-14}$$

where

$$\mathbf{R}^{-1} = \mathbf{\Psi}^T(\mathbf{W}^2)^{-1}\mathbf{\Psi} \ , \tag{7.4-15}$$

$$A_a = \mathbf{\Psi}^T\mathbf{M}_A^*\mathbf{\Psi} \tag{7.4-16}$$

$$B_a = \mathbf{\Psi}^T\mathbf{K}_A^*\mathbf{\Psi} \ . \tag{7.4-17}$$

If the weighting matrix $\mathbf{W}$ is taken such as

$$\mathbf{W}^2 = (\mathbf{M}_A^*)^{-1} \tag{7.4-18}$$

for Eqn. (7.4-13), and

$$\mathbf{W}^2 = (\mathbf{K}_A^*)^{-1} \tag{7.4-19}$$

for Eqn. (7.4-14). Eqns. (7.4-13) and (7.4-14) can then be written as

$$\mathbf{M}^* = \mathbf{M}_A^* + \mathbf{M}_A^*\mathbf{\Psi}A_a^{-1}(\mathbf{I} - A_a)A_a^{-1}\mathbf{\Psi}^T\mathbf{M}_A^* \tag{7.4-20}$$

and

$$\mathbf{K}^* = \mathbf{K}_A^* + \mathbf{K}_A^* \Psi B_a^{-1} (\Lambda - B_a) B_a^{-1} \Psi^T \mathbf{K}_A^* \tag{7.4-21}$$

Eqns (7.4-20) and (7.4-21) are easily evaluated expressions for the corrected mass matrix, damping matrix and stiffness matrix making them consistent with the measured modes.

§ 7.5 APPLICATION OF PSEUDO-INVERSE OF A MATRIX IN STRUCTURAL IDENTIFICATION

The application of the pseudo-inverse of a matrix in structural system identification is discussed in this section. As previously mentioned, a structural model can be identified by using modal parameters obtained in a modal test. The procedure for identification of structural parameters could be developed for two different cases: complete or truncated experimental data. Since the truncated solution can be used for a complete system description, only the truncated solution is studied in this section.

When test data from a structure are experimentally measured, it is impossible to obtain a full modal description, i.e., a complete system is one where the number of defined modes equals the number of structural degrees of freedom. The structure has an almost-infinite number of degrees of freedom, possible coordinates, and modes of vibration. It is, therefore, necessary to make a simplified model using a greatly reduced number of measurement points and, usually, an even smaller number of modes. Often, only a few modes can be identified in the frequency range of interest. When the number of measurement points exceeds the number of measured modes, this is called a truncated modal description. The modal matrix is non-square, so the ordinary matrix inverse cannot be applied. To deal with this, it is necessary to use a special inverse of a rectangular matrix called pseudo-inverse. The properties and

method to generate this inverse are given in Appendix 7.A. The pseudo-inverse is a generalized inverse that can deal with non-square or square but singular matrix. The structural mass, stiffness, and damping can then be found using truncated modal data by use of pseudo-inverse. If the number of measurement stations is less than the number of modes, the full "test" modes can be calculated, as will be discussed in § 7.6. When the number of degrees of freedom considered exceeds the number of modes, the modal matrix also is non-square.

Assuming that $\mathbf{M}^*$ and $\mathbf{K}^*$ are the unknown improved matrices and $\mathbf{M}_A^*$ and $\mathbf{K}_A^*$ are the given analytical matrices. It may be written that

$$\mathbf{\Psi}^T(\mathbf{M}^* - \mathbf{M}_A^*)\mathbf{\Psi} = \mathbf{I} - A_a \tag{7.5-1}$$

where

$$\mathbf{I} = \mathbf{\Psi}^T\mathbf{M}^*\mathbf{\Psi} \tag{7.5-2}$$

and

$$A_a = \mathbf{\Psi}^T\mathbf{M}_A^*\mathbf{\Psi} \tag{7.5-3}$$

When the pseudo-inverse of the incomplete eigenvector matrix is used, the following equation is obtained

$$\mathbf{M}^* - \mathbf{M}_A^* = (\mathbf{\Psi}^T)^+(\mathbf{I} - A_a)\mathbf{\Psi}^+ \tag{7.5-4}$$

where $\mathbf{\Psi}^+$ is the pseudo inverse of matrix $\mathbf{\Psi}$.

The pseudo inverse of matrix $\boldsymbol{\Psi}$ is

$$\boldsymbol{\Psi}^{+} = (\boldsymbol{\Psi}^T \mathbf{V} \boldsymbol{\Psi})^{-1} \boldsymbol{\Psi}^T \boldsymbol{V}$$

where **V** is an arbitrary matrix such that

$$Rank\ (\boldsymbol{\Psi}^T \mathbf{V} \boldsymbol{\Psi}) = Rank\ (\boldsymbol{\Psi})$$

Hence, Eqn. (7.5-4) becomes

$$\mathbf{M}^* = \mathbf{M}_A^* + \mathbf{V}\boldsymbol{\Psi}(\boldsymbol{\Psi}^T \mathbf{V} \boldsymbol{\Psi})^{-1} (\mathbf{I} - A_a)(\boldsymbol{\Psi}^T \mathbf{V} \boldsymbol{\Psi})^{-1} \boldsymbol{\Psi}^T \mathbf{V} \tag{7.5-5}$$

where **V** is a nonsingular weighting matrix.

The matrix $\mathbf{K}^*$ may also be written as

$$\mathbf{K}^* = \mathbf{K}_A^* + \mathbf{V}\boldsymbol{\Psi}(\boldsymbol{\Psi}^T \mathbf{V} \boldsymbol{\Psi})^{-1} (\boldsymbol{\Lambda} - B_a)(\boldsymbol{\Psi}^T \mathbf{V} \boldsymbol{\Psi})^{-1} \boldsymbol{\Psi}^T \mathbf{V} \tag{7.5-6}$$

where

$$B_a = \boldsymbol{\Psi}^T \mathbf{K}_A^* \boldsymbol{\Psi} \tag{7.5-7}$$

When the analytical matrix $\mathbf{M}_A^*$ is taken as the arbitrary matrix **V**, Eqns. (7.5-5) and (7.5-6) become

$$\mathbf{M}^* = \mathbf{M}_A^* + \mathbf{M}_A^* \boldsymbol{\Psi} A_a^{-1} (\mathbf{I} - A_a) A_a^{-1} \boldsymbol{\Psi}^T \mathbf{M}_A^* \tag{7.5-8}$$

and

$$\mathbf{K}^* = \mathbf{K}_A^* + \mathbf{K}_A^* \Psi B_a^{-1} (\Lambda - B_a) B_a^{-1} \Psi^T \mathbf{K}_A^* \tag{7.5-9}$$

Eqns. (7.5-8) and (7.5-9) coincide with the formulas of the proposed method in § 7.4 and hence the same computer algorithm implementation can be used.

§ 7.6 FULL MODE COMPUTATION

The above discussions are based on the assumption that the modes over the full coordinate system are known. The degrees of freedom measured in a test however, may be limited. A method has to be used to transform the limited number of measured mode shapes to the mode shapes over the full coordinate system. There are methods available for this purpose. One method is to reduce the model to the test coordinates, to correct the reduced model, then to perform an "inverse Guyan reduction" (1965). Another approach is to use a geometric interpolation method to estimate the modal displacements at the unmeasured coordinates. The method used here appears as an interpolation method based on the dynamics of the structure, rather than the geometry. Since the analytical model is not limited to the degrees of freedom measured in a test and may be used to derive the coordinates of modes, the relationship between the measured subset and unmeasured subset of a mode shape can be written as

$$\left[\begin{bmatrix} \mathbf{K}_{A1}^* & \mathbf{K}_{A2}^* \\ \mathbf{K}_{A2}^{*T} & \mathbf{K}_{A4}^* \end{bmatrix} + \lambda_i \begin{bmatrix} \mathbf{M}_{A1}^* & \mathbf{M}_{A2}^* \\ \mathbf{M}_{A2}^{*T} & \mathbf{M}_{A4}^* \end{bmatrix} \right] \begin{Bmatrix} \Psi_{1i} \\ \Psi_{2i} \end{Bmatrix} = \mathbf{0} \tag{7.6-1}$$

where the Ψ_{1i} represents the measured elements and Ψ_{2i} represents the unmeasured elements of the i-th mode shape, λ_i is the measured eigenvalue and the analytical

model $\mathbf{M}_A^*$ and $\mathbf{K}_A^*$ should reasonably represent the structure parameters.

The method was used by Berman (1979) for calculation of normal mode shapes and is extended to the complex field for calculation of complex modes in this chapter. From Eqn. (7.6-1)

$$\boldsymbol{\psi}_{2i} = -(\mathbf{K}_{A4}^* + \lambda_i \mathbf{M}_{A4}^*)^{-1}((\mathbf{K}_{A2}^*)^T + \lambda_i (\mathbf{M}_{A2}^*)^T)\boldsymbol{\psi}_{1i} \tag{7.6-2}$$

Eqn. (7.6-1) can be solved at three levels of approximation. If λ_i is considered to be so small that it may be ignored, Eqn. (7.6-2) in effect becomes the Guyan's reduction (1965). If it is small, but can not be ignored, the series approximation of Kidder (1973) could be used. If neither of these options appears reasonable an exact solution is performed by solving the simultaneous equations rather than by inverting the matrix.

At the start of the process for improving the analytical model only approximate mass, damping and stiffness matrices are known. If these matrices are good approximations, $\boldsymbol{\psi}_{2i}$ can be expected to be reasonably accurate. In any case, the analysis that follows results in corrected mass, damping and stiffness matrices which will predict the measured value λ and $\boldsymbol{\psi}$.

When the corrected matrices are obtained, an iteration through the above procedure is an option to improve the results and converge rapidly for "small" changes.

§ 7.7 NUMERICAL EXAMPLES

Two simulated experiments are used to illustrate the application of the present

method. The first simple example is a structure of ten degrees of freedom, whose mass, stiffness and damping parameters are listed in Tables 7.7-1, 7.7-2 and 7.7-3. Thses exact values are used for computing complex modes and data sets of the first seven complex modes are used as the modal data for identification of the structural parameters of the structure.

Table 7.7-1 Comparison of Mass Matrix Identification

		1	2	3	4	5	6	7	8	9	10
1	♣	.15+0	.00+0	.00+0	.00+0	.00+0	.00+0	.00+0	.00+0	.00+0	.00+0
	♦	.10+0	.00+0	.00+0	.00+0	.00+0	.00+0	.00+0	.00+0	.00+0	.00+0
	♥	.12+0	.26-1	.14-1	-.16-1	.62-2	.49-2	-.34-2	.97-2	.95-4	-.59-2
2	♣		.35+0	.00+0	.00+0	.00+0	.00+0	.00+0	.00+0	.00+0	.00+0
	♦		.25+0	.00+0	.00+0	.00+0	.00+0	.00+0	.00+0	.00+0	.00+0
	♥		.30+0	.30-1	-.16-1	.11-1	.75-2	-.93-2	.36-3	.44-2	.57-2
3	♣			.45+0	.00+0	.00+0	.00+0	.00+0	.00+0	.00+0	.00+0
	♦			.35+0	.00+0	.00+0	.00+0	.00+0	.00+0	.00+0	.00+0
	♥			.39+0	.51-1	.99-2	.16-1	.17-2	.42-3	.47-2	.24-2
4	♣				.13+1	.00+0	.00+0	.00+0	.00+0	.00+0	.00+0
	♦				.10+1	.00+0	.00+0	.00+0	.00+0	.00+0	.00+0
	♥				.13+1	.15-1	-.14-1	.14-1	-.13-1	.15-2	.16-2
5	♣					.60+0	.00+0	.00+0	.00+0	.00+0	.00+0
	♦					.50+0	.00+0	.00+0	.00+0	.00+0	.00+0
	♥					.57+0	.44-1	-.88-2	.39-2	-.17-1	.12-1
6	♣						.65+0	.00+0	.00+0	.00+0	.00+0
	♦						.50+0	.00+0	.00+0	.00+0	.00+0
	♥						.58+0	-.65-2	.26-1	-.57-2	.71-2
7	♣							.70+0	.00+0	.00+0	.00+0
	♦			symmetry				.80+0	.00+0	.00+0	.00+0
	♥							.78+0	-.53-1	.73-2	-.62-2
8	♣								.75+0	.00+0	.00+0
	♦								.10+1	.00+0	.00+0
	♥								.77+0	-.10-1	-.21-1
9	♣									.80+0	.00+0
	♦									.70+0	.00+0
	♥									.77+0	-.41-1
10	♣										.90+0
	♦										.75+0
	♥										.84+0

♣ exact value

♦ analytical value

♥ improved value

For the convenience of comparison, the identified mass, damping and stiffness

matrices are also shown in Tables 7.7-1, 7.7-2 and 7.7-3, respectively. The analytical model was assumed. The differences between structural parameters of the analytical model and those of the "exact" model range from between 17% to 30%. The largest difference introduced is with the mass at the 4-th degree of freedom, where a 30% variation is made.

Table 7.7-2 Comparison of Damping Matrix Identification

		1	2	3	4	5	6	7	8	9	10
1	♣	.42+2	-.42+2	.00+0	.00+0	.00+0	.00+0	.00+0	.00+0	.00+0	.00+0
	♦	.32+2	-.32+2	.00+0	.00+0	.00+0	.00+0	.00+0	.00+0	.00+0	.00+0
	♥	.34+2	-.31+2	-.35+0	-.26+1	.89+0	.10+1	-.12+1	.11+1	.16+1	-.21+1
2	♣		.84+2	-.42+2	.00+0	.00+0	.00+0	.00+0	.00+0	.00+0	.00+0
	♦		.64+2	-.32+2	.00+0	.00+0	.00+0	.00+0	.00+0	.00+0	.00+0
	♥		.65+2	-.31+2	.26+1	.78+0	-.17+0	-.15+1	.57-1	.12+1	.23+1
3	♣			.84+2	-.42+2	.00+0	.00+0	.00+0	.00+0	.00+0	.00+0
	♦			.64+2	-.32+2	.00+0	.00+0	.00+0	.00+0	.00+0	.00+0
	♥			.66+2	-.31+2	-.44+1	-.11+1	.49+1	-.22+1	-.67+0	.66+0
4	♣				.84+2	-.42+2	.00+0	.00+0	.00+0	.00+0	.00+0
	♦				.64+2	-.32+2	.00+0	.00+0	.00+0	.00+0	.00+0
	♥				.75+2	.36+2	-.34+1	.16+1	-.92+0	.13+1	-.18+1
5	♣					.84+2	-.42+2	.00+0	.00+0	.00+0	.00+0
	♦					.64+2	-.32+2	.00+0	.00+0	.00+0	.00+0
	♥					.74+2	.30+2	-.92+1	.34+1	-.37+1	.31+1
6	♣						.84+2	-.42+2	.00+0	.00+0	.00+0
	♦						.64+2	-.32+2	.00+0	.00+0	.00+0
	♥						.67+2	-.31+2	-.30+1	.37+1	-.18+1
7	♣							.84+2	-.42+2	.00+0	.00+0
	♦			symmetry				.64+2	-.32+2	.00+0	.00+0
	♥							.76+2	-.41+2	.46+0	-.17+1
8	♣								.84+2	-.42+2	.00+0
	♦								.64+2	-.32+2	.00+0
	♥								.86+2	-.42+2	-.13+1
9	♣									.84+2	-.42+2
	♦									.64+2	-.32+2
	♥									.79+2	-.37+2
10	♣										.84+2
	♦										.64+2
	♥										.81+2

♣ exact value

♦ analytical value

♥ improved value

The first sub-row of each item represents the "exact" values, which are then used to

generate the test eigenvalues and eigenvectors. Some errors are introduced to modify the "exact" values to obtain the analytical values, and these are shown in the second sub-row of each item. The third sub-row of each item represents the improved values by the method presented in this chapter.

Table 7.7-3 Comparison of Stiffness Matrix Identification

		1	2	3	4	5	6	7	8	9	10
1	♣	.73+5	-.73+5	.00+0	.00+0	.00+0	.00+0	.00+0	.00+0	.00+0	.00+0
	♦	.64+5	-.64+5	.00+0	.00+0	.00+0	.00+0	.00+0	.00+0	.00+0	.00+0
	♥	.66+5	-.62+5	-.11+4	-.11+4	.18+4	.41+3	-.18+4	.17+4	.75+3	-.18+4
2	♣		.15+6	-.73+5	.00+0	.00+0	.00+0	.00+0	.00+0	.00+0	.00+0
	♦		.13+6	-.64+5	.00+0	.00+0	.00+0	.00+0	.00+0	.00+0	.00+0
	♥		.13+6	-.64+5	-.34+4	.22+4	-.32+4	-.26+4	.19+4	-.86+3	.11+4
3	♣			.15+6	-.73+5	.00+0	.00+0	.00+0	.00+0	.00+0	.00+0
	♦			.13+6	-.64+5	.00+0	.00+0	.00+0	.00+0	.00+0	.00+0
	♥			.14+6	-.62+5	-.81+4	-.49+3	.75+4	-.58+4	-.53+3	.20+4
4	♣				.15+6	-.73+5	.00+0	.00+0	.00+0	.00+0	.00+0
	♦				.13+6	-.64+5	.00+0	.00+0	.00+0	.00+0	.00+0
	♥				.14+6	-.68+5	-.29+4	.15+4	-.10+4	.17+4	-.13+4
5	♣					.15+6	-.73+5	.00+0	.00+0	.00+0	.00+0
	♦					.13+6	-.64+5	.00+0	.00+0	.00+0	.00+0
	♥					.14+6	-.62+5	-.10+5	.68+4	-.36+4	.19+4
6	♣						.15+6	-.73+5	.00+0	.00+0	.00+0
	♦						.13+6	-.64+5	.00+0	.00+0	.00+0
	♥						.14+6	-.61+5	-.46+4	.39+3	.70+3
7	♣							.15+6	-.73+5	.00+0	.00+0
	♦			symmetry				.13+6	-.64+5	.00+0	.00+0
	♥							.14+6	-.71+5	-.27+3	-.35+3
8	♣								.15+6	-.73+5	.00+0
	♦								.13+6	-.64+5	.00+0
	♥								.15+6	-.68+4	-.45+4
9	♣									.15+6	-.73+5
	♦									.13+6	-.64+5
	♥									.14+6	-.66+5
10	♣										.15+6
	♦										.13+6
	♥										.15+6

♣ exact value

♦ analytical value

♥ improved value

The comparisons indicate the method yield reasonable improvement of the analytical model. The identified results, however, give full matrices rather than the diagonal or

tridiagonal matrices as may be expected. The off-diagonal or off-tridiagonal elements are observed to be of an order of magnitude smaller than those of the diagonal or tridiagonal elements.

The improved structural matrices are then used to recalculate the eigenvalues and eigenvectors of the structure. The frequency and damping ratio comparisons are performed and showed in Table 7.7-4 and 7.7-5.

Table 7.7-4. Frequency Comparison

Mode	Test	Analysis	Improved
1	.8238+2	.5093+2	.8186+2
2	.1712+3	.1504+3	.1717+3
3	.2699+3	.2685+3	.2711+3
4	.3314+3	.3343+3	.3317+3
5	.4133+3	.3957+3	.4176+3
6	.5037+3	.4850+3	.4989+3
7	.5738+3	.5385+3	.5718+3
RSS ERROR		0.409	.000

Table 7.7-5. Damping Ratio Comparison

Mode	Test	Analysis	Improved
1	.9062-2	.1273-1	.9050-2
2	.4240-1	.3776-1	.4248-1
3	.7260-1	.6710-1	.7330-1
4	.9209-1	.8360-1	.9224-1
5	.1162+0	.9845-1	.1181+0
6	.1435+0	.1218+0	.1364+0
7	.1628+0	.1344+0	.1669+0
RSS ERROR		0.516	.003

The comparison of the complex mode shape for the first mode is also shown in Table 7.7-6. It can be seen that the method results in almost the same modal parameters as the "exact" values.

Table 7.7-6 First Mode Comparison

Degree of Freedom	Test	Analysis	Improved
1	.2916-1+.2901-1i	.4045-1+.4045-1i	.2824-1+.2815-1i
2	.2873-1+.2863-1i	.4029-1+.4029-1i	.2913-1+.2907-1i
3	.2847-1+.2842-1i	.3955-1+.3955-1i	.2906-1+.2907-1i
4	.2914-1+.2817-1i	.3816-1+.3815-1i	.2798-1+.2800-1i
5	.2548-1+.2549-1i	.3508-1+.3508-1i	.2585-1+.2586-1i
6	.2238-1+.2239-1i	.3118-1+.3118-1i	.2242-1+.2245-1i
7	.1878-1+.1880-1i	.2648-1+.2648-1i	.1859-1+.1855-1i
8	.1467-1+.1469-1i	.2083-1+.2083-1i	.1464-1+.1463-1i
9	.1010-1+.1012-1i	.1428-1+.1428-1i	.1026-1+.1028-1i
10	.5165-2+.5178-2i	.7255-2+.7255-1i	.4943-2+.4943-2i

Table 7.7-7 shows the Square Root of Sum Squares (RSS) error of the complex mode for the first seven modes.

Table 7.7-7. Complex Mode RSS Error Comparison

Mode	Analysis	Improved
1	.3936-1	.1856-2
2	.1989+0	.1321-2
3	.4460+0	.1389-2
4	.6681+0	.2127-2
5	.8175+0	.2798-2
6	.9044+0	.2719-1
7	.9512+0	.1732-1

The RSS error calculation formulas are

for the frequency

$$RSS\ ERROR = \left[\sum_{i=1}^{m} \left[\frac{\omega_{test}^{i} - \omega^{\frac{i\ analysis}{improved}}}{\omega_{test}^{i}} \right]^2 \right]^{\frac{1}{2}}$$

in which ω^i is the frequency of the i-th mode of the system,

for the damping

$$RSS\ ERROR = \left[\sum_{i=1}^{m} \left[\frac{\zeta_{test}^{i} - \zeta^{\frac{i\ analysis}{improved}}}{\zeta_{test}^{i}} \right]^2 \right]^{\frac{1}{2}}$$

in which ζ^i is the damping ratio of the i-th mode of the system, and for the complex mode

$$RSS\ ERROR\ of\ mode\ j = \left[\sum_{i=1}^{n} \left[\phi_{test}^{ij} - \phi^{\frac{ij\ analysis}{improved}} \right]^2 \right]^{\frac{1}{2}}$$

in which ϕ^{ij} represents the i-th element of the j-th complex mode of the system.

Based on this simple numerical test, it can be seen that the present method are capable of identifying structure parameters, i.e., mass, damping and stiffness matrices, which can reproduce values very close to the original test model data.

The second example is a pair of rigid girder and flexible girder frames to illustrate the proposed method can also be used with normal modes and frequencies. Here, assume that a design engineer has analyzed the frame under the rigid girder assumption and produced an analytical model. The assumption is made in order to

reduce the complex structure to a simple mathematical model. The engineer, however, performs a test on the actual structure and consequently the test data is affected by the flexibility of the girders. A hypothetical forced vibration test is assumed to be performed.

The rigid frame structure used by the design engineer as the analytical model is shown in Fig. 7.7-1.

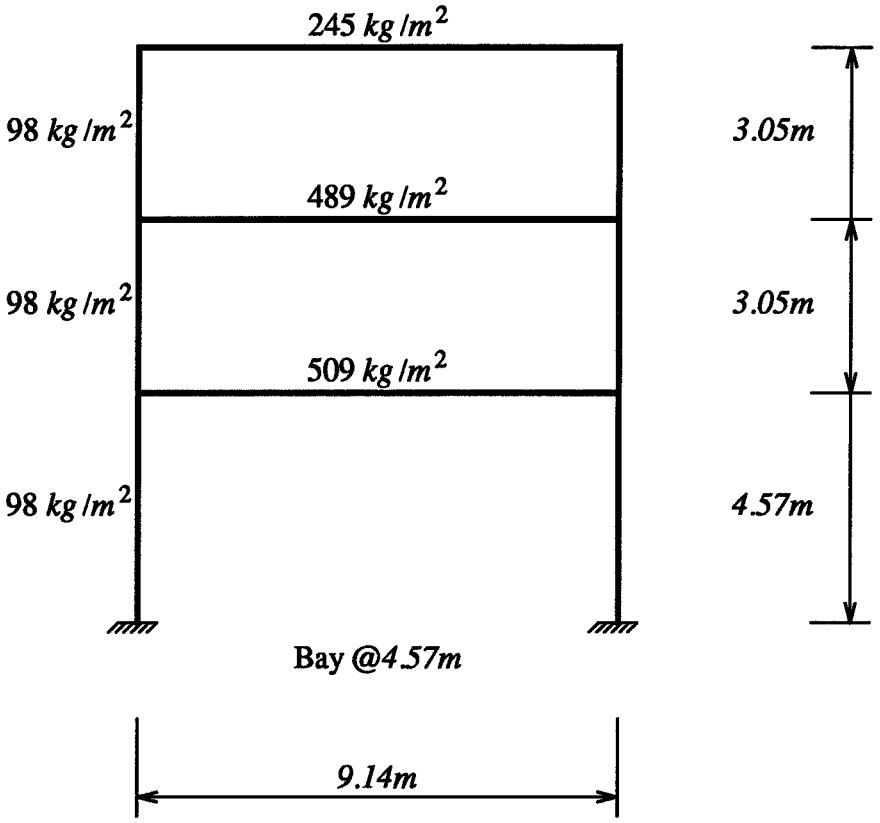

Fig. 7.7-1 Frame with Rigid Girders

The structural parameters of the analytical model with rigid girders are as follows.

$$\mathbf{M}(kg) = \begin{bmatrix} 22967 & 0 & 0 \\ 0 & 21791 & 0 \\ 0 & 0 & 11600 \end{bmatrix}$$

$$\mathbf{K}(10^6\ N/m) = \begin{bmatrix} 13.17 & -7.787 & 0 \\ -7.787 & 15.570 & -7.787 \\ 0 & -7.787 & 7.787 \end{bmatrix}$$

These parameters are now used with the "experimental modal data" to identify the real structural parameters. The analytical modal parameters are computed from the analytical structural parameters and shown in Table 7.7-8.

Table 7.7-8 Modal Parameters of Analytical Model of the Second Example

	Mode 1	Mode 2	Mode 3
Mode Shape	1.0000 1.4781 1.6565	1.0000 -0.0988 -1.0299	1.0000 -2.0841 2.2982
Circular Frequency (rad/sec)	8.5019	24.6356	35.7777
Frequency (Hz)	1.3531	3.9209	5.6942

The experimental modal data are obtained from the real structural parameters of the frame with flexible girders, shown as in Fig. 7.7-2.

The real structural parameters are as follows.

$$\mathbf{M}(kg) = \begin{bmatrix} 22967 & 0 & 0 \\ 0 & 21791 & 0 \\ 0 & 0 & 11600 \end{bmatrix}$$

$$\mathbf{K}(10^6\ N/m) = \begin{bmatrix} 12.73 & -7.752 & 0.386 \\ -7.752 & 14.35 & -7.015 \\ 0.386 & -7.015 & 6.629 \end{bmatrix}$$

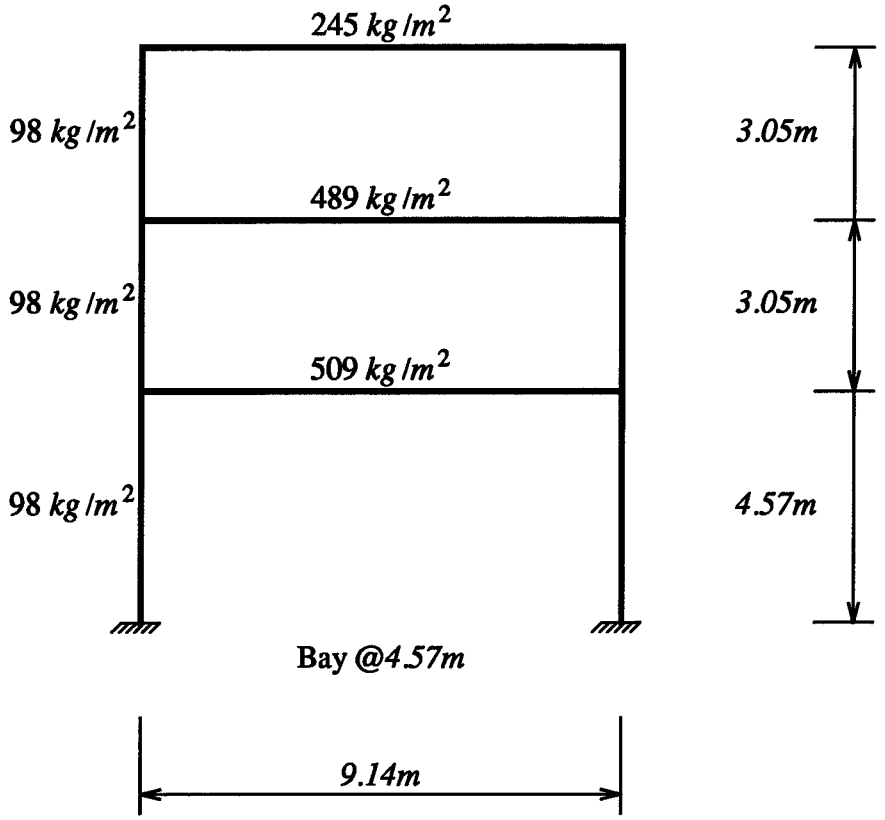

Fig. 7.7-2 Frame with Flexible Girders

The experimental modal data are computed from real structural parameters and shown in Table 7.7-9.

The task is to improve the analytical model, given this experimental modal data. On the basis of the above analytical and experimental data, an improved structural model is identified by the present method. The identified structural parameters are

$$\mathbf{M}(kg) = \begin{bmatrix} 22967 & 0 & 0 \\ 0 & 21791 & 0 \\ 0 & 0 & 11600 \end{bmatrix}$$

and

$$\mathbf{K}(10^6\ N/m) = \begin{bmatrix} 12.67 & -7.78 & 0.33 \\ -7.78 & 14.26 & -7.32 \\ 0.33 & -7.32 & 6.84 \end{bmatrix}$$

Table 7.7-9 Modal Parameters of Real Model of the Second Example

	Mode 1	Mode 2	Mode 3
Mode Shape	1.0000 1.5494 1.7706	1.0000 -0.0065 -1.1074	1.0000 -0.1780 1.8074
Circular Frequency (rad/sec)	7.7139	23.1918	34.4289
Frequency (Hz)	1.2436	3.6911	5.4795

The modal parameters reproduced by the improved model are listed in Table 7.7-10 to compare with analytical and real modal data. It is observed that the comparison of the experimental modal data and modal parameters of the improved model are quite close to each other.

The second example shows that the present method can also be used in improving the analytical model of structures without consideration of damping. It is observed that the improved structural parameters are good enough to describe the real structure and can reproduce reasonable modal data in the example.

Table 7.7-10 Comparison of Improved, Analytical and Real Modal Parameters

	Analytical Model			Real Model			Improved Model		
	1st Mode	2nd Mode	3rd Mode	1st Mode	2nd Mode	3rd Mode	1st Mode	2nd Mode	3rd Mode
ω(*radian/sec*)	8.5019	24.6356	35.7777	7.7139	23.1918	34.4289	7.4909	23.3684	34.5689
f(*Hz*)	1.3531	3.9209	5.6942	1.2436	3.6911	5.4795	1.1763	3.7192	5.5018
Mode	1.0000	1.0000	1.0000	1.0000	1.0000	1.0000	1.0000	1.0000	1.0000
Shape	1.4781	-0.0988	-2.0841	1.5494	-0.0065	-1.7797	1.5622	-0.0294	-1.8406
	1.6565	-1.0299	2.2982	1.7706	-1.1074	1.8074	1.7642	-1.0733	1.9395

§ 7.8 DISCUSSIONS

The proposed method is based on the minimization of the structural parameter changes. From this point of view, it is similar to the Automated Model Improvement (AMI) method developed by Berman et al. (1979). The present method, including identification of the damping parameters of a structure, is however developed in the state space rather than in the configuration space in which AMI method was developed. While the AMI method is aimed at identifying the structure without damping, the present method focuses on the identification of the structure with non-proportional damping.

Only the constraints of orthogonalities are used in the Lagrangian function to develop the algorithm of improvement. The constraint of the equation of the eigen problem is not imposed in the Lagrangian function. This makes the proposed method capable of determining if the measured modal data is contaminated.

The proposed method is based on the orthogonality of the complex eigenvectors, therefore, if the test eigenvectors is not orthogonal, the test modal data sets would not result in a proper structure parameter improvement. In order to illustrate this, the "test" modal data has been contaminated to obtain some amount of non-orthogonality. As expected, they do not yield the improved parameters to reproduce the original modal data base as shown in the Tables 7.8-1 and 7.8-2.

Table 7.8-1 Frequency Comparison by Non-Orthogonal Modal Data

Mode	Test	Improved
1	82.38	62.85
2	171.2	171.0
3	269.9	166.9
4	331.4	323.0
5	413.3	416.2
6	503.7	511.7
7	573.8	553.4
RSS ERROR		0.0057

The AMI method yields the improvement of mass and stiffness parameters which can reproduce the original measured modal data sets, even though the original test modal data is severely contaminated. The reason is that in the AMI method the constraint of the eigen problem was imposed in the Lagrangian function for derivation of the formula to improve the stiffness parameters. The improved mass matrix and test modal data sets were used in the constraint. The improved stiffness matrix together with the improved mass matrix must satisfy the constraint of the eigenvalue problem. Consequently, the improved stiffness and mass matrices will produce the test modal data sets exactly by AMI method. At first, this may appear

good, however, it may conceal the problem of having used bad measured modal data. If the measured modal data is contaminated severely, the "improved structural parameters" may actually not be improved but be contaminated.

Table 7.8-2 Comparison of the First Complex Mode by Non-Orthogonal Modal Data

Degree of Freedom	Test	Improved
1	.2333-1+.2328-1i	.3169-1+.3167-1i
2	.2298-1+.2291-1i	.3346-1+.3346-1i
3	.2847-1+.2842-1i	.2976-1+.2972-1i
4	.2814-1+.2817-1i	.3211-1+.3208-1i
5	.2548-1+.2549-1i	.2732-1+.2726-1i
6	.2238-1+.2239-1i	.2332-1+.2332-1i
7	.1692-1+.1692-1i	.2052-1+.2056-1i
8	.1320-1+.1322-1i	.1360-1+.1363-1i
9	.1010-1+.1012-1i	.9948-2+.9935-2i
10	.5165-2+.5148-2i	.5586-2+.5146-2i
RSS ERROR		1.635

Like the AMI method, the present method, when applied to good modal data base, produces a reasonable improvement of the structure parameters, which can in turn reproduce quite accurately the original modal base. In addition to this, the method can be used to assess the quality of the measured modal data by recalculating the structural modal data with the improved structural parameters and comparing the recalculated modal data with the original test modal data. If the original test modal data can not be reproduced by the improved structural parameters, then original test data is unlikely to be orthogonal and hence contains errors. In this case, the present method can not be used directly to improve structural parameters of a structure.

§ 7.9 SUMMARY

The present method can yield a good improvement of the structural parameters which can reproduce the original test modal data sets, provided the test modal data forms a good data base.

The present method is based on the orthogonality of the test modal data. Therefore, if test modal data is not orthogonal, it can not be used directly to improve structural parameters.

If the improved structural parameters do not reproduce original test modal data, the original test modal data may be severely contaminated and should not be directly used with the present method.

APPENDIX 7A - PSEUDO INVERSE OF A MATRIX

Let **A** be an $n \times m$ matrix of arbitrary rank. The definition of pseudo-inverse, $\mathbf{A}^+$, of a matrix **A** is

1. $\mathbf{A}\mathbf{A}^+\mathbf{A} = \mathbf{A}$
2. $\mathbf{A}^+\mathbf{A}\mathbf{A}^+ = \mathbf{A}^+$
3. $(\mathbf{A}^+\mathbf{A})^T = \mathbf{A}^+\mathbf{A}$
4. $(\mathbf{A}\mathbf{A}^+)^T = \mathbf{A}\mathbf{A}^+$

   where **A** can be rectangular, or square but singular matrix.

Properties of pseudo-inverse

1. the pseudo-inverse is unique
2. for a non-singular matrix, it reduces to the ordinary inverse
3. $(\mathbf{A}^+)^+ = \mathbf{A}$

APPENDIX 7B - A RECURSIVE ALGORITHM FOR COMPUTING THE PSEUDO INVERSE OF A RECTANGULAR MATRIX

The following is a recursive algorithm for computing the pseudo-inverse of a rectangular matrix. Let $\mathbf{a}_k$ denote the kth column of a given matrix $\mathbf{M}^*$, and let $\mathbf{M}^{*_k}$ denote the sub-matrix consisting of the first k columns and consider $\mathbf{A}$ in the partitioned form $[\mathbf{A}_{k-1}, \mathbf{a}_k]$. To initiate the process, it is necessary to compute $\mathbf{A}_1^+$. If $\mathbf{a}_1$ is a zero vector, take $\mathbf{A}_1^+ = \mathbf{0}$; otherwise it is necessary to compute $\mathbf{A}_1^+$ by

$$\mathbf{A}_1^+ = (\mathbf{a}_1^T \mathbf{a}_1)^{-1} \mathbf{a}_1^T \tag{7B-1}$$

It is necessary to then compute

$$\mathbf{d}_k = \mathbf{A}_{k-1}^+ \mathbf{a}_k \tag{7B-2}$$

and

$$\mathbf{C}_k = \mathbf{a}_k - \mathbf{A}_{k-1} \mathbf{d}_k \tag{7B-3}$$

If $\mathbf{C}_k \neq \mathbf{0}$, then set $\mathbf{b}_k = \mathbf{C}_k^+$

If $\mathbf{C}_k = \mathbf{0}$ it is necessary to find

$$\mathbf{b}_k = (1 + \mathbf{d}_k^T \mathbf{d}_k)^{-1} \mathbf{d}_k^T \mathbf{A}_{k-1}^+ \tag{7B-4}$$

and

$$\mathbf{A}_k^+ = \begin{bmatrix} \mathbf{A}_{k-1}^+ - \mathbf{d}_k \mathbf{b}_k \\ \mathbf{b}_k \end{bmatrix} \tag{7B-5}$$

This algorithm can be simply implemented in a computer program. It requires no conventional inversion techniques.

APPENDIX 7C - NUMERICAL COMPUTATION OF FULL MODE SHAPES

The solution for the full mode shapes is the most time consuming component in the proposed method. For efficiency in computation time, a modified LU decomposition algorithm may be used which performs these solutions in 1/8 the storage of the ordinary LU decomposition algorithm. The following algorithm is implemented in the complex field.

The decomposition algorithm takes advantage of the symmetry of the equation coefficients and forms a lower, diagonal, lower transposed matrix decomposition.

Consider a symmetric matrix **A**, which is represented by a product of a lower triangular matrix, **L**, a diagonal matrix **D**, and the transpose of **L**. Introducing the **D** matrix, permits the specification of the diagonal elements of **L** to unity.

$$\mathbf{A} = \mathbf{L}\mathbf{D}\mathbf{L}^T \tag{7C-1}$$

or

$$a_{ij} = \sum_{k=1}^{n} \sum_{l=1}^{n} l_{ik}\, d_{kl}\, l_{lj} \tag{7C-2}$$

$$= \sum_{k=1}^{n} l_{ik}\, l_{jk}\, d_{kk} \quad (since \;\; d_{lk} = 0, \;\; l \neq k)$$

$$= \sum_{k=1}^{min(i,j)} l_{ik}\, l_{jk}\, d_{kk} \quad (since \;\; l_{ik} = 0, \;\; k > i \;\; \text{and} \;\; l_{jk} = 0, \;\; k > j)$$

Since $a_{ij} = a_{ji}$, it is necessary only to work with the lower triangle of matrix **A**

$$a_{ij} = \sum_{k=1}^{j} l_{ik}\, l_{jk}\, d_{kk} \quad \text{for } i \geq j \tag{7C-3}$$

If it is assumed that all the l's are known up to, but not including column j and all the d's are known up to, but not including d_{jj}, then

$$a_{jj} = \sum_{k=1}^{j} l_{jk}^2\, d_{kk} = \sum_{k=1}^{j-1} l_{jk}^2\, d_{kk} + d_{jj} \quad (since \;\; l_{jj} = 1) \tag{7C-4}$$

or

$$d_{jj} = a_{jj} - \sum_{k=1}^{j-1} l_{jk}^2\, d_{kk} \tag{7C-5}$$

where all values on the right hand side are known.

Also

$$a_{ij} = \sum_{k=1}^{j} l_{ik}\, l_{jk}\, d_{kk} = \sum_{k=1}^{j-1} l_{ik}\, l_{jk}\, d_{kk} + l_{ij}\, d_{jj} \quad \text{for } i > j \tag{7C-6a}$$

or

$$l_{ij} = (a_{ij} - \sum_{k=1}^{j-1} l_{ik}\, l_{jk}\, d_{kk}) \,/\, d_{jj} \tag{7C-6b}$$

where all the values on the right hand side are known.

Thus, it is possible, using Eqns. (7C-5), (7C-6a) and (7C-6b)) to read one column of **A** at a time and, starting at the diagonal element, compute the corresponding rows and columns of **L** and $\mathbf{L}^T$. This process requires all the elements of **L**, in the lower rectangle of **L**, which intersects the diagonal. The maximum computer storage space required is then $(n/2)^2$, where n is the order of the matrix.

In the actual algorithm, the decomposition is separated into three phases. A work area of variable dimensions is set up. The first phase loads as many columns of **A** as will fit in this area and computes the corresponding columns of **L**, **D**, $\mathbf{L}^T$. The next phase loads a column of **A** and solves for one column of **L**, **D**, $\mathbf{L}^T$ at a time, starting at the diagonal. The third phase starts when the work area can hold all the remaining rows of **A**. During this entire process, the work area is continually being redimensioned and the rows of **L** and the rows of $\mathbf{L}^T$ are written to a sequential file.

When this process is completed, the solution of the matrix equation $\mathbf{Ax} = \mathbf{LDL}^T\mathbf{x} = \mathbf{b}$ is simply performed as follows

1. solve for $\mathbf{x}_2$, one element at a time from $\mathbf{Lx}_2 = \mathbf{b}$, where $\mathbf{x}_2 = \mathbf{DL}^T\mathbf{x}$ (note **L** is a lower triangular matrix);

2. solve for $\mathbf{x}_1$ from $\mathbf{Dx}_1 = \mathbf{x}_2$, where $\mathbf{x}_1 = \mathbf{L}^T\mathbf{x}$. (note **D** is a diagonal matrix);

3. solve for **x** from $\mathbf{L}^T\mathbf{x} = \mathbf{x}_1$, where **x** is the solution of the original equation (note $\mathbf{L}^T$ is an upper triangular matrix and solution must proceed from bottom up).

Chapter 8

CONCLUSIONS

The art of progress is to preserve order amid change, and to preserve change amid order.

- A. N. Whitehead

§ 8.1 SUMMARY

In the course of conducting the research work in this thesis, attention has been paid to developing some methods for modal and structural identification of vibrating structures in the time domain. Each of the methods developed in this thesis is thus original and, as well, improvements to previously published methods for tackling the same type of identification problem, although strict comparisons in terms of computation time and usage of computer storage have not been carried out. In this

section a summary is made on these newly developed methods in general terms.

Theoretical fundamentals of a linear damped vibrating structure generalized in chapter 2 can be used to develop modal identification methods. Structural models, state models, modal models and response models of a vibrating structure were investigated. The relationships between these models were established which provide a basis for developing modal identification motheds in the time domain. Particularly, relationships between response models in the time domain and various dynamic properties of structures establish the basis for determination of various dynamic properties using the response data in the case of free vibration testing, or the response and excitation data in the case of forced vibration testing in the time domain. The modal parameters of the structure may then be computed from these identified dynamic properties.

The ARMAX model of a vibrating structure obtained in chapter 4 was used to develop two methods for modal identification in the time domain. The response and/or excitation data in the time domain are used to identify the coefficient matrix sequence of the ARMAX model. The identified coefficient matrices of the AR part are then used to calculate the eigenvalues and eigenvectors of the state model of the structure through which the complex mode shapes, natural frequencies and damping ratios of the vibrating structure are computed. The difficulties in use of time domain modal identification methods such as determination of the number of degrees of freedom of the structure being excited in a vibration test, detection of false modes caused by observation noise and numerical ill-conditioning of the test data are also tackled. Some useful techniques are presented to overcome these difficulties. The generality of the direct method was demonstrated by discussion of the reduction of the method to some selected methods reviewed in chapter 3.

The Fourier transformation is a very useful tool in modal identification in the frequency domain. Its counterpart in the time domain, the *Z*-transformation, can play the similar role in modal identification in the time domain. Application of the *Z*-transformation in modal identification was comprehensively investigated. For different vibration test technique, the corresponding method using *Z*-transformation was developed for identification of modal parameters of a vibrating structure. A new technique for derivation of mode shapes of a vibrating structure from its *Z*-transfer function matrix sequence was presented.

Application of the methods presented in this thesis to the actual modal testing is studied. Some techniques for treating the measured data were introduced. The advantages and disadvantages of different types of excitations, choice of sampling rate and presampling filters, estimation of the order of a testing structure and determination of excitation bandwidth, were extensively investigated. Practical procedures for application of the present methods for modal identification to the modal testing are proposed and the results of laboratory experiments on the modal test of a cantilevered beam and a 15 storey steel high rise building model were presented to verify the developed methods.

Finally, identification of structural parameters of vibrating structures using modal test data was investigated as an extension and application of modal identification. A method was developed to identify structural parameters of vibrating structures with nonproportional damping. The method can be used to check whether the modal test data is contaminated. The application of the pseudo inverse of a matrix in the structural system identification was also studied.

§ 8.2 CONCLUSIONS

A substantial portion of the research findings described in this thesis results from original work by the author. Work of others is indicated and used for completeness in the presentation. The main conclusions of this study are summarized as follows.

- Generalization of the fundamental theory of a vibrating structure for structural system identification analysis is the basis for developing various methods of modal identification in both the frequency domain and the time domain.

- Various models representing a vibrating structure and relationships between these models are crucial for development of methods for modal identification.

- The ARMAX model of a vibrating structure can play the role of a bridge for identification of modal parameters, and the response and excitation data in the time domain.

- The direct method is a general method for modal identification in the time domain, while the indirect method is a flexible method which is suitable for different types of excitation and different purposes of testing.

- The coefficient matrix sequence of the ARMAX model of a vibrating structure can be related to the modal parameters of the structure.

- Once the coefficient matrices of the ARMAX model of a vibrating structure are obtained using various numerical methods, the modal parameters of the vibrating structure can be computed using the relationship of coefficient matrices of the ARMAX model to the modal parameters of the structure.

- The natural frequencies and damping ratios of a vibrating structure can be identified using a univariate ARMAX model of the structure.

- The false modes caused by observation noise can be detected by identifying the roots of both AR and MA parts of the ARMAX model.
- The number of degrees of freedom of a structure being excited in modal testing can be assessed from the response data.
- Deterministic or random excitation signals, controlled or uncontrolled excitations can be used with the present methods.
- The methods based on the *Z*-transformation are very efficient in determination of modal parameters of a vibrating structure.
- *Z*-transformation plays an important role in modal identification in the time domain similar to the role of Fourier transformation in the frequency domain.
- Various ARMA models which can be used with different type of excitations in modal identification are developed on the basis of *Z*-transformation.
- Mode shapes of a vibrating structure can be obtained directly from its *Z*-transfer function matrix sequence.
- The closely spaced frequencies of a vibrating structure can be identified by the present methods.
- Sampling rate largely depends on the frequency range of interest in a modal test.
- Aliasing phenomena have to be avoided by use of suitable sampling rates and appropriate response measurement arrangement.
- For different structure and different purpose of a modal testing, different excitation signal should be used.

- Using modal test data, structural parameters of a vibrating structure with nonproportional damping can be identified by use of the method developed in chapter 7.

- The complex modal data from vibration tests can directly be used with the present method.

- The method for structural identification can also be used to assess if the modal test data is contaminated.

§ 8.3 RECOMMENDATION FOR FUTURE RESEARCH WORK

In view of the successful development of the theoretical and experimental work using the methods presented in this thesis, it is considered that the following work may be worth being conducted in future as a continuation of the present efforts.

- The present research has concentrated on the development of several methods for modal and structural identification of a vibrating structure. Although, the algorithms have been applied in the laboratory testing, instructive and comprehensive packages are needed in order to promote the use of these methods. Improvement of these algorithms will also be a good topic for further investigation.

- Many structures, including offshore structures, have some nonlinearity in circumstances. Study of modal identification of non-linear structural system is still a challenging task for structural engineering circle.

- One of the aims of performance of modal identification is to obtain the real modal parameters and/or structural parameters so that these parameters could be

used in the vibration control of the structural system. Investigation of the method for modal identification to cooperate with vibration control is a further promising topic.

- Numerical computing in system identification has always been a problem causing inaccuracy of identified results. Investigation of suitable numerical methods for the present methods would be an interesting and fruitful challenge.

- As discussed in this thesis, detection of noise contained in the test data before identification and identification of the false modes caused by the observation noise are very important for determination of correct modes. In this area, there is still some research which is required.

- Further study of application of the present methods in this thesis to the modal testing of complex structures in the laboratory and field will be worthwhile.

- One of the problems with structural system identification is that the zero off-diagonal elements are not identified as zero in the most identification algorithms. Hence it is desirable to develop method which can produce zero off-diagonal elements of structural matrices in the process of identification with low cost.

BIBLIOGRAPHY

[1] Akaike, H., (1974), "A New Look at the Statistical Model Identification", *IEEE Transactions on Automatic Control*, Vol. AC-19, No. 6, December, pp. 716-723.

[2] Allemang, R. J. and Brown, D. L., (1982), "A Correlation Coefficient for Modal Vector Analysis", *Proceedings of 1st International Modal Analysis Conference*, Orlando, Florida, pp. 110-116.

[3] Allemang, R. J., (1982), "Experimental Modal Analysis Bibliography", *Proceedings of the 1st International Modal Analysis Conference*, Orlando, Florida, pp. 714-726.

[4] Andrew, L. V., (1981), "An Automated Application of Ibrahim's Time Domain Method to Responses of the Space Shuttle", *AIAA/ASME/ASCE/AHS 22nd Structures Structural Dynamics and Materials Conference*, Paper No. 81-0526, April, Atlanta, Georgia, pp. 155-165.

[5] Anderson, J. E., (1981), "Another Look at Sine-Dwell Mode Testing", *AIAA/ASME/ASCE/AHS 22nd Structures, Structural Dynamics and Materials Conference*, Paper No. 81-0532, April, Atlanta, Georgia, pp. 202-212.

[6] Amirouche, M. L. and Huston, R. L., (1985), "Collaborative Techniques in Modal Analysis", *AIAA/ASME/ASCE/AHS 26th Structures, Structural Dynamics and Materials Conference*, Part 2, Paper No. 85-0632, April, Orlando, Florida, pp. 161-165.

[7] Astrom, K. J. and Eykoff, P., (1971), "System Identification - A Survey", *Automatica*, Vol. 7, No. 2, pp. 123-162.

[8] Baruch, M., (1978), "Optimization Procedure to Correct Stiffness and Flexibility Matrices Using Vibration Tests", *AIAA Journal*, Vol. 16, No. 11, November, pp. 1208-1010.

[9] Baruch, M. and Bar Itzhack, I. Y., (1978), "Optimal Weighted Orthogonalization of Measured Modes", *AIAA Journal*, Vol. 16, No. 4, April, pp. 346-351.

[10] Baruch, M. and Bar Itzhack, I. Y., (1979), "Reply by Authors to A. Berman", *AIAA Journal*, Vol. 17, No. 8, August, p. 928.

[11] Baruch, M., (1982), "Methods of Reference Basis for Identification of Linear Dynamic Structures", *AIAA/ASME/ASCE/AHS 23rd Structures, Structural Dynamics and Materials Conference*, Paper No. 82-0729, May, New Orleans, Louisiana, pp. 557-563.

[12] Baruh, H. and Meirovitch, L., (1982), "Identification of the Eigensolution of Distributed Parameter Systems", *AIAA/ASME/ASCE/AHS 23rd Structures, Structural Dynamics and Materials Conference*, Paper No. 82-0771, May, New Orleans, Louisiana, pp. 574-581.

[13] Baruh, H. and Silverberg, L. M., (1985a), "On the Identification of Self-Adjoint Distributed System Using Modal Filters", *AIAA/ASME/ASCE/AHS*

26th Structures, Structural Dynamics and Materials Conference, Part 2, Paper No. 85-0812, April, Orlando, Florida, pp. 673-681.

[14] Baruh, H. and Meirovitch, L., (1985b), "Parameter Identification in Distributed System", *Journal of Sound and Vibration*, Vol. 101, No. 4, pp. 551-564.

[15] Baruh, H. and Khatri, H. P., (1987), "Identification of Modal Parameters in Vibrating Structures", *AIAA/ASME/ASCE/AHS 28th Structures, Structural Dynamics and Materials Conference*, Part 2, Paper No. 87-0744, April, Monterey, CA., pp. 152-162.

[16] Bathe K. J. and Wilson, E. L., (1976), *Numerical Methods in Finite Element Analysis*, Prentice-Hall, Inc., Englewood Cliffs, New Jersey.

[17] Bauer, R. D. and Tung, F. C., (1984), "Application of Maximum Likelihood Estimation of Modal Parameters", *AIAA Guidance and Control Conference*, August, Seattle, WA.

[18] Beliveau, J. G., (1976a), "Identification of Viscous Damping in Structures from Modal Information", *Journal of Applied Mechanics*, Vol. 43, No. 2, June, pp. 335-339.

[19] Beliveau, J. G., (1976b), "Modal Identification for Non-Normal Modes", *Dynamic Response of Structure: Instrumentation Testing Methods and System Identification, ASCE/EMD Technical Conference*, UCLA, March 30.

[20] Beliveau, J. G., (1977), "Eigenrelations in Structural Dynamics", *AIAA Journal*, Vol. 15, No. 7, pp. 1039-1041.

[21] Beliveau, J. G., (1979), "First Order Formulation of Resonance Testing", *Journal of Sound and Vibration*, Volume 65, pp. 319-327.

[22] Beliveau, J. G., (1981), "Parameter Estimation from Full-Scale Cyclic Testing", *Proceedings of the Second Specialty Conference on Dynamic Response of Structures: Experimentation, Observation, Prediction and Control*, January, Atlanta, Georgia, pp. 775-793.

[23] Beliveau, J. G., (1985), "Damping Synthesis Using Complex Substructure Modes and a Hermitian System Representation", *AIAA/ASME/ASCE/AHS 26th Structures, Structural Dynamics and Materials Conference*, Part 2, Paper No. 85-0785, April, Orlando, Florida, pp. 581-586.

[24] Beliveau, J. G., Vigneron, F. R., Soucy, Y., and Draisey, S., (1986), "Modal Parameter Estimation from Base Excitation", *Journal of Sound and Vibration*, Volume 107, pp. 435-449.

[25] Bergman, L. A., Hale, A. L., and Doodding, J. C., (1984a), "Identification of Linear Time-Invariant Systems by the Method of Poisson Moment Function", *AIAA/ASME/ASCE/AHS 25th Structures, Structural Dynamics and Materials Conference*, Paper No. 84-1052, May, Palm Springs, CA., pp. 490-496.

[26] Bergman, L. A. and Hale, A. L., (1984b), "Linear System Identification via Poisson Moment Functionals", *AIAA Journal*, Vol. 22, No. 4, April, pp. 566-568.

[27] Bergman, L. A., Hale, A. L., and Gooding, J. C., (1985), "Identification of Linear Systems by Poisson Moment Functionals in the Presence Noise", *AIAA Journal*, Vol. 23, pp. 1234-1235.

[28] Berman, A. and Flannely, W. G., (1971), "Theory of Incomplete Models of Dynamic Structures", *AIAA Journal*, Vol. 9, No. 8, August, pp. 1481-1487.

[29] Berman, A., (1975a), "Determining Structural Parameters from Dynamic Testing", *Shock and Vibration Digest*, Vol. 7, Jan.

[30] Berman, A., (1975b), "System Identification of a Complex Structure", *AIAA/ASME/ASCE/AHS 16th Structures, Structural Dynamics and Materials Conference*, Paper No. 75-809, May, Denver, Colorado, 6 pp.

[31] Berman, A., (1979a), "Parameter Identification Techniques for Vibrating Structure", *Shock Vibration Digest*, Vol. 11, No. 1, January, pp. 13-16.

[32] Berman, A., (1979b), "Mass Matrix Correction Using an Incomplete Set of Measured Modes", *AIAA Journal*, Vol. 17, October, pp. 1147-1148.

[33] Berman, A., (1979c), "Comment on Optimal Weighted Orthogonalization of Measured Modes", *AIAA Journal*, Vol. 17, No. 8, August, p. 927.

[34] Berman, A., (1980a), "An Improved Orthogonality Check for Measured Modes", *AIAA Journal*, Vol. 18, No. 9, September, pp. 1151-1152.

[35] Berman, A., Wei, F. S. and Sao, K. W., (1980b), "Improvement of Analytical Models Using Modal Test Data", *AIAA/ASME/ASCE/AHS 21st Structures, Structural Dynamics and Materials Conference*, Paper No. 80-0800, May, Seattle, Washington, pp. 809-814.

[36] Berman, A. and Wei, F. S., (1981), *Automated Dynamic Analytical Model Improvement*, NASA Contractor Report 3452, Langley, Virginia.

[37] Berman, A. and Nagy, E. J., (1983), "Improvement of a Large Analytical Modal Using Test Data", *AIAA Journal*, Vol. 21, No. 8, August, pp. 1168-

1173.

[38] Berman, A., (1984), "System Identification of Structural Dynamics Models - Theoretical and Practical Bounds", *AIAA/ASME/ASCE/AHS 25th Structures, Structural Dynamics and Materials Conference*, Paper No. 84-0929 May, Palm Springs, CA, pp. 123-129.

[39] Bishop, R. E. D., and Gladwell, G. M. L., (1963), "An Investigation into the Theory of Resonance Testing", *Philosophical Transactions, Royal Society of London, Series A*, Vol. 244, A 1055, pp. 241-288.

[40] Bierman, G. L., (1977), *Factorization Methods for Discrete Sequential Estimation*, Academic Press, New York.

[41] Blakeley, K., Ibanez, P., Griffith, S., Cooper, B., and Stoessel, J., (1981), "System Identification: Review Examples", *Proceedings of the Second Specialty Conference on Dynamic Response of Structures: Experimentation, Observation, Prediction and Control*, January, Atlanta, Georgia, pp. 846-858.

[42] Brandon, J. A., (1984), "A Discussion of Alternative Duncan Formulations of the Eigenproblem for the Solution of Non-classically Viscously Damped Linear System", *Journal of Applied Mechanics, Transaction of ASME*, Vol. 51, No. 4, December, pp. 904-906.

[43] Braun, S. G. and Ram, Y. M., (1987), "Structural Parameter Identification in the Frequency Domain: the Use of Oversized System", *Journal of Dynamic System, Measurement, and Control, Transaction of ASME*, Vol. 109, June, pp. 120-123.

[44] Broch, J. T., (1980), *Mechanical Vibration and Shock Measurements*, Bruel & Kjar, Denmark.

[45] Bronowicki, A. L., Lukich, M. S., and Kutitz, S. P., (1986), "Application of Physical Parameter Identification to Finite Element Models", *First NASA/DOD CSI Technology Conference*, November, Norfolk, Virginia, pp. 187-206.

[46] Brown, D. L., Allemang, R. J. and Mergeay, M., (1979), "Parameter Estimation Techniques for Modal Analysis", *SAE* Paper No. 790221, February 26-March 2, Detroit.

[47] Brown, D. , Carbon, G. and Ramsey, K., (1977), "Survey of Excitation Techniques Applicable to the Testing of Automotive Structures", *SAE* Paper No. 770029, March, Cobo Hall, Detroit.

[48] Carmichael, D. G., (1979), "The State Estimation Problem in Experimental Structural Mechanics", *Application of Statistics and Probability in Soil and Structural Engineering*, 3rd Ed., International Conference, pp. 802-815.

[49] Caravani, P. and Thomson, W. T., (1974), "Identification of Damping Coefficients in Multidimensional Linear Systems", *AIAA Journal*, Vol. 12, No. 2, pp. 185-190.

[50] Caravani, P., Watson, M. L. and Thomson, W. T., (1977), "Recursive Least-Squares Time Domain Identification of Structural Parameters", *Journal of Applied Mechanics, Transaction of ASME*, Vol. 99, No. 1, March, pp. 135-140.

[51] Carrascosa, L. I., and Busturia, J. M., and Grimenez, J. G., (1985), "Global Experimental Modal Analysis. A Comparison of Different Methods", *Proceedings of the 3rd International Modal Analysis Conference*, Orlando, Florida, Feb., pp. 311-321.

[52] Caughey, T. K., (1960), "Classical Normal Modes in Damped Linear Dynamic Systems', *Journal of Applied Mechanics, Transaction of ASME*, Vol. 27, No. 2, June, pp. 269-271.

[53] Cawley, P. and Rigner, L. G., (1986), "Rapid Measurement of Modal Properties Using FFT Analyzers with Random Excitation", *Journal of Vibration, Acoustics, Stress, and Reliability in Design, Transaction of ASME*, Vol. 108, October, pp. 394-398.

[54] Chen, J. C. and Garba, J. A., (1974), "Determination of Propellant Effective Properties Using Modal Test Data", *Shock and Vibration Bulletin*, No. 45, October, pp. 9-10.

[55] Chen, J. C. and Wada, B. K., (1977), "Matrix Perturbation for Structural Dynamic Analysis", *AIAA Journal*, Vol. 15, No. 8, August, pp. 1095-1100.

[56] Chen, J. C. and Garba, J. A., (1979a), "Matrix Perturbation for Analytical Model Improvement", *AIAA/ASME/ASCE/AHS 20th Structures, Structural Dynamics and Materials Conference*, Paper No. 79-0831, April, St. Louis, Mo., pp. 428-436.

[57] Chen, J. C. and Garba, J. A. (1979b), "Analytical Model Improvement Using Modal Test Results", *AIAA Journal*, vol. 18, No. 6, June, pp. 684-690.

[58] Chen, J. C., Kuo, C. P. and Garba, J. A., (1983), "Direct Structural Parameter Identification by Modal Test Results", *AIAA/ASME/ASCE/AHS 24th Structures, Structural Dynamics and Materials* , Paper No. 83-0812, May, Lake Tahoe, Neveda, pp. 44-49.

[59] Chen, J. C., (1984a), "Evaluations of Modal Testing Methods", *AIAA/ASME/ASCE/AHS 25th Structures, Structural Dynamics and Materials*

Conference, Paper No. 84-1071, May, Palm Sprigns, CA., pp. 561-572.

[60] Chen, J. C., Peretti, L. F. and Garba, J. A. (1984b), "Spacecraft Structural System Identification by Modal Test", *AIAA/ASME/ASCE/AHS 25th Structures, Structural Dynamics and Materials Conference*, Paper No. 84-1051, May, Palm Springs, CA, pp. 478-489.

[61] Chen, J. C. and Trubert, M., (1984c), "Galileo Model Test and Pre-Test Analysis", *Proceedings of the 2nd International Modal Analysis Conference*, February, Orlando, FL., pp. 796-802.

[62] Chen J. C., Rose, T., Trubert, M., and Wada, B., (1986), "Modal Test/Analysis Correlation for Centaur G Prime Launch Vehicle", *AIAA/ASME/ASCE/AHS 27th Structures, Structural Dynamics and Materials Conference*, Part 2, Paper No. 86-1002, May, San Antonio, Texas, pp. 621-633.

[63] Chen, J. C. and Wada, B. K., (1987), "On Sine Dwell or Broad-band Methods for Modal Testing", *AIAA/ASME/ASCE/AHS 28th Structures, Structural Dynamics and Materials Conference*, Part 2, Paper No. 87-0961, April, Monterey, CA., pp. 998-1044.

[64] Chen, S. Y. and Fuh, J. S., (1984), "Application of the Generalized Inverse in Structural System Identification", *AIAA Journal*, Vol. 22, No. 12, December, pp. 1827-1828.

[65] Chen, S. Y. and Fuh, J. S., (1985), "Reply by Authors to J. A. Brandon", *AIAA Journal*, Vol. 23, No. 11, pp. 1840-1841.

[66] Chen, S. Y. and Wei, F. S., (1985), "Systematic Approach for Eigensensitivity Analysis", *AIAA/ASME/ASCE/AHS 26th Structures,*

Structural Dynamics and Materials Conference, Part 2, Paper No. 85-0635, April, Orlando, Florida, pp. 178-183.

[67] Collins, J. D., Hart, G. C., and Kennedy, B., (1971), "Statistical Analysis of the Modal Properties of Large Structural System", *SAE* Paper No. 710785, September, Los Angeles, Calif.

[68] Collins, J. D., Hart, G. C., Hasselman, T. K., and Kennedy, B., (1974), " Statistical Identification of Structures", *AIAA Journal*, Vol. 12, No. 2, February, pp. 185-190.

[69] Coppolino, R. N., (1981), "A Simultaneous Frequency Domain Technique for Estimation of Modal Parameters from Measured Data", *SAE* Paper 811046, October, Anaheim, CA.

[70] Craig, Jr., R. R. and Blair, M. A., (1984), "A Generalized Multiple-Input, Multiple-Output Modal Parameter Estimation Algorithm", *AIAA/ASME/ASCE/AHS 25th Structures, Structural Dynamics and Materials Conference*, Paper No. 84-1050, May, Palm Springs, CA, pp. 469-477.

[71] Crawley, E. F. and O'Donnell, K. J., (1986), "Identification of Nonlinear System Parameters in Joints Using the Force-Stae Mapping Technique", *AIAA/ASME/ASCE/AHS, 27th Structures, Structural Dynamics and Materials Conference*, Part 2, Paper No. 86-1013, May, San Antonio, Texas, pp. 659-667.

[72] Creamer, N. G. and Junkins, J. L., (1987), "An Identification Method for Flexible Structures", *AIAA/ASME/ASCE/AHS 28th Structures, Structural Dynamics and Materials Conference*, Part 2, Paper No. 87-0745, April, Monterey, CA., pp. 163-171.

[73] Cromer, J. C. and Lalanne, M., (1976), "Dynamic Behavior of Complex Structure, Using Part Experiment, Part Theory", *Shock and Vibration Bulletin*, No. 46, Part 5, pp. 177-185.

[74] Cuenod, M. and Sage, A. P., (1968), "Comparison of Some Methods Used for Process Identification", *Automatica*, Vol. 4, pp. 235-269.

[75] Distefano, N. and Rath, A., (1974), "Modeling and Identification in Nonlinear Structural Dynamics. 1: One Degree of Freedom Models", *EERC-74-15*, Earthquake Engineering Research Center, California University, Berkeley, February.

[76] Distefano, N. and Pena-Pardo, B., (1976), "System Identification of Frames under Seismic Loads", *Journal of the Engineering Mechanics Division, ASCE*, Vol. 102, No. EM2, April, pp. 313-331.

[77] Dobbs, M. W., Blakely, K. D. and Gundy, W. E., (1981), "System Identification of Large-Scale Structures", *SAE* Paper 811050, October, Anaheim, CA.

[78] Dunn, W. H., (1977), "Modal Analysis of Transient Response Data Using a Complex Exponential Algorithm", *Soc. Environ. Engr. Proc.*, Imperial College, April, London.

[79] Durham, D. J. and Sussel, R. H., (1976), "Modal Analysis with the /DMS/TSA System", *SAE* Paper No. 760877, November, Town & City, San Diego.

[80] Eykhoff, P., (1981), *Trends and Progress in System Identification*, Pergamon Press, Oxford, England.

[81] Ensminger, R. R. and Turner, M. J., (1979), "Structural Parameter Identification from Measured Vibration Data", *AIAA/ASME/ASCE/AHS 20th Structures, Structural Dynamics and Materials Conference*, Paper No. 79-0829, St. Louis, Mo., pp. 410-416.

[82] Ewins, D. J. and Gleenson, P. T., (1982), "A Method for Modal Identification of Lightly Damped Structures", *Journal of Sound and Vibration*, Vol. 84, No. 1, September, pp. 57-79.

[83] Ewins, D. J., (1981), "State-of the Art Assessment of Mobility Measurements- A Summary of European Results", *Shock and Vibration Bulletin*, Vol. 51, Part 1, pp. 15-35.

[84] Ewins, D. J., (1984), *Modal Testing: Theory and Practice*, John Wiley & Sons, New York.

[85] Fabunmi, J. A., (1985), "Effect of Structural Modes of Vibration Force Determination by the Pseudo Inverse Technique", *AIAA/ASME/ASCE/AHS 26th Structures, Structural Dynamics and Materials Conference*, Part 2, Paper No. 85-0784, pp. 573-580.

[86] Fawzy, I., (1977), "Orthogonality of Generally Normalized Eigenvectors and Eigenrows", *AIAA Journal*, Vol. 15, No. 2, February, pp. 276-278.

[87] Fillod, R., Lallement, G., Piranda, J., and Raynaud, J. L., (1985), "Global Method of Modal Identification", *Proceedings of the 3rd International Modal Analysis Conference*, Orlando, Florida, Feb., pp. 1145-1151.

[88] Flannely, W. G., Fabunmi, J. A., and Nagy, E. J., (1981), *Analytical Testing*, NASA Contractor Report 3429, Langley, Virginia.

[89] Fritzen, C. P., (1986), "Identification of Mass, Damping, and Stiffness Matrices of Mechanical Systems", *Journal of Vibration, Acoustics, and Reliability in Design, Transaction of ASME*, Vol. 108, January, pp. 9-16.

[90] Fuh, J. S., Chen S. Y. and Berman A., (1984), "System Identification of Analytical Models of Damped Structures", *AIAA/ASME/ASCE/AHS 25th Structures, Structural Dynamics and Materials Conference*, Paper No. 84-0926, May, Palm Springs, CA, pp. 112-116.

[91] Fuh, J. S., Gustavson, B. and Berman, A., (1986), "Error Estimation and Compensation in Reduced Dynamic Models of Large Space Structures", *AIAA/ASME/ASCE/AHS 27th Structures, Structural Dynamics and Materials Conference*, Part 2, Paper No. 86-0837, May, San Antonio, Texas, pp. 1-9.

[92] Garba, J. A. and Wada, B. K., (1977), "Application of Perturbation Methods to Improve Analytical Model Correlation with Test Data", *SAE* Paper No. 770959, November, Los Angeles, CA.

[93] Gersch, W., (1970), "Estimation of the Autoregressive Parameters of a Mixed Autoregressive Moving-Average Time Series", *IEEE Transactions on Automatic Control*, Vol. AC-15, No. 10, October, pp. 583-588.

[94] Gersch, W., (1970), "Mean Square Responses in Structural Systems", *Journal of the Acoustical Society of America*, Vol. 48, pp. 403-413.

[95] Gersch, W. and Luo, S., (1972), "Discrete Time Series Synthesis of Randomly Excited Structural System Response", *Journal of the Acoustical Society of America*, Vol. 51, pp. 402-408.

[96] Gersch. W., Nielsen, N. N. and Akaike, H., (1973), " Maximum Likelihood Estimation of Structural Parameters from Random Vibration Data", *Journal*

of Sound and Vibration, Vol. 31, No. 3, pp. 295-308.

[97] Gersch, W., (1974a), "On the Achievable Accuracy of Structural System Parameter Estimates", *Journal of Sound and Vibration*, Vol. 34, No. 1, pp. 63-79.

[98] Gersch, W. and Foutch, D. A., (1974b), "Least Squares Estimates of Structural System Parameters Using Covariance Function Data", *IEEE Transaction on Automatic Control*, Vol. AC-19, No. 6, December, pp. 898-903.

[99] Gersch, W., (1975), "Parameter Identification: Stochastic Process Techniques", *Shock and Vibration Digest*, Vol. 7, No. 11, November, pp. 71-86.

[100] Gersch, W. and Liu, R. S-Z., (1976a), "Time Series Methods for the Synthesis of Random Vibration Systems", *Journal of Applied Mechanics, Transaction of ASME*, Vol. 43, March, pp. 159-165.

[101] Gersch, W., Taoka, G. T., and Liu, R., (1976b), "Structural System Parameter Estimation by Two Stage Least-Squares Method", *Journal of the Engineering Mechanics Division, ASCE*, Vol. 102, No. EM5, October, pp. 883-899.

[102] Gersch, W. and Yonemoto, J., (1977), "Synthesis of Multivariate Random Vibration Systems: A Two-Stage Least Squares AR-MA Model Approach", *Journal of Sound and Vibration*, Vol. 54, No. 4, pp. 553-565.

[103] Graupe, D., (1976), *Identification of Systems*, R. E. Krieger Publishing Co., Malabar, FL.

[104] Goodwin, G. C. and Payne, R. L., (1977) *Dynamic System Identification: Experiment Design and Data Analysis*, Academic Press, New York.

[105] Goyder, H. G. D., (1980), "Methods and Application of Structural Modeling from Measured Structural Frequency Response Data", *Journal of Sound and Vibration*, Vol. 68, No. 2, pp. 209-230.

[106] Grossman, D. T., (1982), "An Automated Technique for Improving Modal Test/Analysis Correlation", *AIAA/ASME/ASCE/AHS 23rd Structures, Structural Dynamics and Materials Conference*, Paper No. 82-0640, May, New Orleans, Louisiana, pp. 68-76.

[107] Guyan, R. J., (1965), "Reduction of Mass and Stiffness Matrices", *AIAA Journal*, Vol. 3, p. 380.

[108] Hamma, G. A., Smith, S. and Stroud, R. C., (1976), "An Evaluation of Excitation and Analysis Methods for Modal Testing", *SAE* Technical Paper No. 760872, December, Town & City, San Diego.

[109] Hanagud, S., Meyyappa, M., Cheng, Y. P. and Craig, J. I., (1984), "Identification of Structural Dynamic Systems with Nonproportional Damping", *AIAA/ASME/ASCE/AHS 25th Structures, Structural Dynamics and Materials Conference*, Paper 84-0993, May, Palm Springs, CA, pp. 283-291.

[110] Hanagud, S. and Glass, B. J., (1987), "Structural Dynamics Model Identification Using Heuristic Search", *AIAA/ASME/ASCE/AHS 28th Structures, Structural Dynamics and Materials Conference*, Part 2 Paper No. 87-0747, April, Monterey, CA, pp. 177-185.

[111] Hanks, B. R., Ibrahim, S. R., Miserentino, R., Lee, S. H. and Wada, B. K., (1978), "Comparison of Modal Test Methods on the Voyager Payload", *SAE* Technical Paper No. 781044, November, Town & City, San Diego.

[112] Hart, G. C. and Yao, J. T. P., (1977), "System Identification in Structural Dynamics", *Journal of the Engineering Mechanics Division, ASCE*, Vol. 103, No. EM6, December, pp. 1089-1105.

[113] Hart, G. C. and Torkamani, M. A. M., (1974), "Structural System Identification", *Stochastic Problems in Mechanics*, University of Waterloo Press, pp. 207-228.

[114] Hasselman, T. K., (1981), "Structural Uncertainty in Dynamic Analysis", *SAE* Technical Paper No. 811049, October, Anaheim, CA.

[115] Horda, L. C. and Juang, J. N., (1985), "Identifying Approximate Linear Models for Siple Nonlinear Systems", *AIAA/ASME/ASCE/AHS 26th Structures, Structural Dynamics and Materials Conference*, Part 2 , Paper No. 85-0686, April, Orlando, Florida, pp. 282-289.

[116] Hoshiya, M. and Saito, E., (1984), "Structural Identification by Extended Kalman Filter", *Journal of the Engineering Mechanics Division, ASCE*, Vol. 110, No. 12, December, pp. 1757-1770.

[117] Hoshiya, M. and Saito, E., (1986), "Structural Identification by Extended Kalman Filter", *The First Asian Conference on Structural Engineering and Construction*, January, Bangkok, pp. 1729-1740.

[118] Hunt, D. L., (1987), "A Modern Approach for Modal Testing Using Multiple Input Sine Excitation", *AIAA/ASME/ASCE/AHS 28th Structures, Structural Dynamics and Materials Conference*, Part 2, Paper No. 87-0964, April,

Monterey, CA., pp. 1016-1023.

[119] Huynh, T. V., (1987), "A New Method of Computing the State Transition Matrix for Linear System", *Journal of Guidance, Control, and Dynamics*, Vol. 10, No. 2, pp. 218-221.

[120] Ibanez, P., (1973), "Identification of Dynamic Parameters of Linear and Non-Linear Structural Models from Experimental Data", *Nuclear Engineering and Design*, Vol. 25, pp. 30-41.

[121] Ibanez, P., (1974), "Methods for the Identification of Dynamic Parameters of Mathematical Structural Models from Experimental Data", *Nuclear Engineering and Design*, Vol. 27, pp. 209-219.

[122] Ibanez, P. (1979), "Review of Analytical and Experimental Techniques for Improving Structural Dynamic Models", Bulletin 249, Welding Research Council, June.

[123] Ibrahim, S. R. and Mikulcik, E. C., (1973), "A Time Domain Vibration Test Technique", *Shock and Vibration Bulletin*, No. 43, Part 4, pp. 21-37.

[124] Ibrahim, S. R. and Mikulcik, E. C., (1976), "The Experimental Determination of Vibration Parameters from Time Responses", *Shock and Vibration Bulletin*, No. 46, Part 5 , Aug., pp. 187-196.

[125] Ibrahim, S. R. and Mikulcik, E. C., (1977), "A Method for the Direct Identification of Vibration Parameters from the Free Response", *Shock and vibration Bulletin*, No. 47, Part 4, September, pp. 183-198.

[126] Ibrahim, S. R., (1977), "Random Decrement Technique for Modal Identification of Structures", *Journal of Spacecraft and Rockets*, Vol. 14, No.

11, pp. 696-701.

[127] Ibrahim, S. R., (1978), "Modal Confidence Factor in Vibration Testing", *Journal of Spacecraft and Rockets*, Vol. 15, No. 5, Sept-Oct, pp. 313-316.

[128] Ibrahim, S. R. and Mikulcik, E. C., (1978), "Time Domain Identification of Standing Wave Parameters in Gas Piping Systems", *Journal of Sound and Vibration*, Vol. 60, Part 1, pp. 21-31.

[129] Ibrahim, S. R., (1979), "Application of Random Time Domain Analysis to Dynamic Flight Measurements", *Shock and Vibration Bulletin*, Vol. 49, Part 2, Sept., pp. 165-170.

[130] Ibrahim, S. R. and Pappa, R. S., (1982), "Large Modal Survey Testing Using the Ibrahim Time Domain Identification Technique", *Journal of Spacecraft and Rockets*, Vol. 19. No. 5, Sept-Oct, pp. 459-465.

[131] Ibrahim, S. R., (1982), "Computation of Normal Modes from Measured Complex Modes", *Shock and Vibration Bulletin*, No. 52, pp. 13-17.

[132] Ibrahim, S. R., (1982), "Dynamic Modeling of Structural from Measured Complex Modes", *AIAA/ASME/ASCE/AHS 23rd Structures, Structural Dynamics and Materials Conference*, Paper No. 82-0770, May, New Orleans, Louisiana, pp. 564-573.

[133] Ibrahim, S. R., (1984), "A Model Identification Algorithm for Higher Accuracy Requirements", *AIAA/ASME/ASCE/AHS 25th Structures, Structural Dynamics and Materials Conference*, Paper No. 84-0928, May, Palm Springs, CA, pp. 117-122.

[134] Ibrahim, S. R., (1980), "Limitation on Random Input Forces in Randomdec Computation for Modal Identification", *Shock and Vibration Bulletin*, No. 50, Part 3, pp. 99-112.

[135] Ibrahim, S. R., (1987), "An Upper Hessenberg Sparse Matrix Algorithm for Modal Identification on Minicomputers", *Journal of Sound and Vibration* , Vol 113, No. 1, pp. 47-57.

[136] Irvine, H. M., (1986), "Research Directions in Offshore Structural Engineering at The University of New South Wales", *Workshop on National Needs, Capabilities, and Resources for Offshore Engineering*, May, Monash University, Australia.

[137] Jazwinski, A. H., (1970), *Stochastic Processes and Filtering Theory*, Academic Press, New York and London.

[138] Jezequel, L., (1986), "Three New Methods of Modal Identification", *Journal of Vibration, Acoustics, Stress, and Reliability in Design, Transaction of ASME*, Vol. 108, No. 1, January, pp. 17-25.

[139] Ljung, L., (1987), *System Identification: Theory for the User*, Prentice-Hall, Inc., Englewood, Cliffs, New Jersy.

[140] Juang, J. N. and Pappa, R. S., (1985), "An Eigensystem Realization Algorithm for Modal Parameter Identification", *Journal of Guidance, Control and Dynamics*, Vol. 8, No. 5, pp. 620-627.

[141] Juang, J. N. and Pappa, R. S., (1986), "Effect of Noise on Modal Parameters Identified by the Eigensystem Realization Algorithm", *Journal of Guidance, Control and Dynamics*, Vol. 9, No. 3, pp. 294-303.

[142] Kabe, A. M., (1985), "Stiffness Matrix Adjustment Using Mode Data", *AIAA Journal*, Vol. 23, No. 9, September, pp. 1431-1436.

[143] Kabe, A. M., (1987), "An Efficient Direct Measurement Mode Survey Test Procedure", *AIAA/ASME/ASCE/AHS Structures, Structural Dynamics and Materials Conference*, Part 2, Paper No. 87-0962, April, Monterey, CA., pp. 1005-1015.

[144] Kammer, D. C., (1987), "An Optimum Approximation for Residual Stiffness in Linear System Identification", *AIAA/ASME/ASCE/AHS 28th Structures, Structural Dynamics and Materials Conference*, Part 2, Paper No. 87-0813, April, Monterey, CA., pp. 277-287.

[145] Kano, H., (1989), "An Identification Method of Multiinput, Multioutput Linear Dynamical Systems for the Experimental Analysis of Mechanical Structures", *Journal of Dynamic Systems, Measurement and Control*, Vol. 111, No. 2, June, pp. 146-152

[146] Kashyap, R. L. and Nasburg, R. E., (1974), "Parameter Estimation in Multivariate Stochastic Difference Equations", *IEEE Transaction on Automatic Control*, Vol. AC-19, No. 6, December, pp. 784-797.

[147] Kennedy, C. C., and Pancu, C. D. P., (1947), "Use of Vectors in Vibration Measurement and Analysis", *Journal of Aeronautical Sciences*, Vol. 14, No. 11, Nov., pp. 603-625.

[148] Kidder, R. L., (1973), "Reduction of Structural Frequency Equations", *AIAA Journal*, Vol. 11, No. 6, p. 892.

[149] Kim, C. G. and Gourishankar, V., (1981), "A Model Reference Adaptive Technique of Identification for Discrete Systems", *Automatica*, Vol. 17, No.

4, pp. 637-640.

[150] Kubomura, K., (1985), "Component Mode Synthesis for Structures with General Stiffness, Damping and Mass Matrices", *AIAA/ASME/ASCE/AHS 26th Structures, Structural Dynamics and Materials Conference*, Part 2, Paper No. 85-0711, April, Orlando, Florida, pp. 337-340.

[151] Kubrusly, D. S., (1977), "Distributed Parameter System Identification A Survey", *International Journal of Control*, Vol. 26, No. 4, pp. 509-535.

[152] Kumar, R. and Moore, J. B., (1981), "Detection Techniques in Least Squares Identification", *Automatica*, Vol. 17, No. 6, pp. 850-819.

[153] Kumar, P. R., and Varaiya, Pravin, (1986), *Stochastic Systems: Estimation, Identification and Adaptive Control*, Prentice-Hall, Inc., Englewood Cliffs, New Jersey.

[154] Kuo, C. P. and Wada, B. K., (1986), "Nonlinear Sensitivity Coefficients and Corrections in System Identification", *AIAA/ASME/ASCE/AHS 27th Structures, Structural Dynamics and Materials Conference*, Paper No. 86-0927, May, San Antonio, Texas, pp. 576-584.

[155] Kuo, C. P. and Wada, B. K., (1987), "System Identification of a Truss Type Space Structure Using the Multiple Boundary Condition Test (MBCT) Method", *AIAA/ASME/ASCE/AHS 28th Structures, Structural Dynamics and Materials Conference*, Part 2, Paper No. 87-0746, April, Monterey, CA., pp. 172-176.

[156] Klosterman, A. and Zimmerman, R., (1975), "Modal Survey Active Via Frequency Response Functions", *SAE*, Paper 751068, November.

[157] Klosterman, A. L., McCleland, W. A., and Sherlock, J. E., (1975), "Dynamic Simulation of Complex System Utilizing Experimental and Analytical Techniques", *ASME* Paper No. 75-WA/Aero-9.

[158] Knauer, Jr. C. D., Peterson, A. J. and Rendahl, W. B., (1975), "Space Vehicle Experimental Modal Definition Using Transfer Function Techniques", *SAE* Paper 751069, November, Culver City, Los Angeles.

[159] Lapidus, L. and Luus, R., (1967), *Optimal Control of Engineering Processes*, Balisdell Publishing Company, Waltham, Massachusetts.

[160] Lawson, C. L. and Hanson, R. J., (1974), *Solving Least Squares Problems*, Prentice-Hall, Inc., Englewood Cliffs, New Jersey.

[161] Lee, R. C. K., (1964), *Optimal Estimation, Identification, and Control*, MIT Press, Cambridge, MA.

[162] Lee, L. T. and Hasselman, T. K., (1978), "Dynamic Modal Verification of Large Structural Systems", *SAE* Technical Paper No. 781047, Town & City, San Diego.

[163] Leonard, J. W. and Khouri, B. R., (1985), "System Identification Using a Standard Finite Element Program", *Engineering Structures*, Vol. 7, July, pp. 190-197.

[164] Leppert, E. L., Wada, B. K., and Miyakawa, R., (1974), "Modal Test Results of Viking Orbiter", *Shock and Vibration Bulletin*, No. 44, Part 2, August, pp. 165-175.

[165] Leppert, E. L., Lee, S. H., Day, F. D., Chapman, P. C. and Wada, B. K., (1976), "Comparison of Modal Test Results: Multipoint Sine Versus Single-

Point Random", *SAE* Technical Paper No. 760879, December, Town & City, San Diego.

[166] Leuridan, J. M., Brown, D. L., and Allemang, R. J., (1982), "Direct System Parameter Identification of Mechanical Structures with Application to Model Analysis", *AIAA/ASME/ASCE/AHS 23rd Structures, Structural Dynamics and Materials Conference*, Paper No. 82-767, May, New Orleans, Louisiana, pp. 548-556.

[167] Leuridan, J. and Vold, H., (1984), "A Time Domain Linear Estimation Technique for Global Modal Parameter Identification", *Proceedings of 2nd International Modal Analysis Conference*, Florida, pp. 443-451.

[168] Leuridan, J. M., Brown, D. L. and Allemang, R. J., (1986), "Time Domain Parameter Identification Methods for Linear Modal Analysis: A Unifying Approach", *Journal of Vibration, Acoustics, Stress, and Reliability in Design, Transaction of ASME*, Vol. 108, January, pp. 1-8.

[169] Lewis, R. C. and Wrisley, D. L., (1950), "A System for the Excitation of Pure Natural Modes of Complex Structures", *Journal of Aeronautical Sciences*, Vol. 17, No. 11, Nov., pp. 705-722.

[170] Lin, P. L. and Wu, Y. C., (1982), "Identification of Multi-Input Multi-Output Linear Systems from Frequency Response Data", *Journal of Dynamic System, Measurement, and Control, Transaction of ASME*, Vol. 104, March, pp. 58-64.

[171] Ljung, L. and Glover, K., (1981), "Frequently Domain Versus Time Domain Methods in System Identification", *Automatica*, Vol. 17, No. 1, pp. 71-86.

[172] Ljung, L. and Soderstrom, T. (1983), *Theory and Practice of Recursive Identification*, MIT Press, Cambridge, MA.

[173] MacKenzie, A., (1974), "Application of the Fast Fourier Transform to Ground Vibration Testing and Flight Flutter Testing on the B1",*Proceedings of the Conference of the Society of Flight Test Engineers*, Aug, Anaheim, California, pp. 3.59-3.73.

[174] Marmarelis, P. Z. and Udwadia, F. E., (1976), "The Identification of Building Structural System: 2. The Nonlinear Case", *Bull. Seismol. Soc. Amer.*, Vol. 66, No. 1, February, pp. 153-171.

[175] Martinez, D. R., Carne, T. G., Gregory, D. L. and Miller, A. K., (1984), "Combined Experimental/Analytical Modeling Using Component Mode Synthesis", *AIAA/ASME/ASCE/AHS 25th Structures, Structural Dynamics and Materials Conference*, Paper No. 84-0941, May, Palm Springs, CA, pp. 140-152.

[176] McGrew, J., (1970), "Orthogonalization of Measured Modes and Calculation of Influence Coefficients", *AIAA Journal*, Vol. 7, No. 4, pp. 774-775.

[177] Meirovitch, L., (1967), *Analytical Methods in Vibrations*, Macmillan, Inc., New York.

[178] Meirovitch, L., (1975), *Elements of Vibration Analysis*, McGraw-Hills, Inc, New York.

[179] Meirovitch, L., (1980), *Computational Methods in Structural Dynamics*, Sijthoff & Noordhoff, The Netherlands.

[180] Meirovitch, L. and Baruh, H., (1981), "Optimal Control of Damped Flexible Gyroscopic Systems", *Journal of Guidance, Control, and Dynamics*, Vol. 4, No. 2, pp. 157-163.

[181] Meirovitch, L. and Baruh, H., (1985), "Implementation of Modal Filters for Control of structures", *Journal of Guidance, Control and Dynamics*, Vol. 8, No. 6, pp. 707-716

[182] Merritt, P. H. and Baker, W. E., "A Method of System Identification with an Experimental Investigation", *Shock and Vibration Bulletin*, No. 47, Part 4, September, pp. 175-181.

[183] Mickleborough, N. C. and Pi, Y. L., "Estimate of Modal Parameters for a Dynamic System Using Z-Transform", *UNICIV Report No. R-253*, The University of New South Wales, July 1988.

[184] Mickleborough, N. C. and Pi, Y. L., "Modal Parameter Identification Using Z-Transforms", *International Journal for Numerical Methods in Engineering* Vol. 28, No. 10, 1989.

[185] Mickleborough, N. C. and Pi, Y. L., " System Modal Identification Using Free Vibration Data", *Structural Engineering/Earthquake Engineering*, Vol. 6, No. 2, 1989.

[186] Miramand, N., Billaud, J. F., Leleux, F., and Kernevex, J. P., (1976), "Identification of Structural Modal Parameters by Dynamic Test at a Single Point", *Shock and Vibration Bulletin*, No. 46, Part 5, pp. 197-211.

[187] Molusis, J. A., Warmbrodt, W., and Bar-Shalom, Y., (1983), "Identification of Helicopter Rotor Dynamic Models", *AIAA/ASME/ASCE/AHS 24th Structures, Structural Dynamics and Materials Conference*, Paper No. 83-

0988, May, Lake Tahoe, Nevada, pp. 547-557.

[188] Moore, J. B., (1978), "On Strong Consistency of Least Squares Identification Algorithms", *Automatica*, Vol. 14, pp. 505-509.

[189] Mottershead, J. E. and Stanway, R., (1986), "Identification of Structural Vibration Parameters by Using a Frequency Domain Filter", *Journal of Sound and Vibration*, Vol. 109, No. 3, pp. 495-506.

[190] Mottershead, J. E., Lees, A. W., and Stanway, R., (1987), "A Linear, Frequency Domain Filter for Parameter Identification of Vibrating Structures", *Journal of Vibration, Acoustics, Stress, and Reliability in Design*, Vol. 109, No. 3, July, pp. 262-269.

[191] Mustain, R. W., (1976), "Survey of Modal Vibration Test/Analysis Techniques", *SAE* Technical Paper No. 760870, December, Town & City San Diego.

[192] Nake, H. G., (1982), *Identification of Vibrating Structures*, Springer-Verlag, Wien, New York.

[193] Nelson, H. D. and Glasgow, D. A., (1979), "Eigenrelations of Second Order Systems", *AIAA Journal*, Vol. 17, No. 7, pp. 795-797.

[194] Niedbal, N., (1984), "Analytical Determination of Real Normal Modes from Measured Complex Responses", *AIAA/ASME/ASCE/AHS 25th Structures, Structural Dynamics and Materials Conference*, Paper No. 84-0995, May, Palm Springs, CA, pp. 292-295.

[195] O'Callahan, J. C., Avitabile, P., and Leung, R., (1984), "Development of Mass and Stiffness Matrices for an Analytical Model Using Experimental

Modal Data", *Proceedings of the 2nd International Modal Analysis Conference,*, Orlando, Florida, Feb., pp. 585-592.

[196] Otter, P. W., (1981), "Identification and Estimation of Discrete State-Vector Model with Stochastic Inputs", *Automatica*, Vol. 17, No. 2, pp. 389-391.

[197] Pandt, S. M., (1977), "Analysis of Vibration Records by Data Dependent Systems", *Shock and Vibration Bulletin*, No. 47, Part 4, September, pp. 161-174.

[198] Pappa, R. S. and Ibrahim, S. R., (1980), "A Parametric Study of the Ibrahim Time Domain Modal Identification Algorithm", *Shock and Vibration Bulletin*, Part No. 51, Part 3, pp. 43-72.

[199] Pappa, R. S., (1982), "Some Statistical Performance Characteristics of the "ITD" Modal Identification Algorithm", *AIAA/ASME/ASCE/AHS 23rd Structures , Structural Dynamics and Materials Conference*, Paper No. 82-0768, May, New Orleans, Louisiana, pp. 622-640.

[200] Pappa, R. S., (1983), "Close-Mode Identification Performance of the ITD Algorithm", *AIAA/ASME/ASCE/AHS 24th Structure, Structural Dynamics and Materials Conference*, Paper No. 83-0878, May, Lake Tahoe, Nevada, pp. 193-205.

[201] Pi, Y. L. and Mickleborough, N. C., " Identification of Parameters for Offshore Structures Using Modal Test Data", *Proc. Eighth Australasian Conference on Coastal and Ocean Engineering*, Institute of Engineers(Australia), Launceston, 1987.

[202] Pi, Y. L. and Mickleborough, N. C., "An Analysis for the Vibration of Marine Riser by Finite Element Method", *Proc. First Australasian Port,*

Harbour and Offshore Engineering Conference, Sydney, 1986.

[203] Pi, Y. L. and Mickleborough, N. C., "Modal Identification from Autoregressive Model Using Free Vibration Data", *Proc. Eleventh Australasian Conference on the Mechanics of Structures and Materials*, Auckland, New Zealand, 1988.

[204] Pi, Y. L. and Mickleborough, N. C., "Determination of Modal Parameters using ARMA Model of Vibrating Structures", *UNICIV Report No. R-250*, The University of New South Wales, 1988.

[205] Pi, Y. L. and Mickleborough, N. C., "Time Domain Modal Identification of a Linear Vibrating Structure", *UNICIV Report, No. R-249,* The University of New South Wales, 1988.

[206] Pi, Y. L. and Mickleborough, N. C., "Identification of Parameters of Vibrating Structure with Non-proportional Damping", *Proc. First Structural Engineering Conference*, Institute of Engineers(Australia), Melbourne, 1987.

[207] Pi, Y. L. and Mickleborough, N. C., "The Calculation of Response Spectral Density for Random Vibration", *Tenth Australasian Conference on the Mechanics of Structures and Materials,* Adelaide, 1986.

[208] Pi, Y. L. and Mickleborough, N. C. "Modal Identification of a Vibrating Structure In the Time Domain", *Computers & Structures*, Vol. 32, N0.5 August, 1989.

[209] Pi, Y. L. and Mickleborough, N. C., "Modal Identification of Vibrating Structures Using ARMA Model", *Journal of Engineering Mechanics, American Society of Civil Engineers*, Vol. 115, No. 10, October, 1989.

[210] Pilkey, W. D. and Cohen, R., (Eds.), (1972), *System Identification of Vibrating Structures*, ASME, New York.

[211] Powell, C., L., (1985), "Analysis of Experimental Complex Modes", *Proceedings of the 3rd International Modal Analysis Conference*, Orlando, Florida, Feb., pp. 223-230.

[212] Rajaram, S. and Lunkins, J. L., (1985), "Identification of Vibrating Flexible Structures", *Journal of Guidance, Control, and Dynamics*, Vol. 8, No. 4, July-August, pp. 463-470.

[213] Rajbman, N. S., (1978), "Minimax, Identification ", *Automatica*, Vol. 14, pp. 129-135.

[214] Raney, J. P., and Howlett, J. T., (1969), "Identification of Complex Structures Using Near-Resonance Testing", *NASA-TN-D*, 5069, 38 pp.

[215] Rao, C. R., and Mitra, S. K., (1971), *Generalized Inverse of Matrices and Its Applications*, John Wiley, & Sons, Inc., New York.

[216] Richardson, M. and Kniskern, J., (1976), "Identifying Modes of Large Structures from Multiple Input and Response Measurements", *SAE* Paper 760875, Town & City, San Diego.

[217] Rodden, W. P., (1967), "A Method for Deriving Structural Influence Coefficients from Ground Vibration Tests", *AIAA Journal*, Vol. 5, No. 5, May, pp. 991-1000.

[218] Ross, Jr. R. G., (1971), "Synthesis of Stiffness and Mass Matrices from Experimental Vibration Modes", *SAE* paper No. 710787.

[219] Rubinstein, R. Y., (1981), *Simulation and the Monte Carlo Method*, John Wiley & Sons, Inc., Somerset, NJ.

[220] Sage, A. P., and Melsa, J. L., (1971), *System Identification* , Academic Press, New York.

[221] Samaras, E., Shinozuka, M., and Tsurui, A., (1985), "ARMA Representation of Random Processes", *Journal of the Engineering Mechanics, ASCE*, Vol. 111, No. 3, March, pp. 449-461.

[222] Saridis, G. N., (1974), "Comparison of Six On-Line Identification Algorithms", *Automatica*, Vol. 10, pp. 69-79.

[223] Shinozuka, M., (1974), "Digital Simulation of Random Processes in Engineering Mechanics with the Aid of FFT Technique", *Stochastic Problems in Mechanics*, University of Waterloo Press, pp. 277-286.

[224] Shinozuka, M., Yun, C. B. and Imai, H., (1982), "Identification of Linear Structural Dynamic Systems", *Journal of Engineering Mechanics, ASCE*, Vol. 108, No. EM6, December, pp. 1371-1390.

[225] Silverberg, L. and Kang, S., (1989), "Variational Modal Identification of Conservative Nongyroscopic Systems", *Journal of Dynamic Systems, Measurement and Control*, Vol. 111, No. 2, June, pp. 160-171.

[226] Skingle, C. W., (1966), "A Method for Analyzing the Response of Resonant System to a Rapid Frequency Sweep Input", *Royal Aircraft Establishment Technical Report*, No. 66379, Dec.

[227] Sloane, E., and McKeever, B., (1975), "Modal Survey Techniques and Theory", *SAE paper*, No. 751067, 27 pp.

[228] Smallwood, D. O. and Gregory, D. L., (1987), "Experimental Determination of the Mass Matrix Using a Constraint Least Squares Solution", *AIAA/ASME/ASCE/AHS 28th Structures, Structural Dynamics and Materials Conference*, Part 2, Paper No. 87-0814, April, Monterey, CA., pp. 288-295.

[229] Smith, S. and Woods, Jr., A. A., (1972), "A Multiple Driver Admittance Technique for Vibration Testing of Complex Structures", *The Shock and Vibration Bulletin*, No. 42, Part 3, Jan., pp. 15-22.

[230] Smith, W. R., (1981), "Least-Squares Time Method for Simultaneous Identification of Vibration Parameters from Multiple Free-Response Record", *AIAA/ASME/ASCE/AHS 22nd Structures, Structural Dynamics and Materials Conference*, Paper No. 81-0530, April, Atlanta, Georgia, pp. 194-201.

[231] Spitznogle, F. R., et al, (1971) "Representation and Analysis of Sonar Signal, Volume 1: Improvements in the Complex Exponential Signal Analysis Computational Algorithm", *Texas Instruments, Inc. Report*, No. U1-829401-5, 37 pp.

[232] Spalding, G. R., (1976), "Distributed System Identification: A Green's Function Approach", *Journal of Dynamic System, Measurement, and Control, Transaction of ASME*, Vol. 98, No. 2, June, pp. 146-151.

[233] Styan, G. P. H., (1973), "Hadammard Products and Multivariate Statistical Analysis", *Linear Algebra and Its Applications*, Vol. 6, pp. 217-240.

[234] Strejc, V., (1981), "Trends in Identification", *Automatica*, Vol. 17, No. 1, pp. 7-21.

[235] Sundararajan, N. and Montgomery, R. C., (1983), "Experiments Using Least Square Lattice Filters for the Identification of Structural Dynamics",

AIAA/ASME/ASCE/AHS 24th Structures, Structural Dynamics and Materials Conference, Paper No. 83-0880, May, Lake Tahoe, Nevada, pp. 206-210.

[236] Tanabe, T. A. and Izawa. J., (1986), "The Identification of Eigen Vectors from Vibration Test Data for Dynamic Analysis of RC Structures", *The First Asian Conference on Structural Engineering and Construction*, January, Bangkok, pp. 1840-1847.

[237] Talbot, C. R. S., Tidbury, G. H., and Jha, S. K., (1975), "Identification of the Vibrational Modes of a Car Driven on the Road", *ASME* Paper No. 75-DET-115, September.

[238] Targoff, W. P., (1976), "Orthogonality Check and Correction of Measured Modes", *AIAA Journal*, Vol. 14, No. 2, February, pp. 164-167.

[239] Thomson, W. T. , Calkins, T. and Caravani, P., (1974), "A Numerical Study of Damping", *Journal of Earthquake Engineering and Structural Dynamics*, Vol. 3, pp. 97-103.

[240] Udwadia, F. E. and Marmarelis, P. Z., (1976), "The Identification of Building Structural System: 1. The Nonlinear Case", Bull. Seismol. Soc. Amer., Vol. 66, No. 1, February, pp. 125-151.

[241] Udwadia, F. E., Garba, J. A., and Ghodsi, A., (1983), "Parameter Identification Problems in Structural and Geotechnical Engineering", *Journal of Engineering Mechanics*, Vol. 110, No. 9, pp. 1409-1432.

[242] Udwadia, F. E., and Flashner, H., (1988) "Trade-Offs between Identification and Control in Dynamic System", *Journal of Applied Mechanics*, Vol. 55, No. 4, December, pp. 939-945.

[243] Unbehauen, H. and Gohring, B., (1974), "Test for Determining Model Order in Parameter Estimation", *Automatica*, Vol. 10, pp. 233-244.

[244] Ushijima, T., (1984), "Modal Parameter Estimation by Z-transformation Method", *Proceedings of 2nd International Modal Analysis Conference*, Orlando, Florida, Feb., pp. 437-442.

[245] Vepa, K., (1984), "Optimal Identification of Vibrating Structures", *Proceedings of 2nd International Modal Analysis Conference*, Orlando, Florida, Feb., pp. 96-105.

[246] Van Den Boom, A. J. W. and Van Den Enden A. W. M., (1974), "The Determination of the Orders of Process-and Noise Dynamics", *Automatica*, Vol. 10, pp. 245-256.

[247] Vigneron, F. R. and Soucy, Y., (1986), "Driven-Base Tests for Modal Parameter Estimation", *AIAA/ASME/ASCE/AHS 27th Structures, Structural Dynamics and Materials Conference*, Part 2, Paper No. 86-0870, May, San Antonio, Texas, pp. 232-241.

[248] Vigneron, F. R., (1976), "A Natural Modes and Modal Identities for Damped Linear Structures", *Journal of Applied Mechanics, Transaction of ASME*, Vol. 53, March, pp. 33-38.

[249] Vold, H., Kundrat, J., Rocklin, G. T. and Russel, R., (1982), "A Multi-Input Modal Estimation Algorithm for Mini-Computers", *SAE* Paper No. 820194, February, Detroit, Michigan.

[250] Vold, H., and Crowley, J., (1985), "A Modal Confidence Factor for the Polyreference Method", *Proceedings of the 3rd International Modal Analysis Conference*, Orlando, Florida, Feb., pp. 305,310.

[251] Wendler, B. H., (1986) "Modal Parameter Identification Using Adaptive Digital Filters", *Shock and Vibration Bulletin*, No. 56, Part 2, pp. 21-27.

[252] Yang, Y., (1985), "A Time Domain Identification Technique: The Oversized Eigenmatrix(OEM) Method", *Journal of Vibration, Acoustics, Stress, and Reliability in Design, Transaction Of ASME*, Vol. 107, No. 1, January, pp. 53-59.

[253] Yoshimura, T., Konishi, K., and Soeda, T., (1981), "A Modified Extended Kalman Filter for Linear Discrete-Time System with Unknown Parameters", *Automatica*, Vol. 17, No. 4, pp. 657-660.

[254] Young, P., Jakeman, A. and McMurtrie, R., (1980), "An Instrumental Variable Method for Model Order Identification", *Automatica*, Vol. 16, pp. 281-294.

[255] Yun, C-B, and Shinozuka, M., (1980). "Identification of Nonlinear Structural Dynamic Systems", *Journal of Structural Mechanics*, Vol. 8, No. ST2, pp. 187-203.

[256] Zak, M., (1983), "Discrete Model Improvement by Eigenvector Updating", *Journal of Engineering Mechanics, ASCE*, Vol. 109, No. 6, December, pp. 1437-1444.